Energy Management Systems For Smart Active Residential Buildings

Stepaniuk, Viktor

DOI (link to publication from Publisher):
10.54337/aau466407828

Publication date:
2021

Document Version
Publisher's PDF, also known as Version of record

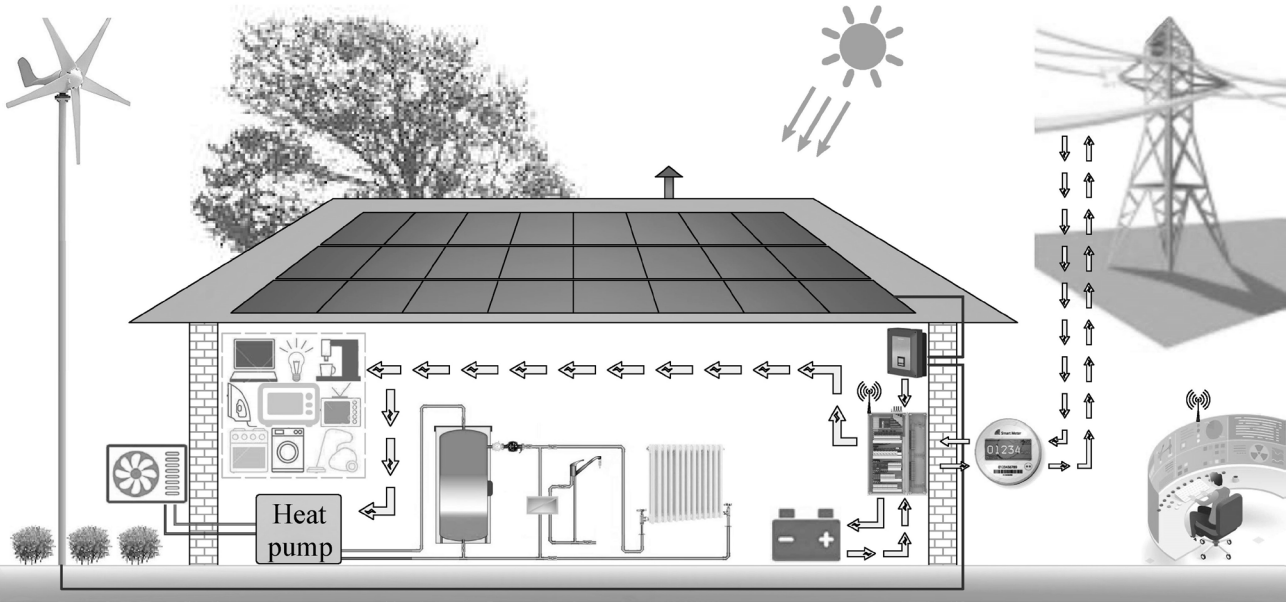

ENERGY MANAGEMENT SYSTEMS FOR SMART ACTIVE RESIDENTIAL BUILDINGS

BY
VIKTOR STEPANIUK

DISSERTATION SUBMITTED 2021

AALBORG UNIVERSITY
DENMARK

ENERGY MANAGEMENT SYSTEMS FOR SMART ACTIVE RESIDENTIAL BUILDINGS

by

Viktor Stepaniuk

AALBORG UNIVERSITY
DENMARK

PhD Dissertation

Submitted November 2021

Dissertation submitted: November 2021

PhD supervisors: Assoc. Prof. Jayakrishnan Radhakrishna Pillai,
Aalborg University

Prof. Birgitte Bak-Jensen,
Aalborg University

PhD committee: Associate Professor Erik Schaltz (chairman)
Aalborg University, Denmark

Professor Johan Driesen
KU Leuven, Belgium

Professor Mohan Kohle
University of Adger, Norway

PhD Series: Faculty of Engineering and Science, Aalborg University

Department: AAU Energy

ISSN (online): 2446-1636
ISBN (online): 978-87-7573-977-6

Published by:
Aalborg University Press
Kroghstræde 3
DK – 9220 Aalborg Ø
Phone: +45 99407140
aauf@forlag.aau.dk
forlag.aau.dk

Printed in Denmark by Rosendahls, 2022

ACKNOWLEDGEMENTS

I would like to express my deepest gratitude to my supervisors Associate Professor Jayakrishnan Radhakrishna Pillai and Professor Birgitte Bak-Jensen for giving me this wonderful opportunity for PhD studies, for their comprehensive support throughout the entire PhD duration and professionalism. I am greatly thankful to them for giving me the freedom to select the research directions and investigate selected topics on my own, at the same time for their openness to discussions, valuable feedbacks, and remarkable guidance.

My deep appreciation to the Department of Energy at Aalborg University for the partial scholarship and funding provided for participation in external courses and conferences. Special acknowledge to Otto Mønsteds Fond, William Demant Fonden, and AAU Doctoral School for supporting me financially during the research stay abroad.

I am sincerely thankful to SINTEF Energy Research for facilitating this wonderful research stay abroad. In particular to Hanne Saele, Merkebu Zenebe Degefa, Venkatachalam Lakshmanan, and Henning Taxt. My highest appreciation to all of them for their hospitality and the ideal research environment they provided during my research stay, for cooperation, interesting and fruitful technical discussions, and for the inexhaustible inspiration and motivation obtained.

I am very grateful to Associate Professor Carsten Bojesen (AAU), Christian Petersen (Vaillant Nordic), Jakob Vestergaard (Viessmann A/S Danmark), and Mikael Brix Falgren (Daikin, BKF-Klima A/S) for their technical guidance on the specifics of the heat pump system operation.

Big thanks go to my former officemate, Pavani Ponnaganti, and former colleague Karthikeyan Nainar, with whom I had countless technical and social discussions during the entire period of PhD studies.

I would like to express my sincere gratitude to Maria Bredvig as the first person I contacted at AAU regarding this PhD opportunity and who forwarded my application to my supervisors.

A particularly huge thank you, from the deepest of my heart, to my family for the immense kindness, support, understanding and love!

ENGLISH SUMMARY

The intention to counteract the climatic changes that our planet is experiencing as a result of human activity has brought a number of green initiatives to the existing traditional energy systems. However, increasing integration of more intermittent Renewable Energy Sources (RESs) into the power grid and the growing electrification of heating and transport sectors, induces a number of operational challenges that are currently faced by system operators in many countries. Limited power output forecasting accuracy of RESs (caused by abrupt changes in weather conditions) and difficulties with foreseeing electricity demand for flexible loads, as well as power generations on the low-voltage 0.4kV level of the power grid, lead to grid congestion issues, reverse power flow, and needs for reinforcement of grid infrastructure. All this radically changes not only the power system structures (that have been vertically integrated previously) but also the mechanisms of interactions between various parties/entities, as well as the management and control schemes.

One of the most promising solutions to address these challenges and to postpone very costly grid reinforcement as of today is found in the utilisation of energy flexibility on the demand side (that is shifting from supply control to demand control). Buildings, in this respect, being the largest energy consumption sector globally, is that particular resource of energy flexibility that receive one of the greatest emphasis today. The emergence of individual local RES generations, heat pumps, electric vehicles, as well as the automation of various indoor processes, in this connection, makes buildings the most attractive platform for introducing new technologies and "smarter" solutions that will enable utilisation of this flexibility in fundamentally new way. Nonetheless, the emergence of new components, as well as the transition to a market-based energy system structure, requires also new schemes for active interaction between these energy-flexible loads and various market participants. Existing demand response schemes were mostly applicable to large industrial or commercial customers and far not always available for such consumers as an average household. Furthermore, in many schemes the fact of market relationships is not taken into account. In addition, a unique generally accepted scheme/methodology for calculating such flexibility that would serve as the basis for both proactive power system operation planning and for financial calculations simply does not exist today.

This dissertation first provides a more detailed overview of the existing problems in power systems, and an overview of market mechanisms for planning, purchasing and selling electricity on the example of Denmark. The importance and complexity of providing ancillary services for

balancing generation and demand, which is getting more complicated every year due to uncertainties caused by the growth of RESs and flexible loads are highlighted. It is described in detail, what actually energy flexibility is, provides an overview of types, resources, existing mechanisms and rules, as well as an overview of various authors works describing the provision of such energy-flexible services. The difficulties with the delivering these services are emphasised from small consumers and the actual lack of schemes, regulations, market mechanisms for interaction between various market players, as well as the actual absence of market platforms where these services can be freely procured today. The importance of estimating the flexibility potential and quantifying the exact amount of energy flexibility in kilowatt-hours (i.e. the amount of peak energy shaved or shifted during active service provision) are discussed. The relevance of detailed modelling of energy-flexible loads for determining the above indices is also emphasized.

At the next stage of the study, models of various household energy system components, such as photovoltaic (PV) panels, micro wind turbine (WT), battery, heat pump (HP) and a hot water storage tank (HWST) were created. Particular attention is paid to the HP and HWST (referred to here as heat pump system (HPS)), as these components are considered as the main resource of energy flexibility in this thesis. The degree of flexibility that can be provided by a heat pump depends largely on the specifics of its operation that includes conversion and restart delays, defrost mode and guaranteed power-on time. Also, it depends on the amount of thermal energy controlled in the tank and its energy state. In order to maximally reflect the HPS operational behaviour and its details model is developed.

Having created models of individual components, the impact of main active components on the household's needs of electricity supplied from the grid was simulated and studied in detail. This has been done by combining different scenarios of these components under a single coordination algorithm. After examining the impact of upgrading the energy systems of a single building, the next step was to investigate the impact of an aggregated group of such buildings. To do so, 25 models of similar smart active residential buildings were created using previously created models of separate components and historically measured base electrical and thermal load data for 25 households. This allowed to analyse energy consumption, as well as to investigate the impact of such modernization of the energy systems of buildings on the voltage deviation of the feeder line that supplies these houses.

To calculate the energy flexibility potential, a rule-based management strategy for responding to demand response signal, and its creation has been developed.

The final stage is the investigation of how the aggregated flexibility of 25 active houses connected to a single feeder can help to address the voltage drop issues occurring in that feeder. For this reason, another centralized coordinating control strategy was designed. The main feature of the proposed strategy is that the thermal comfort of the residents is always the primary priority and thereafter responses to request signals are provided. While the application of this strategy showed the ability to solve 81% of voltage drop periods occurring in that feeder during ordinary operation, applying the worst-case scenario. This confirms that the use of the proposed strategies can be mutually beneficial, both for system operators (in terms of voltage regulation support), and for household owners who will receive incentive payments for activating demand response.

DANSK RESUME

Intentionen om at modvirke de klimaændringer, som vores planet oplever, som følge af menneskelig aktivitet, har bragt en række grønne tiltag til de eksisterende traditionelle energisystemer. Den stigende integration af mere varierende vedvarende energikilder (VE) i elnettet og den voksende elektrificering af varme og transportsektorer fremkalder en række driftsmæssige udfordringer, som systemoperatører i mange lande i øjeblikket står over for. Begrænset nøjagtighed af forudsigelse af produktionen fra VE (forårsaget af pludselige ændringer i vejrforholdene) og vanskeligheder med at forudse efterspørgsel på elektricitet til fleksible belastninger, såvel som at el-produktionen på lavspændingsnettet (0,4 kV), fører til problemer med netbalancering, tilbageløb af effekt fra lavspændingsnettet og behov for forstærkning af netinfrastrukturen. Alt dette ændrer radikalt ikke kun strukturen for elnettet (der tidligere var vertikalt opbygget), men også mekanismerne for interaktioner mellem forskellige parter/enheder, såvel som nye styrings- og kontrolmetoder.

En af de mest lovende løsninger til at imødegå disse udfordringer og til at udskyde en meget kostbar netforstærkning i dag findes i udnyttelsen af energifleksibilitet på forbrugssiden (dvs. at skifte fra udbudskontrol til efterspørgselskontrol). Boliger er i denne henseende den største energiforbrugssektor globalt og er netop en attraktiv ressource til energifleksibilitet med stor mulighed for stor indflydelse. Fremkomsten af individuelle lokale VE-kilder, varmepumper, elektriske køretøjer, samt automatisering af forskellige interne processer, gør bygninger til den mest attraktive platform for introduktion af nye teknologier og "smartere" løsninger, der vil muliggøre udnyttelsen af denne fleksibilitet på en helt ny måde. Fremkomsten af nye komponenter samt overgangen til et markedsbaseret energisystem kræver dog også nye metoder for aktiv interaktion mellem disse energifleksible komponenter i bygningen og de forskellige deltagere på energimarkedet. Eksisterende fleksibilitetsordninger for fleksibelt elforbrug var for det meste gældende for store industrielle eller kommercielle kunder og langtfra altid tilgængelige for forbrugere som en gennemsnitlig husholdning. Desuden tages der i mange ordninger ikke hensyn til markedsforhold. Til dato er der heller ikke én fælles ordning/metode til beregning af fleksibilitet, der kan fungere som grundlag for både proaktiv netværksplanlægning og økonomiske beregninger.

Denne afhandling giver først et mere detaljeret overblik over eksisterende problemer i elsystemet, et overblik over markedsmekanismer for planlægning, køb og salg af el med Danmark som eksempel. Den fremhæver vigtigheden og kompleksiteten af at levere tjenesteydelser for

at balancere produktion og efterspørgsel, hvilket kompliceres år for år på grund af stigningen i VE og fleksible belastninger. Den beskriver i detaljer, hvad der er fleksibilitet, typer, ressourcer, eksisterende mekanismer og regler, samt giver oversigt over forskellige forfatteres værker til at levere sådanne energifleksible tjenester. Afhandlingen understreger vanskelighederne med implementeringen af disse ydelser fra små forbrugere og den faktiske mangel på ordninger, reguleringer og markedsmekanismer for interaktion mellem forskellige markedsdeltagere, såvel som faktiske markedsplatforme, hvor disse tjenester frit kan handles. Den beskriver vigtigheden af at vurdere det fleksibilitetspotentiale, der kræves for proaktiv netplanlægning, samt kvantificering af specifikke kilowatttimers energifleksibilitet, dvs. mængden af elektricitet, der anvendes til amplituderegulering eller flyttes til andre tidspunkter. Vigtigheden af detaljeret modellering af energifleksible belastninger for at bestemme ovenstående indikatorer blev også fremhævet.

I den næste fase af undersøgelsen blev der skabt modeller af forskellige komponenter i husstandens elsystem, såsom solpaneler, en mikrovindmølle, et batteri, en varmepumpe og en varmtvandsbeholder. Der lægges særlig vægt på varmepumpen og tanken, fordi disse komponenter i denne afhandling betragtes som hovedressourcen til energifleksibiliteten. Da mængden af fleksibilitet, der kan ydes af en varmepumpe, i høj grad afhænger af dens drift (inklusive konverterings- og genstartsforsinkelser, afrimning og garanteret opstartstid), samt niveauet af termisk energi i tanken og dens energitilstand, er varmepumpemodellen mere detaljeret for at afspejle dens drift bedst muligt.

Efter at have skabt modeller af individuelle komponenter, blev virkningen af visse komponenter på husstandens behov for elektricitet, leveret fra nettet, simuleret og undersøgt i detaljer. Dette er blevet gjort ved at kombinere forskellige scenarier af disse komponenter under en enkelt koordinationsalgoritme. Efter at have undersøgt virkningen af opgraderingen af energisystemet i en enkelt bygning, var det næste skridt til at undersøge virkningen af en samlet gruppe af sådanne bygninger. For at gøre det, blev der opstillet modeller af 25 lignende smarte aktive boliger ved hjælp af de tidligere oprettede modeller for separate komponenter og historisk målte elektriske samt termiske belastningsdata for 25 forskellige husstande. Dette gjorde det muligt at analysere energiforbruget samt at undersøge påvirkningen på spændingen ved nettilslutningen for disse bygninger.

For at beregne energifleksibilitetspotentialet er der udviklet en regelbaseret styringsstrategi til at reagere på et fleksibelt elforbrugssignal. Tilgangen til at skabe et kunstigt teknisk signal blev præsenteret i detaljer.

Den sidste fase er undersøgelsen af, hvordan den samlede fleksibilitet af 25 aktive huse, forbundet til en enkelt radial på nettet, kan hjælpe med at løse de spændingsfaldsproblemer, der opstår på nettet. Af denne grund blev der designet en koordineret, centraliseret styringsstrategi. Den største fordel ved den foreslåede strategi er, at beboernes termiske komfort altid er i første række, og alle svar på anmodningssignaler gives kun så vidt muligt i forhold til opretholdelsen af komforten. Anvendelsen af denne strategi viser evnen til at løse 81 % af de perioder med spændingsfaldsproblemer, der forekommer i netledningen under almindelig drift, ved anvendelse af det værste scenarie. Dette bekræfter, at anvendelsen af de foreslåede strategier kan være gensidigt fordelagtige, både for systemoperatører (i form af støtte til spændingsregulering) og for husstandsejere, som vil modtage incitamentsbetalinger for dette.

CONTENTS

LIST OF FIGURES

LIST OF TABLES

LIST OF ABBREVIATIONS

A2W	Air-to-Water
AVR	Automatic Voltage Regulator
BEMS	Building Energy Management System
CHP	Combined Heat and Power
CO_2	Carbon dioxide
COP	Coefficient of Performance
CPP	Critical-Peak Pricing
BL	Baseload
BP	Balancing Power
BPM	Balancing Power Market
BRP	Balance Responsible Party
DC/AC	Direct Current / Alternating Current
DER	Distributed Energy Resource
DG	Distributed Generation
DH	District Heating
DHW	Domestic Hot Water
DLC	Direct Load Control
DR	Demand Response
DSO	Distribution System Operator
DS	Distributed Storage
DSF	Demand-Side Flexibility
DSM	Demand-Side Management
DSI	Demand-Side Integration
EB	Electric Boiler
EMS	Energy Management System
ENTSO-E	European Network of Transmission System Operators for Electricity
EPBD	Energy Performance of Buildings Directive
ER	Electricity Retailer
ES	Electricity Supplier
ESCo	Energy Service Company
EV	Electric Vehicle
EU	European Union
EWH	Electrical Water Heater
GBC	Green Building Council
GC	Grid Company
GENCO	Generation Company
GHG	Greenhouse gas
HAWT	Horizontal Axis Wind Turbine
HH	Household
HP	Heat Pump

HPS	Heat Pump System
HVAC	Heating, Ventilation, and Air Conditioning
HWST	Hot Water Storage Tank
ICT	Information Communication Technologies
IEA	International Energy Agency
IES	Integrated Energy Systems
IHWH	Instantaneous Heating Water Heater
ISO	Independent System Operator
LEED	Leadership in Energy and Environmental Design
LV	Low voltage
MDCP	Main Distribution and Control Panel
MPC	Model Predictive Control
Mtoe	Megatonne of oil equivalent/ Millions of tonnes of oil equivalent
MV	Medium Voltage
NBM	Nordic Balancing Model
NEMO	Nominated Electricity Market Operator
nZEB	nearly Zero Energy Building
OECD	Organisation for Economic Co-operation and Development
P2G	Power-to-Gas
P2H	Power-to-Heat
P2T	Power-to-Transport
P2X	Power-to-X
PCM	Phase-Changing Material
PEV	Plug-in Electric Vehicle
PHS	Pumped Hydro Storage
PMU	Phasor Measurement Unit
PO	Plant Owner
POC	Point of Connection
PV	Photovoltaic
RES	Renewable Energy Source
RP	Regulating Power
RPM	Regulating Power Market
RTO	Regional Transmission Organization
RTP	Real-Time Pricing
RTU	Remote Terminal Unit
SARBEMS	Smart Active Residential Building Energy Management System
SDGs	Sustainable Development Goals
SG	Smart Grid
SH	Space Heating
SOE	State of Energy
SOC	State of Charge

STC	Standard Test Conditions
TFC	Total final consumption
TCM	Thermochemical Material
TOU	Time-of-Use
TSO	Transmission System Operator
UNFCCC	The United Nations Framework Convention on Climate Change
V2G	Vehicle-to-Grid
VSC	Voltage Source Converters
WT	Wind Turbine
bat.	Battery
cons.	Consumption
el. or electr.	Electrical
init.	Initial
prod.	Production
therm.	Thermal

LIST OF SYMBOLS

Symbol	Definition	Unit
A	Rotor swept area of the wind turbine (the area of a circle for HAWT, where the radius is the length of the wind turbine blade)	[m²]
A_{array}^{PV}	Total area of the PV array (i.e., the area of a single panel multiplied by the number of panels)	[m²]
A_{panel}^{PV}	Area of a single panel	[m²]
c	Heat capacity of water	[J/(kg K)]
C_{in}^{DR}	Demand response signals (requesting flexibility service, where 1 – flexibility is requested, 0 – not requested)	[-]
C_{out}^{DR}	Binary control signal, which defines the demand response activation (and thus the duration of an actual response), where 1 – activated, 0 – not activated	[-]
$C_{restart}^{DR}$	Binary control signal sent to each active respondent individually signalling the ability to turn ON the heat pump unit	[-]
C_s^{HP}	Binary control signal which defines the activation of the heat pump (basic ON/OFF control, where ON = 1 and OFF = 0)	[-]
C_s^{IHWH}	Binary control signal which defines the activation of the instantaneous heating water heater (basic ON/OFF control, where ON = 1 and OFF = 0)	[-]
C_p	Power coefficient, representing the efficiency of the wind turbine in capturing the wind power	[-]
$COP_{theoretical}$	Maximal theoretical (ideal) efficiency during the energy transformation cycle	[-]
COP^{HP}	Practical coefficient of performance of heat pump or, in other words, transformation coefficient from electric to thermal power	[-]
$dP_{inv.}^{PV}$	Photovoltaic system inverter losses	[-]
$dP_{mod.temp.}^{PV}$	Photovoltaic panels temperature losses	[-]
$dP_{DC\ cable}^{PV}$	Photovoltaic system DC cables losses	[-]
$dP_{AC\ cable}^{PV}$	Photovoltaic system AC cables losses	[-]
$dP_{shad.}^{PV}$	Photovoltaic panels shadings losses	[-]
$dP_{irr.}^{PV}$	Photovoltaic panels weak irradiation losses	[-]
dP_{dust}^{PV}	Photovoltaic panels losses due to dust, snow	[-]
dP_{other}^{PV}	Other losses inherent in the photovoltaic system	[-]

Symbol	Definition	Unit
$E_{cap.}^{BAT}$	Total battery capacity	[kWh]
$E_{chrg.}^{BAT}$	Electrical energy charged into the battery	[kWh]
$E_{disch.}^{BAT}$	Electrical energy discharged from the battery	[kWh]
$E_{inv.}^{BAT}$	Electrical energy that can pass through the battery inverter per single time step	[kWh]
$E_{exp.}^{GRID}$	Electrical energy exported to the grid	[kWh]
$E_{imp.}^{GRIG}$	Electrical energy imported from the grid	[kWh]
$E_{el.cons.}^{HP}$	Electrical energy consumed by the heat pump	[kWh]
$E_{el.cons.}^{IHWH}$	Electrical energy consumed by the instantaneous heating water heater	[kWh]
$E_{prod.}^{PV}$	Electrical energy produced by the photovoltaic system	[kWh]
$E_{prod.}^{WT}$	Electrical energy produced by the wind turbine	[kWh]
ΔE	Excess or shortage of electrical energy (local production)	[kWh]
H	Global solar irradiation on tilted panels (without shadings)	[W/m^2]
H_p	Projected height (wind turbine hub height)	[m]
H_r	Reference height (installation height of anemometer)	[m]
i	Initial time step ($if\ t = 1, i = 1;\ if\ t > 1, i = t - 1$)	[m]
m	Mass of water	[kg]
n	Simulation limit	[-]
$P_{chrg.}^{BAT}$	Battery charging power	[kW]
$P_{disch.}^{BAT}$	Battery discharging power	[kW]
$P_{inv.rt.}^{BAT}$	Battery inverter rated power	[kW]
$P_{exp.}^{GRID}$	Power exported to the grid	[kW]
$P_{imp.}^{GRID}$	Power imported from the grid	[kW]
P_{base}^{HH}	Electric baseload of the household	[kW]
$P_{th.load.}^{HH}$	Thermal load of the household comprising both domestic hot water and space heating	[kW]
$P_{el.dem.}^{HP}$	Electric power demand of the heat pump	[kW]
$P_{el.rt.}^{HP}$	Rated electric power of the heat pump	[kW]
$P_{th.prod.}^{HP}$	Thermal power output of the heat pump	[kW]
$P_{th.prod.2HWST}^{HP}$	Thermal power produced by heat pump that is fed into the hot water storage tank	[kW]
$P_{th.prod.conv.del.}^{HP}$	Thermal power produced by heat pump during the time of conversion delay	[kW]
$P_{th.prod.defr.}^{HP}$	Thermal power produced by heat pump during the defrost cycle	[kW]
$P_{el.dem.}^{IHWH}$	Electric power demand of the instantaneous heating water heater	[kW]

Symbol	Definition	Unit
$P_{el.rt.}^{IHWH}$	Rated electric power of the instantaneous heating water heater	[kW]
$P_{panel.rt.}^{PV}$	Peak power of a single photovoltaic panel under standard test conditions	[W]
$P_{prod.}^{PV}$	Power output of the photovoltaic system	[kW]
PR	Performance ratio or a coefficient for losses	[-]
$P_{prod.}^{RES}$	Power produced by renewable energy sources	[kW]
P_{wind}	Power available in the wind	[W]
$P_{prod.}^{WT}$	Power output of the wind turbine	[kW]
P_{rt}^{WT}	Rated power output of the wind turbine	[kW]
ΔP	Battery charging or discharging power (can be positive or negative)	[kW]
Q_{in}	Energy delivered to the system by a heating process	[J]
Q_{out}	Energy lost by the system due to work done (heat demand)	[J]
ΔQ	Change in the internal energy of the system	[J]
$Q_{th.cons.}^{HH}$	Thermal energy consumption of the household comprising both domestic hot water and space heating	[kWh]
$Q_{th.prod.2HWST}^{HP}$	Thermal energy produced by heat pump that is fed into the hot water storage tank	[kWh]
$Q_{th.prod.}^{HP}$	Overall thermal energy produced by heat pump	[kWh]
$Q_{react.}^{HPS}$	Reactive power demand of the heat pump system	[kVAr]
$Q_{th.loss.}^{HWST}$	Thermal energy losses of the hot water storage tank	[kWh]
Q_{total}^{HWST}	Total thermal energy accumulated in hot water storage tank	[kWh]
ΔQ^{HWST}	Change in the internal energy of the hot water storage tank	[kWh]
$Q_{th.prod.}^{IHWH}$	Thermal energy produced by instantaneous heating water heater	[kWh]
r	Solar panel yield	[%]
SOE^{BAT}	State of energy of the battery	[%]
$SOE_{temp.}^{BAT}$	Preliminary calculated state of energy of the battery	[%]
SOE_{max}^{BAT}	Maximum battery state of energy band	[%]
SOE_{min}^{BAT}	Minimum battery state of energy band	[%]
SOE^{HWST}	State of energy of the hot water storage tank	[%]
$SOE_{min.ctrl.}^{HWST}$	State of energy of the hot water storage tank, minimum controlled level	[%]

Symbol	Definition	Unit
SOE_{max}^{HWST}	State of energy of the hot water storage tank, maximum controlled level	[%]
t	Simulation step that is equivalent to a 1-minute time interval	[m]
$t_{rsv.}$	Desired duration of the reserved heat supply period	[h]
T^{air}	Ambient air temperature	[K]
T_{in}^{air}	Air temperature at the inlet to the heat pump	[°C],[K]
$T_{in.min}^{air}$	Minimum allowable air temperature at the inlet to the heat pump	[°C],[K]
$T_{in.max}^{air}$	Maximum allowable air temperature at the inlet to the heat pump	[°C],[K]
$T_{in.freeze}^{air}$	Temperature level that determines the risk of icing up (considered to be +4°C in this study)	[°C]
T_{out}^{w}	Heat pump outlet water temperature, which is selected to be 338,15 K (65°C) in this study	[K]
T_{cold}^{w}	Minimum possible cold-water temperature	[K]
T_{hot}^{w}	Maximum possible hot water temperature	[K]
ΔT	Water temperature difference	[K]
V	Volume of water inside the tank	[m^3]
v_p	Wind speed at the projected height of the wind turbine	[m/s]
v_r	Wind speed at the reference height of the wind turbine	[m/s]
v_p^{ci}	Cut-in wind speed band of the wind turbine	[m/s]
v_p^{co}	Cut-out wind speed band of the wind turbine	[m/s]
v_p^{rt}	Rated wind speed of the wind turbine	[m/s]
Z	Elevation, including wind turbine's tower high	[m]
η_e	Deviation factor (i.e. empirical deviation from the Carnot cycle, which is equal to 0.38 in this study)	[-]
η_c	Cumulative efficiency involving wind turbine's (internal) transmission and generation losses	[-]
η_t	Transmission efficiency (losses, associated with transferring power to generating unit inside the wind turbine)	[-]
η_g	Generator efficiency (losses of generating unit inside the wind turbine)	[-]
μ	Ground friction coefficient (~1/7 for open land)	[-]
μ_{Carnot}	Carnot efficiency	[-]
ρ_a	Air density at the wind turbine's hub	[kg/m^3]
ρ_w	Density of water	[kg/m^3]

Symbol	Definition	Unit
$\tau_{conv.}$	Binary control signal defining the activation of the conversion delay (where "activated" = 1 and "deactivated" = 0)	[-]
$\tau_{defr.}$	Binary control signal defining the activation of the defrost cycle (activated = 1 and deactivated = 0)	[-]
$\tau_{oper.}$	Binary control signal defining the minimum duration of the heat pump uninterruptible operating time and its availability for a DR response provisioning (1 = activated, which means no DR response can be provided and 0 = deactivated or available)	[-]
$\tau_{rest.}$	Binary control signal defining the activation of the restarting delay (activated = 1 and deactivated = 0)	[-]
φ	Phase angle, which is considered to be 0.32 in this study ($\tan(\varphi)$ = 0.33, $\cos(\varphi)$= 0.95)	[rad]

1 INTRODUCTION

1.1. BACKGROUND AND MOTIVATION

1.1.1. Electrification. Industrialization. Climate change.

The discovery and understanding of the principles of electricity generation have significantly changed the lives and opportunities of mankind. Less than two centuries ago, electricity gradually became available for commercial use and for use in technology. Nowadays, the use of electrical energy finds a place in almost all spheres of human life and for a modern person, it is already difficult to even imagine their existence without it. A variety of appliances and equipment in everyday life, a diversity of industrial equipment, lighting, computers, mobile communications, television, and the Internet – all these require a power supply. Due to the superiority in the efficiency, as well as relatively easy transmission and distribution of electrical energy over long distances compared to some other forms of energy, such as, for instance, mechanical and thermal, as well as easy conversion into these forms of energy, electricity is becoming the dominant energy carrier in the global scale. The rapid technological growth over the past few decades, as well as the rapid growth of the global population, makes the demand for electricity tremendously high and these indices keep growing every year. Referring to the International Energy Agency (**IEA**), total final global electricity consumption has increased more than four times for the period between 1974 – 2018 [1] (Figure 1.1a). Danish Transmission System Operator (**TSO**) Energinet, in its turn, estimates significant growth in electricity consumption in Denmark over the next several decades in new sectors such as data processing, electrified transport, and heating (Figure 1.1b). However, Figure 1.1c indicates that an overwhelming majority of all globally generated electricity today is still produced by centralized power plants, burning various fossil fuels, such as coal, oil, and gas, thereby emitting harmful greenhouse gases into the atmosphere.

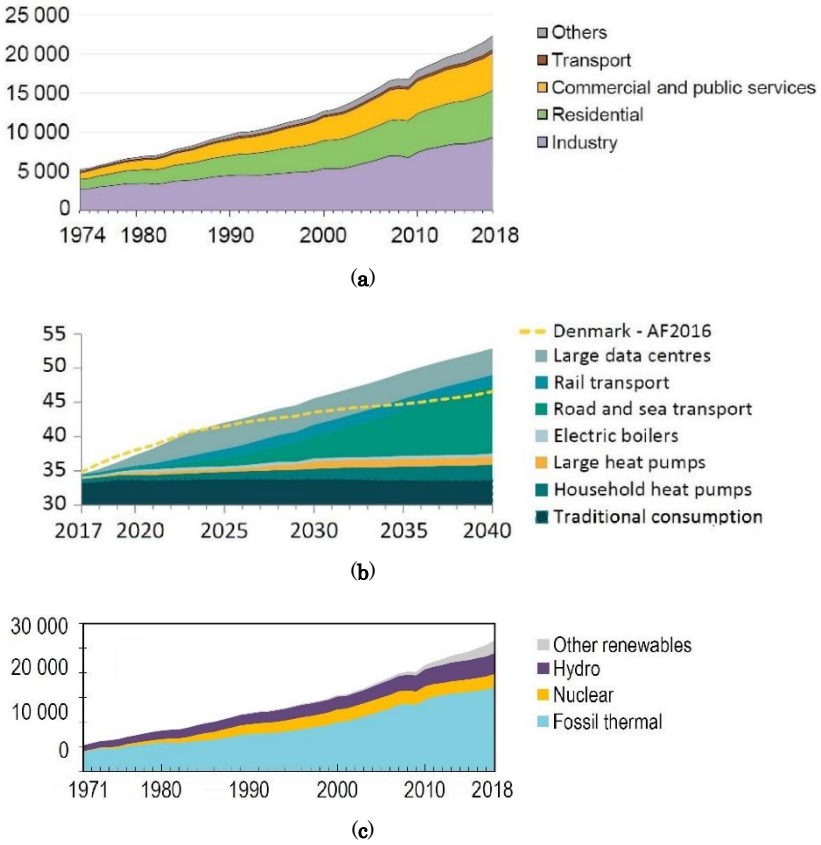

Figure 1.1. (**a**) Total final global electricity consumption by sector in TWh [1]; (**b**) Expected total annual Danish gross electricity consumption in the projection period in TWh, compared with analysis assumptions made in 2016 (AF2016) [2]; (**c**) World electricity generation by source in TWh [1].

Referring to [3], just one decade ago, electricity generation accounted for 31% of the world's total fossil fuel use. The same report specifies that two-thirds of the primary energy used for electricity production is lost during generation (only one-third is transformed into electricity), another 9% is lost during transmission/distribution. In view of the above, and also taking into account the scientific consensus that greenhouse gases emission precisely is the main cause of global warming – electricity production is considered one of the largest environmental pollutants on the planet. The first column in Figure 1.2 visually illustrates the above statement, showing that electricity and heat generation sectors together account for 41% of all global CO_2 emissions. Alongside the other three top polluting sectors such as industry, transport, and buildings, at the same time

considering that electricity feeds a vast share of these sectors this causes significant environmental and climate change.

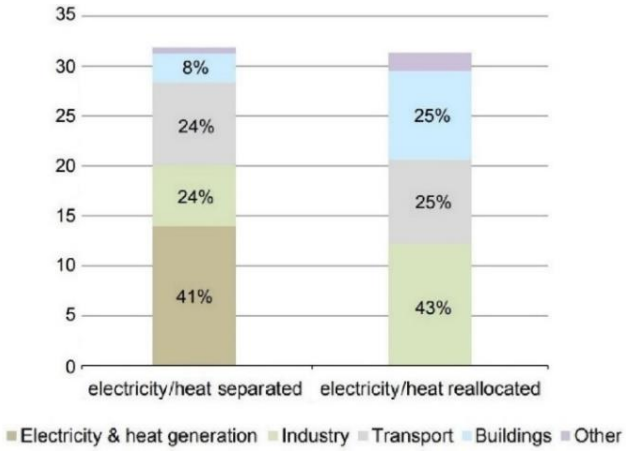

Figure 1.2. Global CO_2 emissions by sector (Gt), 2018 [4].

1.1.2. Environmental-friendly development strategies

The upward trend in global electricity consumption, enormously high growth of fossil fuel use, and potentially endangering climate changes have prompted humanity to search for new environmental-friendly development strategies and new sustainable solutions to minimise this harmful impact. Since 1992, a number of countries have negotiated and signed a number of environmental treaty agreements addressing climate change through the United Nations Framework Convention on Climate Change (**UNFCCC**), followed by the Kyoto Protocol in 1997, which was superseded by the Paris Agreement in 2015. The latter Paris Agreement, as of 2020, was signed and ratified by most of the countries in the world [5], thereby committing to undertake and communicate ambitious efforts to mitigate global warming. In this regard, many countries, have set their national targets, development plans, road maps, and so on.

In the European Union, these climate strategies and targets [6], along with a set of laws, directives, acts, useful documentation, and numerous studies, have been collected under the "2030 climate and energy framework", and "2050 long-term strategy". Three main targets for the period up to 2030 are outlined as follows and illustrated in Figure 1.3.

- 32.5% improvement in energy efficiency (i.e. primary energy and/or final energy use has to be no more than 1 273 Mtoe / 956 Mtoe),

- 55% cuts in greenhouse gas emissions (from 1990 levels), and
- 32% share for renewable energy.

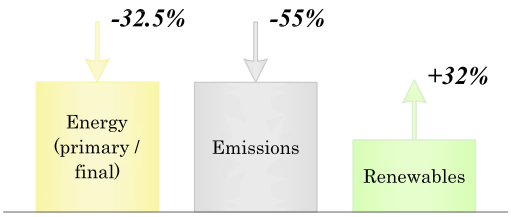

Figure 1.3. The European Union's climate and energy targets to be reached by 2030

While in the long-term strategy by 2050 the EU plans to become fully climate neutral (i.e. with a net-zero greenhouse gas emissions economy).

The electrification of existing fossil-fuelled appliances (which means converting non-electric end-uses to electricity, like, for example, use of heat pumps for space and water heating instead of gas/oil/wood pellet fired boilers or electric transportation instead of conventional gasoline/diesel driven one) has been proven to be one of the best ways to improve energy efficiency and reduce harmful emissions. Since a significant part of greenhouse gases is a consequence of electricity generation by the fossil fuel-based power plants and, at the same time, considering that electrification is so essential today – the transition to alternative, environmentally friendly sources of electricity generation is absolutely necessary. The most promising technologies, as of today, are renewable-based hydro, wind and solar photovoltaic (**PV**) power production. These three, compared to a variety of other sources, demonstrate a predominant increase in power generating capacity installed in the world for the last two decades [7].

The Danish pathway

Denmark, among a number of European countries, is one of the most ambitious supporters of the transition to renewable energy, aiming to become independent of fossil fuels by 2050. The summary of the Danish National Energy and Climate Plan [8] embracing the main objectives and targets to be met by 2030 and 2050 is illustrated in Figure 1.4.

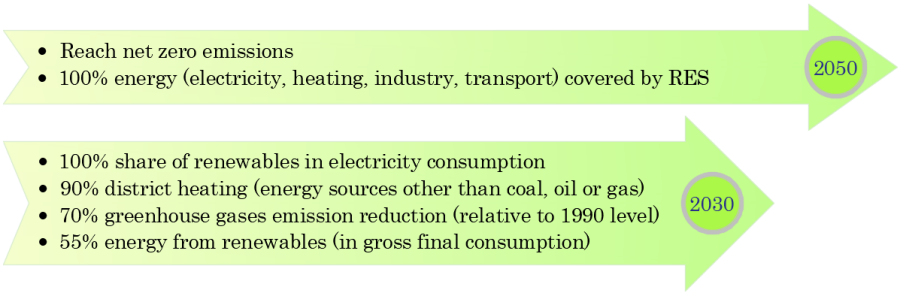

Figure 1.4. Danish national energy and climate targets by-2050 [8]

Nowadays, Denmark has the largest share of Wind Turbines (**WT**s) produced energy per capita in the world, being on top of this list over the last 15 years [9]. September 15, 2019, was the record-breaking day in Danish history when WT production accounted for 100% of the total electricity consumption during 24 consecutive hours. Moreover, the production exceeded demand by 25% for the major part of the day [10]. Wherein the share of WTs' production in total annual domestic electricity supply took 47.2%, which, together with the solar panels share of 2.8% allowed Denmark to reach one of the set goals (i.e. 50% of RES delivered energy by 2020) faster than anticipated [11]. The realization of this task entailed considerable changes both in policy and energy systems. However, in order to provide 100% renewable-based energy supply during a whole year, as well as meet the aforementioned targets and commitments, today's power systems must undergo much more comprehensive changes and overcome a number of ongoing challenges and difficulties.

1.2. POWER SYSTEM

1.2.1. Power system structure

Not so long time ago, a "traditional" has been called vertically integrated power systems in which all electricity has normally been generated by centralised power plants, then transmitted and distributed to the end-use consumer by transmission and distribution lines. More and more stringent environmental mandates have led to the emergence of a large number of small distributed renewable-based power generations, such as solar panels and wind turbines, Combined Heat and Power (**CHP**) plants in the energy systems. This led to power systems reconversion and decentralisation. Figure 1.5 demonstrates the evolution of the distributed generation in Denmark, which is nowadays a pioneering country in terms

of the reconversion of its energy system and among the best in the world at integrating wind energy into the electricity system.

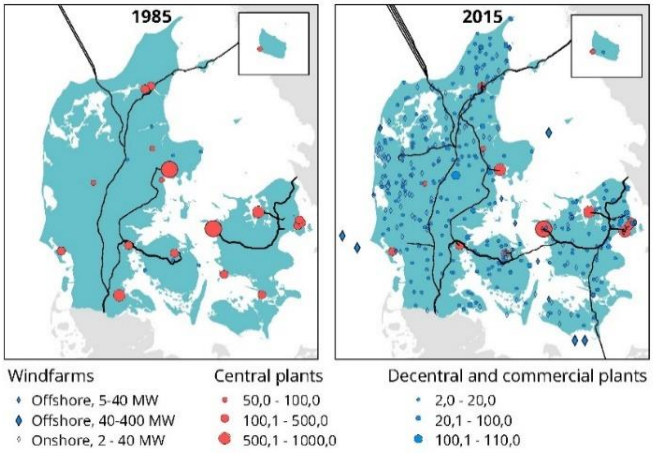

Figure 1.5. Evolution of the Distributed Generation in Denmark [12]

Both in older centralised power systems and more decentralised contemporary systems, the generation, transmission, and distribution of electric energy is handled by special entities [13], [14], namely:

- Generation Companies (**GENCO**s) / Plant Owners (**PO**s)
- Transmission System Operators (**TSO**s)
- Distribution System Operators (**DSO**s) / Grid Companies (**GC**s)
- Electricity Retailers (**ER**s) / Electricity Suppliers (**ES**s)

Electricity production is the primary responsibility of GENCOs / POs, wherein GENCOs referred to an older power system and POs to a more contemporary system comprising both large- and small-scale electricity-generating facilities.

TSOs are responsible for transmitting the bulk electric power over long distances, on a national and international scale, and are normally associated with a high voltage range (from 110 kV to 750 kV). The core service of TSOs is the security of supply, which is done by initiating ancillary services when the imbalance between consumption and generation occurs.

Whereas DSOs, which are also interchangeably referred to as GCs (especially in the context of the electricity market), are companies that

operate in a lower voltage range (between 0.4 kV and 60 kV) and dealt with distributing power on a trans-regional, regional, or local scale. These companies own the electricity infrastructure from the transmission level to the consumer and are also responsible for connecting new customers, for a smooth reliable operation of the distribution grid, for the maintenance, development, and timely reinforcement of the grid infrastructure.

The other entities referred to as Electricity Retailers / Electricity Suppliers are in charge of selling electrical energy to end-use consumers. These companies are closely related to DSOs, and commonly refer to as the same entity, however, they have no deal with a technical layer (i.e. maintenance, reinforcement and so on) of the distribution electricity grid and have to pay the GCs for transporting electricity to the customers and transmitting meter data for settlement purposes. The typical layout of a modern power system is illustrated in Figure 1.6

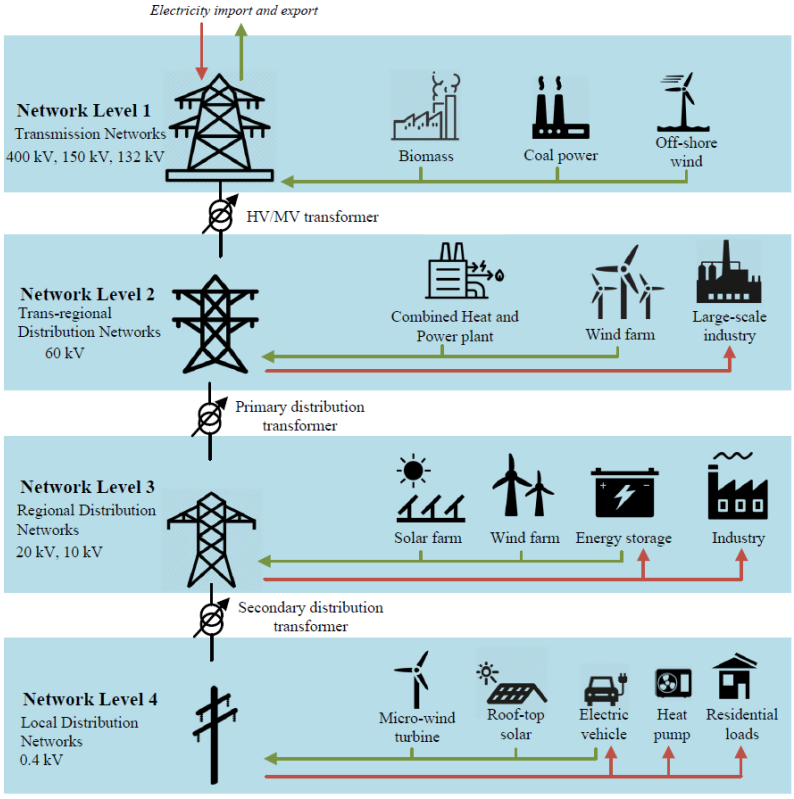

Figure 1.6. Layout of a modern power system [15]

1.2.2. Power system operation and Electricity Market

As known, maintaining a balance between demand and supply is the basis for the high-quality power supply services provisioning and one of the main prerequisites for efficient use of energy resources. Following changes in the power system structure, with the advent of more intermittent and volatile Renewable Energy Sources (**RES**s) into the power grid, the process of maintaining such a balance, as well as the frequency and voltage magnitude within the standardized tolerance is also gradually evolving.

Older power system

In older power system structures, all active imbalances that occur during the power system operation have been eliminated through the direct dynamic interaction between GENCOs and ERs, wherein an overwhelming majority of energy flexibility being delivered to the power system came from large centralized power plants. Ancillary services such as, for instance, frequency control and voltage regulation have similarly been provided centrally by frequency-sensitive / spinning generators, and voltage regulators. All management and control, in such systems, have typically been executed in a hierarchical manner, wherein the generation has strictly followed the electricity demand. Whereas the whole system operation has usually been coordinated by one governmental institution.

Modern power system

In nowadays power systems, all interactions between POs and ESs are executed via the electricity market. Since generating and consuming facilities have a significant impact on the physical power system balance, market players who trade electricity on their own behalf usually have to be prequalified as Balance Responsible Parties (**BRP**s) for production or consumption respectively. Those parties wishing to sell or buy electricity without balance obligation must assign BRPs to perform this task on their behalf (i.e. BRPs for trade) [16]. The BRPs, in turn, every new day have to submit schedules of power production and consumption 24 hours forward in time [17]. If any imbalances between planned and real production or consumption arise during the actual operation, these imbalances will be eliminated by TSOs through the market mechanism however, the cost of this will be invoiced to the BRPs. Ancillary services that have traditionally been provided centrally is another area that undergoes significant changes. Energy flexibility being delivered to the nowadays electricity system is, to a major extent, already coming from the wholesale electricity market with neighbouring countries, to a still large extent from centralised power plants, and, to a lesser extent, from other energy sources such as CHP plants, biomass/waste/biogas fired plants, energy storages. This topic will be more thoroughly discussed in the following chapters.

Electricity Markets

The wholesale electricity market is a virtual IT platform that was designed to address variations in demand and supply on a short basis. As of today, the Danish electricity markets can be classified as wholesale and retail. The wholesale market consists of 3 sub-markets, namely, *day-ahead* or spot market, *intraday* or adjusting market, and *real-time* market, which is a combination of regulating and balancing power markets, in the Danish case. The day-ahead hourly market has initially been designed to facilitate the operational restrictions (such as slow start-up, ramping-up, and -down) of centralised power plants. Nowadays almost 80% of all electricity consumption in Nordic countries is traded through this market. An intraday market is a market where less predictable loads are traded on an hour-ahead basis. While all active imbalances that occur during real-time operation are counterbalanced by running various ancillary services, part of which is procured through regulating and balancing markets. The retail market is the market where all end-use consumers, such as ordinary household, buy their electricity via ERs/ESs.

1.2.3. Power system monitoring and automation

Remote monitoring and control of the power distribution grid is another important link to ensure a quick response to any changes that occur during the operation process. This can relate to both observing active load changes (for further estimating the load distribution) and power quality (i.e. voltage, frequency, harmonics, power factor, phase angle, etc.), as well as monitoring the state of protective devices for fault detection and operational switching. To date, remote monitoring/control in low voltage (**LV**) distribution grids in Denmark is very limited. Remotely-controlled substations with on-load tap changing transformers for voltage regulation are only available at MV/LV 60/20 kV, 60/10 kV levels. Whereas, transformer substations at 20/0.4 kV, 10/0.4 kV levels are not automated, as well as not equipped with automatic voltage regulators, reactive power compensation units [15]. Those parts of the distribution grid infrastructure at 0.4 kV level are most commonly very simple, with a radial feeder structure, therefore, any switching or reconfiguration there is performed only manually. There are also no substations/feeder lines monitoring and all monitoring in this part of the grid is limited to just interval (smart) meters at the point of connection (**POC**) of consumers. Moreover, even though having 100% coverage with smart meters [18] that provide an opportunity to extract reading once 15 minutes or even shorter intervals and can measure all network variables, the full potential of these meters is not exploited and is just limited to energy data for billing purposes. In addition, due to fact that there are still quite large data transferring issues connected with infrastructure, processing, refining,

storing and security, these energy data are transferred only once a day at best, even though read once 15 minutes.

1.2.4. Issues in contemporary Power Systems

Issues on the Supply-side

Since wind turbines and solar panels are inherently intermittent and completely dependent on weather conditions, maintaining an energy balance to ensure stable and safe operation of the electrical system and guarantee secure electricity supply in a new, decentralized, and RES-based power system is a serious challenge and difficult task for all system operators and BRPs. Dependence on weather conditions and limited power output forecasting accuracy (caused by abrupt changes in weather conditions) creates a number of control and operational complexities. In particular, as mentioned earlier, on the 15th of September 2019 the total wind turbine production in Denmark exceeded the overall country's demand by 25% for most of the day. Similarly, on the 1st of April 2019, between 03:00 – 10:00, the overall domestic wind turbines' production was very close to zero. [10]. Having an installed capacity of 6,103 MW, as of the end of 2019, total production in the same year amounted to only 16,158,977 MWh [19], that is equivalent to 30,2% in relation to the nominal installed capacity (i.e. to the energy that potentially could have been produced, but not produced due to the periodical absence of wind or down-regulation/ curtailment in case of low demand and no export possibilities). Danish projection of annual load and wind turbines production (Figure 1.7a), as well as capacity (Figure 1.7b), can clearly illustrate these discrepancies.

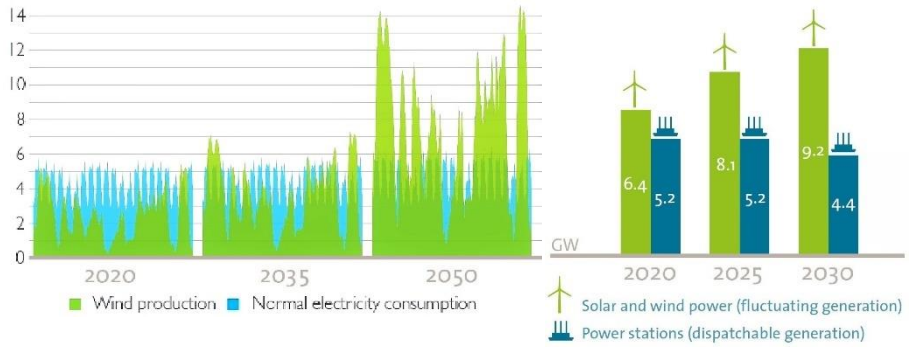

(a) (b)

Figure 1.7. (**a**) Projection of annual load and electricity generation by wind turbines in Denmark up to 2050 in GW [20]; (**b**) Projection of capacity in GW [21].

Another example of abrupt fluctuation in power generated by wind turbines is given by [22] on the example of Horns Rev offshore wind farm, located in Danish waters in the North Sea. Figure 1.8 illustrates the situation, in which the high and rapid increase of wind speed (above the 25m/s, appeared almost instantly across the whole wind farm) caused a simultaneous shutdown of all 80 turbines (each having 2MW), as a consequence, ramping down of about 140 MW of production within a few minutes. This phenomenon occurred several times during one night.

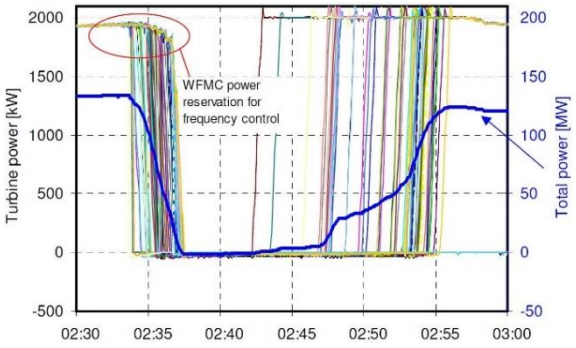

Figure 1.8. A shutdown of the wind farm due to a sharp change in weather conditions. [22].

Summarising the above examples, electricity production during peak wind or solar activity combined with low and uncontrolled power demand (or vice versa), as well as fast ramping-down and -up of a high volume of power can be the cause of grid problems such as overvoltage/undervoltage, reverse power flow, grid congestion, and, as a consequence, further actuation of network protection devices and frequency imbalance [21], [23]. Ancillary services, in particular operating reserve services (i.e. the availability of ready-to-use generating capacity, that can quickly be dispatched to balancing supply and demand on a short-term basis) – is another large challenge for the reliable and economical operation of the power system. As the green transition accelerates (also considering that a large share of flexibility still comes from centralised/dispatchable power plants), the decreasing number of available power plants will very soon be unable to deliver the degree of flexibility required by the power system to balance the high volume of fluctuated generation. In this regard, it is expected that this flexibility potential is offset by demand-side flexibility.

Another grid issue may be driven by a drastically rising number of small distributed renewable-based generations, such as roof-top PV panels and individual micro wind turbines. The problem is that all of these

generations are located at 0.4kV level where the radial feeder structure is most commonly used. There is no active grid monitoring, no options for remote grid reconfiguration at this level and in this grid topology. Consequently, the power generated by these energy sources may lead to reverse power flow and overvoltage issues, as well as be the main driver for limiting larger, more efficient, and more economically feasible power generation capacities at regional, trans-regional, or even at a transmission level. Nowadays, to assure the reliable operation of the grid, these generations are most commonly restricted on their grid export [24], [25]. Wherein all allowable limits are yet regulated centrally by national regulatory authorities based on technical-economic analysis considering grid infrastructure and capacity. All energy produced above these limits have to be either locally consumed, or stored, otherwise curtailed. However, there may be another, more beneficial solution for both grid operators, as well as micro RES owners.

Issues on the Demand side

Increased electrification of heating, transport, and data processing sectors (i.e. replacement of fossil fuel heat sources with highly efficient, but power-intensive heat pumps (**HP**s) or electric boilers (**EB**s), the displacement of traditional combustion engine cars with electric vehicles (**EV**s), as well as building new power-intensive data centres) impose another series of issues on the other (demand) side. Simultaneous charging events of a large number of EVs may lead to other issues like overloading and undervoltage of transformers and lines [26]. Nowadays it is connected with the fact that existing power grids of many countries are, to a great extent, not designed to accommodate a large amount of such sizeable loads, and, therefore, it will very soon may lead to grid reinforcement and expansion needs.

Balancing issues due to mismatch between supply and demand (caused by the deficit or surplus of RES generation), fast ramping-down and -up issues (caused by abrupt changes in weather conditions), operating reserve and flexibility needs issues (caused by the high volume of fluctuated generation), small distributed generation issues, as well as demand-side issues, have already been discussed. To address these issues, scientific society foresees the following solutions.

1.2.5. Prospective solutions

To maximize the utilization of intermittent RES-based generation, to minimize curtailment, and to address the aforementioned supply-side issues, four main solutions can be highlighted:

- Conventional Energy Storage;

- Flexible Technologies - Integrated Energy Systems, including:
  - Power-to-Heat (**P2H**) that implies the utilisation of heat pumps, Electrical Water Heaters (**EWH**s), and CHP plants to produce both heat and electricity;
  - Power-to-Gas (**P2G**), aimed at using electrolysers to produce hydrogen or methanol, which can be stored and further be used for the different reasons, such as, for instance, transport, or reconverted into electricity back when needed, using fuel cells;
  - Power-to-transport (**P2T**), similar to the previous one, is focused on decarbonizing the power and transportation sector, using electrolysers to produce hydrogen for transportation purposes;
  - Vehicle-to-grid (**V2G**) using Plug-in electric vehicles (**PEV**s) as a distributed energy storage thereby providing ancillary system services such as load regulation (controlled charging) or spinning reserves (discharging power back to the grid through bi-directional power flow) when the system needs it;
- Interconnected systems (implies creating links in power system infrastructure on different layers, starting from local, regional, to national, and international layers, so that to make possible the trade of high volumes of electricity across great distances (including cross-border markets) thereby bring power from where it is in surplus, to where it is needed most in a cost-effective manner);
- Demand-side flexibility (**DSF**), which is a shift from conventional supply control (where power generation follows demand) to demand control (where growing flexible demand will continually be reshaped to match fluctuated power production) [27].

When considering the first "Energy Storage" solution, which seems to be able to solve all the above balancing issues, the option of using Electrochemical storage in a form of batteries is so far extraordinary expensive to be used in large-scale projects. Even despite the steadily decreasing cost, and technical viability to compensate the intermittency of RES generations (implying configurable power-to-energy ratio, high round-trip efficiency) [28], far not all power systems can afford this option today without subsidy policy. Wherein the potential of Mechanical storages (such as pumped hydro storage (**PHS**) that have the largest share of the quantity of energy stored globally, as well as considered to be the most cost-beneficial technology today) is not applicable in many countries due to inappropriate terrain. Flywheels and electrical supercapacitors are also limited to power (not for energy) application due to their short charge/discharge durations. Most other storage options such as Thermal (i.e. hot water, molten salt, phase changing materials, etc.) or Chemical

(i.e. Hydrogen, Methanol, synthetic natural gas) require flexible technologies and integrated energy systems.

Flexible technologies such as P2H, P2G, P2T aimed at converting, reconverting, and storing of energy (which are also commonly referred to as Power-to-X (**P2X**)), are very well suitable to both accommodating surplus of RESs generated energy and coping with ancillary services provisioning. In addition to the abovementioned solutions, to maintain ancillary services (such as frequency control and voltage regulation) in a modern, distributed generations-based energy system, it is also expected to get support from decentralized generators' side, namely, variable-speed wind turbine generators, power-electronics-based PV converters, biomass/waste/biogas fired plants, or furthermore, from various sources on the demand side, such as PEVs or thermostatically controlled loads. The practical example of utilizing V2G technology to stabilize the power grid (i.e. primary frequency support) and the biomass plants for secondary frequency regulation can be found in [29].

Making interconnected energy systems and deploying demand-side flexibility in a new market-based power system structure seems to be an economically and technically more attractive solution rather than the utilisation of large-scale storages for system balancing. This is, to a great extent, due to the perspective of making the grid operation process much more intelligent. However, it should also be noted that solutions such as cross-border interconnections increase the country's energy dependency.

To address issues that may arise due to small distributed RES generations, it is vital to create an environment in which these generations can interact with the grid in a more intelligent manner (not just exporting the excess of their own use). The environment that will be attractive/beneficial to both for power system operation, and for RES owners. A flexibility market, where flexibility (derived from these on-site RESs coupled with batteries) can be traded for ancillary services provisioning, is the most promising solution.

To overcome the potential demand-side issues (due to increasing electricity demand), also considering the grid capacity inadequacy (caused by the high volume of fluctuated generation), there are two broadly accepted solutions: grid reinforcement/expansion (or at least, for the first time, reconfiguration) and DSF implying a new type of control for constantly reshaping demand to fit fluctuated generation patterns [30]. Upgrading or expanding the existing grids is generally very expensive. Therefore, special importance as of now is given to the latter one, i.e. shifting to a

demand-controlled system. This is where the Demand-Side Management (**DSM**) and Demand Response (**DR**) solutions play a crucial role.

1.3. ROLE OF DEMAND-SIDE FLEXIBILITY

DSM is the mechanism including a set of technologies, various programs, and activities directed to proactively and/or reactively reshape the consumption or local generation patterns of consumers/prosumers in distribution electricity grids. DR programs are considered the primary solution for implementing DSM strategies and one of the main methods for maintaining the energy flexibility provided by power-intensive flexible loads on the demand side. While energy flexibility is considered the most promising paradigm today to address both the challenges of balancing supply and demand and postponing a very expensive reinforcement of the grid [31]. If to take a close look, a variety of industrial and commercial enterprises with loads of sizeable power ratings and high grid stability impact are already utilising their energy flexibility in the electricity market. Nevertheless, this will very soon be not enough to cover the recent future needs. To maximize the exploitation of this flexibility, particular attention is paid to buildings as they occupy one of the largest shares of total final energy consumption globally. (More information about the importance of DSF including DSM concept, DR programs will be presented in Chapter 2, Section 2.2).

1.4. ROLE OF BUILDINGS

Buildings account around 40% of total final energy consumption (followed by transport - 33%, industry - 25%, and agriculture - 2%), around 55% of common electricity consumption and 36% of the CO2 emissions in Europe (see Figure 1.9a) [32]. The share of energy consumption of buildings in Denmark is one of the largest in Europe and occupies about 44% [33]. The energy sources delivered to buildings are mainly gas, biomass, oil, heat or electricity. Even though the end-use of energy is highly dependent on the type of building, Figure 1.9b shows that in the residential sector most of the energy consumption is ascribed to space and water heating (taking together a share over 78%); followed by lighting and appliances – 14%; and by cooking equipment, space cooling and ventilation, and other end-use, taking together – 7.5%. Referring to [32], the share of residential buildings in the EU accounts for around 75%. At the same time, the EU's statistic estimates that around 35% of all buildings stock are older than 50 years, and virtually 75% of them are energy inefficient, wherein the only very minor share of 0.4-1.2% is renovated each year. These factors, create a large potential for energy savings from the buildings' side.

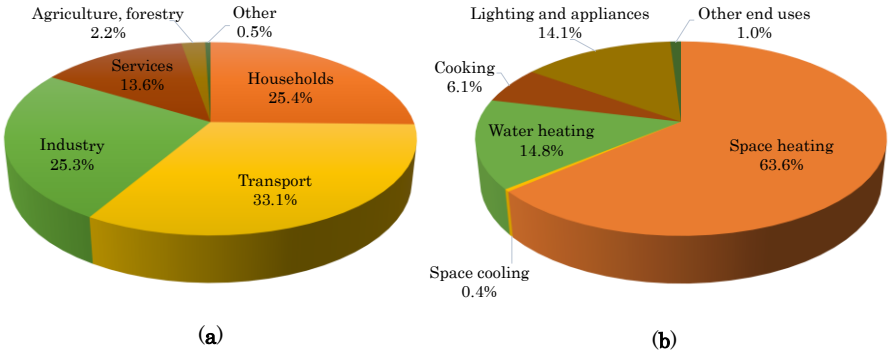

Figure 1.9. (**a**) Final energy consumption by sector, EU-28, 2015 (% of total, based on tonnes of oil equivalent) [34]; (**b**) Energy consumption in the residential sector by use, EU-27, 2018 [35].

The EU has three main directives concerning buildings and the transition to a more sustainable future:

- Energy Efficiency Directive [36] that basically aims at forcing a competitive low carbon economy and contains measures and prescriptions to save energy (in relation to final energy indices) by utilizing it in a more efficient manner, however, its scope comprises buildings and appliances.
- Eco-design [37] that predefines energy efficiency classes (from A+ to G) for each energy-related product. In this regard, a new labelling is required to show how good or bad the product is in relation to the effectiveness of the energy use.
- Energy Performance of Building Directive (**EPBD**) [38], which stipulates that any new public building since 2021 should be nearly Zero Energy Building (**nZEB**). Wherein, the ability of a building to rapidly reshape its load, as well as the ability to actively interact with the power system by providing energy flexibility services, is considered one of three key building functionalities in the methodology for defining its "smart readiness" indicator.

The first two have a strict relation to the Passive House concept, which generally means an extremely well insulated high-performance building that consumes 85-90% less energy than conventional existing building today. The annual heat demand in such kinds of buildings is very low and normally does not exceed 15 kWh/m2 (for comparison, in conventional buildings this demand ranging from 100 kWh/m^2 and more in bad insulated buildings). This means simplified requirements for the heating

system, and thereby lower bills and lower CO2 emissions. The overall energy efficiency of such kinds of buildings is very high.

nZEB is basically defined as very high energy performance and a low energy consumption building that covers a very significant share of its energy demand by using on-site or local RES. However, the exact energy standard (to which extent) is varying for each EU member state. Utilizing the on-site RES, generally means that the energy system of new buildings starting from 2021 is also evolving and should be considered not only in terms of consumption but also in terms of production, supply and energy storage (i.e. photovoltaic panels or micro wind turbine coupled with battery, or a heat pump or solar collectors coupled with a hot water storage tank or other forms of thermal energy storage). These types of buildings (which are also so-called Prosumers), containing these small-scale distributed generations (**DG**s), storages, and flexible loads (which are also commonly referred to as Distributed Energy Resources (**DER**s) [39]), can contribute to the transformation of energy systems through active interaction with the network and by providing energy flexibility services. However, a large entry barrier to the energy market remains a key obstacle, as of now, towards enabling flexibility utilization from the building's side. An introduction of new players such as Aggregators to the energy market may substantially facilitate this task.

Being the largest end-use energy sector, buildings play one of the most essential roles in this green transformation cycle while having an opportunity to significantly contribute to both improving energy efficiency, reducing CO2 emission, and helping to solve grid issues. That is why the buildings are considered the most attractive sector for developing and demonstrating new smarter technologies and integrated energy systems for facilitating this transition.

1.5. CHALLENGES TOWARDS DEMAND-SIDE FLEXIBILITY UTILISATION

As can be seen from the above sections, the DSF can be beneficial both in solving the supply- and demand-side issues. Furthermore, enabling DSF will greatly expand the capabilities of grids, bringing them to a whole new Smart Grids (**SG**s) level. However, the implementation of DSM and thus exploitation of DSF still face a number of challenges. Among them:

- Information Communication Technologies (**ICT**) associated with extracting, exchanging, processing, storing, and security of data (i.e. to transmit meter readings from the end-use consumer to the

data hub, to exchange technical control actions/price signals, etc). This implies both expansion of data infrastructure and building new data centres.

- Grid infrastructure monitoring (implying substation/feeders monitoring, power/load estimates, forecasts, and so on) aimed at observation of active load changes and power quality.
- Grid infrastructure automation (implies Machine-to-Machine communication for remote operational switching or network reconfiguration, and so on).
- New grid operation and control schemes considering demand-side flexibility utilisation.
- Market and regulatory conditions and legislation have to be improved allowing small customers to trade their energy flexibility or provide ancillary services (i.e. introduction of new market players such as *Aggregators* for harvesting flexibility from a variety of small end-uses, or introduction of new *Flexibility markets*).
- Market participation mechanisms suitable for small end-user customers on the demand side have to be progressed. This implies new incentives schemes or price response schemes describing how buildings equipped with on-site renewables, flexible loads, and storages can contribute to energy flexibility or ancillary services provision, by interacting with the electricity grid via aggregators or retailers/suppliers.
- Activation of energy assets of the existing buildings has to be substantially improved (implying automation, control, and energy management schemes within the building).
- Shortage of solutions for estimating energy flexibility potential (required for proactive power system operation, when there is no access to flexibility data of individual consumer).
- Shortage of practical solutions for energy flexibility quantification (both for proactive and reactive power system operation, as well as for actual settlements in the flexibility market).

It is obvious that demand-side flexibility enabling is far more complicated, perhaps also more expensive, than grid reinforcement/expansion. However, implementing this bid advantageous attributes both for the grid operation (by minimizing grid losses, enhancing reliability, and facilitating planning due to the availability of data), as well as for the consumer (enabling the option to gain on energy flexibility trading). The report [39] argues that the creation of Smart Grid – compared with traditional expansion – is the best socio-economic perspective and the most efficient method of addressing future challenges inherent in using RESs.

1.6. HYPOTHESIS, RESEARCH QUESTIONS AND OBJECTIVES

Assuming that some of the challenges outlined in Section 1.5 will successfully be managed within the nearest future, namely ICT, distribution grid automation, and the flexibility market will soon be developed, the information given in the previous sections lead to the following ***hypothesis:***

"Through improvement of the coordination and energy management systems for buildings, it is possible to improve the entire energy efficiency of building stock, improve the integration of renewable energy sources, as well as support the enhanced operation and control of the underlying energy networks and infrastructures"

This is realised by integrating and utilising active DER elements (i.e. RESs and flexible loads in combination with backup electrical and thermal energy storages) into the buildings, developing new schemes for integrated energy systems management and interaction, and provisioning energy flexibility services.

In order to confirm or refute the hypothesis aspects, this dissertation intends to ascertain the following ***research questions***:

- How does the emergence of on-site RESs affect the *energy needs* of the household and whether the presence of a battery can completely reduce dependence on the grid, including the need to export excess RESs generation? In this regard, could on-site RESs generation be considered *load reduction* to the power system *and* hence an improvement of *energy efficiency*? Furthermore, how can the replacement of the domestic heat source (where fossil fuel might have been employed) with HP increase the energy efficiency of the household when this substitution significantly increases its electricity demand? Can on-site RESs coupled with battery compensate for this heat source shift by covering the increased power demand with local generation?
- What *energy flexibility* can a single average household, equipped with one or another DER, provide and how the combination of

different DER elements under single management and control solution affects the potential for flexibility? In this connection, how does energy storage capacity (both electrical and thermal) affect the degree of flexibility and the duration of the activation period, without compromising the comfort of residents? What energy flexibility can an aggregate group of such kinds of houses provide?

- How does the electrification of heat sources in buildings, the presence of on-site RESs, and the coordinated control by a group of such kinds of buildings *affect the existing LV grid*, considering peak hours periods, transformer/buses/feeder lines loading, voltage deviation? How does this in general impact the peak hours periods in the local low-voltage grid?
- What are *schemes of interaction* in the energy markets exist *today*? Can these schemes be utilised for energy flexibility services provisioning from small consumers such as households? Can wholesale spot market prices be used for flexibility provisioning in local LV (i.e. 0.4 kV) grids? If not, why not?

  How exactly can the activation of energy assets of building with new control and management schemes and further utilisation of energy flexibility from these DERs *support the grid* operation? In this connection, can the voltage-based DR control strategy for such kinds of active buildings help to solve grid peak hours issues (i.e. overloading, undervoltage) thereby reducing or postponing the need for grid reinforcement?

Considering the above hypothesis and research questions, the overall ***objective*** of this dissertation is formulated as follows:

"To develop a versatile solution for energy management of residential buildings, integrated with renewable energy sources, energy storages and flexible loads".

To achieve this objective, the specific tasks conducted are as follows:

- Create RES energy models (power output profiles of PV and WT for the domestic use);
- Create a battery energy storage model (management algorithm);
- Create a model of heavy-intensive flexible load unit with the backup storage, namely Air-to-Water (**A2W**) type source heat pump

with Hot Water Storage Tank (**HWST**) and Instantaneous Heating Water Heater (**IHWH**);

- Create a power flow model of the active grid-tied residential building with battery backup and flexible load unit;
- Investigate on single building energy flexibility potential through DR signal.
- Investigate aggregated energy flexibility for a group of such kinds of buildings and the potential effect on the power distribution grid;
- Develop the DR strategy for the economic motivation of household owners while simultaneously considering the technical constraint of the distribution grid. Evaluate the suitability to provide power system services. Investigate DR application and assess the grid impact on the example of 25 buildings.

1.7. SCOPE OF WORK AND LIMITATIONS

The scope and limitation of this thesis are as follows:

- All studies performed in relation to this thesis concern only the Northern Jutland region of Denmark with relatively strong wind activity and low solar insolation. Considering that the power output of the RESs may substantially differ in southern countries, the results may also vary.
- Phase imbalance is a quite common issue in many LV networks. In particular in those with very long feeder lines where a single consumer or group of consumers are supplied with a single-phase connection. All single-family detached dwellings in the Danish low voltage grid have a three-phase supply to their home switchboards [40]. Furthermore, three phases are evenly distributed within the household's switchboard and throughout the house, so that to proactively balance the load. Therefore, the extent of unbalancing in Danish LV grids is very low. Since the study performed based on the Danish case, asymmetrical networks and unbalanced loading have not been considered for network analysis. In this regard, all active DER models incorporated in this study, which are based on manufacturers' technical datasheets, are also selected three-phase connections.
- Energy efficiency measures within the household, such as classes for each energy-related product, labelling of appliances (from A+ to G) are not investigated and are not a scope of this study. In this study, energy efficiency improvement is considered as a reduction in the total household demand for power supplied from the grid (by

means of substituting this share with on-site renewable energy generation).

- In-building automation and ICT parts, associated with enabling automated control of different baseload appliances and processes, such as lighting, blinds & shades, as well as software/hardware compatibility, compatibility of ICT protocols, standardisation for data exchange, and so on, are not included in the scope of this study.
- In detail modelling of the household's enclosing structures, envelope, calculation of heat losses, thermal inertia, the efficiency of the heat exchanger, occupant behaviour, schedule modelling, are not the prime target of this study and therefore are not included in the scope of this thesis. The thermal demand is historically recorded time series data.
- The utilisation and estimation of energy flexibility within a building are limited to Air-to-Water type HP coupled with HWST and the electric battery. Wherein base electrical loads such as lighting, appliances, laundry, cooking equipment such as refrigerator, freezer, kettle, and others are historically recorded time-series data. Furthermore, as the Scandinavian climate is relatively cold, the heat pump is modelled only for heat delivery purposes, although it can work in both heating and cooling modes.
- Modelling of the HWST is limited to an energy model using the specific heat capacity equation. Due to the relatively small volume of the storage tank (comparing to industrial storage), this study does not take into account the thermocline effect and stratification of different water layers. It is assumed that water inside the tank is constantly mixed using a circulation pump for space heating and frequent use of hot water for domestic purposes.
- Both thermal and electric load profiles are historically recorded time-series data, supplied by Aalborg University and concern only the Northern Jutland region of Denmark. Although profiles are obtained from different households, with different time resolutions, this should not affect the accuracy of the results obtained, and should not be considered as a critical limitation. Electricity consumption in the residential sector in Denmark has remained more or less at the same level over a decade [40], All heat load profiles, in turn, were selected only for households without electric heating. Considering these two aspects it can be clearly stated that these input data profiles do not overlap (meaning that electrical and heat systems within these houses are, in principle, two completely independent systems) and that the replacement of the heat source has no effect on the electric baseload, hence, it will not alter the finding of the research.

- Although forecasting of electrical and thermal energy consumption, as well as weather forecast and prediction of the behaviour of different system components, is highly important, this is not conducted in this study. Future time series are considered as already known due to the availability of data.
- Payback periods and profitability of various equipment such as the battery, HP, RESs, as well as electricity price reshaping, economic benefits/incentives that can be provided to household owners for their involvement in the DR program, as well as any other cost-benefit analysis have not conducted within the scope of this work.
- A grid study is limited to steady-state analysis (i.e. load flow analysis, using the Newton-Raphson method) on voltage magnitude and buses/feeder lines/transformer loading of the local 0.4 kV grid.

1.8. CONTRIBUTIONS OF THE THESIS

The significance of this thesis is about the development of an energy management algorithm that will enable coordination and flexible operation of power-intensive load, related to both heat and electricity systems, RES generation and storage units. This work is applied for:

- improving energy efficiency in building stock;
- providing energy flexibility for enhanced operation of electricity networks and infrastructures;
- increasing the renewable energy penetration in energy networks;
- creating new opportunities, new interaction schemes for prosumers and other energy market players, allowing all parties concerned to benefit from energy flexibility provided by buildings.

The exact outcomes are architecture for the active building control for effective energy management, the applications to estimate building energy flexibility and demand response control for efficient distribution grid management set up with active buildings.

1.9. THESIS OUTLINE AND PUBLICATIONS

The dissertation is written as a monograph, nonetheless, part of this PhD work has already been published by means of two conference papers and one journal article. The main content of the dissertation is organised into 6 chapters as below:

Chapter 1 consist of background information and motivation related to the composition of work performed. A new tendency in climate change is signified first. The impact of new environmental-friendly development strategies on the operation and planning processes of the traditional power system is indicated. The ongoing transformation of the power system induced by increased penetration of the renewable sources, electrification of fossil-fuel driven sectors, as well as the emergence of flexible and movable loads are highlighted. The importance of building stock, demand-side management, and energy flexibility services provisioning are emphasised. Finally, the opportunities and challenges are presented.

Chapter 2 presents the literature review while concentrating on the state of the art in the power system, that is recent developments and contemporary practices to solve the identified issues associated with Demand Response, energy flexibility service provisioning and in overall, prosumers-to-grid interaction through the market mechanisms.

Chapter 3 is focused on creating an energy *model* of a building consisting of DERs and integrating these active building components into a single coordinating and management solution. The integration of all these DERs components within a single management solution gives us an opportunity to explore the behaviour of both each individual component and the entire integrated energy system of the household as a whole, and also allows applying Demand Response signals, and hence investigating and evaluating the flexibility potential.

Chapter 4 aims to answer multi-purpose questions. It will begin with clarifying the first group of research questions (under the first bullet point) and investigating two DSM technologies (i.e. Strategic load growth and *Energy efficiency*), namely how the presence of on-site RESs, a battery, as well as the replacement of a non-electric end-use with an electric one, affects the energy needs of a household. This will follow with creating 25 separate models of grid-tied houses using the same principle and further *aggregating* them into one group. The purpose of such aggregation is to investigate how the combination of certain components in a group of houses changes the simultaneous use of energy from the grid and thus affects the grid peak hour periods.

Chapter 5 first investigates the energy *flexibility potential* of a single building by simulating a DR application. The DR signal required for this purpose has artificially been generated on the basis of the peak load of a transformer substation in the local LV grid. This potential is explored in two stages. First, the flexibility range that can be achieved is estimated by combining different scenarios with respect to DERs. Second, the actual

amount of peak-hour energy that can be shaved through DR application in an active residential building equipped with a HP and HWST will be quantified. The second section of this chapter will analyse the *impact* of the expansion of smart active buildings on the local distribution grid applying different scenarios of DERs and running load flow studies. A *voltage-based control strategy* for peak shaving in the distribution feeder will be demonstrated and the ability of buildings to cope with undervoltage issues (when receiving the feedback voltage-based DR signal) will be investigated and evaluated.

Chapter 6 concludes the thesis by summarising the major outcomes and scientific contributions of this research, while at the same time opens up the discussion for future work highlighting opportunities for improvement.

PUBLICATIONS

The following manuscripts are the outcome of the research performed during the PhD study. All publications are freely available online. The relevant hyperlinks are listed below.

Journal article

J1 V. Stepaniuk, J. R. Pillai, and B. Bak-Jensen, "Estimation of Energy Activity and Flexibility Range in Smart Active Residential Building," Smart Cities, vol. 2, no. 4, pp. 471–495, 2019, [Online]. Available: https://doi.org/10.3390/smartcities2040029.

Conference papers

C.1 V. Stepaniuk, J. R. Pillai, and B. Bak-Jensen, "Battery Energy Storage Management for Smart Residential Buildings," in Proceedings - 2018 53rd International Universities Power Engineering Conference, UPEC 2018, 2018, pp. 1–6, [Online]. Available: https://bit.ly/3cE8M2i

C.2 V. Stepaniuk, J. R. Pillai, and B. Bak-Jensen, "Quantification of demand-side flexibility of a smart active residential building," The 9th International Conference on Renewable Power Generation . IET Conference Proceeding, 2021, [Online]. Available: https://bit.ly/30Nlf1F

2 LITERATURE REVIEW

This chapter provides an overview of the various most relevant sources of information used in this dissertation. The main attention in the first section is paid to energy markets, their structures, and mechanisms of interaction between various participants. The importance of providing ancillary services for balanced stable operation of the network is also emphasized. The second section deals with energy flexibility and provides an overview of types, resources, existing mechanisms, and rules that currently exist for enabling this service. Existing challenges with delivering this service from small consumers are also highlighted. The relevance of detailed modelling of active energy-flexible building components for determining the energy flexibility indices and investigating the grid impact through DR application is discussed in the third section.

2.1. ELECTRICITY MARKET

The competitive electricity market was established with the single main purpose – to deregulate the price of electricity in accordance with the cost of production. The first full-fledged competitive energy market was established in the UK between England and Wales in 1990, following Norway in 1991, Australia and New Zealand in 1996, and the US at the end of the century [41], [42]. All these markets are quite distinct in different countries, in terms of their structure and trading mechanisms, since they were all introduced differently considering local legislation and power systems topologies [43], [44]. However, the fundamental principles of all competitive energy markets are the same, namely, to separate generation, transmission, distribution and retail operations, thereby preventing monopolies in the energy sector and creating a competitive environment for both different producers and consumers.

All markets associated with electricity that exist today can be broadly divided into *energy* and *capacity*, wherein they are very closely interconnected and complement each other. The background for such distribution is taken from the principle of operation of any power plant. All power generating units without exception have a nominal and maximum allowable power/capacity, calculated at the stage of their

manufacture to operate under certain conditions for a long time. However, for various reasons, only part of their potential is often used in practice. In this connection, the energy market is the place where the actual energy produced by one or another generation resource is traded. Whereas, the capacity market is the place where maximum available capacities are reserved by those power generating units, the potential of which is either only partially used or may not be used at all [45].

2.1.1. Energy markets

All energy markets consist of *wholesale* and *retail* markets. The wholesale markets, in turn, also usually divided by several markets in terms of energy delivery. Particularly, the *day-ahead* (or spot) and *real-time* (i.e. balancing or regulating) markets, and, as it is nowadays progressing in the European energy exchange area, an *intraday* (i.e. an hour ahead) market as well [45]. The day-ahead and intraday markets in Europe are administered by Nominated Electricity Market Operators (NEMOs), whereas the real-time markets are usually managed by local TSOs [46]. Figure 2.1 illustrates the abovementioned.

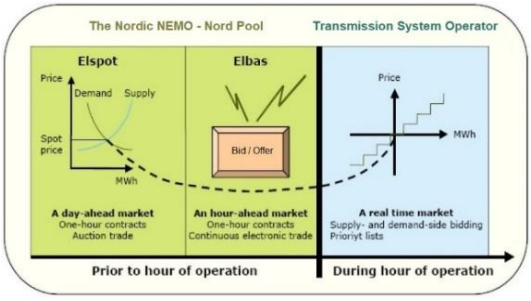

Figure 2.1. The Nordic Power Exchange Market (adapted from [47])

Day-ahead and intraday markets

Nord Pool is the pioneering European NEMO, owned by the largest stock exchange in Europe, Euronext Nordics Holding AS (66%) and TSO Holding AS (34%) consisting of Nordic and Baltic countries' transmission system operators. As of today, 16 countries from Northern, North-eastern, Central, North-western, and Western Europe trade their electric power through the Nord Pool-managed day-ahead and intraday web-based power exchange platforms [48]. The main advantage of NEMOs over other power exchanges around the world is that the trading mechanisms in the aforementioned two markets allow schedule changes (i.e. market participants are allowed to place, modify and delete their orders) until the market gate closure.

In the case of Nord Pool's *day-ahead* ***Elspot*** market, these gates are closing at 12:00 the day before the day of operation. Elspot market is a web-based platform in which the major part of all electricity in the Nordic and Baltic countries is traded. During 2019, this volume accounted for 381.5 TWh of power (which is equivalent to 77.2%) out of a total of 494 TWh that was traded through Nord Pool. For comparison, the volume traded in Nord Pool's intraday markets for the same year accounted 15.8 TWh (i.e. 3.2%) [49]. Several types of demand/supply order can be submitted to this market, namely, hourly orders, block orders for several hours, and flexible orders. All orders without exception should indicate an energy volume and electricity price. The energy volume offered for sale from the supply side must be constant or increasing, whereas purchasing bids from the demand side – constant or decreasing. For hourly orders, these indices should reflect the specific hour of the day of operation. Block orders must indicate the start and stop time, an average electricity price for at least three consecutive hours, the applicable minimum acceptance ratio and price limits in case of partial acceptance. Whereas flexible orders must specify the volume, the applicable upper and lower price limits, and the delivery periods that/for which/during which the participant would be willing to purchase or sell the power [50]. Following specific matching criteria for each type of demand/supply orders, also considering the transmission capacity in the electricity grid, the electricity prices (spot prices) for each hour of the following day are computed using an optimization algorithm. This is done between 12:00 and 13:00. When supply and demand are matched, 24-hour electricity prices are published and all traders are informed of the quantities they have traded. All buyers and sellers are consequently invoiced between 13:00 and 15:00 (wherein settlements are done on an hourly basis). The minimum trade lot size that can be ordered in this marker is 0,1 MW [51].

Three hours after closing the spot market gates (i.e. at 15:00), the intraday market opens its gates for further trading and balance adjustment. An *intraday* ***Elbas*** (Electricity Balance Adjustment Service) market serves as a supplement market to the day-ahead market and is considered the major advantage of Nord Pool's power exchange structure allowing market players to continuously trade power (i.e. to enter, modify and remove their orders) up to one hour prior to the actual delivery take place through the real-time market. This option allows adjusting their trade imbalances that may occur due to forecast errors after the closing of the day-ahead market. The participants have the opportunity to review and diminish their out-of-balance risks thereby avoiding costly imbalance payments, which is highly important for those plant owners with variable RES-based plants in their portfolio [45], [52]. In this manner, the intraday market helps to more accurately ensure the equilibrium between supply and demand, therefore

smoothing the overall power system operation. As of the beginning of 2020, this market accounts for 3.2% of all energy traded [49]. As seen, the volumes traded through the Elbas are much less than those traded through the Elspot. However, the imbalances are expected to become greater over the coming years due to increased penetration of intermittent RESs into the power grid, therefore this difference will also most likely be reduced (for comparison, in 2012 this share was 0.7% [53]). Two types of demand/supply orders can be submitted to this market, namely, curve orders and block orders. Each curve order must contain information about energy volume for the applicable delivery period, price, and the lower and upper price limits. The values between these limits may be interpolated and the order may be matched at any point on the curve. In each block order, the trader should indicate the start and stop time, price limit, and hourly energy volume. The energy volume offered for sale from the supply side must be constant or increasing, whereas purchasing bids from the demand-side – constant or decreasing [54]. Since intraday trading is carried out on an ongoing basis, prices are mounted following a first-come, first-served rule, with the best prices coming first (that is, the highest purchase price and the lowest selling price). Accordingly, all settlements are done to the pay-as-bid principle [48], [55]. The settlement period is currently one hour and the minimum trade lot size that can be ordered in the Elbas is 0,1 MW [51].

Real-time market

The real-time market is the last stage in the wholesale energy trade, which serves as a tool for system operators to resolve the imbalances that remained after the first two markets. This market is fully managed by local TSO, namely, Energinet* in the Danish case (the data, however, are shared with the Nord Pool) and is generally considered a platform to trade upward and downward regulating and balancing power. In this regard, it is also divided into two submarkets, namely Regulating Power Market (**RPM**) and a Balancing Power Market (**BPM**).

The regulating power is mainly associated with the physical deficit or surplus of power in the system during its actual real-time operation. In case of consumption exceeds production (if a deficit of power occurs), the Energinet must ensure that some producers will increase their production, or some consumers will reduce their consumption, thus neutralising this discrepancy. In this case, the Energinet buys the equivalent volume of increased power/reduced load from one or several producers/consumers by activating their bids for upward regulation. Conversely, in the case of

* Energinet is the national TSO, an independent public enterprise owned by the Danish state, which is responsible for operating the Danish power grid within Continental Europe's (as well as Nordic's) synchronous transmission area.

surplus production, a reduction in power output from the supply-side (or increase of consumption from the demand-side) of the power grid has to be ensured by the Energinet. In this case, the Energinet sells the equivalent volume of decreased power or increased load to one or several producers/consumers by activating their bids for downward regulation [56]–[58]. Generally, both upward and downward regulation can be provided either by generating or by consuming units, however, as of now in Denmark, only the generating side of the grid is employed. Furthermore, the market is primarily used to define Regulating Power (**RP**) prices and consequently for the formation of Balancing Power (**BP**) prices as well as serves for commissioning (activating) the manual Frequency Restoration Reserve with a response time of 15 minutes. The latter, in turn, serves to release the automatic reserve (if one has been activated) thereby restoring its availability to counteract rapidly other possible fluctuation and, in this way, preventing its excessive use (which is very costly) [59]. For the formation of RP prices, the same fundamental principles as on the spot market are used. The price is determined following the marginal price principle and is formatted on an hourly basis. Settlement for those players whose bids have been activated is done based on the metered time series values, derived at the end of each day of operation [60].

The balancing power is required for BRPs to eliminate their trade imbalances, i.e. deviations from submitted notifications/schedules caused by a mismatch between their forecasts and the system behaviour during its real-time operation. Energinet eliminates these imbalances by purchasing upward/downward regulating power in RPM and selling this power in BPM to all BRPs that incurred imbalances. All imbalances incurred by BRPs are settled based on the difference between their power schedules and the actual metered values employing different RP prices. Whereas, the RP price, in turn, depends on whether it is an ordinary imbalance, or an automatic reserve has also been involved. A one-hour imbalance settlement period is currently used [60], [56].

As seen from the above, the existing nowadays wholesale energy markets are functioning very well in the short-term time horizon. This is mainly due to the fact that market-clearing for a longer time horizon requires more complex and accurate forecasts of demand and generation. In energy systems with a high penetration share of RESs as well as flexible and movable loads, this is currently a very difficult task [45].

Retail electricity market

Following the deregulation of the electricity sector and the emergence of competitive wholesale energy markets, the retail electricity trade has also

undergone (and is yet undergoing) profound changes [61]. One of the main questions faced by all parties concerned with the transition is how to transfer the benefits of the wholesale competition to end-use customers. The creation of a retail electricity market has been considered one of the first prerequisites to do so. In this connection, the European Parliament and the Council of the European Union have established a clear set of rules for the retail electricity market design. These common rules for all EU member countries are nowadays outlined in two main documents, namely, the DIRECTIVE (EU) 2019/944 [62] and the REGULATION (EU) 2019/943 [63]. These documents stipulate the creation of the necessary regulatory framework and environment that will enable/allow/provide:

- different electricity service suppliers to easily enter the market;
- the end-use customers to easily switch electricity supplier;
- all electricity consumer groups, including ordinary households, to directly participate in the market by managing/adjusting/shaping their consumption (i.e. trading their energy flexibility) in response to different technical or real-time price signals, thereby receiving incentive payments or benefiting from the price reduction;
- all customer to trade their self-generated electricity;
- participation in a non-discriminatory manner, meaning that those consumers who choose not to participate in the dynamic electricity price scheme, for instance, are not penalised;
- an appropriate implementation model for independent aggregation;
- incentives to DSOs to procure flexibility services;
- the highest level of cybersecurity and customer data protection;
- and many other highly important aspects related to energy storage facilities, electric vehicles integration, tariff approval, and others.

Denmark switched to a supplier-centric retail market model in April 2016. Supplier-centric, in this context, means model where the consumer has contact to the market through the electricity supplier and where all market processes, all data exchange, subscriptions, all communications between the various parties involved in the trade take place through the Datahub*. Date Hub was established with the main purpose - to simplify, standardize, and organize all these processes. Graphically, this model is illustrated in Figure 2.2 and described in detail in [64]. Today the Danish consumer can easily change the supplier and receive only one single bill (unlike those countries where the transportation fee is charged separately). The consumer, in turn, has a choice between two price categories – fixed (where the price is fixed for at least three months and is

* Datahub is an IT platform owned and operated by Energinet, which handles measurement data, master data, necessary transactions and communication between the electricity market players in Denmark [269].

thus known in advance) and variable (the main purpose of which is to reflect the wholesale electricity prices fluctuation and enable the consumer to save on electricity use during periods when the wholesale price is cheap) [65]. Nevertheless, the composition of the bill, that is, the composition of the retail electricity tariff yet remains a large obstacle for encouraging consumers to choose the dynamic prices scheme and thus enabling DSF. Since the overwhelming share of the retail tariff is flat Electricity taxes, Grid/transportation charges and PSO, and the actual variable electricity price share, in the Danish case, is less than 20% of the total cost (as illustrated in Figure 2.3), such a tariff does not reflect all the advantages of a competitive wholesale market and is not attractive to the consumer, both in terms of savings and for the provision of energy flexibility services.

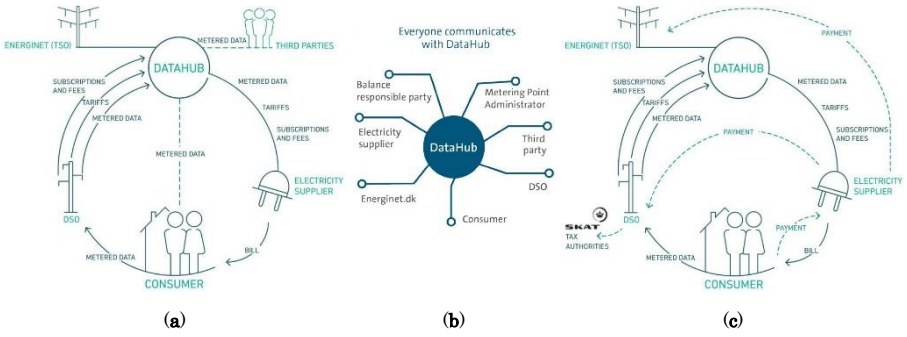

Figure 2.2. Denmark's retail electricity market model [64]: (**a**) Data flow; (**b**) Communication model; (**c**) Billing process.

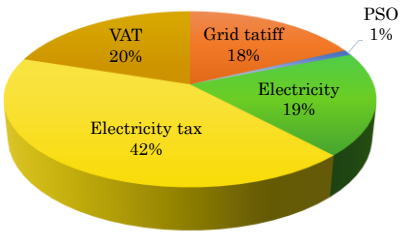

Figure 2.3. Composition of electricity price for households with an annual consumption of 4,000 kWh in Denmark (adapted from [66])

For those consumers who have on-site grid-connected RESs (i.e. for prosumers), Denmark proposes a special scheme called flexible settlement. In this scheme, the prosumer is offered to buy the entire volume of imported energy from the grid at the supplier's price and pay VAT on the entire volume of imported energy, while Grid tariff, Electricity tax and PSO should be paid only for the net consumption (that is, for the difference between imported and exported energy). Prosumer as a supplier will be

settled according to the Nord Pool's spot price and adjusted once a year depending on their contracts. More details about this model can be found in [67], [68], while the composition of residential electricity prices for all EU countries can be found in [69]. In order to increase the competition, support the development of new flexible products and services, and take full advantage of this, referring to the Directive and Regulation mentioned above – it is obvious that the competitive variable share of the retail tariff has to be increased, whereas the fixed part, conversely, should be reduced. When it comes to retail tariff formation it can be said that a unique model that is appropriate for all EU countries simply does not exist. A wide variety of pricing methods based on the grid congestion, cost of providing capacity at peak, line losses, operational expenditure, maintenance, and investment cost can nowadays be found in science [70]–[76]. Nonetheless, NordREG [77] summarizes the overall principles of retail tariffs design, stipulating that prices must be set in a fair, transparent, non-discriminatory and cost-reflective way (i.e. an efficient grid operation and DSOs' services revenue cap should be considered). Summarising this section, the author in [78] argues that as of the end of 2019, neither the main question outlined at the beginning of this section nor the goals of the modern retail electricity market design have not been solved/achieved, therefore a lot of work in this direction yet have to be done.

2.1.2. Capacity markets and Ancillary services

Capacity markets

When referring to capacity in relation to the power system, it usually involves two equally important aspects:

- capacity, applicable to overall power system planning and
- capacity for the power system operations planning.

The former involves measures for assessing the need for investment in new generating facilities, transmission and distribution grid infrastructure expansion/reinforcement. Whereas the latter implies activities that determine the scheduling and operation of available resources to meet expected seasonal, monthly, or daily demand fluctuation [79], as well as to cover a possible outage of the largest generation unit, the loss of international link, the shortage of imported power, or to neutralise other system and energy trading imbalances that may arise during the actual real-time power system operation [56]. However, the way of assuring capacity for power system operation is also undergoing a profound change in parallel with the evolution of energy systems.

In traditional power systems, special additional capacities, so-called strategic or operating reserves, were usually reserved to counterbalance

daily and seasonal peaks. Due to limited observability, lack of measuring infrastructure, ICT, load flow analyses, also due to the varying nature of the load and inability of controlling the demand-side of the grid, i.e. managing peak loads, these reserve capacities were not utilised for power supplying during normal system operation and have been activated only during peak load periods. The owners of these generating units, however, received availability payments per kW/period [77] for being on standby mode and the ability to being activated at any time. These payments, of course, were then reflected in the component of the retail electricity tariff. For the same reason, investing in new capacities and reinforcing/expanding the grid (in traditional regulated power systems) has been much more attractive to most utilities than investing in DSF.

Nowadays, the capacity market is dedicated to addressing this task by scheduling and operating these resources via the market mechanisms, wherein providing feedback price signal (or price data) to all parties involved in power system planning, such as TSO, DSOs, and POs. These data (while elaborating on it in the annual statement) serve as a litmus test for their assessment of the overall system adequacy, payback periods, and needs for further investment in new generating units, grid infrastructure expansion/reinforcement, or in other solutions, like, for instance, DSM [79]. However, the situation in those countries that don't have capacity markets established, indeed, is much more diffuse. As of today, far not all countries have capacity markets and active discussions are still going on around its design, remuneration mechanisms, and the most economically viable strategy of its implementation [80]. Denmark, having energy-only markets [81], strong national and international connections, rapid regulation properties, as well as being focusing on implementing DSF, is also among those counties that actively working on the aforementioned aspects while measuring all pros and cons [21], [82]. In this connection, four Nordic TSOs have represented the roadmap for establishing a joint Nordic Balancing Model (**NBM**), which includes the creation of different capacity markets in different time frames [83], [84].

In the literature, everything related to reserve capacity for power system operation is also interpreted very ambiguously. According to the following references, most European countries have energy-only markets [44] and capacity payments or strategic/operating reserves [21]. In this connection, the author in [80] defines all services associated with active power management, which are supplemental for energy planning, as an operating reserve, simultaneously stating that part of these services is procured via the day-ahead and real-time markets. The study, at the same time, separates capacity and ancillary service markets, showing that the primary target of the former ones is to "*evaluate potential capacity*

shortfalls after considering bilateral contracts or other power purchase agreements" as well as to assure that "*generation is developed on time to meet resource adequacy targets and help these resources recover their capital costs"*. Whereas the latter ones are strictly focused on the power system reliability. Meanwhile, Figure 2-2 in [79] associates the term "*operating reserves"* with a former vertically integrated energy system, while in a more contemporary market-based system it is treated as an "*ancillary service markets"*. The same reference associates these markets with Regional Transmission Organization (**RTO**)- or Independent System Operator (**ISO**)- managed markets in the US (like with NEMO- and TSO-managed markets in Europe). Besides the abovementioned, the author in [43] specifies that both energy and ancillary services are procured via the real-time markets, which are usually administered by local TSOs. Whereas the European real-time markets are usually divided into regulating and balancing power markets (as illustrated in Figure 2.4).

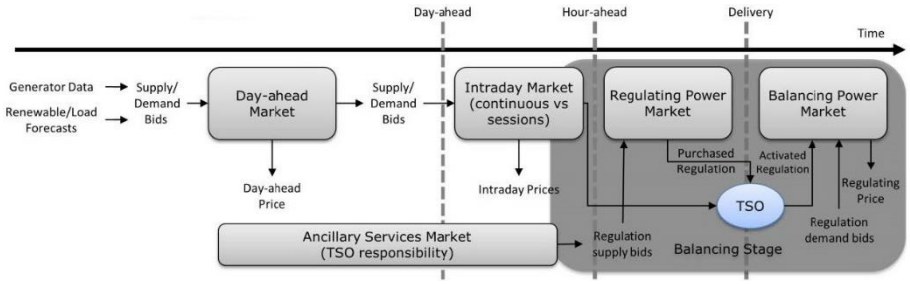

Figure 2.4. Electricity markets design (adapted from [43]).

Contrary, the author in [41] considers the balancing market as the energy-only market, not including reserves or ancillary services, while, at the same time, considering balancing, regulating, or real-time markets as those that could be called interchangeably.

In practice, the resource adequacy assessment together with the task of ensuring the appropriate level of reserve capacity for maintaining stable and secure power system operation in Denmark nowadays are handled by the Energinet. The task of organising different ancillary services, where these reserve capacities to be used both for energy supply regulating purposes (thereby for system balancing) and assuring the reliable power system operation, is also under Energinet's responsibility. This is realised both through the real-time ***market*** divided into two-stage markets, i.e. RPM and BPM (as mentioned in Section 2.1.1 above, stated in [43], [60] and illustrated in Figure 2.4 above) and through bilateral capability supply ***contracts*** and capacity ***auctions*** [17], [59]. Whereas these auctions can be held through the day-ahead and intraday markets as well. The EU

Regulation 2015/1222 in this regards [46] provides a clear legal framework for cooperation between NEMOs and TSOs for their efficient and modern capacity allocation through the day-ahead and intraday markets. Respectively, these markets can be considered a combined energy and capacity markets. Moreover, [85] specifies that the modern intraday solution supports both explicit (i.e. capacity only) and implicit (i.e. capacity and energy together) trading. In Denmark, in particular, the trade takes place as a continuous implicit allocation. Furthermore, all generating units can be allocated for delivering either energy, or ancillary services, or a combination of the above (if the potential is not fully exploited for something one). In the case of activation in the capacity market, the electricity generated during the activation will also be paid using RP or BP prices, the activation, however, is fully competitive. This is considered the main difference between traditional strategic/operating reserves and today's capacity or energy-capacity markets [21], [86].

Ancillary services (operating reserves)

Ancillary services are an integral part of a well-coordinated and well-balanced functioning of the network required to support the transmission and distribution of electricity between selling and purchasing entities. In a power system, the load changes instantaneously. In more contemporary power systems (with a large penetration share of RESs), generation units may also experience quite a high variability of and uncertainty in power output, due to their weather dependant nature. These instantaneous imbalances at any moment of time cause grid frequency and voltage deviation from its nominal value and may lead to power system operation disturbances, and hence, generator shutdown or load shed [45]. To overcome this and guarantee system security, power system operators provide a range of ancillary services. Reference [87] provides an overview and technical specifications for the various services that exist nowadays. These services usually involve the use of the aforementioned generating capacities that are not employed/not fully employed for normal energy supply (from the supply side of the power grid), network devices, and/or controllable loads to provide load reduction, load rise, or, in other words, load shape activities, on the demand side of the grid, respectively. All ancillary services are commonly categorised by those related to *frequency* control, *voltage* control, and system *black-start* (i.e. the ability to restart a grid following a blackout) [80], [43], [88], [87]. The information regarding services offered in North America and Europe is presented in [88]–[90]. In the Danish case, these services, according to [59], can be grouped as:

- Frequency-controlled reserves;
- Properties required to maintain power system stability, including checks of reactive reserves, analysis of load flow, short-circuit

power, and other contingency situations such as failures of generation plants, transformers, lines, etc. (applicable only to central power plants that are connected to the high-voltage grid).

In general, it can be said that almost all services offered in Denmark are associated with maintaining system frequency with automatic and very fast responses (without or with very limited energy supply), as well as with providing additional energy supply to the system when it is required. In more detail, these frequency-controlled services are provided in the following way. Firstly, by concluding agreements between Energinet and potential capacity reserves suppliers on the delivery of ancillary or balancing services. By signing agreements, the latter ones gain access to different capacity auctions, place bids and receive availability payments (in case of acceptance of their bids). The bids must normally indicate the volume which they are offering to make available, in MW (at 5-minute intervals during an hour, an hour-by-hour during a day, or a single value for the full month depending on service) and a price per MW, asked by them to make this volume available during the prespecified operation periods. Energinet selects bids so that the total volume required is met at the lowest possible cost. All suppliers, whose bids are accepted, must in fact be available for activation at any time. Whereas the activation is possible in three different ways:

- either employing supplier's frequency-deviation sensitive control equipment (i.e. fully autonomous);
- or through the signal sent by Energinet (either directly to the supplier or via BRPs);
- or by actively participating in the regulating power market (by bidding for activation at this time).

The latter option is applicable to the manual reserve only, where all accepted suppliers receive payments for both energy (supplied during the activation period) and capacity (while being available for regulation). In this case, Energinet buys the necessary volume of upward or downward regulating power (from these suppliers) in the RPM and sells these volumes afterwards in the BPM to all parties that have experienced energy or trade imbalances. Unlike the latter option, the former two options provide an availability payment only. In case of not activating (i.e. not being able to supply capacity, when requested), these suppliers are financially responsible for the replacement purchase. Table 2.1 summarises the information regarding all frequency-controlled services offered in Denmark as of today, including procurement procedures, the minimum size for participant bids, response time requirements, the way of activation, and other general technical/financial information. While more information on this topic can be found in [59], [60], [91], [92].

Table 2.1. Summary of ancillary services offered in Denmark (adapted from [59]).

Ancillary service		*Procurement: market auction (day/month ahead) or supply capability contract*	*Offered in the Danish pricing areas: DK1 - western, DK2 - eastern Denmark*	*Provided by: G - generation, D - demand units*	*Type of product: U - upward, D - downward regulation, E – energy*	*Response time in western (eastern) Denmark*	*Required volume in western (eastern) Denmark, MW*	*Minimum bid size, MW*	*Volume to be indicated in each bid, MW*	*Way of submitting bids*	*Availability payment is settled corresponding to: H - highest bid price (marginal pricing scheme), P - pay-as-bid*	*To receive an availability payment bidder must: A - bid for activation, B - be available*	*Way of activation: F - supplier's own frequency measure, S - signal to BRP with reference to the bid, RPM - via the regulating power market*	*Combined deliveries (from several generations or demand units)*	*Payment for energy delivery (if activated)*
FCR	*Frequency Containment Reserve*	Day-ahead	DK1	G, D	U, D	15 sec.	20	1.0	six 4-hour blocks	www.regelleistung.net	H	B	F	Yes	*No*
FFR	*Fast Frequency Reserve*	Day-ahead	DK2	G, D	U	0.7 sec.	0-45	0.3	hour-by-hour	Self-service Energinet	H	B	F	Yes	*No*
FCR-D	*Frequency Containment Reserve for **disturbances***	Day/two days ahead	DK2	G, D	U	5 sec.	44	0.3	hour-by-hour	Self-service Energinet	P	B	F	Yes	*No*
FCR-N	*Frequency Containment Reserve for **normal operation***	Day/two days ahead	DK2	G, D	U, D, E	150 sec.	18	0.3	hour-by-hour	Self-service Energinet	P	B	F	Yes	*RP price* [1]
aFRR	*automatic Frequency Restoration Reserve*	Contract	DK1, DK2	G, D	U, D, E	15 (5) min.	90 (12)	1.0	one value/ month	email to Energinet	P	A	S	Yes	*Yes*[2]
aFRR	*automatic Frequency Restoration Reserve*	Month ahead	DK1	G, D	U, D, E	15 min.	100	1.0	one value/ month	email to Energinet	P	B	S	Yes	*Yes*[2]
mFRR	*manual Frequency Restoration Reserve*	Day-ahead	DK1, DK2	G, D	U, E	15 min.	vary	5.0	hour-by-hour	Self-service Energinet	H	A, B	RPM	Yes	*RP price* [1]
mFRR	*manual Frequency Restoration Reserve*	Month ahead	DK2	G, D	U, E	90 or 15 min.	<300 or >300+	5.0	hour-by-hour	email to Energinet	H	A, B	RPM	Yes	*RP price* [1]

[1] *RP price - regulating power price for upward/downward regulation, per MWh*
[2] *The energy supplied from upward regulation reserves is settled with the spot price plus DKK 100/MWh (based at least on the RP price for upward regulation). The energy supplied from downward regulation reserves is settled with the spot price less DKK 100/MWh (not exceeding the RP price for downward regulation).*

Summing up the information given above it can be said that de jure, all services indicated in Table 2.1 could be delivered both from generating capacities or demand units, which are not fully employed during normal operation and are reserved for being available for activation at any time automatically (i.e. by means of a control system and signals) or manually. De facto only generating capacities and transmission system elements are involved. In particular, services are still, to a large extent, coming from centralised power plants and, to a lesser extent, from other energy sources such as biomass/waste/biogas-fired and CHP plants. Moreover, local regulation prohibits RESs (such as WTs or PV panels) from submitting bids on their own. Participation is only allowed along with other types of generation to ensure the power supply in case if RESs fail in delivering due to weather conditions [59].

Grid voltage in Denmark is controlled at 132 kV and 400 kV levels by regulating the reactive power production and consumption. This is done by utilising system reactive power components such as synchronous compensators complemented with flywheels, Voltage Source Converters (**VSC**s) of HVDC links, static var compensators, as well as by automatic adjustment of conventional power plants' reactive power generation/demand in response to grid voltage variation at the point of connection [57], [93]. (The power plant's reactive power injection or absorption varies as a function of voltage and is continuously controlled by an Automatic Voltage Regulator (**AVR**) device by increasing or reducing the generator's excitation. Whereas the voltage setpoint of AVR is a function of a signal dispatched by the Energinet and can also be adjusted in case if the use of the aforementioned system components alone is insufficient to assure the reactive power balance and, respectively, voltage magnitude within the tolerance band margins [59], [94], [88]). Furthermore, due to the increasing number of underground cables that have a much higher capacitance and generates much more reactive power than overhead lines [95], [96] (in Denmark, overhead lines have been actively replaced over the past several decades and are currently being replaced by underground cables), a large number of shunt reactors (i.e. absorbers of reactive power) are expected to be installed in the coming years [94]. The capacitance in power lines is one of the reasons why reactive power transmission for a long distance is tried to be avoided, as it leads to losses and provokes even greater imbalances, which, in turn, can lead to voltage collapse. The voltage stability can also be compromised including due to the rapid variation in power output (e.g. from wind turbines) or changes in load. Usually, those power grid nodes, where the balance of active and reactive power and, consequently, voltage stability are violated, are "treated" locally. This is typically done in several ways:

- by injecting/absorbing the reactive power,

- by changing the position of the tap-changers, or
- by reducing the load [87].

The inability of the power system to locally meet reactive power demand is considered the main reason for voltage instability. Danish distribution grids are heavily permeated with intermittent wind power generations and dispersed generating plants, therefore dynamic voltage stability at this level of the power grid is becoming very important nowadays.

In overall, it can be said that the Danish voltage control system uses a centralised control scheme fully managed by the Energinet [94]. The limit of responsibility of Energinet ends with the low-voltage side of transformer substations 150/60 kV, 132/60 kV, 132/50 kV, and 132/10 kV, including transformers' tap changers [97]. In this regard, it worth mentioning that the role of DSOs in this process is very limited even though multiple scientific studies demonstrate that it is the low-voltage side of the power grid (i.e. 0.4 kV level) that will experience the voltage and hosting capacity issues due to the progressive electrification of the heating and transport sectors [40], [98]–[101]. Therefore, in order to reach very ambitious national targets (indicated in Figure 1.4, Section 1.1.2 above), more localised solutions for maintaining active and reactive power balance and for controlling voltage stability have to be introduced. Special attention, in this connection, is paid to DSF.

Despite the variety of other options on DSOs' responsibility side, such as, for example, the use of wind farms with variable-speed wind turbine generators (which can contribute to both primary frequency control by the pitch control system and inertial response [102]–[104] and voltage control by compensating reactive power with predefined power factor [105]–[107]) and PV farms with power-electronics-based converters [108]–[110], as well as utilising the DSF that could be delivered from large industrial or small aggregated consumers, such as HPs, EWHs, residential PV systems coupled with batteries, and PEVs [29], [111], [112] – all ancillary services offered in Denmark are mainly limited to TSO's responsibility side of the power grid, where Energinet is in charge of maintaining the power grid security and stability employing mainly traditional solutions.

Reference [88] indicates that most European DSOs as of the end of 2019 – beginning of 2020 (excluding those in Spain, Switzerland, the Netherland, and Sweden) do not participate in voltage control. Most European counties, as of April 2020, use the same market mechanisms and activation procedures for load participation as for generation, which are, in fact, not accessible to small consumers. Furthermore, there are no specific market solutions (including ones for aggregators) applicable to load providers of balancing services in most of Europe. Only some

countries have already implemented this, allowing large consumers (the UK, Belgium, France, Poland, Spain, and Portugal) and aggregated small consumers (the UK, Belgium, France, Poland) to participate in the balancing services. As centralised fossil fuel-based power plants are being forced to phase out of service soon (see Section 1.1.2 above), the system may potentially lack the reserve capacities required for both frequency- and voltage-controlled services provisioning. Therefore, the power/energy flexibility of DERs for ancillary services purposes (delivered particularly from the distribution side of the grid) will have a crucial impact on the proper management of a modern power system.

2.2. DEMAND-SIDE ENERGY FLEXIBILITY

This section will address the following questions: What is energy flexibility? Who needs flexibility? Who offers and what are the sources of flexibility? What are DSF's strategies, objectives? What are the mechanisms for enabling DSF? Is any marketplace for DSF exist nowadays? How is DSF handled, by whom? How is DSF activated? What are the control strategies? Why should DSF be estimated or quantified? How is DSF quantified? What are the largest barriers to implementing DSF?

2.2.1. What is energy flexibility?

The term "*flexibility*" is not new in power system studies. Before variable RESs became widely deployed around the world, this term has frequently been used for describing the capability of generation to follow demand [113]. From the electricity system perspective, flexibility is very closely related to grid frequency and voltage control, power upward and downward regulation, and shaping demand. It is commonly associated with overcoming supply and demand balancing issues and considered a solution for coping with grid uncertainty and variability, caused by the large-scale integration of RESs and DERs, and different power system contingencies. Not least important, that it is also seen as one of the most promising solutions that will enable to delay very costly grid reinforcement and expansion, at the same time enabling both consumers and producers to receive financial benefits from their flexible use of energy resources thereby maximising the utilisation of local RES-based energy and hence reducing national dependence on cross-border electricity imports. A variety of interpretations of flexibility definitions can be found in different scientific papers. A good collection of references and review of flexibility definitions was made by [114]. Some of them sound like: ***"The possibility to deviate the electricity consumption from the business as usual***

consumption at a certain point in time and during a certain time span" proposed by De Coninck and Helsen [115] The authors presented a methodology to assess the amount of flexibility and the corresponding cost of the associated DR actions for an energy system saturated with DERs. The same authors in [116] showed that no general metric or indicator for quantifying energy flexibility exists nowadays. They had elaborated a generic method that results in cost curves allowing to aggregate the energy flexibility of various distributed energy resources or buildings. The flexibility there was defined as ***"The ability to deviate from its reference electric load profile"***. Junker et al. [117] defined flexibility as a ***"Dynamic function suitable for control".*** The authors have demonstrated how to characterize flexibility as a dynamic function and furthermore how to compute it based on this function. The presented function describes a response of a single building or group of buildings to a flexibility signal. (that can be technical, price, CO2 signal, etc.). One of the most recent and the most comprehensive clarifications of this topic, including a review of references, definitions, classification and characterisation of different flexibility sources, as well as the applicability of these resources for different purposes, is given by Degefa et al. [118]. The author defined flexibility as ***"The ability of power system operation, power system assets, loads, energy storage assets and generators, to change or modify their routine operation for a limited duration, and responding to external service request signals, without inducing unplanned disruptions".***

2.2.2. Who needs flexibility?

The simple answer will be TSOs, DSOs, and BRPs. The flexibility is required by them in form of capacity reserves (both generating and load units) and network components to ensure stable, secure and well-balanced operation of the power grid during its normal conditions, as well as to withstand system disturbances such as loss of interconnection line, generating units, etc. Considering that most traditional fossil-fuelled plants will soon be displaced with environmentally friendly, but variable ones, the DSF would find a high demand from the aforementioned parties. Basically, this means that in order to accommodate as much as possible variable generation from RESs the load should be flexible so that to be able to easily shape the generation pattern. Domestic power-intensive HPs and EVs ideally should run when RESs produce a lot of power and the price for this power is low. Contrarily, the extensive use should be limited in hours when RES-based production is low, so that not to force activation of remaining traditional reserve capacities, leading to high electricity price [21]. By enabling flexibility on the demand side, DSOs, for instance, may alleviate the potential challenges such as excessive voltage drop/rise, grid equipment overload, planned/unplanned outages, manage constraints

such as insufficient transfer capacity at an efficient cost and thus delay or avoid grid reinforcement needs. Reference [86] defined all DSF services that may potentially be requested by TSOs, DSOs, and BRPs, and categorised these services into four main classes. In particular, *Balancing* (implying frequency regulation), *Wholesale* (i.e. aggregating and providing flexibility to various BRPs), *Adequacy* (improving the security of supply and cost-effectiveness of capacity allocation by using DERs and forming long-term peak or non-peak periods), and *Constraint management* (i.e. supporting voltage control, congestion management, etc.). Besides these, DSF services can also be (should be) potentially interesting for consumers/prosumers who have flexible assets in their portfolio, in terms of generating additional profit from the provision of these services.

2.2.3. Who offers and what are the sources of flexibility?

As well as a variety of definitions, the diversity of sources from which flexibility can be derived exist nowadays. In conventional power systems (that is systems with relatively low penetration levels of RESs and DERs), power and energy flexibility services have traditionally been provided by supply-side assets [119]. In contemporary systems, these services can be offered by different parties. In this connection, the author in [118] differentiates four main places in the power system, that exist at the present time, from which the flexibility can be delivered. Namely,

- the flexibility provided by the supply-side,
- the flexibility provided by the network-side,
- the flexibility provided by the demand-side (DSF), and
- other sources, such as energy storages or well-designed markets.

Wherein, the supply-side, DSF, and storages comprise actual flexibility sources, and the network-side and markets are considered key enablers [118]. All flexibility services in Denmark are currently provided by the supply-, network-side assets and markets only. This has extensively been described in Section 2.1 above. It can just be added that apart from cross-border interconnections, the network-side flexibility may also be considered in form of grid reconfiguration/sectioning (switching, with the help of motorised switches, contactors, etc.), parallel operation of transformers, meshed or other forms of interconnected operation.

When referring to DSF, authors in [120] argued that based on a study made in Denmark, large-scale integration of HPs in combination with buffer tanks or building's thermal mass in the domestic sector outside areas with district heating (**DH**) networks helps to utilize up to 20% of excess energy production from the wind turbines (i.e. wasteful energy that would otherwise be sold very cheap, for free, or at even negative price).

They argue that water tanks, in general, are better suitable for provisioning short-term flexibility services, whereas phase-changing material (**PCM**) and thermochemical material (**TCM**) tanks are better at providing long-term services. Authors in [121], demonstrated flexibility potentials on an example of the specific atomic loads i.e. those, the working cycle of which is non-interruptible, but could be postponed in time (for example, dishwashers, washing machines, cloth dryers, etc.). The demonstrated data-driven flexibility modelling methodology comprises data mining of historically measured data to determine peculiarities such as the likelihood of appliance start-up and average consumption profile per cycle. While in [122] the study is aimed at creating a very detailed model of the building's HVAC system with the main purpose of further integrating this model into the buildings management system and optimizing the energy use. The flexibility strategies there are based on in-house climate settings readjustments. The authors in [115] showed a quantitative comparison of energy flexibility service provision on the example of the application of two different cold emission systems within the office building environment. Table 2.2 summarizes the references to scientific papers that contain examples of utilising different sources for DSF provisioning.

Table 2.2. Examples of sources of DSF.

Source	*Reference*
HPs with buffer tanks	[27], [123], [124], [125], [126], [127], [128], [129], [130], [131]
HPs with building's thermal mass	[131], [132], [133]
Electric boilers	[98], [134]
Appliances	[121]
Building's HVAC system	[115], [131]
Electric vehicles	[26], [135], [136], [137], [138], [139]
Batteries	[28], [140], [141], [142], [143], [144]

2.2.4. What are DSF's strategies, objectives?

As discussed in the preceding chapter, shifting to a demand-controlled system is considered one of the most promising solutions to address forthcoming challenges inherent in using RESs and DERs. Despite the fact that the necessity for this transition and the DSF is a fairly hot topic today, all nowadays called DSF strategies are closely related and, it can be said, take their origin from the well-known demand-side management (DSM). The term DSM itself is not new and originate from the late 70s early 80s [145]. One of the first definitions of the DSM sounds as: "***DSM activities are those which involve actions on the demand (i.e. customer) side of the electric meter, either directly caused or indirectly stimulated by the utility***" [146]. There were a lot of different interpretations of the DSM

concept since that time. A literature review (involving 389 documents) made by [147] indicates that definitions of DSM have varied over time in what they include or exclude. According to this, some authors associate DSM only with the peak load shaving, others only with the demand response, some refers to DSM synonymously as Smart Grid, which is not fully correct. The author in [147] went further and collated the definitions published since the 1980s with energy policy objectives of different countries, including regulatory, market-based, voluntarily, and others (such as energy security, electricity price reduction, increasing share for RESs, and CO_2 emissions reductions) that had existed as of 2015, hence establishing more concrete definitional boundaries. Based on his definition ***"DSM refers to technologies, actions and programmes on the demand-side of energy meters, as implemented by governments, utilities, third parties or consumers, to manage or decrease energy consumption through energy efficiency, energy conservation, demand response or on-site generation and storage, in order to reduce total energy system expenditures or to contribute to the achievement of policy objectives, such as emissions reduction, balancing supply and demand or reducing consumer energy bills"***. The definition acknowledges that DSM refers to a broad category of end-use consumer solutions and covers a wide range of technologies and processes, including on-site generation and storage. Describing the DSM in other words, it can be said that the DSM constitutes a broad set of means involving proactive analysis of the situation in the system, planning, implementing different actions, and management that usually involves human intervention (may include estimates, forecasts, filtering, monitoring, etc.). Assumes that something will be needed an hour/day/week/month/season ahead or another basis.

A decade ago, the world reputable organisation CIGRE, based on observations from interactions with diverse organisations internationally, defined new terminology for six DSM load shaping objectives with respect to restructured, i.e. competitive electricity market-based environment. Furthermore, objectives are grouped into three major categories, namely *Strategic load growth*, *Energy efficiency*, and *Demand response* [148], [149]. Figure 2.5 illustrates an overview and a brief description of each objective. The DSF, in this connection, is straightforwardly associated with the later four objectives, grouped as demand response. Whereas, these objectives can be applied for both energy management and ancillary services provisioning purposes, depending on flexibility resources, responsiveness time (fast/slow response), ramping-up and -down duration (similar to power generation), and how long the activation period can last. The overall benefits of the DSM or Demand-Side Integration (**DSI**), as it is also commonly called in a new restructured power system, can be found in [150], [151].

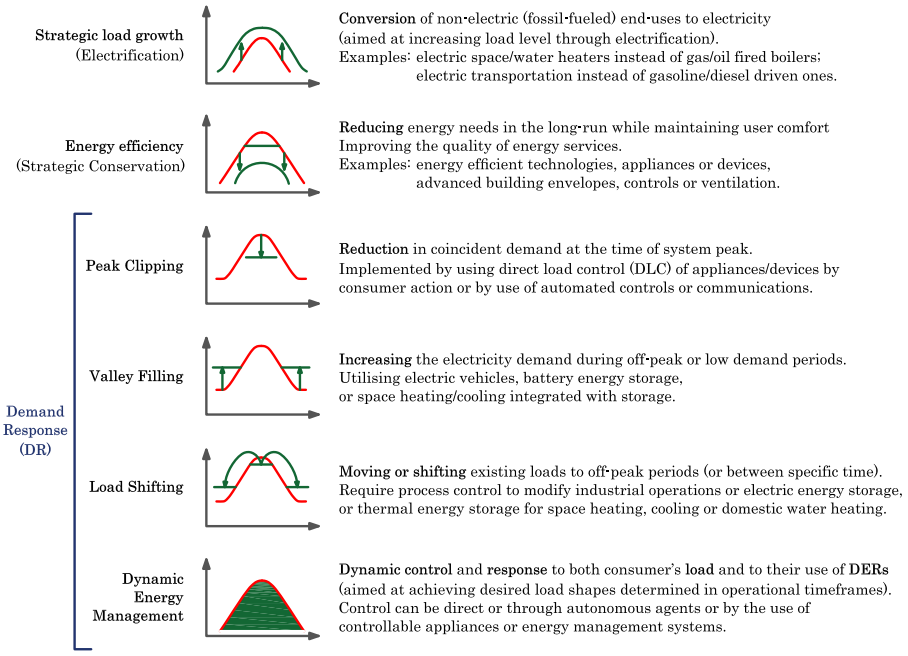

Figure 2.5. A summary of DSM objectives for deregulated electricity markets (adapted from [145], [148], [149])

2.2.5. What are the mechanisms for enabling DSF?

As seen from Figure 2.5 above, Demand Response is a subset of DSM and should be considered as a characterisation of certain DSM objectives, while at the same time as a solution, including programs and activities, for implementing/enabling DSF [145]. DR may work with or without human intervention and is linked to a situation that is happening at a specific moment of time. As mentioned in the previous section the term DSM is not new. A wide range of DR programs and activities have been developed and periodically modified since their origin. All this is thoroughly described in science and ordered by utilities in many countries. Nowadays DR programs can broadly be classified as incentive-based and price-based according to the way of how consumers are motivated to participate in these programs and hence how load changes are induced. Some programs focus on system reliability, while others, as illustrated in Figure 2.6, are strictly economic [79], [152].

		Motivation Method	
		Load Response	Price Response
Trigger Criteria	Reliability	Direct Load Control Curtailable Load Interruptible Load	Critical Peak Pricing Demand Bidding
	Economic	Direct Load Control Curtailable Load	Time-of-Use Pricing Critical-Peak Pricing Real-Time Pricing Demand Bidding

Figure 2.6. Classification criteria for DR programs [152]

To reduce electric energy price for consumers, [153]–[155] propose variable *price-based* activities, where users are encouraged to individually manage their loads, for instance by reducing (or contrarily rising) the energy consumption of certain appliances/devices such as pool pump, HP, HVAC equipment, or PEV, in response to electricity price fluctuation. In this regard, critical-peak pricing (**CPP**), that includes a pre-specified extra-high rate for a limited number of hours [153]; time-of-use (**TOU**) pricing, where price rates are fixed for a specific time of day [154]; and real-time pricing (**RTP**), where rates are varied continually in connection with wholesale energy market [155], are the most popular options.

Alternatives to price-based are *incentive-based* DR activities, such as Direct Load Control (**DLC**), interruptible/curtailable load, emergency DR, demand bidding, capacity and ancillary service market programs. These activities are based on cooperation agreements between end-use customers and program providers, or market-based. In this case, consumers (prosumers) receive financial rewards for adjusting their load (generation) profiles following system needs. This adjustment can be done either at customers personal choice (i.e. manually), or employing their automation system (customized according to specific preferences), or by allowing the program provider or aggregator to remotely control operation and energy consumption of different power-intensive load appliances without the client's participation in this process.

According to [86], [156]–[158] these price- and incentive-based activities are interchangeably referred to as *Implicit* and *Explicit* DSF. All DR programs are thoroughly described in [79], [149], [152]. Table 2.3 contains a summary made based on these papers. Whereas the applicability of different programs in different timescales of electricity system management is shown in Figure 2.7.

Table 2.3. A summary of DR programs based on [79], [149], [152]

Program	Brief description		Customer Size	Advance notification	Reflect	Enabling	Incentives example	Penalties
Price-based programs (Implicit DSF)								
Time-of-use (TOU)	Load shifting (via rates)	Price vary by time of day (peak/off-peak periods) and by season	Large industrial and commercial	Pre-determined for a period of several months or years	Cost of generating and delivering power	Interval meter	Bill reduction	-
Real-time pricing (RTP)		Price fluctuates hourly	All	Prices known on a day-ahead or hour-ahead basis	Wholesale electricity price	Interval meter, web data (Internet)	Locational marginal price	-
Critical Peak Pricing (CPP)		Hybrid of the TOU and RTP (basic structure - TOU, peak price replaced with a much higher CPP event price)	All	Short notice for a limited number of days and/or hours per year	System reliability contingencies or very high supply price	Interval meter, web data (Internet)	Price discount during non-CPP periods	-
Incentive-based programs (Explicit DSF)								
Direct Load Control (DLC)	Load reduction (classical)	Shutting down or cycling a customer's electrical equipment remotely by the program operator	Residential and small commercial, <100 kW	Short notice (minutes to hours) / None	System or local reliability contingencies	Load switches	Bill credit	May or may not levy
Curtailable Load		Curtailment or reduction of customer's load	Medium industrial and commercial, >100 kW	Minutes to hours, up to a day ahead	System contingencies	Manually or automated control	Rate discount or bill credit	Yes
Interruptible Load		Switch off major portions or all of a facility's load for specified periods of time	Largest industrial or commercial, >500 kW	Minutes to hours, up to a day ahead	System contingencies	Power is not supplied from the grid	Bill reduction or bill credit	Yes
Emergency Demand Response	Load reduction (market based)	Load curtailments are offered as supplemental resources that help restore system reserves (when all capacity reserves are deployed)	>100 kW, aggregation is allowed	Hours or day ahead	Reserve shortfalls or reliability-triggered events	Automated control	Rate discount or bill credit	May or may not levy
Demand Bidding		Customers bid load reduction into a wholesale electricity market	All (who passed the market entry barrier)	Hours or day ahead	Customer's proposed price or amount of load that can be curtailed based on provider's price	Web data (Internet), market trading mechanisms	Locational marginal price	Yes
Capacity Market		Load curtailment is offered to replace conventional generation or delivery resources	Large industrial and commercial	Day-of notice	System contingencies (generation shortage)	Web data (Internet), market mechanisms	Up-front reservation payments (market prices)	Yes
Ancillary Services Market		Customers bid load curtailment as operating reserves	Large industrial and commercial	Committed to being on standby	System reliability contingencies	Web data (Internet), market mechanisms	Locational marginal price	Yes

In the power system, all energy consumers can broadly be categorized into industrial, commercial, and residential. As seen from Table 2.3 above, half of all programs are designed to be used for medium-large industrial or commercial customers. Large industrial consumers have a great advantage, comparing to the other two segments, of shifting large volumes of loads. However, most of their technological processes require advanced planning and customisation of special equipment. An unexpected short-term or unplanned power outage can cause serious production disruptions.

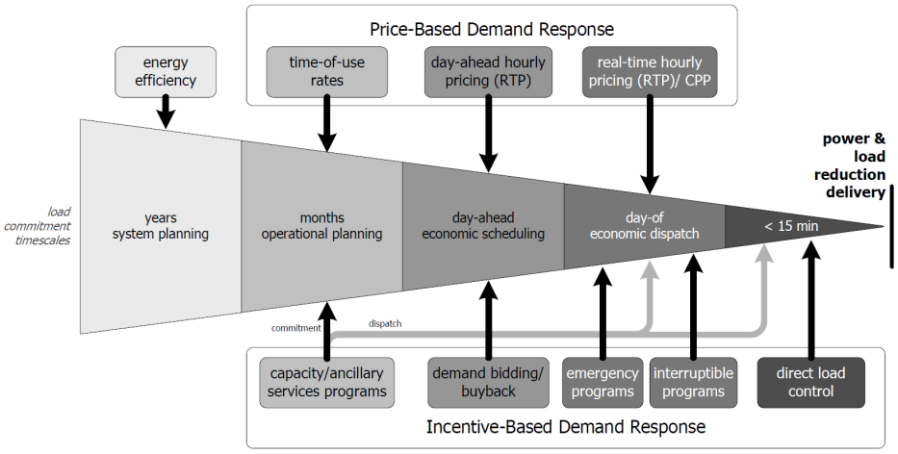

Figure 2.7. Applicability of DR with respect to Electric System Planning and Operation [79]

That is why programs that allow advance planning like, for example, TOU or energy flexibility trading via day-ahead market are more relevant for such consumers. Participation in programs such as curtailable or interruptible loads usually involves the use of a backup power source, such as a diesel generator, or massive storage batteries, the cost-efficient use of which is questionable. Unlike industrial, small consumers such as households are more flexible in this regard. The availability of equipment that does not require complex settings readjustments and reprogramming (such as refrigerator, pool pump, HP controlled by a simple controller and sensors), as well as the similarity of equipment in each household, makes the residential sector more attractive to participate in almost every program. Entry barriers reduction for participating in one or another program, aggregation, coordinated control, and management are the key factors for enabling this.

2.2.6. Is any marketplace for DSF exist nowadays?

As noted in the previous section, nowadays, de jure, it is possible to trade energy flexibility in any of the existing markets. All energy markets offer both implicit and explicit auctions (both energy and capacity allocation), however, from the description of day-ahead and intraday markets (Section 2.1.1 above), it can be seen that only upward regulation (from the supply side) and load reduction (from the demand side) can be procured in these markets. From the perspective of implementing DSM, this generally means that, as of now, only peak shaving strategies can, to some extent, be realized in these markets. The load rise, and hence valley feeling, load

shifting, and dynamic load shape (discussed in Section 2.2.4 above) are not applicable. Furthermore, even though Energinet de jure has a national marketplace for activating energy flexibility (real-time market), nowadays it is not possible to add geographical information (so-called "geotag") to the bids for determining where the facilities and players are located. Therefore, solving very localised distribution grid bottleneck issues via this market is nowadays simply not possible [82]. This clarifies one more time that the demand side of the grid is de facto not utilized and that the market was designed primarily to accommodate flexible production units, not flexible demand units. Therefore, the mechanisms for delivering flexibility from small consumers, such as households, the business models of interaction between various players, as well as issue of how to transfer all the benefits of the wholesale competition to the end consumer (i.e. the potential provider of DSF) are not yet solved/established [21], [82], [92]. There should be separate parties, responsible for handling these tasks.

2.2.7. How is DSF handled, by whom?

Since in deregulated power system structure, DSOs and TSOs cannot incentivise their consumers/prosumers directly, authors in [159], [86] proposed several market design models aimed at maximizing the valorisation of prosumer's flexibility via implicit and explicit DSF mechanisms. The first model (related to implicit DSF) proposes serving prosumers with the help of an independent *Energy Service Company* (**ESCo**) that provides a broad range of energy-related services, such as, for instance, the remote operation and maintenance of equipment, information services related to energy savings, energy optimisation based on specific tariffs, risk management, etc. Whereas the second model (related to explicit DSF) emphasizes the role of *Aggregators* as a key middle chain between prosumers and different market players, such as DSOs, TSOs, and BRPs, who request flexibility on the market. The third model is considered a combination of these two. To employ the DSF in the Danish market, [156] proposed four different models for aggregators. In the first model, referred to as *Model 0* (current option), the existing ES/BRP and aggregator are the same entity. In *Model 1*, the aggregator is acting as a separate market player that focuses only on services, related to frequency control. *Model 2* designates an aggregator for delivering flexibility to all electricity markets, without being responsible for the power supply. Whereas in the last *Model 3* the aggregator's activities are covering both flexibility and electricity supply services. On the European scale, the framework for DSF service provision via aggregators are addressed in Articles 13, 17 in [62].

2.2.8. How is DSF activated? What are the control strategies?

Similar to activating various traditional ancillary services (described in Section 2.1.2 above), DSF activation is possible in different ways, however, various authors interpret these strategies differently.

Author in [160], for example, characterise control strategies according to their impact on the distribution system, highlighting different application perspectives (such as Local network support, System-level balancing, Market support), goals (such as Economic, Economic/Technical, Technical), control perspectives (such as Consumer/Prosumer, Aggregator/System operator, Grid operator), and type of resource to be controlled (such as Electric vehicle, Heat pump, or local solar PV array). Authors in [161], [162] divide all DSF control strategies in general into ***direct*** and ***indirect*** control. Indirect control, in turn, is classified by the latter reference into four different classes, namely: *control with indirect functional variables* (or pure aggregation based indirect control), *indirect control via price signals, independent local control* (also commonly referred to as autonomous), and *control with the internal market platform* (also known as a transaction or bid-based control). Authors in [163], in turn, classified control with respect to the location of the decision-maker (i.e. a ***local*** or ***centralised*** controller is employed) and communication type (i.e. communicating in one-way, two-way or no communication at all), thereby separating autonomous and transaction control from the indirect control class.

In their interpretation, *Direct control* is the one that realised employing an external centralised decision-making controller that has sufficient knowledge about localised DERs and their statuses for remote control through one- or two-way communication. This control can be executed either by ESCo or aggregator (see Section 2.2.7 above) wherein each DERs, in turn, must be equipped with a local low-level hardware controller. In the case of using one-way communication, the local controller must obey the signal/command sent by the centralised decision-maker. A bi-directional link, unlike the former one, implies no compulsory reaction. The aggregator only notifies the flexible resource owner about the need for flexibility, but the decision is made exclusively locally wherein sending a feedback signal [164]–[166]. *Control with indirect functional variables* is a control in which the DER operation, and hence the power demand, can be influenced by a signal containing a functional variable, such as, for example, the thermostat temperature set-point for a local heating system. The signal is sent by an external controller using one-way communication, meaning that no feedback is expected. In this case, the controller should not necessarily have to have in-deep knowledge of the local DER system

as well as their status. The response to such signals is also not compulsory [167]. *Indirect control via price signals* is a scheme in which the local controller makes decisions solely relying on external electricity price signals sent by the program provider (i.e., aggregator or ESCo), reflecting instant or planned price variation. If the program provider has information about the state of the grid, prices can then be formed to addressing, for example, grid balancing or congestion issues [162], [168]. *Autonomous* control is one where the collection of information from local sensors (such as measuring frequency and voltage), recognition and processing of this information, as well as decision-making for further system behaviour (including the improvement of the system performance), are taken exclusively locally and autonomously, i.e., without any external intervention. Accordingly, control does not require higher-level supervision, as well as communication infrastructure [169]–[173]. *Transactional control* (or control with the internal market platform) implies active participation in various wholesale electricity markets by bidding to activate load reduction, load rise, or a load shift. Whereas the decision on bidding amount, as well as further control (in case of acceptance), is completely carried out locally and autonomously [174], [175].

2.2.9. Why should DSF be estimated or quantified?

First of all, worth noting that, unlike electricity production or consumption, energy flexibility cannot be measured using an ordinary energy meter. In order for DSF to obtain real market value (similar to the generated and consumed energy traded in the market), this potential change of electricity demand (which can be either shaped or shifted in time, as shown in Figure 2.5 above) have to be estimated or quantified. The accuracy of these estimates or quantified values should subsequently be validated and the delivered flexibility should finally be settled in accordance with the service provided [176].

Estimation in this context applies to those cases where some market players, such as GCs or TSO, may not have access to the flexibility potential of individual consumers, but this potential is highly important for their proactive power system operation planning (e.g. to foreseeing and managing potential grid congestions or as part of the resource adequacy assessment and possible substitute of reserve capacity). Referring to different interaction and data exchange schemes between various market players (see Sections 2.1, 2.2.7 above, also [64], [156], [177], [178] for more details), far not all market participants nowadays may have access to the flexibility potential of each end-use customers since some of these players (like, for instance, the aforementioned GCs or TSO) could be the buyers of

this commodity, whereas others (like aggregators) the sellers. This is where aggregated profiles can be applied. Nevertheless, referring to [13], the more disaggregated values (i.e. the flexibility potential of each consumer/device), the better accuracy of estimates.

More accurate *quantification* of flexibility is equally important both for proactive power system operation planning and for billing/settlement purposes. Proactive planning in this regard implies that all BRPs, aggregators have to submit their preliminary schedules, whereby indicating the exact amount of flexible power demand in kW that could be shaped or shifted and for how long it would be possible, i.e. time and energy in kWh. These schedules can be used, for example, for ordering the regulating power (see [17], [60], [86], Section 1.2.2 and 2.1 above).

2.2.10. How is DSF quantified?

A literature review shows that a unique common method or technique for quantifying energy flexibility applicable to all resources so far simply does not exist. The author in [117] argues that the flexibility potential can be obtained either deductively (using various building simulation tools) or inductively (applying different data-driven techniques and statistical time-series analyses, wherein historically measured data serves as an input). Since the flexibility potential of one or another resource largely depends on the state of this resource at a certain time, obtaining such information requires dynamic modelling [179]. Deriving information on the flexibility available in the household during a given time of the day (e.g., the possible deviation of energy consumption of space heating and hot water appliances) requires detailed modelling of energy systems integrated into the household, which in turn requires consideration of different technical and climatic characteristics, operating modes and various limitations, state and boundary conditions of different equipment, as well as residents' preferences, habits, behaviour [117]. This is far not the easiest task. In this connection, authors in [180]–[186] interpret that all models, in general, are classified as *white-box*, *black-box*, and *grey-box* models. *White-box* models are those, where in-depth prior physical knowledge of the investigated system, deterministic equations and detailed modelling are laid down in the conceptual base. These models are well suitable e.g., for building energy modelling, energy-efficient designing and deriving the flexibility potential of new buildings, where historical data are not yet available. Well-designed models are in general very precise, but can rapidly increase in size and complexity (especially when integrating various interconnected systems and their controls into a single model), so they are often resource-intensive and require powerful computers, otherwise, computation/simulation time may be excessive.

Black-box models are those, where the concept solely relies on historically recorded time-series data and statistical methods. These models do not require prior knowledge about modelled systems, run very fast and are well fit, e.g., for predicting the energy consumption of existing functional buildings based on previous energy use patterns. *Grey-box* models combine physical knowledge and the information obtained from data, thus bridging the gap between the first two. Models can ideally be used for those buildings that need to be modernised, as well as those studies, where detailed analysis of the system behaviour (in response to, e.g., DR signal) is matters. These models have also an advantage over the first two by allowing the use of a model for forecasting, simulation, and control, which is vital in flexibility studies.

2.2.11. What are the largest barriers to implementing DSF?

Despite a clearly defined market framework to enabling DSF, a number of obstacles yet have to be overcome in the coming years. One of the key barriers to enabling implicit flexibility is the tariff design. A relatively small variable share of tariff reflecting the actual electricity cost compared to the fixed share (consisting of taxes and other levies) seems unattractive to encourage customers to participate. Among the most common barriers to enabling explicit flexibility the following can be highlighted:

- Inappropriate market design for small consumers like household;
- Restrictions on ancillary services provision by RESs and DERs;
- Market entry barriers (i.e. minimum bid/offer sizes for both energy and ancillary services provisioning purposes are not affordable for small/small aggregated consumers);
- Lack of market-ready solutions allowing explicit DR to be enabled;
- Difficulty predicting the flexibility potential (i.e. the exact amount of power demand that could be shifted and for how long) with the level of accuracy sufficient to correctly allocate DR signals;
- Flexibility quantification, validation and settlement issues (i.e. lack of solutions for quantifying the exact amount of energy shaped (i.e. curtailed or raised) during a specific period of time or shifted in time, as well as too high imbalance settlement period, which is currently set to 60 minutes in all Nordic markets);
- Most of the programs prescribe mandatory load reductions and levy penalties in case of not responding, which is not applicable to control schemes where user preferences are in the first priority;
- Prices in the wholesale markets do not reflect the dynamics of load changes in the LV grid. Accordingly, the flexibility schemes based

on wholesale market prices cannot be applied for LV levels and hence, cannot be applied to small consumers such as a household.

All these barriers and more are thoroughly described in [92], [176], [187], [188].

2.3. BUILDING

2.3.1. What is Smart Active Building?

Considering that many different interpretations of the definition of "Smart building" and "Active building" can nowadays be found in the global network, it should be clearly defined what is meant by these terms in this thesis. One of the most commonly used definitions of the Active House concept is given by an international Active House Alliance, which mainly identified Active House as a proceeder (i.e. next development step towards the user-centric focus) of Passive House concept buildings [189]. However, this definition is mainly related to a building's topology and has no relation to the electricity grid, electricity market, and hence to this dissertation.

Since huge hopes toward achieving the flexibility (required for adapting the electricity system to variable RESs and DERs) are placed on energy consumers, these energy consumers must take an *active* part in the electricity market. Consequently, in relation to the power system and the electricity market, these consumers are called "Active customers". A holistic definition of these market players is given in point (8) of Article 2 of DIRECTIVE (EU) 2019/944 [62], and sounds as: *"'active customer' means a final customer, or a group of jointly acting final customers, who consumes or stores electricity generated within its premises located within confined boundaries or, where permitted by a Member State, within other premises, or who sells self-generated electricity or participates in flexibility or energy efficiency schemes, provided that those activities do not constitute its primary commercial or professional activity".*

In this connection, buildings consisting of active flexible loads, and/or on-site generating units, energy storage facilities, which actively interact with the power grid by delivering various flexibility services in the way of shaping and shifting their demand/generation profiles, thereby actively participating in the power system operation process are defined in this thesis as "*Active buildings*". The term "*Smart building*" here assumes the presence of an intelligent control system for enabling this interaction via different DR and market mechanisms. Consequently, "*Smart Active building*" is considered a combination of these two. Starting from this point and further in the text, the terms building, house, and household are used

interchangeably. Unless otherwise explicitly stated, both building, house, and household denote a single-family detached or semi-detached dwelling.

2.3.2. The importance of detailed modelling of building's dynamic systems

Nowadays, detailed low-resolution modelling of a building's energy systems is, first of all, required to quantify more accurately the flexibility potential that can be provided by a building's assets and to properly allocate various DR signals that serve as a tool for enabling DSF. In this regard, it is very important to clearly understand that predicting consumption and quantifying flexibility are two closely related, but not the same things, and that predicting consumption far not always the key action that leads to accurate DFS quantification/utilisation.

Predicting consumption can be most relevant for enabling implicit flexibility, e.g., via real-time pricing DR program, where optimal scheduling or predictive control of energy storage devices and various flexible/schedulable loads considering known day-ahead electricity price is the core feature that allows the program to be used effectively. This is where the use of black-box models (see Section 2.2.10) is the most appropriate solution. On the household scale, the load forecasting can be utilised e.g., for filling up the local storage with energy in times when there is a surplus of own rooftop PV production or the grid power is cheap, and thereafter utilise this energy when the PV production shortage occurs, or the price is high.

However, for enabling explicit flexibility, load forecasting based on aggregated profiles is not sufficient. In contrast to load that can be predicted based on such profiles, the explicit energy flexibility and *impact* of this flexibility *on household's integrated energy systems and power grid* can only be investigated either by performing practical experimentation or via detailed modelling of these dynamic systems in combination with load flow studies [117]. Physical experiments are expensive and time-consuming. In dynamic systems, the output signals' value depends on both the input signals' value and the past behaviour and state of these integrated systems. A great example of this is the calculation of the State of Energy (**SOE**) of an electric battery and HWST. In case when flexible loads such as EVs or HPs coupled with HWSTs take place, and when these loads are requested to be curtailed or risen up to address various power system contingency situations via technical DR signals, then detailed modelling is absolutely essential. The flexibility potential of these sources is greatly dependant on the amount of energy (i.e., SOE) available in their storages at a particular time. The SOE, in turn, is directly and indirectly

influenced by various factors. Considering the HWST, for example, these factors are the thermal demand (which, in turn, depends on the residents' in-house climate preferences, habits, behaviour, outdoor air temperature), thermal insulation and losses, heat pump system operating modes and various limitations.

If the flexibility potential of these sources is obtained (similar to load forecasting) based on aggregated profiles, i.e. without considering systems dynamics, the DR request signals will most likely be allocated incorrectly and hence the responses and effectiveness of this DR application are questionable.

Antithetically, detailed modelling of dynamic systems (implying white- or grey-box models) allows simulating the application of DR signals and makes it possible to investigate the feedback reaction to these signals [92]. Namely, the behaviour of multi-energy systems integrated into the building, whether the residents' comfort preferences are not violated, accurate duration of each response, load changes, as well as the impact of these responses on a power grid (e.g., reflection in grid voltage magnitude by performing load flow studies). These responses (or activation periods, as they are referred to in the context of the electricity market), in the case of the household equipped with HP and HWST for instance, can last, in some situations, less than 15 minutes, or may not be provided at all. Detailed low time resolution modelling allows seeing all causes and consequences of such responses.

Since flexible loads of the household such as HP with HWST, electric batteries of the PV system or EV can provide only short-term flexibility (due to their limited energy storage capacity), also considering that most existing DR programs may levy penalties for not responding (see Table 2.3 above) – the proper analysis of the system behaviour and accordingly the accuracy of calculation of the flexibility potential are highly essential. In the same context, since the 60-minute imbalance settlement interval is still commonly used nowadays [84], [92], the detailed modelling is also necessary to clarify the need to switch to settlements with a lower time resolution and graphically show changes in demand that occur behind an hourly interval (i.e. those changes, which are counted as a mean value over an hour today). The more detailed the system behaviour simulated/mimicked, the more accurately the signals are allocated, and hence, the higher the overall efficiency of such a flexibility service.

2.4. CHAPTER SUMMARY

In this chapter, an overview of the most actual matters for implementing flexibility services from the demand side (in particular, buildings' side) has been made. To see the current situation in the provision of these services, a detailed overview of today's market mechanisms and ancillary services has been made first. An overview showed that even though Denmark is a pioneer in the reconversion of its energy system and among the best in the world at integrating variable wind power into the electricity system, ancillary services are mainly limited to the TSO's responsibility side of the power grid. The DSOs side and buildings that have large flexibility potential do not practically yet have the ability to provide these services today. This chapter also highlighted in detail what these services are and emphasized the importance of DSF in the transformation path. Contemporary practices, including existing control strategies and interaction models, have been revealed. The necessity and complexity of quantifying the flexibility that can be provided by building assets are highlighted, and the fact that today there is no single unique methodology for quantifying flexibility is underscored. The difference between load forecasting and flexibility quantification has been explicitly clarified, as well as the importance of detailed modelling for determining the latter has also been emphasized.

3 MODELLING OF ACTIVE RESIDENTIAL BUILDING FOR ITS ENERGY MANAGEMENT

This chapter introduces the process of creating mathematical models for various active flexible components of a modern residential building. The process of creating such models combines physical knowledge of the simulated systems, mathematical equations and the information received from data. Some models are simplified, while others are created applying a more detailed modelling approach. This is all to investigate and highlight various aspects of the overall interactive analysis, to understand and evaluate the behaviour and performance of different modelled systems simultaneously, when combining them under a single coordinating solution. Since space heating demand accounts for the major share of the energy consumed by a household, special attention is paid to the heat pump system model as one of the largest potential sources of energy flexibility. All models will, later on, be theoretically verified (in Chapter 4) by comparing simulation results from different scenarios and analysing correlations, while the overall validation relies on science and technical data where all these models have already been validated and empirically examined.

3.1. MODEL OVERVIEW

The process of creating an energy model of a building, in general, is possible by applying the white-, black-, or grey-box modelling approach (this has already been disclosed in Section 2.2.10). Having sufficiently high quality historically recorded time-series data (i.e. households' electric baseload, thermal load and weather data representatives provided by Aalborg University during the project), as well as the technical characteristics of various investigated equipment – a grey-box modelling approach was chosen to execute this task. The building model in this case includes the following components. Rooftop PV array and small WT, which represent small-scale distributed generations (**DGs**); electric battery and HWST representing distributed storages (**DSs**); active flexible loads represented by HP and IHWH (instantaneous heater); and the baseload,

which is time-series data. An overview of integrated energy systems being modelled in this study is shown in Figure 3.1, while the process of creating such a building model and an overview of components is illustrated in Figure 3.2 and described below.

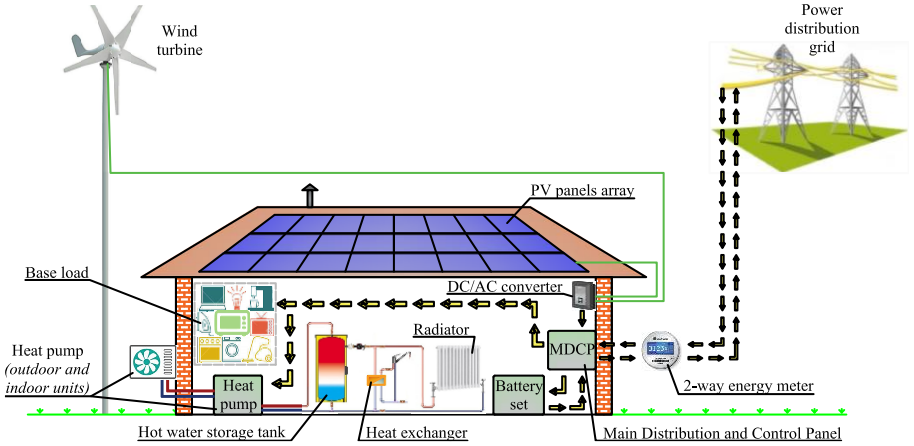

Figure 3.1. Household's integrated energy systems overview [190].

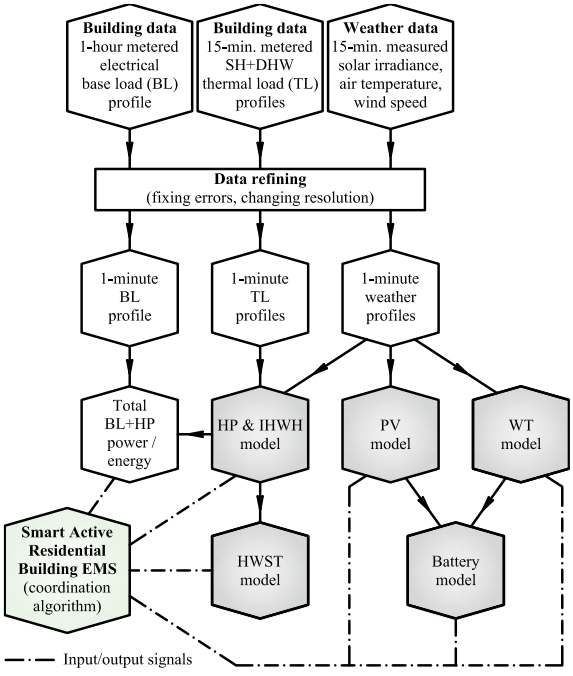

Figure 3.2. An overview of model components and workflow.

At the first stage, all the data obtained were analysed for errors, the coincidence of the resolution, etc. After data refinement, separate energy models were created for each of the above-mentioned components. For the creation of models of PV array, WT and battery it was decided to apply a simplified approach, whereas the HP and HWST models have been developed to mimic the system performance/behaviour as closely as possible to a real system, reflecting different delays and operating modes. Thereafter, all created models were combined under a single coordination algorithm referred to as Smart Active Residential Building Energy Management System (SARBEMS) in this thesis. The heat pump model receives special attention mainly due to the fact that most of the energy consumption in the residential sector is attributed to space and water heating (see Figure 1.9 **b**). The heat pump, in this regard, is considered the potential heat source that is likely to be used to replace the currently used fossil fuel-based sources. Furthermore, the heat pump system (incl. HWST) is seen as the primary source of energy flexibility in the context of this study. Since the provision of flexibility largely depends on the specifics of the HP operation and SOE of the WHST, estimating this flexibility requires a more detailed approach.

The general idea of creating such a combined model is to analyse how the replacement of heat source such as district heating (**DH**) or oil burners by HP and also the application of various scenarios of DG and DS capacity influence the amount of energy imported/exported to/from the grid, as well as the energy flexibility potential of a single house. This is made with the perspective of further spreading this model to a group of such kinds of buildings to investigating their impact on the grid and DR application (which will be done in the next chapters). All models have been developed and simulated in a Matlab environment. The process is as follows.

3.2. TIME-SERIES DATA

This thesis provides only a very brief overview of building load profiles and weather data representatives obtained, since the comprehensive analysis of very similar types of building (including both electrical and thermal load profiles) as well as weather data and part of the distribution grid, has already been done for the same location in [191].

3.2.1. Building load profiles

Electrical baseload (BL)

Time-series data is considered one of the main prerequisites for developing any grey-box model. In this dissertation, the baseload data consist of hourly measurements of power demand (energy consumption) derived

from smart meters of 129 buildings located in the Northern Jutland region of Denmark. Data are obtained for a period of time of one calendar year. The vast majority of these buildings are detached or semi-detached houses without an electrified heat source, meaning that heat is supplied to buildings either by DH networks or another source (like gas/oil/wood pellet fired boiler). Therefore, it can be said that data generally represent various appliances, lighting, cooking equipment and so on. The available database also contains a number of agricultural and small commercial premises, as well as several households with an electrified heat source, common annual consumption of which does not exceed 35% of total consumption. All buildings are fed by the same transformer substation with a total capacity of 315 kVA. These cumulative data of all 129 buildings will, later on, be used for comparing peak hour periods on a local and national scale (in Chapter 5) and serve for simulating the technical load-based DR signal required for quantifying energy flexibility potential. Part of this data, in particular, 25 buildings, which belong to the same feeder line, will be used for performing load flow analysis and developing a voltage-based DR control strategy. At this stage, all data were analysed for errors and similarity, consequently, an average house without electrified heating was selected. The annual, monthly, weekly and daily consumption profiles of this house are showh in Figure 3.3 and the main baseload characteristics in relation to the heating season are summarized in Table 3.1. The heating season in Denmark is considered a period from early October to late April.

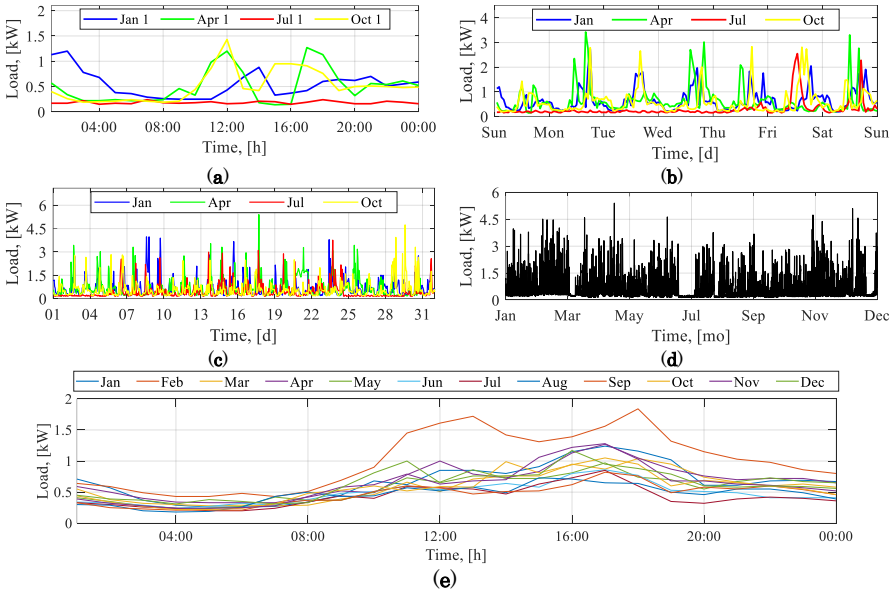

Figure 3.3. Electrical baseload profile of the household: (**a**) Daily; (**b**) Weekly; (**c**) Monthly; (**d**) Yearly; (**e**) Average hourly demand at a specific month.

Table 3.1. A summary of the household electrical baseload profile [190].

Season	*Total cons., kWh*	*Average monthly cons., kWh*	*Average daily cons., kWh*	*Average power demand, kW*	*Maximal power demand, kW*
Heating *(Oct.-Apr.)*	3417	488	16.2	0.67	5.4
Non-heating *(May-Sep.)*	1762	352	11.5	0.48	4.6
Whole year	5179	432	14.3	0.59	5.4

As can be seen from the table and graphs, the maximal and average loads during the heating and non-heating seasons are slightly varying, however, this difference is very minor, which once again confirms the fact that the baseload has no direct relation to the heating. The discrepancy in total annual consumption can be easily explained by the fact that the heating season in Denmark is slightly prolonged compared to central Europe and lasts a full seven months compared to the remaining five months of the non-heating season.

Thermal load

The thermal load database includes historically measured data about space heating (**SH**) and domestic hot water (**DHW**) demand of 25 households located in the same area (i.e. Northern Jutland, Denmark). The thermal load is presented in kW (thermal) with a 15 minutes metering resolution over a time span of one year. All data readings have been provided to Aalborg University by the local DH company. Following the same principle as with electrical baseload, data were carefully analysed for errors and similarity and an average household has consequently been selected for further exploration. At this stage, the investigation implies the substitution of heat supply source (i.e. DH) with individual, domestic HP coupled with HWST and supplemented with instantaneous heater. Once the model of a single building is established, the data from the remaining 24 buildings will be used to create a group of similar households and study their impact on the local LV grid and the DR application. The summary of the main thermal load characteristics of the investigated house is given in Table 3.2, while the daily, weekly, monthly, and yearly demand curves are depicted in Figure 3.4.

The table shows that the main share of annual consumption, as well as the maximum peak load, is taken by space heating during the heating season. DHW demand accounts for a significantly smaller share of the total thermal load. This ratio is also clearly traced graphically, especially when comparing Figure 3.4 a1 and b1, as well as a5 and b5. The same graphs show that DHW consumption is relatively stable throughout the year, wherein SH is strictly seasonal. Figure 3.4 b5 also clearly illustrates that the heating season lasts from mid-September / early October to late April.

Table 3.2. A summary of the household thermal load profile [190].

Type of load	*Season*	*Total cons., kWh*	*Average monthly cons., kWh*	*Average daily cons., kWh*	*Average power demand, kW*	*Maximal power demand, kW*
Domestic hot water (DHW)	Heating	1 502	215	7.1	0.3	3.2
	Non-heating	863	173	5.6	0.2	3.2
	Whole year	2 365	197	6.5	0.3	3.2
Space heating (SH)	Heating	9 097	1 300	42.9	1.8	9.0
	Non-heating	1 025	205	6.7	0.3	6.6
	Whole year	10 122	844	27.7	1.2	9.0
Total (DHW + SH)	Heating	10 598	1 514	49.9	2.0	11.5
	Non-heating	1 888	378	12.4	0.5	8
	Whole year	12 486	1 041	34.2	1.4	11.5

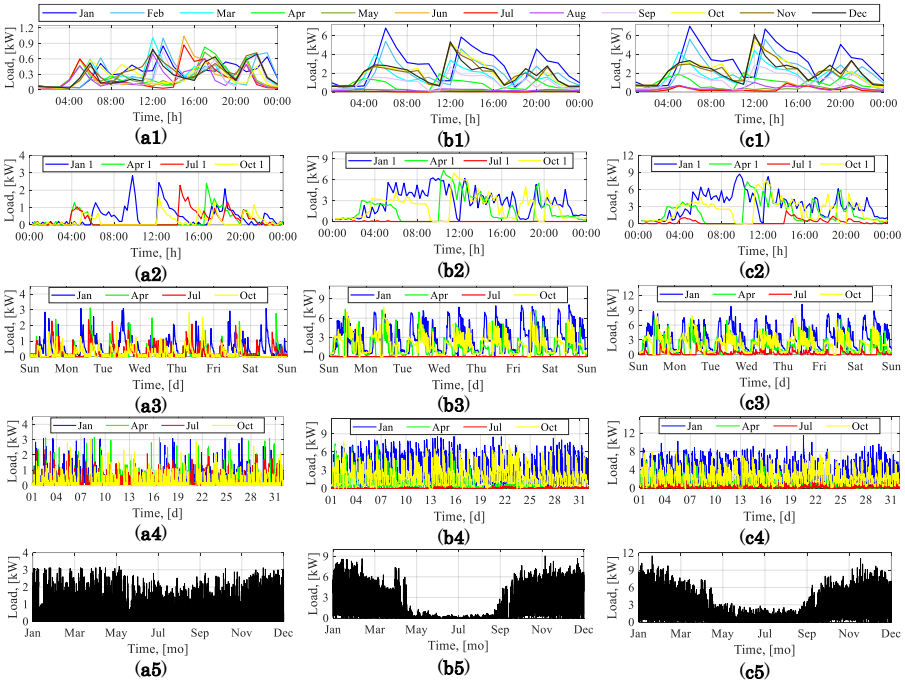

Figure 3.4. Thermal load profile of the household.: (**a**) DHW; (**b**) SH; (**c**) DHW+SH; 1) average hourly demand at a specific month; 2) one day at a specific month; 3) one week at a specific month; 4) four months; 5) a whole year.

3.2.2. Weather data

The weather data shown in Figure 3.5 include *solar irradiance*, required to calculate the output power of PV panels (first column); *wind speed*, required to calculate the output power of the WT (second column); and the *air temperature*, required to calculate the heat pump consumption (third column). Each graph (top to bottom) represents the hourly averages for a specific month, as well as daily, weekly, monthly and yearly curves.

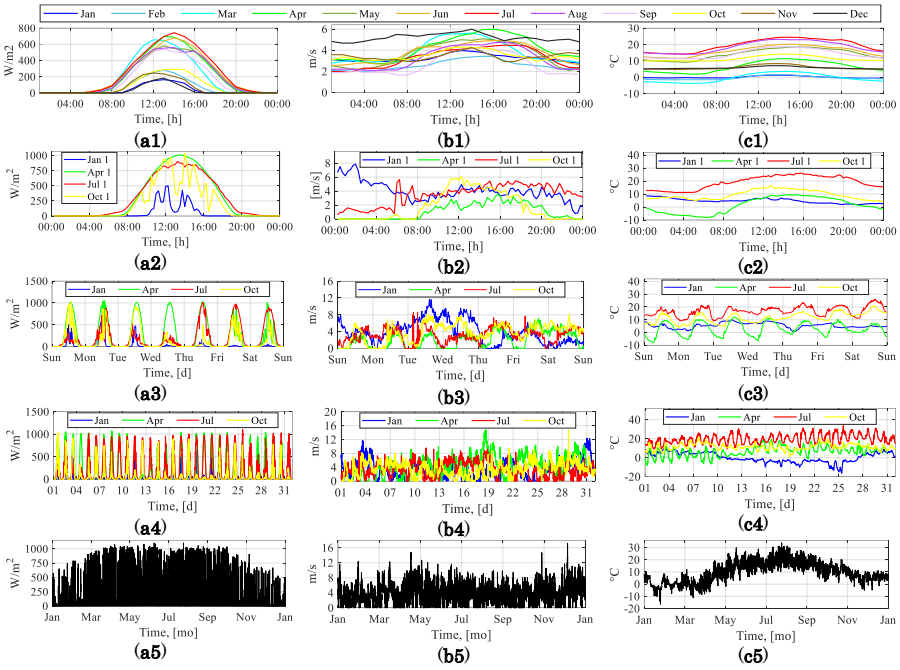

Figure 3.5. Weather data: **(a)** Solar irradiance; **(b)** Wind speed; **(c)** Air temperature; 1) hourly mean values at a specific month; 2) one day at a specific month; 3) one week at a specific month; 4) four months; 5) a whole year.

From graphs a1 and a5 it can be seen that the period from November to January solar activity is very low. In September, October and February, the level of irradiation is higher and often exceeds 500 W/m², while from mid-March to mid-September, solar irradiation is most active. Nevertheless, as seen from graph a5, even in the most active months, the radiation level very rarely reaches 1000 W/m², which is considered standard for PV panels. From the third column, graphs c1 and c5, it is also clearly observed that in the period from early October to late April, the temperature rarely exceeds +10°C, even despite the relatively higher solar activity in October and March. All this may also find its reflection in the

prolonged heating season. In contrast to the first and third columns, all graphs in the second column show a stable and consistent wind throughout the year, which is considered a major advantage for wind turbines.

All data sets have been obtained with 15-minute and hourly intervals from two different sources. In particular, the weather module installed at Aalborg University laboratory and EnergyPRO software. Data sets have been derived for the same location so that to be in line with the aforementioned load profiles. In the instances of not having weather data representatives, a collection of different sources from which these data can be obtained is given by [192].

3.2.3. Data refining

All load profiles have been obtained already pre-edited containing no errors. The weather data derived from two different sources were collated and carefully analysed. Very minor errors have been simply eliminated and blank fields were filled in using linear interpolation. Since the data were acquired at different measurement intervals, they had to be corrected to a single common time step. The initial idea was to convert all data with hourly time intervals into a 15-minute interval so that to perform the first simulations comprising one or a combination of several sub-models (such as PV and battery or a combination of PV, WT and battery). The simulations have been successfully executed, however when it came to combining all model components under a single coordinating solution, the interval of 15 minutes turned out to be insufficient to studying deeper the systems behaviour as well as the flexibility that these systems can provide (this issue will be more comprehensively described in Section 3.6.4). Therefore, it was eventually decided to convert all existing data with an hourly interval and a 15-minute interval into a 1-minute time interval. Since electrical baseload data were obtained with a measurement step of one hour, it is assumed in this study that the load behind an hourly interval is very stable (i.e. that an instantaneous power and mean value over an hour are equal, implying the same value for 60 steps in minute scale). The conversion of household thermal power demand and energy consumption from a 15-minute time step to a 1-minute step is calculated following the same principle.

3.3. HEAT PUMP SYSTEM (HPS)

In this thesis, a heat pump, an instantaneous heating water heater and a hot water storage tank are considered a single system referred to in short here as the Heat Pump System (**HPS**). There are several major types of

heat pumps most commonly used nowadays. In relation to the primary energy source and to where this energy is redirected, they can be easily differentiated as Ground-to-Water (or geothermal), Water-to-Water (using a body of water as a heat source), Air-to-Air and Air-to-Water (**A2W**) types [193]. The first two types are considered the most efficient, however, requires a sufficient amount of land/water on the site and have much higher investment/installation expenditures. The latter two types are gaining more and more popularity in recent years, which is mainly due to much lower investment, as well as steadily growing efficiency indices. Considering the performance of an A2W type heat pump in combination with a buffer tank, which (according to [194], [195]) is capable to cover 95-98% of the heat demand of the household, these HPs offer very promising technology for domestic heat supply in the near future.

One of the main ideas of this study is to investigate how the replacement of heat source affects the household's electric energy needs; the impact of such substitution on the grid; the energy flexibility potential that can be obtained by utilizing an HP in conjunction with energy storage and renewable sources; and, most importantly, the ability of such flexibility to support/facilitate ancillary services in the distribution grid (such as e.g., voltage control). Since the heat demand of the household accounts for the largest share of the total energy used by the building (as shown in Figure 1.9b above), the substitution of the heat source deserves special attention. The heat pump is the core of this research and it is the heat pump coupled with the HWST that is considered one the largest sources of energy flexibility that can be provided by a household [120].

In this context, it is important to choose the right model that will be as simple as possible and at the same time be able to reflect the main processes and general behaviour of the system as close as possible to the real one (in terms of energy use). At the same time, which will be capable to capture responses to the external DR signals and will provide an opportunity to conduct a detailed analysis of these responses with satisfactory accuracy. Complex full-fledged white-box models of dynamic systems, as for example [196], [197], are usually the most accurate and allow to see all the processes in detail. However, such models are computational resourceful and time-demanding. Data-driven black-box models are fast and accurate in quantifying, however, limit the possibility to perform in-depth analysis. In the current case, a grey-box modelling approach applying fundamental equations along with technical documentation and empirical test results is considered as the most appropriate solution to clarify the aforementioned aspects. Thus, this study is aimed at creating a grey-box model of an A2W type vapour compression HP in combination with HWST and supplemental IHWH.

3.3.1. Heat Pump

Prior knowledge. Physical attributes of the system. Parametrization.

After detailed studying of service and maintenance manual and also personal communication with other researchers who have research and practical experience in this field, a heat supply scheme most commonly used in Denmark is selected as shown in Figure 3.6. A heat pump modelled here is selected as a complete monoblock appliance comprising indoor and outdoor units.

- The indoor unit includes a circulation pump for the secondary circuit, 3-way diverter valve (dedicated separating heating and DHW circuits in a case of an application without a buffer tank), pressure safety valve, flow switch, IHWH and control unit.
- The outdoor unit consists of an output-dependent inverter-controlled scroll type compressor, condenser, evaporator, 4-way diverter valve, electronic expansion valve, and variable speed fans.

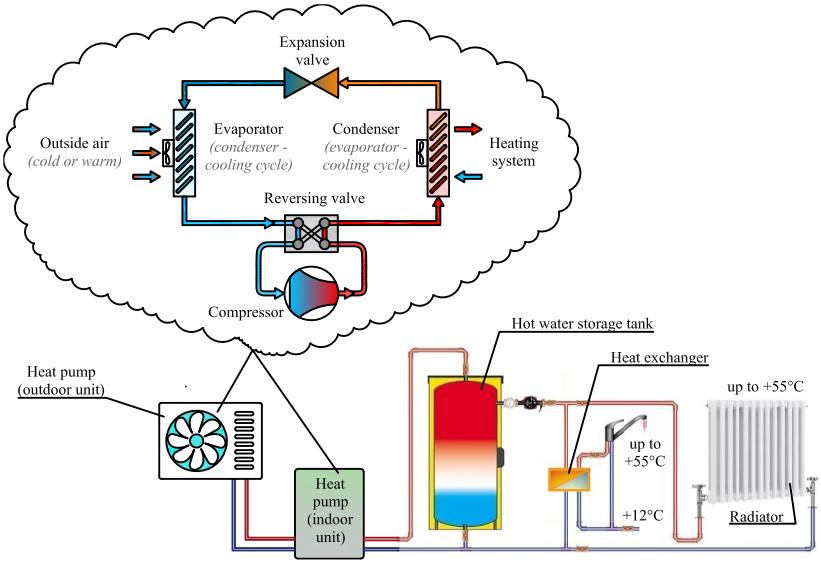

Figure 3.6. Overview of the heat supply scheme (adapted from [190]).

The inverter-controlled type compressor has been selected for several reasons: a) these types of compressors, unlike traditional non-inverter-based ones, have the inrush current of nearly the same order of magnitude as its nominal steady-state current value, hence a much "softer" and less harmful starting-up; b) high power factor varying in between 0.95 and 1.00 [198]. These two factors are quite relevant for the DR application study

which will be disclosed in Chapter 5. Apart from this, it is worth noting that inverter-based control does not necessarily mean that the compressor works continuously without cutting off. The turning-on and -off cycles in this type of compressors are realised as in conventional compressors using thermostatic control, nevertheless, the speed of pumping refrigerant is varied depending on the thermal load.

For the creation of a grey-box model, it is usually required to know at least the basic operating parameters of the modelled system. In the current case, these parameters were obtained from the technical documentation of manufacturers represented in nowadays market [194], [199], [200]. The required parameters are:

- inlet air limits (minimum/maximum levels),
- secondary circuit water temperature.
- rated electric power,
- rated thermal power,

Inlet air limits

Apart from the geothermal HPs, where the primary source temperature is very stable throughout the year (around +6°C), air-source HP performance and hence power output, as well as the operation in general significantly depend on the outdoor air temperature. The efficiency of HP in producing heat significantly decreases when the air temperature exceeds +35°C and the operation of many existing models is simply not possible when the temperature drops to the level below –15°C (although newer contemporary models are able to supply heat even in a range from –25°C to +43°C [199], [200]).

Secondary circuit water temperature

The temperature level demanded by a secondary circuit largely depends on the environmental conditions, the heating system installed in the household, and whether the DHW supply is separated from the SH or not. In those cases, when the inhouse space heating is realised through the hydronic low temperature "underfloor heating" system, and the DHW is supplied by another source (such as condensing boiler, or so), the inflow water temperature of +35°C is considered to be fully sufficient to keep the average insulated building warm enough during the winter season [201]. Systems using radiators for space heating usually require a higher temperature level, up to +55°C [202]. The technical guide [201] indicates that for domestic hot water a temperature level of +45°C is considered a level that does not compromise the comfort of inhabitants. However, in Denmark, this temperature limit is clearly regulated by the Danish

Standards for DHW supply [203] specifying that it should not drop below +50°C at any part of the water installation and only at peak load +45°C is allowed. Furthermore, for combined systems with indirect heating, such as the one investigated in the current work, where HWST is used, a temperature level of at least +60°C is also one of the rules to be followed to eliminate the proliferation of bacteria inside the hot water tank [203]. Thus, to deliver +50°C to the taps (considering heat losses in pipe network and fittings), the water temperature at the outlet of the HWST should be around or above +55°C. In turn, to ensure a stable +55°C inside the HWST (considering the return water temperature) and to prevent the bacteria growth, the supply water temperature has to be at least +60 ~ +65°C.

From the supply-side perspective, i.e. from the heat pump side, the temperature of the outlet water is, to the largest extent, depending on the properties of the HP medium (that is the circulating liquid refrigerant), its chemistry and thermodynamic properties in terms of phase transition. Depending on the HP application this temperature may be as high as +90°C (i.e. at hotels and hospitals for sterilisation purposes, while using a dual cascade refrigerating system) [204] and even higher in some other cases [205]. Nevertheless, high-temperature A2W type HPs, using cascade technology, are usually quite complex, expensive and therefore rarely applied for domestic use. Most conventional models, which can nowadays be commonly found in private houses, not so long time ago experienced serious difficulties in delivering water temperature higher than +45°C ~ +55°C over a wide outdoor temperature range [202], [206]. To heat the water up to the required temperature, a backup electric heater was typically applied, the frequent use of which significantly increased the electricity bill. Recent development in this area allows more modern HPs (using new types of refrigerant or double injection compressors) to achieve a water temperature of +65°C at an outdoor temperature of –15°C [201], [200], [207], and +55°C water at –20°C air [199] in mono mode application. In the Danish climate, where the temperature rarely drops below –10°C, the use of such heat pumps is more than sufficient for both domestic hot water and space heating purposes, while the use of an additional electric heater is essentially minimized. Therefore, the supply temperature of +65°C is taken as a basis in this study.

Rated thermal power

The rated thermal power (provided by manufacturers) is usually required just for selecting the appropriate heat pump system size, to see how well it can match the thermal load of the household. While the equation for calculating the thermal power output will be shown later on in this section.

Rated electric power

Since the creation of this model considers an inverter-controlled type compressor, the rated electric power (required for calculating the HP thermal power output) is not a single constant value. All manufacturers' technical guides represent these power rate variations as a function of air temperature and typically indicate only a limited number of values (in accordance with the standard test conditions of EN 14511). In the model setup, this correlation is expressed as shown in (3.1).

$$P_{el.rt.}^{HP}(t) = \begin{cases} 0, & if \quad T_{in}^{air}(t) > +43°C \\ P_{el.rt.+20}^{HP*}, & if \quad T_{in}^{air}(t) = +20°C \\ P_{el.rt.+12}^{HP}, & if \quad T_{in}^{air}(t) = +12°C \\ P_{el.rt.+07}^{HP}, & if \quad T_{in}^{air}(t) = +07°C \\ P_{el.rt.+02}^{HP}, & if \quad T_{in}^{air}(t) = +02°C \\ P_{el.rt.-07}^{HP}, & if \quad T_{in}^{air}(t) = -07°C \\ P_{el.rt.-15}^{HP}, & if \quad T_{in}^{air}(t) = -15°C \\ P_{el.rt.-20}^{HP*}, & if \quad T_{in}^{air}(t) = -20°C \\ 0, & if \quad T_{in}^{air}(t) < -20°C \end{cases} \quad for\ each\ t \in \{0,1,\dots,n\} \quad (3.1)$$

where,

$P_{el.rt.}^{HP}$ – rated electric power for different air temperature levels [kW],

T_{in}^{air} – inlet air temperature [°C],

t – simulation step that is equivalent to a 1-minute time interval [m],

n – simulation limit.

Although the information provided by the manufacturers' datasheets gives a fairly clear overview of the rated power change, in order to derive more variations (and hence to obtain more accurate results), the intermediate values between every two nearest known data points can be interpolated. This is what has been done initially. Interpolation also greatly simplifies the HP sizing process, which will be described in more detail in Section 3.3.6. For this study, a full range of rated power reflecting all temperature data points, have been provided as reference information by [208].

Despite the fact that the basic parameters for creating a model have already been revealed above, there are also several operational features and limitations that affect the heat delivery process, productivity, energy consumption, and, therefore, the flexibility potential. Among them:

* Rated electric power at an outlet water temperature of +55°C. To achieve the required water temperature setpoint, hot water heating is boosted by a backup electric heater.

- conversion delay,
- defrost cycle,
- restart delay,
- minimum operating time.

Figure 3.7 graphically illustrates all of these limitations, while a more detailed description of each is given below.

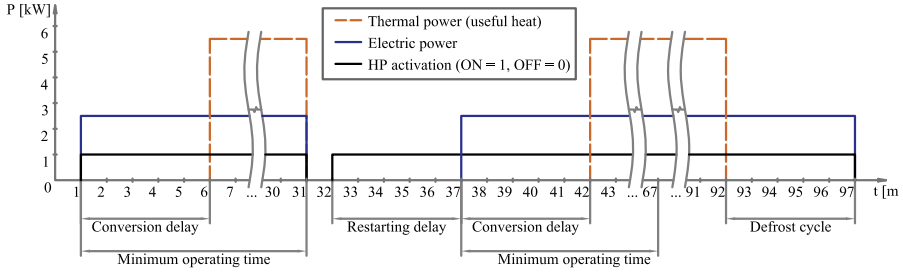

Figure 3.7. Operational limitations of the heat pump.

Conversion delay

The HP operation is built in such a way so that the useful heat is not delivered instantaneously right after turning it ON after prolonged power OFF period. Similar to traditional power generators, HP requires a certain "ramping-up" time to meet secondary circuit temperature set-point and to reach a steady-state to supply heat to the HWST. Depending on the HP size, the type of the compressor and the circulating liquid refrigerant, as well as on the secondary circuit temperature requirements, this preparation process may take up to 15 minutes [128], [191]. For the domestic heat pumps, 5 minutes is considered a default time. Graphically, this step response is illustrated in Figure 3.7 above, while the conditions for its activation with respect to time (t) are represented as follows:

$$\tau_{conv.}(t, \dots, t+4) = \begin{cases} 1, & if\ \ C_s^{HP}(i) = 0\ \ \&\ \ C_s^{HP}(t) = 1 \\ 0, & otherwise \end{cases} \tag{3.2}$$

where,

$\tau_{conv.}$ – binary control signal defining the activation of the conversion delay (where "activated" = 1 and "deactivated" = 0),

i – initial time step ($if\ t = 1,\ i = 1;\quad if\ t > 1,\ i = t - 1$) [m],

C_s^{HP} – binary control signal which defines the activation of the HP (basic ON/OFF control, where ON = 1 and OFF = 0). All the conditions defining the activation are disclosed in (3.25), Section 3.3.3.

Operating cycles

Most Air-to-Water heat pumps have three operating cycles: heating cycle, cooling cycle and, defrost cycle [209].

A *heating cycle* can be explained as follows. The working fluid (i.e. refrigerant, coolant, or heat carrier in other words), being in a liquid state with low pressure and having a temperature lower than the outside air temperature, reaches the outdoor coil. The outdoor coil acts as an "evaporator" in this case and is considered a first heat exchanger. Being within the evaporator, it absorbs heat from the external air and heats up. Having a low boiling point – boils and turns itself into a gas (a low-temperature vapour). This vapour then goes to the reversing valve and accumulator where all remaining liquid is separated and collected so that not to damage the compressor. The compressor then pressurises this vapour, thereby reducing its volume and raising up its temperature. Pressurised hot gas is then passed by the reversing valve to the indoor coil, which acts as a "condenser" and is considered a second heat exchanger. Being hotter than the secondary source (flow water of the heating system), dissipates its heat to this source, thereby partially cooling down and condensing back into a high-pressure vapour/liquid mixture. The liquid/vapour mixture finally flows through the expansion valve which releases the pressure. As the pressure drops, the above mixture is rapidly cooled and returned to the evaporator as a low-pressure cold liquid. The cycle is repeated. Figure 3.6 above shows an overview of the household's heating system, modelled in this study, and the heat pump's heating cycle.

The *cooling cycle* is described as a reverse of the heating cycle during which heat is taken out of the indoor air and is released outdoor. The indoor coil, in this case, acts as an evaporator while an outdoor coil as a condenser respectively. However, even if the heat pump can operate in both modes, heat production in the Danish climate is much more in demand, therefore, the cooling cycle is not investigated in this work.

The *defrost cycle* is important both in terms of ensuring the efficient operation of the system and for electrical energy-related studies. A sharp change in pressure (at the moment when the expansion valve releases the pressure during the heating cycle) contributes to the cooling of not only the refrigerant liquid but also the valve itself, the tube through which this liquid enters the evaporator, the evaporator coil itself and the air that blows them outside. Moisture in the air with a sharp loss of heat condenses on the above-mentioned surfaces and turns into frost (then ice). In the case when the heat pump works under heavy load (i.e. when the thermal demand is high), and especially when the outdoor temperature falls to near or below freezing, as well as when the humidity is high – the

likelihood of frost formation is extremely high. The ice accumulated on the evaporator coil significantly reduces the heat transferring ability of this coil (i.e. the ability of coolant to absorb heat from the external air) thereby reducing the overall system efficiency. To prevent freezing of the outer coil and massive accumulation of ice, the reversing valve switches cycles from heating to cooling, thereby changing the flow direction of the hot gas, and hence melting the frost. The cycle can be initiated either by differential pressure, flow or temperature sensors or by pre-set interval timer. In this model, it is initiated for 5 minutes at the end of each working hour of HP, when the inlet air temperature is below +4°C. This cycle is of interest for energy research, since even though no useful heat is delivered to the indoor heating system, electrical energy continues to be consumed. Graphically this is illustrated in Figure 3.7 above, while all the conditions for its initiation with respect to time (t) are expressed as below:

$$\tau_{defr.}(t,\dots,t+4)=\begin{cases}1, & if \quad t>55 \\ & \& \quad C_s^{HP}(t-55,\dots,t)=1 \\ & \& \quad T_{in}^{air}(t-55,\dots,t)<T_{in.freeze}^{air} \\ 0, & otherwise\end{cases} \tag{3.3}$$

where,

$\tau_{defr.}$ – binary control signal defining the activation of the defrost cycle (activated = 1 and deactivated = 0),

$T_{in.freeze}^{air}$– temperature level that determines the risk of icing up (considered to be +4°C in this study) [°C].

Minimum operating time

To avoid short operating cycles of the HP unit that may occur following different DSF/DR control strategies (disclosed in Section 2.2.8 above), Viessmann technical guide [194] recommends pre-setting a specific minimum operating (power-ON) time between two power-OFF cycles. For simplicity, a power ON time of 30 minutes is considered a reasonable interval to guarantee uninterruptible operation. The limitation is graphically illustrated in Figure 3.7 above, while the conditions for its activation are expressed as follows:

$$\tau_{oper.}(t,\dots,t+29)=\begin{cases}1, & if \quad C_s^{HP}(i)=0 \quad \& \quad C_s^{HP}(t)=1 \\ 0, & otherwise\end{cases} \tag{3.4}$$

where,

$\tau_{oper.}$ – binary control signal defining the minimum duration of the HP uninterruptible operating time and its availability for a DR

response provisioning (1 = activated, which means no DR response can be provided and 0 = deactivated or available).

Restarting delay

Most if not all modern HPs have a built-in start-up (restarting) delay set with the main purpose to prevent the compressor from turning itself ON and OFF repeatedly within a short period of time. This may be caused, for example, by the series of demand response signals, a rapid considerable change in demand, a malfunction such as low refrigerant level, grid outages, and others. The delay, in this case, is required to equalize the refrigerant pressure on both sides of the compressor (inlet and outlet) and thus protecting the compressor from damage since pumping the refrigerant against high pressure is very difficult and harmful task. This delay can normally last from several seconds to 10 minutes (depending on the manufacturer), however, for the domestic heat pumps, a power-OFF period of 5 minutes is usually sufficient. Visually, this limitation is depicted in Figure 3.7 above. The conditions for activating the restarting delay can be expressed as shown below:

$$\tau_{rest.}(t,\dots,t+3)=\begin{cases}1, & if \quad t\geq 3 \\ & \& \quad C_s^{HP}(t-2)=1 \\ & \& \quad C_s^{HP}(t-1)=0 \\ 0, & otherwise\end{cases} \tag{3.5}$$

where,

$\tau_{rest.}$ – binary control signal defining the activation of the restarting delay (activated = 1 and deactivated = 0).

Mathematical formulation. Fundamental equations.

Energy models of heat pumps [193], [210]–[213] are usually built applying the coefficient of performance (COP) approach. From the thermodynamics side, this coefficient denotes the source and sink temperature difference. However, it is also considered the main attribute of any HP and is defined as a ratio of thermal power output and electric power input. To obtain the thermal power output of the HP, while having known its electrical rated power, some authors derive COP from the technical datasheets provided by various manufacturers. In some cases, for example in [214], this COP can be expressed as a single fixed value, which can be suitable enough to create models of ground-source HPs, where the primary source (soil) temperature is very stable. However, applying such a concept to air-source HPs may cause a large inaccuracy of results due to the variable nature of the primary energy source (which is air). In other cases, such as in [191], [193], polynomial interpolation is applied to define the COP variation with

respect to air temperature change. However, the secondary circuit (water flow) temperature is not considered in that process. In this dissertation, the COP is expressed by the inverse Carnot efficiency considering both the air inlet and water flow temperature as well as a specific empirical factor (η_e), which is a deviation from the ideal Carnot cycle.

The COP determined by the inverse Carnot efficiency (shown in Eq. 3.6, 3.7) is, in general, considered maximal theoretical, or an ideal efficiency that can ever be obtained during the energy transformation cycle. However, in practice, the cumulative efficiency and performance of various components of an HP system, such as compressor, circulation pumps, fans, valves, condenser, evaporator, coolant, and others, as well as losses that appeared during operation, make this energy transformation cycle far from ideal [213]. In a study carried out by [210] (based on the empirical examination results demonstrating real COP for different types of HPs [215]), the above-mentioned coefficient of deviation (η_e) has been obtained for Air-to-Water type heat pumps. The authors argued that for this type of HPs, the averaged factor is equal to 0.38. This information is taken as a basis for the following calculations. Thus, the practical COP is determined using equation (3.8).

$$COP_{theoretical} \cong \frac{1}{\mu_{Carnot}} \quad where \quad \mu_{Carnot} = \frac{T_{out}^{w} - T_{in}^{air}}{T_{out}^{w}} \tag{3.6}$$

thus,

$$COP_{theoretical} = \frac{T_{out}^{w}}{T_{out}^{w} - T_{in}^{air}} \tag{3.7}$$

and practical,

$$COP^{HP} = COP_{theoretical} \times \eta_e \tag{3.8}$$

Considering that COP is also defined as a ratio between thermal and electric power, another COP expression is as follows:

$$COP^{HP} = \frac{P_{th.prod.}^{HP}}{P_{el.dem.}^{HP}} \tag{3.9}$$

where,

$COP_{theoretical}$ – maximal theoretical (ideal) efficiency during the energy transformation cycle [-],

COP^{HP} – practical coefficient of performance of HP or, in other words, transformation coefficient from electric to thermal power [-],

μ_{Carnot} – Carnot efficiency [-],

T_{in}^{air} – heat pump inlet air temperature [K],

T_{out}^{w} – heat pump outlet water temperature [K], which is selected to be 338,15 K (65°C) in this study.

η_e – deviation factor (i.e. empirical deviation from the Carnot cycle, which is, following the above reference, equal to 0.38) [-].

$P_{th.prod.}^{HP}$ – thermal power output of the HP [kW],

$P_{el.dem.}^{HP}$ – electric power demand of the HP [kW].

Combining the latter two equations, also taking into account that the HP has an inverter-based type compressor (and thus varied power input) and that the flow water temperature is considered constant value – the **overall** thermal power production of the HP, for all (t), is expressed as follows:

$$P_{th.prod.}^{HP}(t) = \frac{P_{el.dem.}^{HP}(t) \times T_{out}^{w} \times \eta_e}{T_{out}^{w} - T_{in}^{air}(t)}, \tag{3.10}$$

in which:

$$P_{el.dem.}^{HP}(t) = P_{el.rt.}^{HP}(t) \times C_s^{HP}(t), \tag{3.11}$$

where,

C_s^{HP} – control signal, which defines the activation of the HP (see (3.25)).

However, due to the aforementioned conversion delay and defrost cycle, only part (**useful** part) of heat enters the HWST, and it is this part that should be taken into account, unlike electricity, which is counted in all cases. Therefore, it is important to segregate this part from the overall heat production. Such separation is essential, firstly, to compare and analyse the useful and wasteful shares, and secondly, to employ only a useful part of thermal energy when quantifying the SOE of the HWST (which is the main decision-making parameter for activating the HP) and, later on, when assessing energy flexibility potential of HPS. Hence, the segregation is realised as follows:

$$N(t) = \begin{cases} 1, & if \;\; \tau_{conv.}(t) = 0 \;\; | \;\; \tau_{defr.}(t) = 0 \\ 0, & if \;\; \tau_{conv.}(t) = 1 \;\; | \;\; \tau_{defr.}(t) = 1 \end{cases} \tag{3.12}$$

$$P_{th.prod.2HWST}^{HP}(t) = P_{th.prod.}^{HP}(t) \times N(t), \tag{3.13}$$

$$P^{HP}_{th.prod.conv.del.}(t) = P^{HP}_{th.prod.}(t) \times \tau_{conv.}(t), \tag{3.14}$$

$$P^{HP}_{th.prod.defr.}(t) = P^{HP}_{th.prod.}(t) \times \tau_{defr.}(t), \tag{3.15}$$

The thermal energy production is accordingly equal to:

$$Q^{HP}_{th.prod.2HWST} = \frac{1}{60} \int P^{HP}_{th.prod.2HWST} \times dt \tag{3.16}$$

$$Q^{HP}_{th.prod.} = \frac{1}{60} \int P^{HP}_{th.prod.} \times dt \tag{3.17}$$

where,

N – intermediate variable [-],

$P^{HP}_{th.prod.2HWST}$, $P^{HP}_{th.prod.conv.del.}$, $P^{HP}_{th.prod.defr.}$ – thermal power produced by HP that is fed into the HWST; produced during the time of conversion delay; produced during the defrost cycle [kW],

$Q^{HP}_{th.prod.2HWST}$, $Q^{HP}_{th.prod.}$ – thermal energy produced by HP that is fed into the HWST and the overall thermal energy produced by HP [kWh] (per minute).

Electric power demand and energy consumption shares are segregated following the same principle, nevertheless, for the following calculations, it makes sense to visualize only the overall energy consumption.

$$E^{HP}_{el.cons.} = \frac{1}{60} \int P^{HP}_{el.dem.} \times dt \tag{3.18}$$

where,

$E^{HP}_{el.cons.}$ – electrical energy consumed by the HP [kWh] (per minute)

As noted previously, the HP activation events, as well as the duration of activation periods, are fully dependant on the thermal demand of the household and the state of energy of the HWST (reflecting the HWST charging cycles up to the maximum level). The SOE of the HWST is defined in the following Section 3.3.2, while all conditions for activating the HP unit are disclosed in Section 3.3.3.

3.3.2. Hot Water Storage Tank

The HWST is considered one of the most commonly used solutions nowadays for accompanying the HP system [27], [123]. Scientific literature proposes a variety of models of such thermal tanks, including single-mass

(or fully mixed) model, two-mass (or moving boundary) model, multi-node (or multi-layer) stratified model, black-box, zonal and others [124], [128], [210], [212], [196], [216]–[219]. Depending on the prospective application of the model, some of them intend to demonstrate all the fluid dynamic and heat transfer processes occurring inside the tank, being very precise from one side, but saturated with partial differential equations and thus, requiring high computation time on the other side. Other models propose simple and fast execution, however relatively lower computation accuracy. The classification of different models including a brief overview of each, their prospective application and references are given by [220]. Their work serves as a guide for selecting the most appropriate modelling approach.

The approach selected in this study does not involve the creation of a model for in-depth analysis of fluid flow and heat transfer properties. Due to the relatively small volume of the HWST (compared to industrial storage tanks), this study does not consider the thermocline effect and stratified distribution of water inside it. The study assumes that water inside the tank is a homogeneous mixture with a uniform temperature, i.e. constantly mixed using a circulation pump for a secondary circuit (for both space heating and domestic hot water). Therefore, the model selected for this study is solely based on the first law of thermodynamics for a closed system and the specific heat capacity equation. Following the first law of thermodynamics, the energy balance is expressed as:

$$\Delta Q = Q_{in} - Q_{out} \tag{3.19}$$

where,

ΔQ – change in the internal energy of the system [J],

Q_{in} – energy delivered to the system by a heating process [J],

Q_{out} – energy lost by the system due to work done (heat demand) [J]

To quantify the total heat energy that can be stored in an HWST and its initial energy level, to be able to start a simulation, as well as setting up the maximal and minimal energy bands required to control the charging and discharging cycles, it is first assumed that the energy lost due to work (Q_{out}) is zero (meaning no heat demand, no losses). Based on equation (3.19), the overall energy change (ΔQ) in this case is equal to (Q_{in}) and can be quantified using a specific heat capacity equation shown in (3.20). According to [221] the specific heat capacity (c) is defined as the amount of heat energy required to raise the temperature of one unit mass of substance by one degree. Considering that the water is essentially an incompressible substance under normal conditions, the heat capacity of water is considered a constant value of 4184 [J/(kg K)]. Taking also into

account that mass is equal to density times volume and that the density of water inside the HWST is also relatively an unaltered value, the amount of heat energy required to raise the temperature of that water is highly dependent on the temperature difference and volume. In this study, it is assumed that the cold water supplied to the household remains at the same level throughout the year and that the HWST is placed indoors, therefore the minimum possible cold water temperature (T_{cold}^{w}) is considered to be +12°C (or 285.15 K), whereas the maximum possible hot water temperature (T_{hot}^{w}), as mentioned earlier, is +65°C (or 338.15 K). Knowing the volume of HWST, the total energy accumulated in it can be easily quantified using the following equation. The initial energy level, in turn, can be obtained proportionally, depending on the level at which the simulation is intended to be started.

$$c = \frac{\Delta Q}{m\Delta T} = \frac{Q_{in}}{m\Delta T}, \qquad where \;\; m = V\rho_w; \;\; and \;\; \Delta T = T_{hot}^{w} - T_{cold}^{w} \tag{3.20}$$

thus

$$\Delta Q = Q_{in} = Q_{total}^{HWST} = \frac{cV\rho_w(T_{hot}^{w} - T_{cold}^{w})}{3.6 \times 10^{6}} \tag{3.21}$$

where,

Q_{total}^{HWST} – total thermal energy accumulated in HWST [kWh],

c – heat capacity [J/(kg K)],

m – mass of water [kg],

V – volume of water inside the tank [m^3],

ρ_w – density of water [kg/m^3],

ΔT – water temperature difference [K],

T_{cold}^{w} – minimum possible cold-water temperature [K],

T_{hot}^{w} – maximum possible hot water temperature [K].

Since the total energy of the HWST and its initial energy level have already been defined, also considering that the heat demand is not zero by default, the energy added or released from the HWST (while referring back to (3.19)), is then expressed as:

$$\Delta Q^{HWST}(t) = Q_{th.prod.2HWST}^{HP}(t) + Q_{th.prod.}^{IHWH}(t) - Q_{th.cons.}^{HH}(t) - Q_{th.loss}^{HWST}(t) \tag{3.22}$$

Whereas, the state of internal energy of the HWST, at each time step (t), in percentage equivalent, is calculated as:

$$SOE^{HWST}(t) = SOE^{HWST}(i) + \frac{\Delta Q^{HWST}(t)}{Q_{total}^{HWST}} \times 100 \tag{3.23}$$

where,

SOE^{HWST} – state of energy of the HWST [%],

ΔQ^{HWST} – change in the internal energy of the HWST [kWh],

$Q_{th.prod.}^{IHWH}$ – thermal energy produced by IHWH [kWh] (per minute, see Section 3.3.4 below),

$Q_{th.cons.}^{HH}$ – thermal energy consumption of the household comprising both domestic hot water and space heating [kWh] (per-minute),

$Q_{th.loss.}^{HWST}$ – thermal energy losses of the HWST [kWh] (per-minute, see below).

It is a known fact that the thermal tank loses some energy accumulated in it over time. Thermal energy losses mainly depend on the insulation of the tank and the environment in which it is placed. After communicating with other researchers who have a wealth of experience in this field, it was determined that HWSTs, which are commonly used in the domestic sector nowadays, may lose around 1% of the thermal energy accumulated in it (residual energy) every 24 hours (or 1/24 per cent per hour). This ratio is accepted for investigating the HPS behaviour in this study. Mathematically, these losses can be expressed as follows:

$$Q_{th.loss.}^{HWST} = \frac{1}{60} \int \left(\frac{SOE^{HWST}(i) \times Q_{total}^{HWST}}{24 \times 10^4} \right) \times dt \tag{3.24}$$

3.3.3. Basic control of the HPS

The HPS is generally considered a thermostatic load and is regulated using ordinary hysteresis control. The lower- and upper-temperature setpoints for the HWST are selected to be +55°C (328.15 K) and +65°C (338.15 K), where +55°C is the temperature of water at the outlet of the HWST, required to ensure +50°C at the taps (standard requirements), and +65°C is the temperature level that contemporary A2W type HPs for the domestic use can produce with very minimal or without the need for an additional electric heater. Equivalent energy setpoints for these temperature levels (i.e. lower and upper SOE bands of the HWST) are also determined using equation (3.21), where the ΔT value required to calculate the lower (turn-on) energy band is equal to 43 K (i.e. 328.15 K – 285.15 K) and the upper (cut-off) energy band is simply considered the value of the

total thermal energy. Thus, in other words, it can be said that the HP flow water temperature controller will turn the unit ON ($C_s^{HP} = 1$) when the state of energy of the HWST drops to the lower energy band ($SOE_{min.ctrl.}^{HWST}$) and switch it OFF by reaching the maximum energy level (SOE_{max}^{HWST}) as it is shown in (3.25). For clarity, using the example of an HWST with a volume of 0.2 m^3 (200 litres), the total energy value will be 12.3 kWh, and the control will be executed in between 10.0 and 12.3 kWh, which in SOE equivalent is 81% and 100%. The controlled amount of energy is accordingly – 2.3 kWh.

The activation and deactivation of the HP unit for all (t) are realised as shown in (3.25). The first condition (from top to bottom) describes a situation where the HP should be turned ON due to the fact that the SOE level fell to (or below) a minimum controllable level. This condition is suitable for the first start or the end of a discharge cycle. The second condition stands for the continuation of work, i.e. charging the HWST to the maximum SOE level. The third and fourth conditions depict backward situations when the HP unit should be switched OFF by reaching the maximum SOE level and continue to be in power OFF mode until the minimum controllable SOE level. The last two conditions indicate that the HP should be switched OFF due to exceeding outdoor air temperature limits or due to a restart delay.

$$C_s^{HP}(t) = \begin{cases} 1, & if \;\; SOE^{HWST}(t) \le SOE_{min.ctrl.}^{HWST}; \\ 1, & if \;\; SOE_{min.ctrl.}^{HWST} < SOE^{HWST}(t) < SOE_{max}^{HWST} \\ & \& \;\; C_s^{HP}(i) = 1; \\ 0, & if \;\; SOE^{HWST}(t) = SOE_{max}^{HWST} \\ & \& \;\; C_s^{HP}(i) = 1; \\ 0, & if \;\; SOE_{min.ctrl.}^{HWST} < SOE^{HWST}(t) \le SOE_{max}^{HWST} \\ & \& \;\; C_s^{HP}(i) = 0; \\ 0, & if \;\; T_{in.}^{air}(t) < T_{in.min}^{air} \;\; | \;\; T_{in.}^{air}(t) > T_{in.max}^{air}; \\ 0, & if \;\; \tau_{rest.} = 1; \end{cases} \tag{3.25}$$

where,

$\tau_{rest.}^{HP}$ – is the restarting delay set to guarantee the power-off status of the HP unit during at least 5 minutes after each new power-off event (thus avoiding its frequent ON/OFF switching).

SOE^{HWST}, $SOE_{min.ctrl.}^{HWST}$, SOE_{max}^{HWST} – state of energy of the HWST, it's minimum and maximum controlled levels [%],

$T_{in.min}^{air}$, $T_{in.max}^{air}$ – minimum/maximum inlet air temperature limits [°C].

3.3.4. Instantaneous Heating Water Heater

In cases where the heat pump is unable to cover high heat demand on its own and the energy stored in the tank is not enough, as well as those cases when the outdoor air temperature is below the HP working limits or when the HP runs the defrost cycle – an IHWH is applied to cover this demand. Normally the IHWH is turned OFF and if the HP and HWST sizes are chosen correctly, the share of energy produced by IHWH is very small, usually does not exceed 2-5% per year. The IHWH can be integrated either directly into the HWST (i.e. immersion heater or resistor in other words) or into the secondary circuit. In this study, the IHWH is selected as an indoor HP unit accessory integrated into the secondary circuit. Since the coefficient of performance (COP) and the power factor of this unit are equal to one, the electric power input and thermal power output (i.e. $P_{el.dem.}^{IHWH}$ and $P_{th.prod.}^{IHWH}$) [kW] are equal and can be represented for each time step (t) as:

$$P_{el.dem.}^{IHWH}(t) = P_{th.prod.}^{IHWH}(t) = P_{el.rt.}^{IHWH} \times C_s^{IHWH}(t) \tag{3.26}$$

where,

$P_{el.rt.}^{IHWH}$ – rated electric power [kW],

C_s^{IHWH} – binary control signal which defines the activation of the IHWH (basic ON/OFF control, where ON = 1 and OFF = 0) [-].

To avoid very frequent turning it ON and OFF, which is an undesirable activity due to high rated power, the minimum working time of 5 minutes was introduced after each turning ON event. The conditions for activating an IHWH, with respect to time (t), are expressed as follows:

$$C_s^{IHWH}(t, \dots, t+4) = \begin{cases} 1, & if \;\; Q_{th.prod.2HWST}^{HP}(t) < Q_{th.cons.}^{HH}(t) \\ & \& \;\; SOE^{HWST}(t) < SOE_{min.ctrl.}^{HWST} \\ 1, & if \;\; T_{in.}^{air}(t) < T_{in.min}^{air} \;\; | \;\; T_{in.}^{air}(t) > T_{in.max}^{air}; \\ & \& \;\; Q_{th.cons.}^{HH}(t) > 0 \\ & \& \;\; SOE^{HWST}(t) < SOE_{min.ctrl.}^{HWST} \\ 0, & otherwise \end{cases} \tag{3.27}$$

The electrical energy consumed ($E_{el.cons.}^{IHWH}$), as well as thermal energy produced $Q_{th.prod.}^{IHWH}$) [kWh] (per minute) are accordingly equal to:

$$E_{el.cons.}^{IHWH} = Q_{th.prod.}^{IHWH} = \frac{1}{60} \int P_{el.dem.}^{IHWH} \times dt \tag{3.28}$$

3.3.5. Total power demand

The overall active power demand [kW] of the HPS (required for the following load flow study) is the summation of the power demand of the HP and IHWH.

$$P_{el.dem.}^{HPS}(t) = P_{el.dem.}^{HP}(t) + P_{el.dem.}^{IHWH}(t) \tag{3.29}$$

Since IHWS has a purely resistive nature, there is no reactive power consumed or produced by this unit (all power is active and converted into heat), therefore the overall reactive power of the HPS [kVAr] only takes into account the HP unit.

$$Q_{react.}^{HPS}(t) = P_{el.dem.}^{HP}(t) \times tan\,(\varphi) \tag{3.30}$$

where,

$Q_{react.}^{HPS}$ – reactive power demand of the heat pump system [kVAr],

φ – phase angle, which is considered to be 0.32 in this study ($\tan(\varphi)$ = 0.33, $\cos(\varphi)$= 0.95) [rad].

3.3.6. Sizing of HPS

Sizing of HP and IHWH

For determining the size of the HP, recommendations provided in [194] and [209] were used as a basis. In the first reference, the authors recommend selecting the size so that its thermal output covered 70 to 85% of the maximum thermal demand of the household (in accordance with EN 12831). The authors of the second reference affirm that by choosing a heat pump capable of covering 60 to 70% of the maximum heat load (including both SH and DHW demand), the maximum cost-effectiveness of the HP operation is achieved. In this study, 70% was taken as a basis.

As recommended above, the maximum heat load of the household and the share of this load to be covered by the heat pump were defined first. For the investigated household, this is 11.5 kW and accordingly 11.5 x 0.7 = 8.1 kW. In the next step, having historically recorded time-series data for an ambient air temperature, it was determined at what temperature ($T_{in.}^{air}$) such a load occurred (–3,9°C in the current case). Having obtained the air temperature and knowing the supply water temperature requirements (i.e. +65°C in the current study), in the next step the COP was determined

using Eq. (3.8) above. The obtained COP is equal to 1.86. Consequently, the electric rated power was calculated using equation (3.9) above and is equal to 4.31 kW. The calculated load was subsequently compared with the manufacturer's tabular data [199], [208]. Since most nowadays HPs have a variable load (due to an inverter-controlled type compressor), and also, since most manufacturers provide only partial data for certain temperatures, to more accurately determine the HP size and simplify the matching process, intermediate values between indicated data points should be interpolated. In this study, as mentioned above, these variations have been provided by the manufacturer [191]. The parameters of the selected HP are shown in Table 3.3.

The sizing process of an IHWH is greatly simplified. Since IHWH is a supplementary unit supplied in demand as an accessory for the HP, the whole sizing process comes down to what is offered by manufacturers. Manufacturers [199] offers only one size, 8.6 kW, whereas indicating that the power can be adjusted. Given the fact that the efficiency of IHWH is equal to 1 (i.e. produces 1 kW of heat, consuming 1 kW of electric power), it is important that this power is not overestimated, since it significantly changes the consumption profile of the entire HPS (as illustrated in Figure 3 in [195]). Considering that the HP operating envelope is the temperature of –20° C to + 43°C and that the bulk of the heat load is covered by the HP in mono mode, as well as the fact that for the situations mentioned in Section 3.3.4 above the heat pump is also coupled with a hot water storage tank, the main role of an IHWH in this process is to swiftly heat the already pre-heated water up to the required temperature. In this regard, it was decided to select the value of 6 kW. This is also shown in Table 3.3.

Sizing of HWST

Author in [195] shows that the typical size of the HWST used for DHW purposes (such as showering, dish washing, etc.) together with heat pumps installed in single-family houses is around 150-200 litres. For minimising very frequent ON/OFF switching, the HP unit is often additionally equipped with a buffer tank of around 40-80 litres. However, according to the author, such volumes are usually not enough to ensure flexible operation of the heat pump to be able to turn off for hours. For such purposes, heat storage tanks with a capacity of up to 1000 litres are installed, which are also connected to the space heating circuit. Nevertheless, when a larger volume is required, the question of the limit of the available free space usually arises, since, given the insulation, such installations take up a fairly large area. The sizing methods selected for this study are solely based on technical recommendations given by [194]. The technical guide provides two different methodologies used depending on the purpose of the application.

The first sizing method, expressed in (3.31), is very simple/rough and is suitable for the HP run-time optimization* purpose. According to this method, the buffer tank should be dimensioned for a volume of about 20 litres per kW of HP thermal power output.

$$V = P_{th.prod.}^{HP} \times 20 \tag{3.31}$$

where:

V – volume of the hot water storage tank [l],

$P_{th.prod.}^{HP}$ – thermal power output of the HP at the temperature at which the maximum load occurred [kW].

Another purpose, why the HWST can be used, is to provide a reserve heat supply (including DHW supply) when the power supply is OFF. The latter can be associated with planned/unplanned outages, high electricity price periods, or, for example, with the provision of DR services. For these purposes the size of the HWST is calculated following the equation below:

$$V = \frac{P_{th.load.}^{HH} \times t_{rsv.}}{c \times \Delta T} \tag{3.32}$$

where:

$P_{th.load.}^{HH}$ – thermal load of the household comprising both domestic hot water and space heating [kW],

$t_{rsv.}$ – desired duration of the reserved heat supply period [h],

c – heat capacity [kWh/(kg K)],

ΔT – water temperature difference [K],

Having the rated electric power of the selected HP of 5.3 kW (at –3.9°C, as shown in Table 3.3 below) and multiplying this power by the aforementioned COP will give us the thermal power output of 9.9 kW. The required volume of the HWST for run-time optimisation purposes is then equal to 198 litres. Various manufacturers usually offer 200-litre tanks. This size will be designated as Scenario 1 while assessing flexibility potential. Assuming that one hour of backup heat supply is a minimum requirement of inhabitants for not violating their thermal comfort preferences, the required volume (using the second method) will then be equal to 1000 litres. This volume will be referred to as Scenario 2. The equivalent energy value for both cases can then be easily derived from (3.21). All parameters are listed in Table 3.3.

* Optimising run-time in this context implies minimising the number of start-ups of the HP unit, thus ensuring its smooth operation and thereby extending its technical lifetime.

Table 3.3. Heat pump system parameters.

Parameter	*Description*	*Value*	*Unit*
	HP		
$P^{HP}_{el.rt.+31}, \dots, P^{HP}_{el.rt.+35}$	Rated electric power ($T^{air}_{in.}$ from +30°C to +35°C)	4.2*	[kW]
$P^{HP}_{el.rt.+21}, \dots, P^{HP}_{el.rt.+30}$	Rated electric power ($T^{air}_{in.}$ from +21°C to +29°C)	4.4*	[kW]
$P^{HP}_{el.rt.+18}, \dots, P^{HP}_{el.rt.+20}$	Rated electric power ($T^{air}_{in.}$ from +19°C to +20°C)	4.7	[kW]
$P^{HP}_{el.rt.+15}, \dots, P^{HP}_{el.rt.+17}$	Rated electric power ($T^{air}_{in.}$ from +15°C to +17°C)	5.0	[kW]
$P^{HP}_{el.rt.+09}, \dots, P^{HP}_{el.rt.+14}$	Rated electric power ($T^{air}_{in.}$ from +09°C to +14°C)	5.3	[kW]
$P^{HP}_{el.rt.+04}, \dots, P^{HP}_{el.rt.+08}$	Rated electric power ($T^{air}_{in.}$ from +04°C to +08°C)	5.4	[kW]
$P^{HP}_{el.rt.-13}, \dots, P^{HP}_{el.rt.+03}$	Rated electric power ($T^{air}_{in.}$ from –13°C to +03°C)	5.3	[kW]
$P^{HP}_{el.rt.-15}, \dots, P^{HP}_{el.rt.-14}$	Rated electric power ($T^{air}_{in.}$ from –15°C to –14°C)	4.5*	[kW]
$P^{HP}_{el.rt.-20}, \dots, P^{HP}_{el.rt.-16}$	Rated electric power ($T^{air}_{in.}$ from –20°C to –16°C)	4.4*	[kW]
$T^{air}_{in.min}$	Minimum inlet air temperature band	+35	[°C]
$T^{air}_{in.max}$	Maximum inlet air temperature band	–20	[°C]
$T^{air}_{in.freeze}$	Temperature determining the risk of icing up	+4	[°C]
T^{w}_{out}	Outlet water temperature	+65	[°C]
η_e	Deviation factor from the Carnot cycle	0.38	[-]
	Duration of the conversion delay	5	[m]
	Duration of the restart delay	5	[m]
	Duration of the defrost cycle	5	[m]
	Duration of the minimum operating time	30	[m]
	IHWH		
$P^{IHWH}_{el.r.t.}$	Rated power (both thermal and electric)	6	[kW]
	Duration of the minimum operating time	5	[m]
	WHST		
V	Volume of the hot water storage tank (Scenario 1)	0.20	[m³]
V	Volume of the hot water storage tank (Scenario 2)	1.00	[m³]
c	Specific heat capacity of water (at +20°C)	4184	[J/(kg K)]
ρ	Density of water	997	[kg/m³]
T^{w}_{hot}	Maximum possible hot water temperature	+65	[°C]
T^{w}_{cold}	Minimum possible cold-water temperature	+12	[°C]
$T^{w}_{max.contr.}$	Upper temperature setpoint (for the HP control)	+65	[°C]
$T^{w}_{min.contr.}$	Lower temperature setpoint (for the HP control)	+55	[°C]
SOE^{HWST}_{max}	Maximum SOE band (for the HP control)	100	[%]
$SOE^{HWST}_{min.ctrl.}$	Minimum SOE band (for the HP control)	81	[%]
	Thermal losses per every 24 hours	1	[%]

* Rated electric power at an outlet water temperature of +55°C. Values at an outdoor temperature from +21°C to +35°C have been extrapolated. Extrapolation to +43°C does not make sense as the maximum outdoor temperature determined in the available datasets is +34°C.

3.4. PV PANELS

Solar panels have gained considerable popularity over the past few decades. A variety of different models can be found in the literature today. They are all very multidirectional. Some models are focused on studying special cells' properties, such as e.g. transmittance through the glass and thin anti-reflective coating [222], or the operating cell temperature [223] with the main target of improving the efficiency of one or another element of the PV module. Others, such as [224], [225] demonstrate the modelling approach highlighting the output current-voltage (**I-V**) characteristic of the solar cells, while [226] is focussed on special properties of inverters, which are relevant for in-deep grid stability/reliability studies. Authors in [170] proposed an integrated adaptive control solution for compensating overvoltage caused by PV arrays with the help of EWH. Another solution for mitigating this impact with the help of a PV-battery system, comprising the I-V equation-based solar PV model, is proposed by [227]. The method of using an inverter-based PV system for supporting the voltage regulation in a local LV grid is proposed by [228], while for congestion management by [229]. Authors in [230] proposed a neural network-based methodology for short-term solar power forecast, which can be employed in grid operation planning. Another example of data-driven modelling of a PV system (i.e. black-box modelling) is given by [231]. While the library comprising simple mathematical models of solar cells/module/array, battery, controller, inverter and load (i.e. full set of components of a stand-alone PV system) is presented in [225].

The focus of this study is aimed at precisely investigating the energy interaction with the power grid considering that the PV array is connected to the grid through the power converter. Therefore, the main purpose of creating a model, in this case, is to explore the total power output of the entire PV array at a given time/season rather than reflecting the dynamics of processes of a single panel on the other side of a power converter. In this regard, the correlations of output power to the change of weather conditions, amount of energy imported/exported to/from the grid, as well as the possibility of accumulating and shifting the use of this power in time (thereby delivering energy flexibility to the power grid) are the main factors to which the primary attention is riveted in this study.

The generating capacity of a PV panel, in general, depends on a number of various factors. Among them is the intensity of the solar irradiation (insolation), the spectral distribution of this irradiation, incidence/tilt angle, module temperature, shading, as well as different losses, such as those due to dust, snow, cable, inverter losses etc. Ideal conditions, during which maximum peak capacity can be derived, are those which

corresponds to the irradiance level of 1000 W/m² with an absolute air mass spectral distribution of 1.5 (AM1.5) perpendicular to the PV panels surface and a module temperature of +25 °C [213]. These conditions are also commonly referred to as laboratory Standard Test Conditions (**STC**). The power output can also be reduced if any of these conditions are violated, i.e. the irradiation is lower, angle differs or the cell temperature is higher.

Solar irradiation is considered the most dominant environmental factor influencing voltage-current and voltage-power output characteristics of PV panels. The significance of this irradiance, as well as its correlation to current, voltage and output power, is clearly described and graphically illustrated in [226]. From Figure 3.5a (Section 3.2.2 above) it can be seen that solar insolation in Denmark very rarely reaches STC. Figure 3.5c demonstrates that the outdoor air temperature, in turn, also very rarely exceeds +25 °C (i.e. 184 hours out of 8760 for this data). Since Denmark is located in a climatic zone with a relatively cold and rainy climate, it can be said that the module surface temperature is in almost ideal conditions most of the year. The temperature factor, in this study, has a significantly smaller effect on generation than the intensity of solar radiation, and that is why it was decided not to take it into account. In addition, referring to [213], which illustrates data of historical measurements for 10 years, relatively equal shares of direct and diffuse components of light give a very high degree of freedom in solar panels orientation (both in terms of tilt angle and orientation South/West).

Therefore, a simplified model of PV panels array using a commonly known *Global formula* to estimate the electricity output of a PV system, shown in Eq. (3.33), was chosen to perform these tasks. Of course, such a model will not reflect a complete picture of all processes, as is possible by applying a modelling approach proposed by for example [225], however, such a model is fully sufficient to answer the research questions posed at the beginning of this thesis. It is also worth noting that this study assumes that PV panels are installed on the rooftop of a house, thus any option of increasing power output efficiency with the help of tracking systems, as well as the use of bifacial photovoltaic panels is not considered in this work.

The calculation of power output of a PV array ($P^{PV}_{prod.}$) in [kW] with respect to time (t) is presented as follows:

$$P^{PV}_{prod.}(t) = A^{PV}_{array} \times H(t) \times r \times PR \times 10^{-3} \tag{3.33}$$

where,

A^{PV}_{array} – total area of the PV array (i.e. the area of a single panel multiplied by the number of panels) [m²],

H – global solar irradiation on tilted panels (without shadings) [W/m^2],

r – solar panel yield [%],

PR – performance ratio or a coefficient for losses [-].

r is calculated as:

$$r = \frac{P^{PV}_{panel.rt.}}{A^{PV}_{panel}} \tag{3.34}$$

where,

$P^{PV}_{panel.rt.}$ – peak power of a single PV panel under STC [W],

A^{PV}_{panel} – area of a single panel [m^2].

and PR is calculated as:

$$\begin{aligned} PR = (1 - dP^{PV}_{inv.}) \times \left(1 - dP^{PV}_{mod.temp.}\right) \times (1 - dP^{PV}_{DC\ cable}) \\ \times (1 - dP^{PV}_{AC\ cable}) \times (1 - dP^{PV}_{shad.}) \times (1 - dP^{PV}_{irr.}) \\ \times (1 - dP^{PV}_{dust}) \times (1 - dP^{PV}_{other}) \end{aligned} \tag{3.35}$$

where,

$dP^{PV}_{inv.}$ – inverter losses [-],

$dP^{PV}_{mod.temp.}$ – temperature losses [-],

$dP^{PV}_{DC\ cable}$ – DC cables losses [-],

$dP^{PV}_{AC\ cable}$ – AC cables losses [-],

$dP^{PV}_{shad.}$ – shadings losses [-],

$dP^{PV}_{irr.}$ – weak irradiation losses [-],

dP^{PV}_{dust} – losses due to dust, snow [-],

dP^{PV}_{other}– other losses [-].

The electrical energy produced by the PV array ($E^{PV}_{prod.}$) [kWh] (per minute) is accordingly equal to:

$$E^{PV}_{prod.} = \frac{1}{60} \int P^{PV}_{prod.} \times dt \tag{3.36}$$

3.4.1. Sizing of PV array

Nowadays, in many countries, installed capacities of grid-connected residential rooftop PV systems are thoroughly regulated. This is mainly associated with a number of issues such as reverse power flow and overvoltage that may be caused by large-scale integration, very low power demand, or poor infrastructures (especially sensitive in grid structures consisting of long radial feeder lines). In this regard, each country has its own limitations on the power that can be fed into the grid instantly, and on the amount of energy that can be exported to the grid per year. All these are usually regulated by means of the rated power of the inverter. For example, in Germany, the limit has been set at 10 kW for over a decade and has recently been increased to 30 kW (subject to a number of preconditions) [25]. In Denmark, this limitation is even more stringent and is set to 6 kW [24]. The authors [140], [166], [232], [233], in turn, argue that the installed capacity of 3 – 6 kW is quite typical for residential grid-tied rooftop PV systems. Therefore, the size of 6 kW was chosen for further research and is considered the size noteworthy to be investigated. A set of input PV system parameters required to execute the simulation can normally be derived from the technical specification of different manufacturers. Parameters used in this research work have been obtained from [234] and are summarised in Table 3.4.

Table 3.4. PV array parameters.

Name	*Parameter*	*Description*	*Value*	*Unit*
Main parameters	L^{PV}	Length	1.559	[m]
	W^{PV}	Width	1.046	[m]
	A^{PV}_{panel}	Area of a single panel	1.631	[m²]
	r	Solar panel yield	0.193	[%]
	$P^{PV}_{panel.rt.}$	Rated power	0.315	[kW]
	n	Number of panels	19	[-]
Losses*	$dP^{PV}_{inv.}$	Inverter losses	0.08	[-]
	$dP^{PV}_{mod.temp.}$	Temperature losses	0.08	[-]
	$dP^{PV}_{DC\ cable}$	DC cables losses	0.02	[-]
	$dP^{PV}_{AC\ cable}$	AC cables losses	0.02	[-]
	$dP^{PV}_{shad.}$	Shadings losses	0.03	[-]
	$dP^{PV}_{irr.}$	Weak irradiation losses	0.03	[-]
	dP^{PV}_{dust}	Losses due to dust, snow	0.02	[-]
	dP^{PV}_{other}	Other losses	0.00	[-]

* The values under the field "*Losses*" in Table 3.4 are the standard values set by default.

3.5. WIND TURBINE

Similar to PV panels, there are a variety of models that focus on improving various physical aerodynamic properties (i.e. design of tower, nacelle housing and rotor blades), mechanical properties (i.e. gearbox, yaw, pitch and brake systems), electrical systems (i.e. generator, power converter or transformer), control systems, as well as power output models of the wind turbines exist nowadays. This thesis is not intended to improve any specific component of the WT and is therefore simply focused on modelling its output power. Different approaches to wind turbine power output modelling can nowadays be found in multiple scientific papers. All these approaches can broadly be classified into two categories:

- those, which are based on fundamental equations of wind power;
- models based on the concept of the power curve of WT.

Models created within the latter category framework are considered more accurate and usually used for predicting WT's behaviour and performance. All models in this group can be divided by parametric (such as the piecewise linear model, probabilistic model, models built using polynomial equations, dynamical power curve, maximum principle method and others) and non-parametric (such as cubic spline interpolation, copula power curve model, fuzzy, neural network and data derived models). A comprehensive review of each of these models, as well as methodologies for the creation, is made by [235]–[237].

Considering that the framework of this work excludes prediction of the WT behaviour as well as in-deep investigation of WT's performance, for the creation of a model in this study, a simplified approach involving fundamental equations of power available in wind has been selected. This approach yet yields satisfactory accuracy for analysing the power output potential required for further estimating the energy efficiency as well as energy flexibility potential of the household. The study, at the same time, does not intend to demonstrate the widest possible range of different WT's configurations and is concentrated on those that are most common in the commercial domain for domestic use nowadays. Namely, the three-bladed, variable-speed, upwind, horizontal axes wind turbine (**HAWT**), without pitch-control. For creating a model, the following studies/books have been used as a basis [238]–[240].

From the fundamental equation of the kinetic energy of wind flow, the power available in the wind (P_{wind}) in [W] passing perpendicularly through

the area swept by the rotor of a wind turbine, at each moment of time (t), can be expressed as follows:

$$P_{wind}(t) = \frac{1}{2}\rho_a(t) \times A \times v_p^3(t) \tag{3.37}$$

where,

ρ_a – air density at the turbine's hub [kg/m^3],

A – rotor swept area of the WT (the area of a circle for HAWT, where the radius is the length of the wind turbine blade) [m^2],

v_p – wind speed at the projected height [m/s],

As can be seen, this power is most dependent on the dynamics of wind speed, nevertheless, another important parameter influencing this power is density. The density of air is not a constant value and depends on temperature, pressure and the amount of moisture in the air. With relatively small daily temperature changes, density fluctuations can be neglected. However, in the context of seasonal temperature variation (from –20°C to +30°C, as shown in Figure 3.5 c5 above), the density deviation is more notable and can change the wind power value (and hence power output of the WT) by up to 20%. In this study, the density of air at the WT's hub is calculated by [239]:

$$\rho_a(t) = \frac{353.049}{T^{air}(t)} e^{\left(-0.034\frac{Z}{T^{air}(t)}\right)} \tag{3.38}$$

where,

T^{air} – ambient air temperature [K],

Z – elevation, including turbine's tower high [m].

Wind speed is considered to be the main characteristic of wind, but it changes randomly and is distributed very unevenly. To represent these variations in specific areas over a period of time, various probability distribution functions (PDF) such as Weibull, Ryleigh and others [241]–[243] are widely applied. However, the use of these functions is mainly in demand where statistical techniques are applied to improve the accuracy of estimates of wind parameters and the performance of WTs. This is very important for the design of new wind farms and for the operation of existing ones (i.e. to improve control algorithms etc). Since the purpose of this study is to evaluate the performance of a WT based on historical data (and not to predict the output power or operating mode), the application of such functions is not required. It is also obvious that the wind speed and

hence the power output of the wind turbine is dependent on the height at which the WT is installed (both the high of the WT tower and elevation of terrain). The height of the wind turbine positioning, as well as the ground friction coefficient, noticeably impact the output power. Therefore, to eliminate the mismatch between the installation height of the weather module and the height of the WT hub, the following equation is applied:

$$v_p\,(t) = v_r(t) \times \left(\frac{H_p}{H_r}\right)^{\mu} \tag{3.39}$$

where,

v_p – wind speed at the projected height [m/s],

v_r – wind speed at the reference height [m/s],

H_p– projected height (hub height) [m],

H_r – reference height (installation height of anemometer) [m],

μ – ground friction coefficient (~1/7 for open land) [-].

In addition, each WT has individual wind speed limits at which it is capable of delivering power. These wind speed bands are commonly known as the *cut-in* speed (v_p^{ci}), *rated* speed (v_p^{rt}), and *cut-out* speed (v_p^{co}). Cut-in is considered a wind speed at which the wind turbine starts producing useful electric power. Rated is considered the wind speed level at which the maximum power can be obtained. While the cut-out is the maximum wind speed band at which the WT is allowed to operate and is considered a safety constraint exceeding which the operation should be interrupted. These limits are set by each WT manufacturer and are usually depicted on a wind turbine power curve in the technical documentation.

However, only part of the power carried out by wind (expressed in Eq. 3.37) can be captured by the WT and then converted into mechanical and electric power. According to the Betz Law, the theoretical maximum of the kinetic energy that can be converted into mechanical energy, that is into rotation of the WT rotor, is equal to 0.593 (or 59.3%). In practice, however, even the best wind turbines cannot reach this maximum. The real power coefficient values for high-speed two blades HAWTs are in the range of 40-50% and for slow speed WTs with a greater number of blades, it ranges between 20-40% respectively [238], [244]. In relation to modern wind turbines, the value of this coefficient is mainly dependant on the tip speed ratio and pitch-blade angle. Considering that most of the domestic use WTs are not equipped with the pitch control system, it is decided to simplify the calculation and fix this coefficient to 0.40%.

Apart from the power coefficient, the power conversion process also includes a number of losses in the gearbox, bearings and frictions of different parts, (i.e. those losses, associated with transferring power to generating unit inside the WT) referred to as transmission efficiency (η_t) and generator losses, called generator efficiency (η_g). Considering fact that most small WTs are gearless, for simplicity of calculation, it is assumed that the cumulative value for both coefficients (η_t) and (η_g) is fixed to:

$$\eta_c = \eta_t + \eta_g = 0.8 \tag{3.40}$$

Consequently, the electric power output of the WT ($P_{prod.}^{WT}$) [kW] is calculated as:

$$P_{prod.}^{WT}(t) = P_{wind}(t) \times C_p \times \eta_c \times 10^{-3} \tag{3.41}$$

where,

C_p – power coefficient, representing the efficiency of the wind turbine in capturing the wind power [-],

η_c – cumulative efficiency involving WT's (internal) transmission and generation losses [-].

Considering also cut-in, cut-out, and rated wind speed bands, the power output of the wind turbine ($P_{prod.}^{WT}$) in [kW] is expressed as follows:

$$P_{prod.}^{WT}(t) = \begin{cases} 0, & if \quad v_p\,(t) < v_p^{ci} \\ P_{wind}(t) \times C_p \times \eta_c \times 10^{-3}, & if \quad v_p^{ci} \le v_p\,(t) < v_p^{rt} \\ P_{rt}^{WT}, & if \quad v_p^{rt} \le v_p\,(t) < v_p^{co} \\ 0, & if \quad v_p\,(t) \ge v_p^{co} \end{cases} \tag{3.42}$$

where,

P_{rt}^{WT} – rated power output of the WT, according to the manufacturer's technical datasheet [kW].

v_p^{ci}, v_p^{co}, v_p^{rt} – cut-in, cut-out, and rated wind speed bands of the WT [m/s].

In those cases, when the calculated power output value exceeds the rated power value (i.e. $P_{prod.}^{WT}(t) > P_{rt}^{WT}$), the power output of the WT is considered

to be equal to the rated power ($P_{prod.}^{WT}(t) = P_{rt}^{WT}$). The electrical energy produced by the WT ($E_{prod.}^{WT}$) in [kWh] (per minute) is accordingly equal to:

$$E_{prod.}^{WT} = \frac{1}{60} \int P_{prod.}^{WT} \times dt \tag{3.43}$$

3.5.1. Sizing of WT

Wind turbines are considered to be among the most energy-efficient, cost-efficient and cleanest renewable energy sources. Thanks to these positive properties, WTs have become ubiquitous and are considered today one of the most promising solutions to stop the rapid global climate change. However, apart from all the positive properties, these resources also have a negative impact on both the environment and human life. These resources produce noise, vibration, interfere with different radio or television equipment by disrupting the strength of signals and are harmful for the wildlife [245]. That is why, in contrast to PV panels, the requirements for the installation of WTs (especially in populated areas) are much more stringent. In Denmark, it is determined by local municipalities, whether the wind turbine (even individual micro turbine) can be placed within the residential area. In addition to local municipalities, there are also a number of rules and regulations (including safety and environmental certification, noise, vibrations, grid connection, etc.) that have to be complied with before installing any size WT. Reference [246] defines three different options. The first option covers wind turbines with a rotor swept area of 5 m² (blade length of 1.26 m) or less. These WTs can be exempted from registration if they are to be used for very specific purposes like teaching, research, experiments; if the use takes place in demarcated territories without public access; as well as in compliance with all necessary safety requirements, environmental protection, as well as other considerations related to human and domestic animal health. The WTs with an area of 5 – 40 m² (blade length of 3.57 m) must comply with local Danish rules. Whereas the latter option, related to the maximum allowable size up to 200 m² (blade length of 7.98 m), prescribes mandatory certification by ISO 61400-22. The maximum power limit and the maximum length of the wind turbine's mast is allowed to be no more than 25 (kW and metres respectively).

The need to comply with all of these requirements makes the use of micro WTs rather occasional than common in areas with a high population density (more suitable for remote estates or farmsteads). Therefore, the size of the WT of 6 kW is selected not so much for reasons of optimal work or cost-effectiveness, but simply for a visual assessment of performance and for comparison with the performance of PV panels of a similar rate,

while assuming that all of the aforementioned requirements are met. Selected parameters are summarised below.

Table 3.5. Wind turbine parameters.

Parameter	*Description*	*Value*	*Unit*
P_{rt}^{WT}	Rated power	6	[kW]
R	Rotor radius (the length of the wind turbine blade)	2.75	[m]
A	Rotor swept area	23.76	[m²]
H_p	Projected height (hub height)	15	[m]
C_p	Power coefficient (efficiency)	0.4	[-]
η_c	Cumulative efficiency factor	0.8	[-]
v_p^{ci}	Cut-in wind speed band	2.5	[m/s]
v_p^{co}	Cut-out wind speed band	65	[m/s]
v_p^{rt}	Rated wind speed	12	[m/s]
μ	Ground friction coefficient (power-law exponent)	0.143	[-]

3.6. BATTERY

The use of electric batteries is becoming more and more popular every year. Demand for batteries in the residential sector is growing along with growing demand for electric vehicles and private renewables such as rooftop PV panels or individual WTs. Batteries are widely recognized in the scientific community as a resource of energy flexibility and therefore the creation of a battery model and its integration into the overall household model for investigating energy flexibility is a rather interesting aspect of the analysis of this study. Comparison of various electrochemical features of several most widely used battery technologies, made by [247], [248], demonstrates that the lithium-based technologies have the most promising indices nowadays, both in terms of power/energy density, life cycles, efficiency, as well as a rapid trend of price reductions. These metrics prompt concentrating the analysis on this particular (Li-ion) technology. Since the study is focused on performing a long-term dynamic simulation, also, considering that the battery model is only a part of a building model – the complexity of the model created and hence a computational time is of great importance. The created model should be reasonably accurate, but at the same time not very demanding to compute the results.

Authors in [249] highlight that among the variety of models that exist in science, the main attention is paid to improving the design, optimizing some of the physicochemical characteristics and simulating the electrical

circuit. Electrochemical models, which can often be found in science [250], [251] usually focus on the first two aspects and are considered quite resource-demanding models due to their richness with complex numerical algorithms used to coupling a number of partial differential equations. Other common models are electrical. These models are normally used to representing circuit parameters and are often interchangeably called electrical equivalent circuit models involving voltage sources, capacitors and resistors. Models can be, in turn, categorised by Thevenin, impedance and run-time[193]. All of them are, in general, precise and intuitive allowing one to explore different aspects. However, setting up requires rather detailed technical specifications of the investigated equipment, which, depending on the focus of the study, may not always be reasonable. The last group is mathematical models focussed on estimating system-level attributes such as efficiency, run-time, capacity**,** based on empirical mathematical equations [252]. These models are usually made to be fast enough for co-design and co-simulation, however, they do not take into account in-depth electrical circuit characteristics and are not always as accurate as models of the former two groups. Combination of several groups can also in [253].

According to [254], all models, which are focussed on studying the charging characteristics are termed as voltage, lifetime, and performance models [253]. Voltage models can be considered a subset of the aforementioned electrical models, focussing mainly on the terminal voltage for further battery management system modelling. Lifetime models are those, which usually aimed at studying the impact of different operating modes and control schemes on the processes of degradation/ageing of battery cells. While the latter, performance group models are focussed primarily on the capacity (i.e. SOC, SOE). Models laid under this category are by far one of the most commonly used models in energy studies since the level of energy stored in the battery is considered single and the most influencing factor in system assessment. These models are simple enough for co-simulation, co-design and well fitted in the context of this study.

3.6.1. Battery SOE

The capacity of the battery can be expressed in either Ah or kWh. The percentage of available capacity (out of total capacity in Ah), at any given time (t) during a charge or discharge cycle, is commonly known as the State of Charge, while the percentage of available (residual) energy (out of total energy in kWh) is referred to as the State of Energy [255]. Since the study does not intend to analyse the voltage-current or Coulomb characteristics of a battery pack, representation in terms of kWh is more

appropriate. The modelling approach of the dynamics of SOE selected for this study can be expressed by the following equation:

$$SOE^{BAT}(t) = SOE^{BAT}(i) + \frac{\frac{1}{60}\int \Delta P \times dt}{E_{cap.}^{BAT}} \times 100 \tag{3.44}$$

where,

SOE^{BAT} – state of energy of the battery with respect to time (t) [%],

$E_{cap.}^{BAT}$ – total battery capacity [kWh],

ΔP – charging or discharging power (can be positive or negative) [kW].

From the equation above, it can be seen that the SOE of the battery at each new time step is derived by adding energy to the currently available energy level. Depending on the delta power sign (on whether it is positive or negative) the energy is added or retrieved to/from the battery (i.e. the battery is charged or discharged).

Various scientific studies have shown that the power (ΔP) added to or subtracted from the initial capacity can be calculated either linearly or nonlinearly. In the reality, part of the actual power exchanged during charge and discharge cycles is lost differently (indicating nonlinearity). This is mainly due to the inverter/charger efficiency, which is commonly known as round-trip efficiency, and also due to the battery self-discharge over the time. Even though the battery self-discharge can be as high as 5% per day (or 0.208% per hour, as indicated in [140]), and the round trip efficiency can be as low as 58% in some cases [142], the author in [254] argues that the use of linear approximation for energy studies is fairly sufficient and that all advantages of using a nonlinear one are very minor to justify an increase in computing time. This conclusion was made based on the analysis of the following works [256], [257], which demonstrate on the example of electric vehicles that the use of nonlinear approximation does not shorten the time intervals between charging cycles and the difference in charging schedules between two cases is very insignificant. In addition to the aforementioned, the well-known manufacturer [258] indicates the efficiency of their units ranging from 95.2% to 98%. Hence, to simplify and linearize this process it was decided to neglect all system losses, simply assuming that 100% of the energy put into storage can be retrieved back.

Another important factor included in this analysis is the C-rate. The C-rate is defined as the rate at which the capacity of a battery is discharged to cover the load. Usually, it is represented as C/x, where x stands for the

number of hours required to discharge this capacity, however since it is accepted to neglect all the round-trip losses, this C-rate corresponds equally to both discharge and charge. On the other hand, it can also be said that the C-rate defines the maximum possible current that can be charged/discharged (or power, in the context of this study, that can be supplied/retrieved) to/from the battery. For instance, $C/2$ stands for to the current that will discharge the capacity of a battery to its minimum level in two hours [248]. In this study, it is simply assumed that this maximum charge/discharge power corresponds to the inverter charger rated power.

It is also assumed that the battery pack uses a multi-flow technology hybrid inverter charger [258], meaning that the battery converter (which is normally used to convert the current from AC to DC to charge the battery) and the battery inverter (used converting back from DC to AC to feed the load and hence discharge the battery) are the single unit and the maximum allowable power that can pass through this unit (i.e. rated power) is the same in both directions. The energy that can pass through that inverter ($E_{inv.}^{BAT}$) in kWh per one-minute interval, is then equal to:

$$E_{inv.}^{BAT} = \frac{1}{60} \int P_{inv.rt.}^{BAT} \times dt \tag{3.45}$$

where:

$P_{inv.rt.}^{BAT}$ – battery inverter rated power [kW].

3.6.2. The role of the battery in the building model. Equipment layout.

Having such DER components, two different layouts of system equipment (as shown in Figure 3.8) are considered the most popular in terms of grid connectivity (interoperability with the grid) nowadays.

The first scheme (Figure 3.8 a) is aimed at maximizing the use of on-site renewable energy and does not support charging a battery from the grid. With this layout, all electricity generated by on-site RESs will be used primarily to meet the household's own demand. In the case when own generation exceeds consumption, excess energy will be accumulated in the battery and only when the battery charge reaches its maximum level, generation will be redirected (exported) to the grid. Conversely, in case of a lack of own production occurs, the energy stored in the battery will be used first and only when the battery is completely discharged – it will be imported from the grid. All energy flexibility in such an arrangement will mainly depend on the thermal energy storage and control system.

The second scheme (Figure 3.8 b), hypothetically, can provide greater energy flexibility, making it possible to accumulate grid-supplied energy. However, this requires very precise prediction and a following model predictive control so that not to neglect local RES production. The demands accurate prediction of the behaviour of most of the system components. Firstly, it is relevant for weather data so as to consequently predict the potential output of local RESs and estimate the thermal demand, secondly, to predict charging/discharging cycles of the HWST as well as shift the HP load in time, and lastly the SOE of the battery so that to optimally distribute and accumulate power.

It will be interesting to investigate and compare energy flexibility and grid impact simultaneously in both layouts, however, this dissertation is devoted to studying the first scheme.

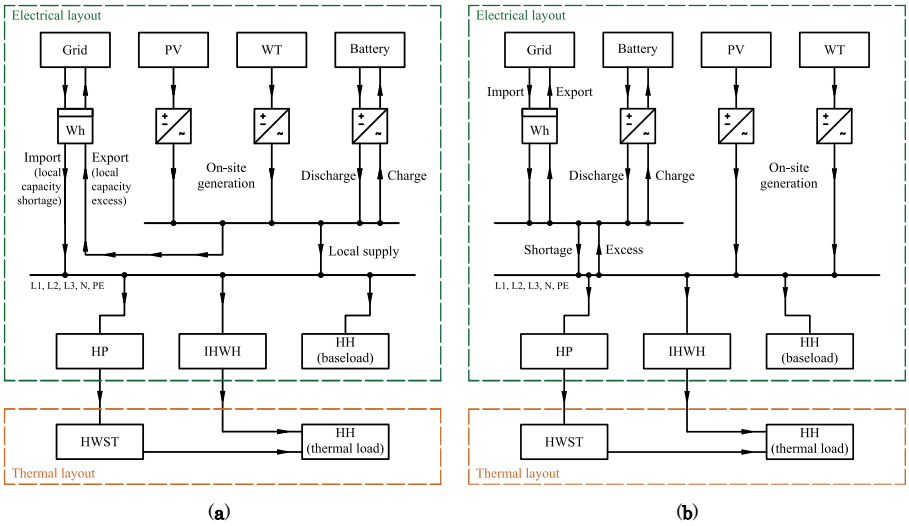

Figure 3.8. The layout of equipment of energy systems integrated into a building: (**a**) the battery is not charged from the grid; (**b**) the battery is charged from the grid.

3.6.3. RES-Battery-Grid power exchange

Considering the aforementioned C-rate, also taking into account the fact that the battery can only be charged using on-site generating capacities, the calculation of SOE of the battery and the conditions for battery charging and discharging, as well as grid export and import (in a case of excess and shortage of local production with respect to demand) are formulated in the following way.

First of all, the laws of physics (in particular, the law of conservation of energy) require the energy balance. For the selected system topology, the electric power balance at each new time step (t) is represented as follows:

$$\Delta P(t) = P^{RES}_{prod.}(t) - P^{HH}_{base}(t) - P^{HP}_{el.dem.}(t) - P^{IHWH}_{el.dem.}(t) \tag{3.46}$$

The ΔP in this equation denotes first battery charging/dischagring power ($P^{BAT}_{chrg.(disch.)}$), and thereafter (depending on the preliminary battery SOE value obtained using Eq. 3.44 above), the grid imported or exported power ($P^{GRID}_{imp.(exp.)}$). The $P^{RES}_{prod.}$ represents the summation of the power outputs of a PV array and a wind turbine (according to Eq. 3.33 and 3.41):

$$P^{RES}_{prod.}(t) = P^{PV}_{prod.}(t) + P^{WT}_{prod.}(t) \tag{3.47}$$

where:

$P^{RES}_{prod.}$ – power produced by RESs [kW],

P^{HH}_{base} – baseload of the household (without HP) [kW],

$P^{HP}_{el.dem.}$ – electric power demand of the HP [kW],

$P^{IHWH}_{el.dem.}$ – electric power demand of the IHWH [kW].

The delta energy (ΔE) in [kWh] per one-minute interval is respectively:

$$\Delta E = \frac{1}{60} \int \Delta P \times dt \tag{3.48}$$

All the conditions for calculating the SOE, are split into two main parts reflecting the excess (i.e. when the $\Delta P > 0$) and the shortage of local RES production (i.e. when the $\Delta P < 0$). To calculate the SOE, in this study, it is decided to introduce the temporary variable ($SOC^{BAT}_{temp.}$), which serves just for pre-quantifying the actual SOE value. The actual final SOE value depends on whether the delta power (ΔP), at each new time step (t), exceeds the rated power of the battery inverter ($P^{BAT}_{inv.rt.}$) and whether the upper/lower charge/discharge limits are reached. Thus, there will also be several sub-parts related to the rated power of the battery inverter and the maximum and minimum battery levels, respectively. For ease of understanding, these conditions are reflected in the flowchart, Figure 3.9.

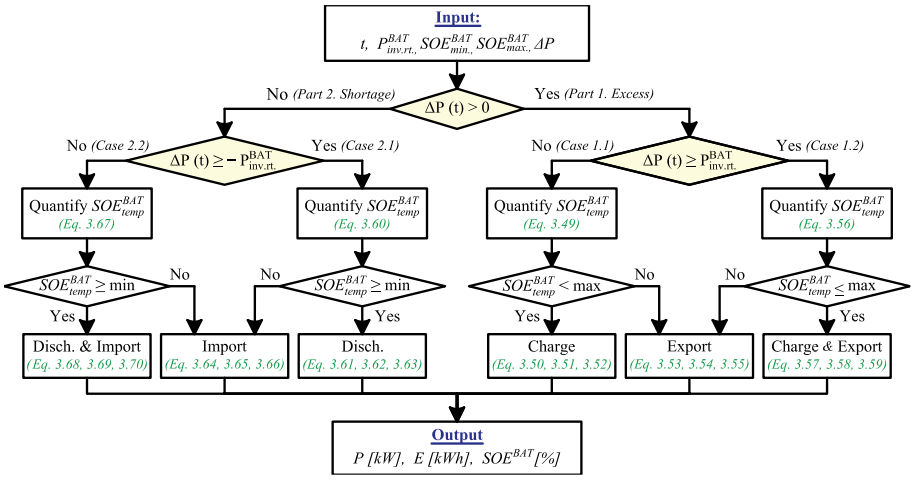

Figure 3.9. Flowchart of the RES-Battery-Grid power exchange.

Part 1. Excess. $\Delta P(t) > 0$

When the excess of local production occurs, the excessed energy can be either stored in the battery or exported to the grid depending on the inverter rated power and the maximum energy level of the battery.

Case 1.1. $\Delta P(t) < P^{BAT}_{inv.rt.}$

In the first case, when the delta power is lower than the inverter rated power, battery charging is only constrained by the maximum SOE band. The preliminary SOE value, in this case, is quantified as:

$$SOE^{BAT}_{temp.}(t) = SOE^{BAT}(i) + \frac{\Delta E(t)}{E^{BAT}_{cap.}} \times 100 \tag{3.49}$$

When the value is already known, then it is checked whether it does not exceed the maximum battery limit and, thus, whether this energy can be charged into the battery or should be partially or fully exported to the grid.

If $SOE^{BAT}_{temp.}(t) < SOE^{BAT}_{max}$, all excess power/energy production is added to the battery. There is no export to the grid, in this case, the SOE of the battery is equal to the preliminary calculated value.

$$P^{BAT}_{chrg.}(t) = \Delta P(t) \quad and \quad E^{BAT}_{chrg.}(t) = \Delta E(t) \tag{3.50}$$

$$P^{GRID}_{exp.}(t) = 0 \quad and \quad E^{GRID}_{exp.}(t) = 0 \tag{3.51}$$

$$SOE^{BAT}(t) = SOE^{BAT}_{temp.}(t) \tag{3.52}$$

If $\boldsymbol{SOE^{BAT}_{temp.}(t) \geq SOE^{BAT}_{max}}$, all excess power production is, accordingly, exported to the grid and the SOE remains unchanged from its previous value.

$$P^{BAT}_{chrg.}(t) = 0 \quad and \quad E^{BAT}_{chrg.}(t) = 0 \tag{3.53}$$

$$P^{GRID}_{exp.}(t) = \Delta P(t) \quad and \quad E^{GRID}_{exp.}(t) = \Delta E(t) \tag{3.54}$$

$$SOE^{BAT}(t) = SOE^{BAT}(i) \tag{3.55}$$

where:

$P^{BAT}_{chrg.}, P^{GRID}_{exp.}$ – battery charging power and power exported to the grid [kW],

$E^{BAT}_{chrg.}, E^{GRID}_{exp.}$ – energy charged into the battery and exported to the grid per minute time interval [kWh],

SOE^{BAT}_{max} – maximum battery state of energy band [%].

Case 1.2. $\boldsymbol{\Delta P(t) \geq P^{BAT}_{inv.rt.}}$

In the case when the delta power is greater or equal to the inverter rated power, the amount of energy that can be charged to the battery within a single time step (t) is even smaller when compared to *Case 1.1* (i.e. constrained also by the inverter rated power). Accordingly, the export of energy to the grid will take place even in those cases when the battery is not fully charged. The temporary SOE value, in this case, is quantified as:

$$SOE^{BAT}_{temp.}(t) = SOE^{BAT}(i) + \frac{E^{BAT}_{inv.}}{E^{BAT}_{cap.}} \times 100 \tag{3.56}$$

As in the previous case, it is then checked the relation to the maximum SOE band.

If $\boldsymbol{SOE^{BAT}_{temp.}(t) \leq SOE^{BAT}_{max}}$, one part of the power that can pass through the inverter is charged to the battery, while the remaining part is exported to the grid. The SOE of the battery is equal to the pre-calculated value:

$$P^{BAT}_{chrg.}(t) = P^{BAT}_{inv.rt.} \quad and \quad E^{BAT}_{chrg.}(t) = E^{BAT}_{inv.}(t) \tag{3.57}$$

$$P^{GRID}_{exp.}(t) = \Delta P(t) - P^{BAT}_{inv.rt.} \quad and \quad E^{GRID}_{exp.}(t) = \Delta E(t) - E^{BAT}_{inv.}(t) \tag{3.58}$$

$$SOE^{BAT}(t) = SOE^{BAT}_{temp.}(t) \tag{3.59}$$

If $\boldsymbol{SOE^{BAT}_{temp.}(t) > SOE^{BAT}_{max}}$, as in *Case 1.1*, all excess power is exported to the grid. The power/energy and SOE values are obtained as shown in (Eq. 3.53, 3.54, 3.55).

Part 2. Shortage. $\boldsymbol{\Delta P(t) < 0}$

The second part depicts the situation when there is a shortage of local production occurs. The energy required to cover demand, in this instance, can be either discharged from the battery or imported from the grid depending on the inverter rated power and the minimum energy level of the battery.

Case 2.1. $\boldsymbol{\Delta P(t) \geq -P^{BAT}_{inv.rt.}}$

In the first case, when the delta power is greater or equal to the negative value of the inverter rated power, the battery discharging is only constrained by the minimum SOE band. The preliminary SOE value, in this case, is quantified as:

$$SOE^{BAT}_{temp.}(t) = SOE^{BAT}(i) + \frac{\Delta E(t)}{E^{BAT}_{cap.}} \times 100 \tag{3.60}$$

Following the procedure described in *Part 1*, this temporary $\mathrm{SOE}^{\mathrm{BAT}}_{\mathrm{temp.}}$value is then checked in relation to the minimum battery band and, thus, whether this shortage energy can be discharged from the battery or should be partially or fully imported from the grid.

If $\boldsymbol{SOE^{BAT}_{temp.}(t) \geq SOE^{BAT}_{min}}$ the power is only extracted from the battery. There is no import from the grid and the actual SOE of the battery is equal to the preliminary calculated value:

$$P^{BAT}_{disch.}(t) = \Delta P(t) \quad and \quad E^{BAT}_{disch.}(t) = \Delta E(t) \tag{3.61}$$

$$P^{GRID}_{imp.}(t) = 0 \quad and \quad E^{GRID}_{imp.}(t) = 0 \tag{3.62}$$

$$SOE^{BAT}(t) = SOE^{BAT}_{temp.}(t) \tag{3.63}$$

If $\boldsymbol{SOE^{BAT}_{temp.}(t) < SOE^{BAT}_{min}}$ all power is, respectively, imported from the grid and the SOE remains unchanged from its previous value:

$$P^{BAT}_{disch.}(t) = 0 \quad and \quad E^{BAT}_{disch.}(t) = 0 \tag{3.64}$$

$$P_{imp.}^{GRID}(t) = \Delta P(t) \quad and \quad E_{imp.}^{GRID}(t) = \Delta E(t) \tag{3.65}$$

$$SOE^{BAT}(t) = SOE^{BAT}(i) \tag{3.66}$$

where:

$P_{disch.}^{BAT}$, $P_{imp.}^{GRID}$ – battery discharging power and imported power [kW],

$E_{disch.}^{BAT}$, $E_{imp.}^{GRID}$ – energy discharged from the battery and imported from the grid per minute time interval [kWh],

SOE_{min}^{BAT} – minimum battery state of energy band [%].

Case 2.2. $\boldsymbol{\Delta P(t) < -P_{inv.rt.}^{BAT}}$

This case describes a situation opposite to *Case 1.2*, i.e. when the discharge power is limited by the inverter rated power. Respectively, the import of power from the grid will occur, even when the battery is not completely discharged and the share of energy imported from the grid at the end will be greater than in *Case 2.1.* The temporary SOE value, in this case, is quantified as:

$$SOE_{temp.}^{BAT}(t) = SOE^{BAT}(i) - \frac{E_{inv.}^{BAT}}{E_{cap.}^{BAT}} \times 100 \tag{3.67}$$

Similar to the previous case, this preliminary calculated value is then checked in relation to the lower battery band.

If $\boldsymbol{SOE_{temp.}^{BAT}(t) \geq SOE_{min}^{BAT}}$, the part of the power that is limited by the inverter rated power is discharged from the battery and the rest is imported from the grid. The actual SOE of the battery is equal to the pre-calculated value.

$$P_{disch.}^{BAT}(t) = -P_{inv.rt.}^{BAT} \quad and \quad E_{disch.}^{BAT}(t) = -E_{inv.}^{BAT}(t) \tag{3.68}$$

$$P_{imp.}^{GRID}(t) = \Delta P(t) + P_{inv.rt.}^{BAT} \quad and \quad E_{imp.}^{GRID}(t) = \Delta E(t) + E_{inv.}^{BAT}(t) \tag{3.69}$$

$$SOE^{BAT}(t) = SOE_{temp.}^{BAT}(t) \tag{3.70}$$

If $\boldsymbol{SOE_{temp.}^{BAT}(t) < SOE_{min}^{BAT}}$, as in *Case 2.1.* all shortage power is imported from the grid. The power/energy and actual SOE values are obtained as shown in (Eq. 3.64, 3.65, 3.66).

3.6.4. Sizing of Battery

For determining the size of the battery, the study investigated the trade-off between battery ageing and cost minimization. The objective function is to minimize the total annual expenditures of the household owner, that is the electricity bill per annum, whereas taking into account the battery investment cost, its lifetime, and payback period. The calculation considers the following:

- the electric power demand of the households (incl. heat pump load);
- PV array power output;
- the total amount energy imported from and exported to the grid, per annum;
- electricity price for households in Denmark (i.e. DKK 2.25 [66]) and hence the cost of energy imported from the grid;
- the weighted average of the spot price in both Danish price zones DK1, DK2 for the last 5 years (i.e. DKK 0.25 per kWh [259]). This price has been used for several purposes:
    - to quantify the cost of energy exported to the grid. In this regard, it is worth mentioning that the flexible settlement scheme described in Section 2.1.1 is not fully taken into account (only its flexible part), therefore the total cost is approximate and can be somewhat underestimated;
    - to calculate the payback of the battery, where a price of DKK 0.25 (same as for export) has been assigned for each kWh of energy charged or discharged to or from the battery;
- battery lifespan of 10 years;
- Li-ion battery price (DKK 400 per kWh).

Battery lifespan and price per kWh have been selected based on information provided on the official Tesla Powerwall webpage. The manufacturer provides a 10-year unlimited cycle warranty, at the same time declaring a loss of capacity of no more than 30% over a period of 10 years [260]. The battery price per kWh is determined from the total cost of the Powerwall as of April 2021, i.e. USD 8500 / 13.5 kWh (total usable energy) / 10 (lifespan) x DKK 6.3 (exchange rate) ≈ DKK 400.

The optimal battery size (total energy value) is calculated using GLPK linear programming optimizer within the Python environment and is equal to 14.1 kWh. The battery power (or, in other words, the rated power of the inverter charger) is selected based on the specification given in [258], which indicates the nominal charging power of 66% of the total energy. The same reference indicates that only 80% of total energy can be used,

therefore, the minimum and maximum SOE bands, are set to 10% and 90%, respectively. The selected battery parameters are as shown below.

Table 3.6. Battery parameters.

Parameter	*Description*	*Value*	*Unit*
$E_{cap.}^{BAT}$	Total energy	14.1	[kWh]
$P_{inv.rt.}^{BAT}$	Inverter charger rated power (37% of total energy)	9.3	[kW]
SOE_{max}^{BAT}	Maximum battery state of energy band	90	[%]
SOE_{min}^{BAT}	Minimum battery state of energy band	10	[%]

3.7. CHAPTER SUMMARY

The chapter demonstrates the process of creating models of the following building components: heat pump, hot water storage tank, instantaneous heating water heater, PV array, micro wind turbine, and battery. Each section provides a literature review and basic information, including some physical attributes and main parameters on each component. Special attention is paid to the model of a heat pump system, highlighting such features of the system's operation as conversion delay, defrosting mode, restart delay and prespecified power on time. Since heating accounts for the major share of a building's total energy consumption, the heat pump and hot water storage tank are considered the largest source of energy flexibility of the household. Therefore, these models are created in more detail. Each section of this chapter also describes the principles and methodologies based on which the size of one or another component was selected. All models shown in this chapter are well suited to perform a simulation with a one-minute step. The one-minute step has significant advantages over the 15-minute step, providing the ability to visually analyse the behaviour of the simulated systems, and also greatly simplifies the process of quantifying energy flexibility, which is one of the main aspects of the analysis in this study.

4 PERFORMANCE ANALYSIS OF A SINGLE BUILDING AND A GROUP OF BUILDINGS EQUIPPED WITH DISTRIBUTED ENERGY RESOURCES

This section demonstrates the performance of an energy system of a single house and a group of 25 houses by combining different DERs. Six simulation scenarios with different combinations of local distributed energy resources are applied to conduct the study/evaluations. The purpose of this analysis is to demonstrate how the increase in household load impact the overall power demand and energy consumption of a single house and group of houses. Furthermore, how the emergence of own renewable sources and battery changes the need for power supply from the grid (referred to here as an import), and the amount of excessed energy fed into the grid (referred to here as an export). This is to provide answers to the following research questions.

«How does the emergence of on-site RESs affect the energy needs of the household and whether the presence of a battery can completely reduce dependence on the grid, including the need to export excess RESs generation? In this regard, could on-site RESs generation be considered load reduction to the power system and hence an improvement of energy efficiency? Furthermore, how can the replacement of the domestic heat source (where fossil fuel might have been employed) with HP increase the energy efficiency of the household when this substitution significantly increases its electricity demand? Can on-site RESs coupled with battery compensate for this heat source shift by covering the increased power demand with local generation»?

4.1. PERFORMANCE ANALYSIS OF A SINGLE BUILDING

This section aims to investigate, analyse, and evaluate the performance of modelled systems using basic settings and basic control, as described in the previous chapter. Six different scenarios for combining the created models under a single coordination algorithm are considered as likely scenarios for the modernization of household energy systems. The scenarios are as follows.

- S1. Baseload (serves as a reference point)
- S2. Baseload + RESs (including PV or WT, or both PV & WT);
- S3. Baseload + RESs + Battery (incl. two different battery sizes);
- S4. Baseload + HPS (incl. two different HWST sizes);
- S5. Baseload + HPS + PV;
- S6. Baseload + HPS + PV + Battery.

4.1.1. S1. Baseload

The baseload used for this study is historically measured time-series data for an average single-family dwelling located in Northern Denmark. The load profile of this house has already been presented and described in the previous chapter (Section 3.2.1, Figure 3.3).

4.1.2. S2. Baseload + RESs

The system setup for the second scenario including both electrical layout and the sequence of combining model components within the Matlab environment is presented in Figure 4.1.

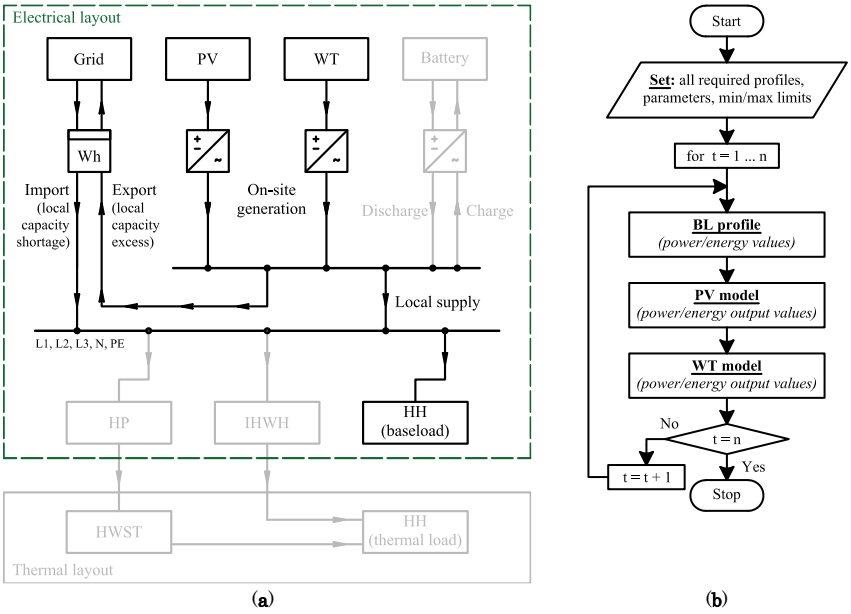

Figure 4.1. Building energy system setup according to scenario S2: (a) layout of electrical components; (b) layout of Matlab models.

Table 4.1 and Figure 4.2 below represent the power output profiles of both PV panels and wind turbine. The left column refers to PV panels, the right one to the WT. It is clearly seen from graphs **a2** and **a3** (depicting the daily and weekly profiles of PV production) that generation is present only in the daytime. This emphasizes the direct dependence of PV panels on the presence of the sun and clearly reflects the solar radiation profile shown in Figure 3.5 **a** (Section 3.2). The WT output, in turn, also clearly reflects the wind speed profile shown in Figure 3.5 **b**. Since solar radiation in Denmark rarely reaches the nominal 1000 W/m^2, the maximum peak generation (as can be seen from Figure 4.2 **a4**, **a5**) is only 4.9 kW, with an installed capacity of 6 kW. The situation with the wind is the opposite. As the wind activity in Denmark is quite high, the wind turbine reaches its peak generation of 6 kW quite often (graphs **b4**, **b5** in Figure 4.2). However, wind activity in the residential sector is still significantly less than in open areas or offshore. Thus, having a nominal wind speed of 12 m/s (for a given WT), a relatively low generation can be observed for many months throughout the year (Figure 4.2 **b4**, **b5, c**). Bar chart Figure 4.2 **c** and Table 4.1 below summarize the monthly electricity generation indices and show that PV generation has higher average production than the wind turbine from March to September. In October, February and April, the difference between the two resources is insignificant. Whereas, from November to January, much higher average performance is demonstrated by the wind turbine. The pie chart shows that the share of energy generated during the year, in the case of a WT, is 10% less than PV panels.

Table 4.1. Performance summary of PV panels versus wind turbine.

Months	*PV panes*		*Wind turbine*		*Total energy production [kWh]*
	Peak power [kW]	*Energy [kWh]*	*Peak power [kW]*	*Energy [kWh]*	
January	3.3	115	6.0	374	489
February	4.1	194	4.6	134	328
March	4.6	619	6.0	501	1,120
April	4.8	666	6.0	597	1,263
May	4.9	659	6.0	380	1,039
June	4.9	708	6.0	351	1,059
July	4.9	794	4.1	274	1,068
August	4.7	639	4.5	250	889
September	4.7	513	3.9	192	705
October	4.7	267	6.0	291	558
November	4.1	182	5.8	334	516
December	3.0	101	6.0	811	912
Total per year	**5,458**			**4,493**	**9,951**

Lower generation indices and much more stringent installation requirements in the residential sector make micro wind turbines much less attractive for individual use. Nevertheless, it is interesting to examine

both of these resources (separately and together) in relation to household consumption.

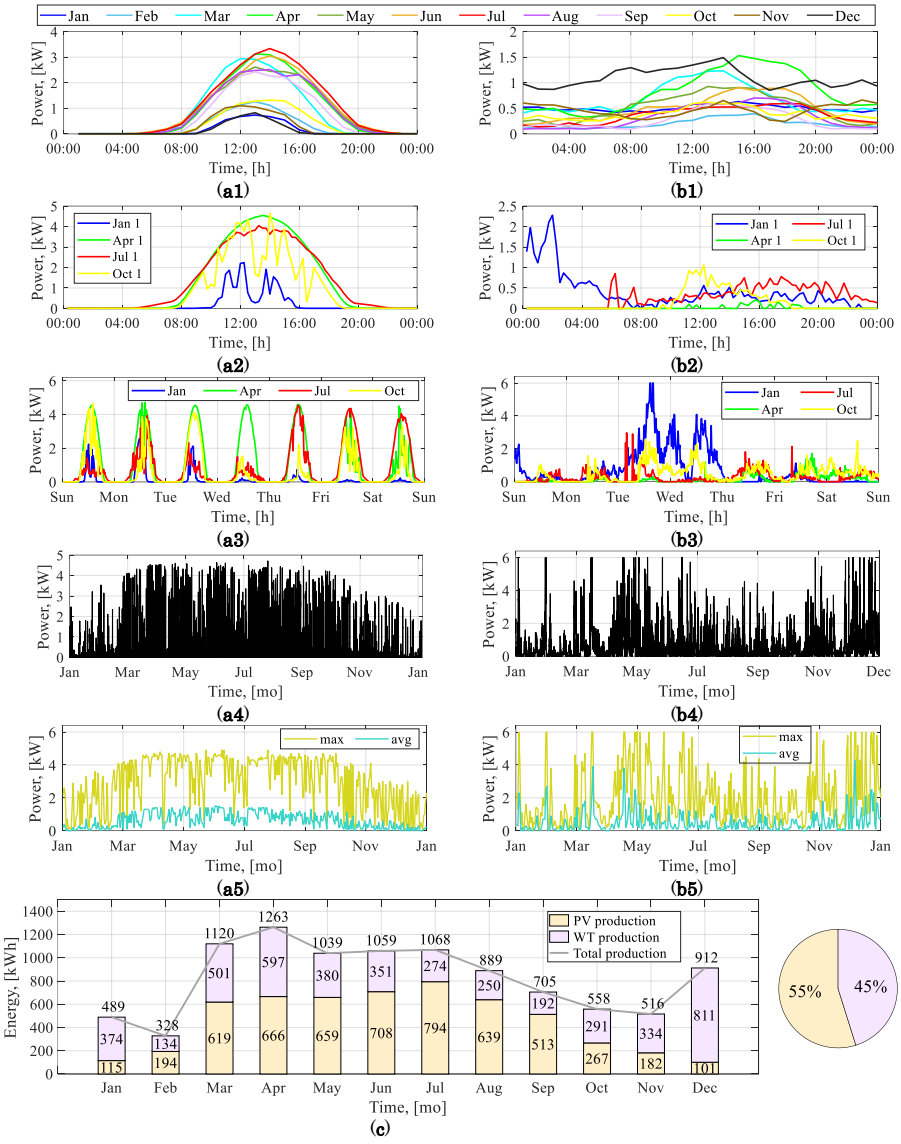

Figure 4.2. Power output profiles of RESs: (**a**) PV array; (**b**) Wind turbine; 1) hourly mean values at a specific month; 2) one day at a specific month; 3) one week at a specific month; 4) a whole year; 5); daily maximum and daily mean throughout the year; 6) monthly energy production; (**c**) monthly summary.

The following paragraphs represent the performance indices of PV, WT, and co-production of PV and WT taking into account the baseload of the household. The two graphs in Figure 4.3 represent the total production of PV panels and wind turbine, as well as the delta power (i.e. excess and shortage of own production) for a period of three days in April (April 20-22). Since there is no energy storage option, in this case, all excess PV generation is fed into the power grid (i.e. exported). Conversely, the shortage of own production is fully compensated by the import of electricity from the grid. Figure 4.3 shows an export during periods of high generation and low consumption (mainly daytime) and import when the production is low (in the evening, night and in the morning time).

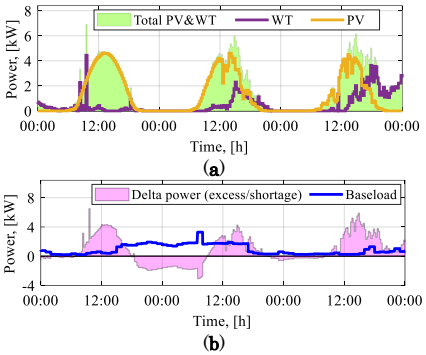

Figure 4.3. Three days in April demonstrating the performance of RESs in relation to baseload: (**a**) power output of PV array and WT; (**b**) excess and shortage of own production.

The following bar and pie charts in Figure 4.4 represent monthly and yearly self-sufficiency indices for three applications of RESs (PV, WT, PV+WT). Due to the fact that the electricity consumption of the household in cold months is larger than in the warm period (blue line), as well as given the fact that the wind turbine shows better performance in the cold months (Figure 4.2 **c**), it can be seen that the self-sufficiency rate in WT case is 2% better than in PV (pie charts (**a**) and (**b**) in Figure 4.4). Whereas the presence of both PV panels and a wind turbine in the household reduces the annual need for electricity supply from the grid (i.e. the imported share) down to 43%, which is a fairly good result, considering the absence of any energy storage. However, as can be seen from the bar charts (**a**) and (**c**), the export share (marked with light brown background) in the case of solar panels, as well as in joint PV&WT application is also quite significant. From the perspective of the DSOs, it is always important that the share of export is within reasonable limits. The consequences of high export may result in voltage peaks, which may significantly affect the

sensitivity and different parameters of the protection system. In some cases, it may also be harmful to the grid operation and its infrastructure.

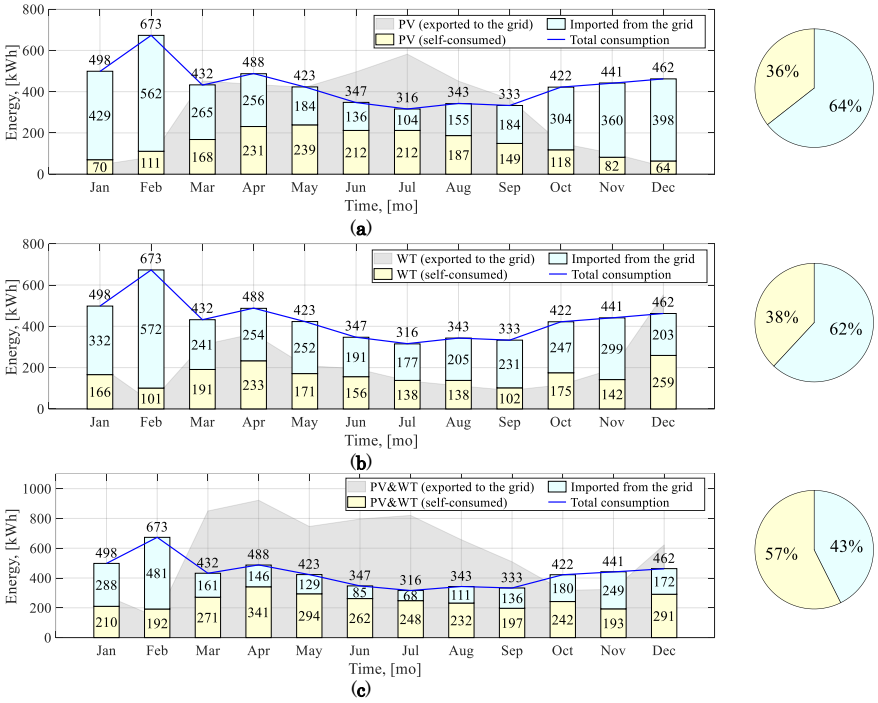

Figure 4.4. Monthly and annual self-sufficiency* indices, in the case of application of (**a**) PV array; (**b**) WT; (**c**) combined PV and WT.

Figure 4.5 below depicts shares of own consumption and energy exported to the grid in all three cases. The bar- and pie charts show that the WT (pie chart **b**) has the smallest share of export and the largest share of own consumption. This can simply be explained by the fact that the WT generated less energy than PV on an annual basis (see Table 4.3 above), as well as by the fact of the presence of load in the evening and night when there is WT production. Table 4.2 summarise all the aforementioned indices and numerically confirms the above statement.

All the existing, technical and regulatory aspects (discussed in Section 2.1 and 2.2) encourage focussing not so much on the financial benefit from exported energy, as on maximizing self-sufficiency and own consumption share as well as on providing additional services of flexible energy use. The use of an electric battery, in this context, is one of the potential methods for implementing the above.

* Self-sufficiency, in this context, is the share of energy consumption (out of the total consumption) covered by an on-site generating unit.

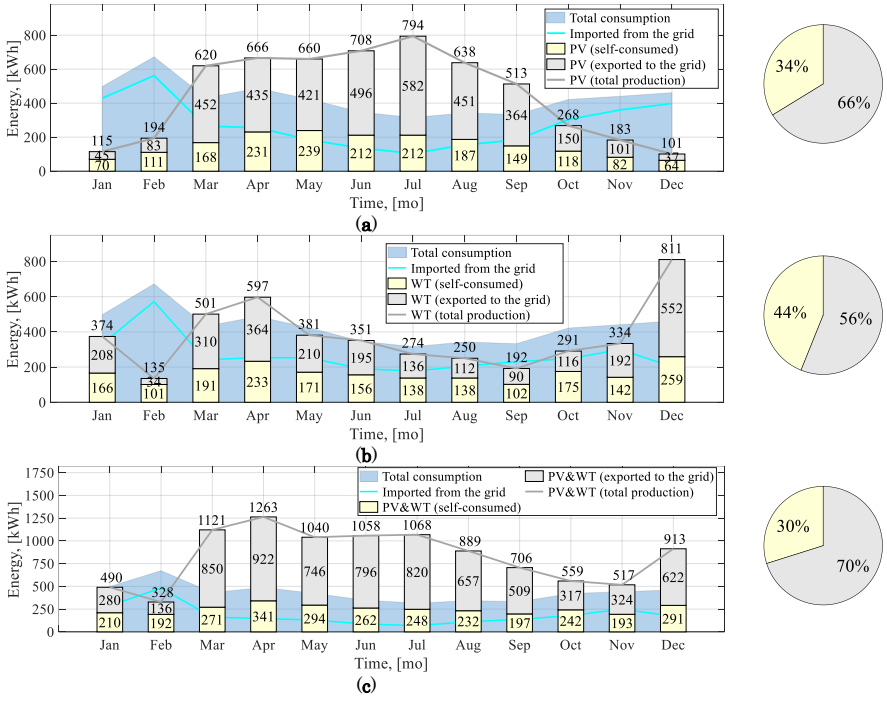

Figure 4.5. Monthly and annual own consumption* indices, in the case of application of (**a**) PV array; (**b**) WT; (**c**) combined PV and WT.

Table 4.2. Summary of the production of PV panels, WT, and co-production of PV and WT in relation to baseload.

Months	***Energy in [kWh]***									
	Baseload	**Imported** from the grid			*Own production* ***self-consumed***			*Own production* ***exported*** *to the grid*		
		PV	*WT*	*PV&WT*	*PV*	*WT*	*PV&WT*	*PV*	*WT*	*PV&WT*
Jan	498	429	332	288	70	166	210	45	208	280
Feb	673	562	572	481	111	101	192	83	34	136
Mar	432	265	241	161	168	191	271	452	310	850
Apr	488	256	254	146	231	233	341	435	364	922
May	423	184	252	129	239	171	294	421	210	746
June	347	136	191	85	212	156	262	496	195	796
July	316	104	177	68	212	138	248	582	136	820
Aug	343	155	205	111	187	138	232	451	112	657
Sept	333	184	231	136	149	102	197	364	90	509
Oct	422	304	247	180	118	175	242	150	116	317
Nov	441	360	299	249	82	142	193	101	192	324
Dec	462	398	203	172	64	259	291	37	552	622
Total	**5,179**	**3,337**	**3,205**	**2,207**	**1,842**	**1,974**	**2,972**	**3,616**	**2,519**	**6,979**

* Own consumption is the share of self-consumed energy out of the total production of an on-site generating unit.

4.1.3. S3. Baseload + RESs + Battery

Following the logic of the previous sections, the system setup for the third scenario is presented in Figure 4.6.

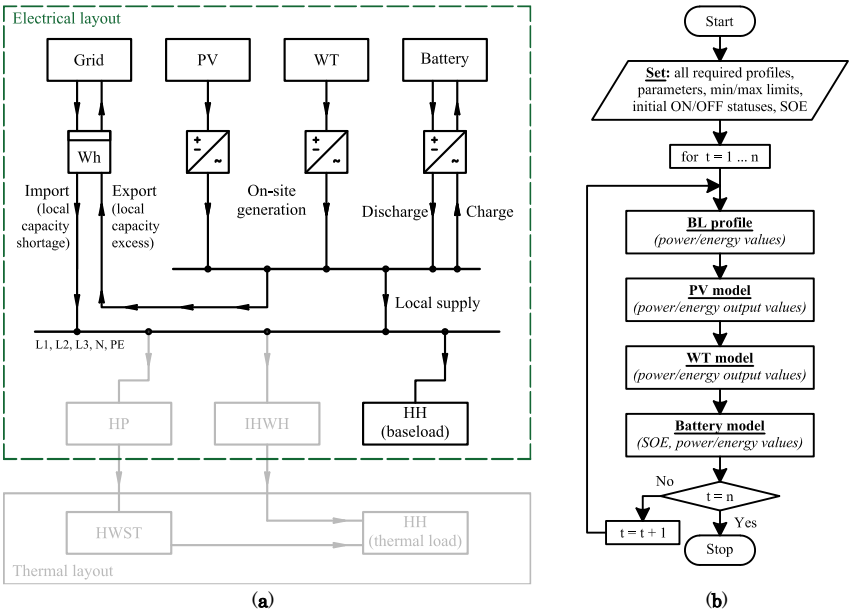

Figure 4.6. Building energy system setup according to scenario S3: (a) layout of electrical components; (b) layout of Matlab models.

Although the optimal battery size has been determined in the previous chapter (i.e. energy – **14.1 kWh**, power **9.3 kW**), one of the aspects of the study is also to analyse the impact of battery size on the amount of electricity imported from the grid, and thus the ability of the battery to significantly increase own renewable energy use and the ability to provide autonomy of power supply. For this purpose, it was decided to analyse one more scenario of the battery size, which is the double-size of the first one, namely, **28.2 kWh**, **18.6 kW**. Considering that the typical battery size for residential PV installations is varied between 4.5–12 kWh [140], also taking into account that the maximum peak load of the selected house recorded during the simulation is 12.5kW (i.e. 1.1 kW – baseload, 5.4 kW – HP load, and 6.0 kW – IHWH load) and that the maximum simultaneous output power of RESs is 10.4 kW (i.e. 4.4 kW – PV, 6.0 kW – WT), this battery size is, in principle, enormously large for an average household. Just for comparison, this size is about half of the battery capacity installed in electric vehicles suchlike the Nissan Leaf (~40 to 60 kWh) and from half to one-third of the Tesla Model 3 (~52 to 82 kWh).

The figures below show an example of energy exchange in the RES-battery-grid connected power supply system of the household. The system performance is demonstrated in the month with the best generation (namely April, as shown in Figure 4.2 above). For the demonstration, the same period of April 20-22 (as shown in Figure 4.3 above) is selected. These three days have an advantage by showing the full discharge and charge cycle of both batteries and are also one of the best periods for demonstrating the distribution of energy between own consumption, accumulation in the battery and export to the grid. All graphs in Figure 4.7 below depict the performance with PV&WT co-production and baseload only (excluding heat pump share). The left column (graphs **a1** – **a4**) shows the performance with the battery №1, the right with the battery №2. Graphs **a1**, **b1** show the total production of both RESs, delta power and baseload; **a2**, **b2** – SOE for both batteries; **a3**, **b3** – the amount of power charged to/discharged from the battery; **a4**, **b4** – the amount of power imported to/exported from the grid. From graph **b2** it can be seen that since the second battery is larger, the discharge/charge cycle lasts longer with the same load and generation. Graphs **a3**, **a4** and **b3**, **b4** show the distribution of delta power depending on battery SOE and show that with a lack of own production of RESs, energy is first taken from the battery (**a3**, **b3**, around 00:00), and when the battery reaches a minimum SOE – imported from the grid (**a4**, **b4** between 00:00 and 12:00 in the second day). And the same with excess energy. The period around 12:00 on the second day shows the charge of this energy in the battery, and upon reaching the maximum level of SOE - export to the grid. Three days show that in those periods when there is no own generation and the battery has previously been fully charged, even a double battery size cannot provide autonomy of power supply for a long period of time. Even with considerable co-generation of PV and WT and only the baseload, a full discharge can be seen in less than a 12-hour period. And the graphs **a1**, **b1** in Figure 4.8, on the example of SOE for both batteries, show that in months with a very low level of generation, self-sufficiency is simply not possible. February and April are selected for visual comparison of the difference since it is in these months both PV panels and WT (as shown in Figure 4.2 **c** above) have demonstrated the lowest (February) and the highest (April) energy production during the year.

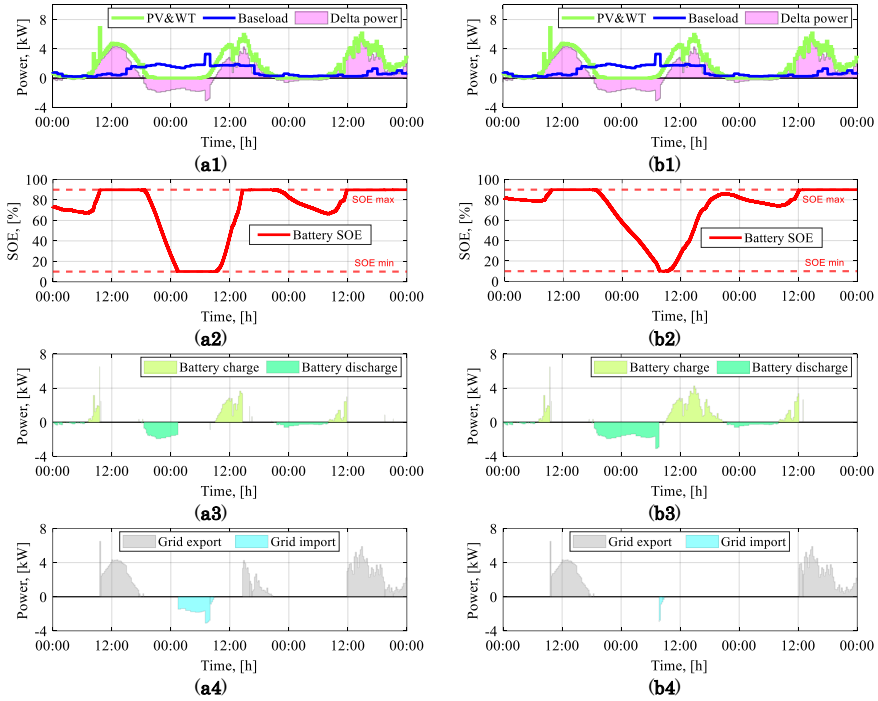

Figure 4.7. The performance of the energy system of building under scenario S3 (simulation results): (**a**) performance of RESs in relation to baseload; (**b**) SOE of the battery; (**c**) battery charge/discharge power; (**d**) power imported/exported to the grid; 1) battery №1; 2) battery №2.

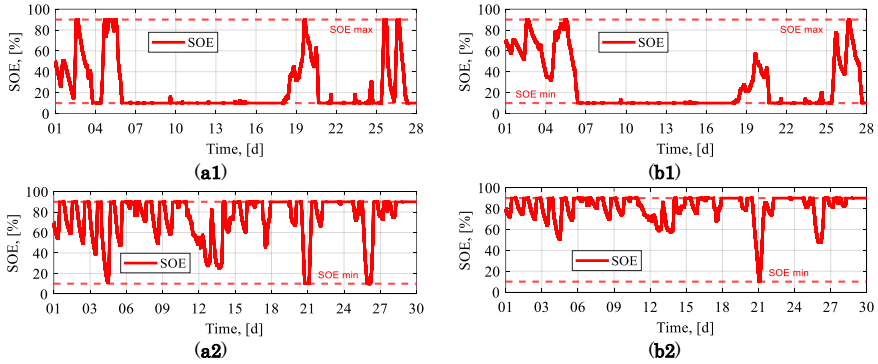

Figure 4.8. SOE of two batteries at a specific month: (**a**) Battery №1; (**b**) Battery №2; 1) February; 2) April.

The figures below illustrate self-sufficiency and own -consumption indices for three different scenarios of application of RESs and two batteries. It can be seen that double battery size has a very small effect on the

autonomy in all three cases of RESs application. The difference between the scenario with battery 1 and battery 2 varies from 2% to 6%, which in principle is a very small difference against the background of double size. Thus, the demonstration of the scenario with battery 2 is meaningless and all further comparisons will apply only to battery 1. Nonetheless, the mere fact of having a battery, in the case of PV (Figure 4.9 **a1**), almost doubled these indices, compared with the case without the battery at all (see Figure 4.4 a). In the case of PV, the share of import decreased by –28% (from 64% to 36%), WT by –19% (from 62% to 43% compared to Figure 4.4 **b**, above). From Figure 4.9 **c1**, it can be seen that the presence of the battery also significantly increased the share of consumption covered by both RESs (by 27% compared to Figure 4.4 **c**). However, in the case of combined PV&WT use, the export share depicted in Figure 4.10 **c1** decreased non-linearly, compared to the case without the battery (Figure 4.5 **c**), only by –14% (from 70% to 56%). This once again testifies to the uneven power generation in different months and the inability of the battery (while having a low power demand of the household) to accumulate all excess energy. Whereas in PV this dependence is almost mirror-like –26% (from 66% to 40%) and in the case of WT –22% (from 56% to 28%).

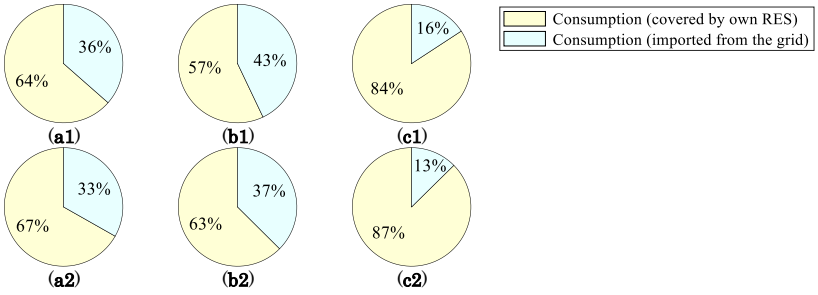

Figure 4.9. Annual self-sufficiency indices for different RESs and batteries (**a**) PV panels; (**b**) WT; (**c**) both PV and WT; (**1**) – battery №1; (**2**) – battery №2.

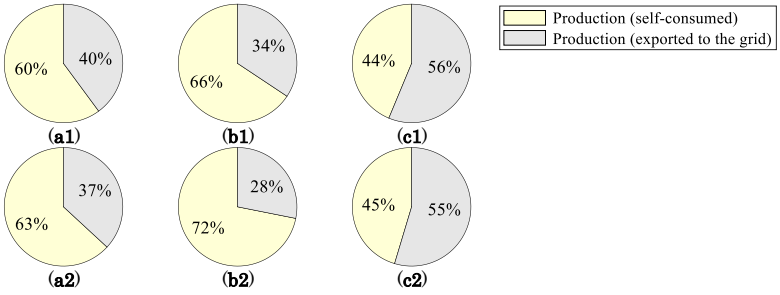

Figure 4.10. Annual own consumption indices for different RESs and batteries (**a**) PV panels; (**b**) WT; (**c**) both PV and WT; (**1**) – battery №1; (**2**) – battery №2.

All monthly indices for each of the above cases of RESs application are summarized in Table 4.3 below. The table shows very insignificant imports from May to September in the case of PV and battery 1, while in the case of battery 2 there is no import in these months, which cannot be said for the wind turbine. The data of the co-production of PV and WT are given only for visual, more detailed, clarification in which months the largest import/export is and why full autonomy is impossible.

Table 4.3. Summary of the production of PV panels, WT, and co-production of PV and WT for two different battery scenarios.

		Energy in [kWh]								
Months	**Battery scenario**	**Imported** from the grid having			*Own production* ***self-consumed***			*Own production* ***exported*** *to the grid*		
		PV	*WT*	*PV&WT*	*PV*	*WT*	*PV&WT*	*PV*	*WT*	*PV&WT*
Jan	**Battery 1** (14.1 kWh, 9.3 kW)	372	272	205	115	220	288	0	154	202
Feb		499	544	396	176	134	281	17	0	47
Mar		87	162	8	351	260	423	269	241	698
Apr		67	173	13	421	326	477	245	271	786
May		20	123	0	401	288	419	258	92	620
June		10	125	2	341	233	348	367	118	710
July		0	91	0	314	214	315	479	60	753
Aug		3	122	0	339	232	344	300	18	545
Sept		17	158	0	316	164	331	197	29	374
Oct		181	152	25	231	270	391	36	21	167
Nov		267	220	115	174	222	322	8	113	194
Dec		361	76	51	101	386	411	0	425	501
Total		**1,885**	**2,217**	**815**	**3,282**	**2,950**	**4,352**	**2,176**	**1,542**	**5,598**
Jan	**Battery 2** (28.2 kWh, 18.6 kW)	361	257	183	115	235	310	0	139	180
Feb		483	532	367	193	134	311	1	0	17
Mar		61	135	0	389	287	430	231	214	690
Apr		30	150	1	459	360	489	207	237	774
May		0	87	0	421	314	419	238	67	620
June		0	102	0	351	267	350	357	84	708
July		0	68	0	314	226	315	479	49	753
Aug		0	112	0	342	250	344	296	0	545
Sept		0	128	0	333	185	331	180	7	374
Oct		157	138	10	244	284	406	23	6	152
Nov		259	186	68	182	255	358	0	79	159
Dec		361	37	22	101	430	449	0	381	463
Total		**1,711**	**1,931**	**652**	**3,445**	**3,229**	**4,514**	**2,013**	**1,263**	**5,437**

Thus, summarizing the above information, it can be said that in the case of battery 1 and battery 2, PV shows better self-sufficiency than WT during most of the year, and also demonstrate an almost linear relationship between a decrease in imports and a decrease in exports with the emergence of a battery (while at the same time increasing self-sufficiency and own consumption shares). With joint PV and WT utilization, this

relation is non-linear, which may be reflected in the cost-effectiveness of the system installed and might cause grid congestions (when exporting simultaneously by a group of houses). On the other hand, certification requirements of WT installations, as well as strict noise restrictions on their operation near the neighbouring properties (the noise may not exceed the limit of 37-44 dB (A) depending on the area [261]), significantly limit and even make it impossible of the latter to work in the residential sector. All this calls into question the feasibility of further research of micro wind turbine for individual use, even with better energy performance in some months. Moreover, since even both RESs with a large battery are not able to provide autonomy for the baseload, it makes no sense to consider all possible scenarios in further research. The focus will thus be made only on PV panels in combination with the battery №1.

4.1.4. S4. Baseload + HPS

The system setup for the fourth scenario is presented in Figure 4.11.

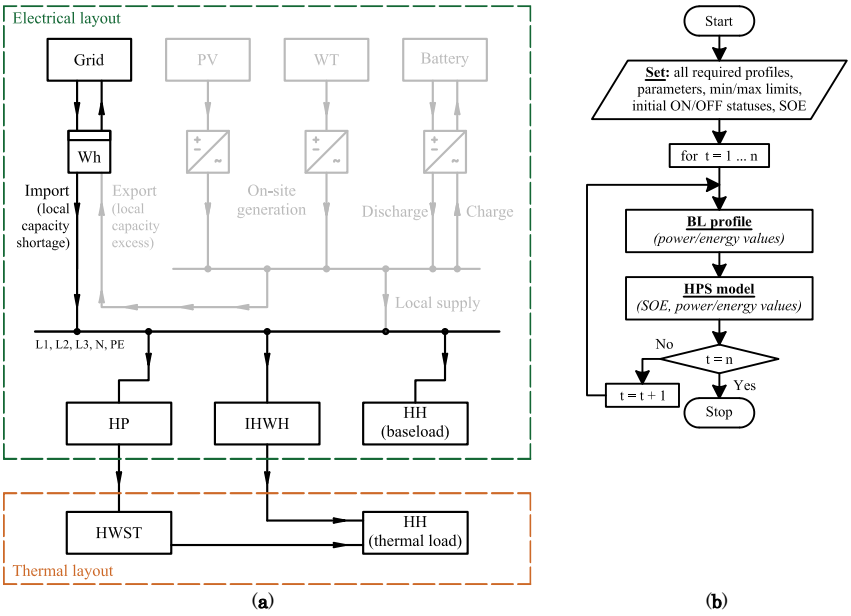

Figure 4.11. Building energy system setup according to scenario S4: (a) layout of electrical components; (b) layout of Matlab models.

The performance of a heat pump system is evaluated by comparing its operation with two different HWST volumes. The left column in Figure 4.12 depicts operation with a **200-litre** storage tank (marked here as **Scenario 1**), and the right column – with a volume of **1000 litres** (as a

Scenario 2). Both scenarios represent work in the winter season, with high heat demand. The left column – at a positive temperature (January 1st), the right column – at a temperature below zero (January 15th). The simulation of the heat pump behaviour (under Scenario 1) is started assuming that the initial energy level in the tank is 70%. The arrow, in the first minutes of operation (Figure 4.12 **a3** and **a4**), shows the conversion delay required to reach the hot water temperature setpoint (i.e. +65°C). As the initial energy level in the tank is less than the minimum controllable (<81%), and there is also some heat demand, the heating is supported by the auxiliary electric heater. This, in turn, led to a significant increase in the electrical load (see arrow on graph **a4**). Since the volume of the first tank (and, accordingly, its total energy capacity) is much smaller than the second, in order to maintain the water temperature and SOE within acceptable limits, the heat pump must be switched ON more often. This is also clearly seen in graphs **a2, a3, a4**. On the contrary, five times larger HWST volume allows HP to run smoother and makes the duration of ON/OFF cycles longer (as visible in graphs **b2**, **b3**, **b4**).

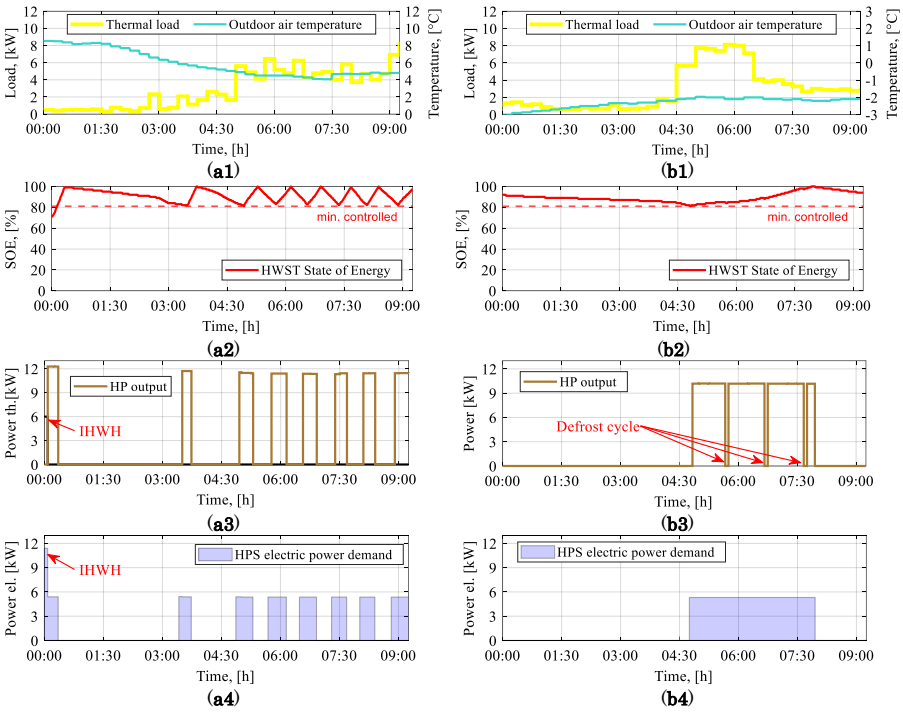

Figure 4.12. Performance of the HPS with two HWST volumes: (**a**) HWST 1 (0.2m³); (**b**) HWST 2 (1m³); 1) thermal load of the household and an outdoor air temperature; 2) SOE of the HWST; 3) thermal power output; 4) electric power input.

Nevertheless, as can be seen from graph **b3**, the HWST thermal energy charging cycles are also interrupted (meaning no useful heat is delivered to the HWST). The reason for these interruptions is the defrost cycle, which, in this case, is a consequence of working with high heat demand and an inlet air temperature below freezing point. The electric power demand though (as shown in graph **b4**) remains continuous, nonetheless, this cycle can be the reason for not providing a response to the DR signal (which will be disclosed in the next chapter).

Figure 4.13 and Table 4.4 show the performance of HPS in heat production for two different scenarios and demonstrates the difference between useful and wasteful energy (that is used only for defrosting an external heat exchanger). Since in this model the defrost cycle is only initiated after prolonged operation at an outdoor air temperature below the freezing point, a very small amount of wasteful energy can be observed. A one-minute simulation step, in this respect, also helped to obtain a more accurate result. The larger share of energy used for defrosting in the second scenario can be explained simply by the longer operating cycles. Longer run time, in turn, as already noted earlier, is directly related to more heat energy that must be supplied to the HWST (as can be seen in Table 4.5).

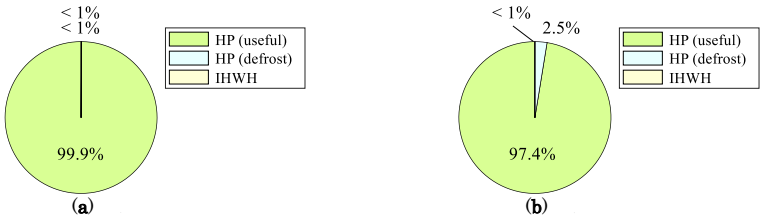

Figure 4.13. Heat energy shares, including useful and wasteful shares, which are produced by the heat pump and the IHWH per annum applying two different HWST scenarios: (**a**) Scenario with 0.2 m^3 HWST; (**b**) Scenario with 1 m^3 HWST.

The table below illustrates another phenomenon that is not entirely clear at first glance. That is when the same HP with a larger storage tank size consumes less electricity and produce more heat than is the case with a smaller tank. Although this is not initially obvious, this phenomenon is an explicit demonstration of the impact of heat conversion delay. The smaller the storage size, the shorter the charging cycle. The greater amount of short charging cycles – HP should start more times with conversion delay. An HPS with a larger HWST spent 66.5 hours on heat preparation per year, while in the case of using a smaller tank, this number is 338.6 hours.

Table 4.4. Summary of the HPS performance on an annual basis.

HWST volume [m³]	*Thermal energy production [kWh]*				*Electrical energy consumption [kWh]*				COP
	HP (useful)	*HP (defrost)*	*IHWH*	*Total HPS*	*HP (useful)*	*HP (defrost)*	*IHWH*	*Total HPS*	
0.2	12,524	8	4	12,536	7,530	4	4	7,538	1.66
1.0	12,707	332	1	13,040	6,173	171	1	6,345	2.06

Table 4.5 below shows the amount of energy involved in the HPS operation for both HWST scenarios, considering temperature control between + 55°C and + 65°C (i.e. the energy used to heat the water inside the storage tank from +55° to +65°C). According to (3.21), this energy is different for different volumes. For illustrative purposes, the table also shows the number of hours of backup heat supply considering the peak and average heat load of the household, which is equivalent to this amount of energy.

Table 4.5. The usable capacity of the HWST considering regulation limits and its equivalent in hours of backup heat supply.

HWST volume [m³]	*Regulation boundaries [°C]*	*An equivalent amount of energy used for regulation [kWh]*	*Hours of backup heat supply considering peak load [h]*	*Hours of backup heat supply considering average load [h]*
0.2	between +55 and +65	2.3	0h 12min.	1h 7min.
1.0		11.6	1h 1min.	5h 32min.

Two graphs, bars and pie charts in Figure 4.14 illustrate the updated (compared to Figure 3.3 **d**) annual household load profiles taking into account the heat pump share for both HWST scenarios. From the first two graphs (**a1**, **a2**), one can visually see how much the emergence of the heat pump increases the overall power demand in relation to the baseload. It is also clearly seen that due to the larger tank and longer cycles, the consumption during the year, in the case of using the HWST 1m^3 (especially in summer), is less, which gives an annual energy savings of 1.2 MWh (i.e. 7,538-6,345 = 1,194kWh ~1.2MWh, see Table 4.4 above). Bar charts **b1** and **b2** also clearly visualize the dependence of electricity use on the heat demand of the household, and the pie charts next to the bars show the annual shares of energy consumed by the baseload and HPS.

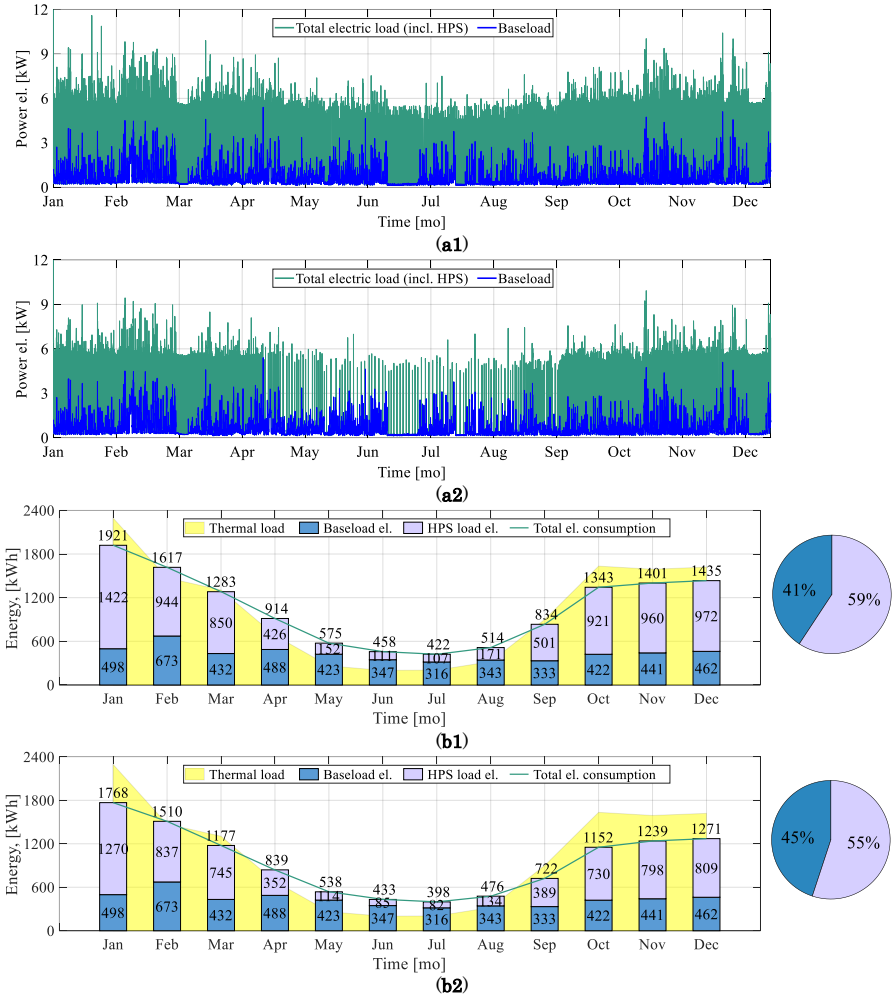

Figure 4.14. Updated electric load profile of the house, taking into account the HP share: (**a**) power demand; (**b**) monthly and annual energy consumption indices under scenario S4; 1) HWST scenario №1 (0.2m³); 2) HWST scenario №2 (1m³).

Table 4.6 below summarizes the building's energy system performance under scenario S4 and shows an annual increase in load due to the emergence of a heat pump system for two HWST case studies.

Table 4.6. Summary of the building's energy system performance under scenario S4.

HWST volume [m³]	*Electrical energy consumption per year [kWh]*			*Percentage increase [%]*
	Baseload	**HPS**	**Total**	
0.2	5,179	7,538	12,716	246
1.0		6,345	11,523	223

4.1.5. S5. Baseload + HPS + PV

The system setup for the scenario S5 is presented Figure 4.15.

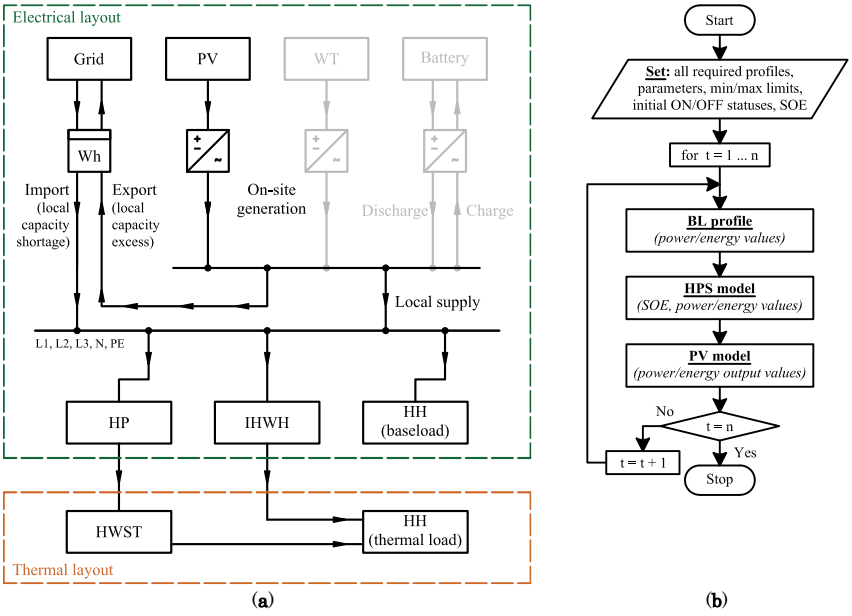

Figure 4.15. Building energy system setup according to scenario S5: (a) layout of electrical components; (b) layout of Matlab models.

The focus of this section is concentrated on the analysis of the combination of baseload, heat pump system and PV panels. Considering the fact that the presence of an enormously large battery does not provide 100% self-sufficiency, as well as the fact that the battery price is still high, it is this combination that is one of the most likely scenarios for the development of in-house energy systems in the near future. The purpose of this analysis is to investigate what part of the increase in electricity consumption (due to the emergence of a heat pump) can be compensated by PV panels. For this case study, it was also decided to highlight here only one scenario of HWST with the volume of one cubic meter, since, as the simulation results showed, the difference in results between the two sizes in the context of self-sufficiency and own consumption is only 2% -4%, which is very insignificant. However, selecting a size of $1m^3$ is more practical for further investigating, the energy flexibility potential.

Figure 4.16 below illustrates almost all the interesting processes, associated with this scenario, which are specially collected and combined in one graph for ease of perception. The period of three days in April (April

20-22) depicts the total household load (including baseload and HPS load), SOE of the HWST, power output curve of PV array and import and export of power. The graph shows that each activation of the HP (turquoise line, around 19:00 on the first day, 12:00 on the second day, and close to 13:00 on the third day) significantly increases the total load of the house. At the same time, it can be seen that in almost all cases, these activations are accompanied by a high import of electricity from the grid. The presence of high imports, even with a sufficiently large PV generation, first of all, indicates that the permitted installed capacity of the PV array (i.e. 6 kW) is insufficient to cover the entire demand. On the other hand, in those moments when the HP is switched off and generation is present (e.g., at noon on the first day), it can be seen that most of the energy generated on-site is exported to the grid. This also indicates a discrepancy between the periods of maximum load (which, in the case of baseload is in between 15:30 – 19:30, as shown in Figure 3.3 **e**) and generation (which, in the case of PV is usually in between 10:00 – 17:30, see Figure 4.2 **a1**).

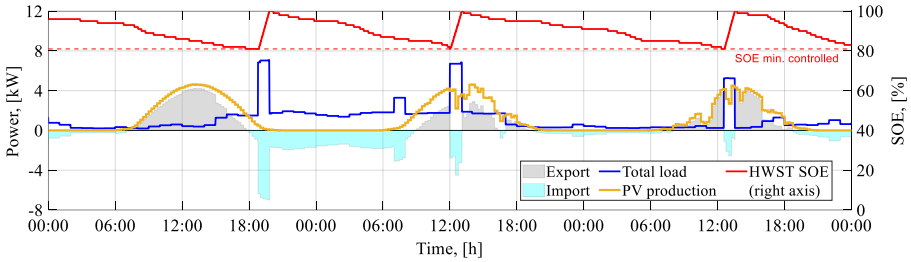

Figure 4.16. The performance of the energy system of building under scenario S5 (simulation results).

Bar and pie charts in Figure 4.17 **a** and **b** demonstrate self-sufficiency and own consumption indices. When comparing these indices with the scenario S2 (i.e. Baseload + PV, shown in Figure 4.4 **a**, Figure 4.5 **a**) it can be seen that appearance of HPS within the household reduces the self-sufficiency index by –17% (from 36% to 19%), while at the same time increasing the share of import by +17% (from 64% to 81%). On the other hand, the own consumption index is increased only by +7% (from 34% to 41%), and the share of export decreased by –7% (from 66% to 59%). This very small percentage (against the background of a significant increase in load) indicates that the increase in load does not help to accommodate more locally produced power, and again indicates the aforementioned mismatch between maximum load and generation periods. Let us check whether the battery can make a difference.

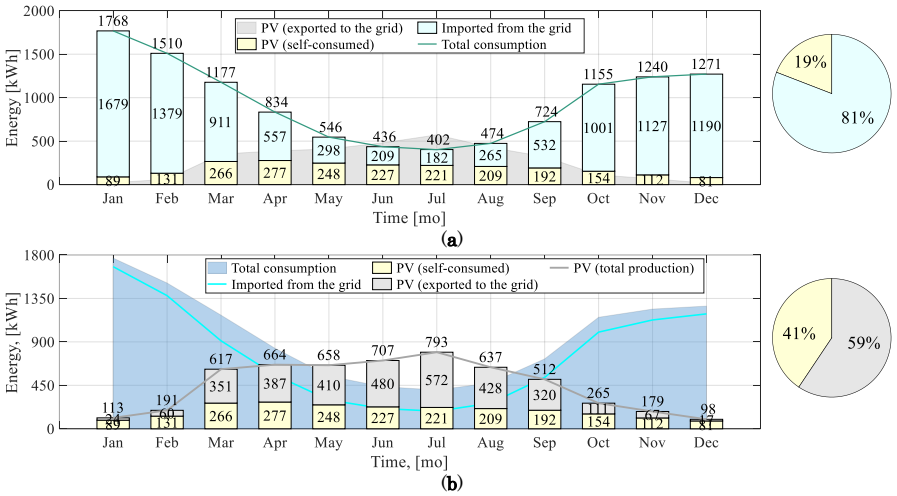

Figure 4.17. Monthly and annual self-sufficiency and own consumption indices under scenario S5: (**a**) self-sufficiency; (**b**) own consumption.

Table 4.7 summarizes all above-mentioned self-sufficiency and own consumption indices on an annual basis.

Table 4.7. Summary of the building's energy system performance under scenario S5.

Energy per year [kWh]			
Total load	*Imported from the grid*	*Own PV array production, which is*	
		Self-consumed	*Exported to the grid*
11,523	9,331	2,192	3,230

4.1.6. S6. Baseload + HPS + PV + Battery

The system setup for the latter scenario S6 is presented in Figure 4.6.

The last part of the analysis of the rearrangement of a building energy system is adding the battery to the above components. The main purpose of this analysis is to investigate whether the emergence of a battery in addition to the available own PV panels, can significantly affect the self-sufficiency, import and export indices while having a significantly increased load (due to a heat pump). In this scenario, the baseload, heat pump with storage tank №2 (volume 1m^3), PV panels with an installed capacity of 6 kW and the battery №1 (14.1 kWh, 9.3 kW) are investigated.

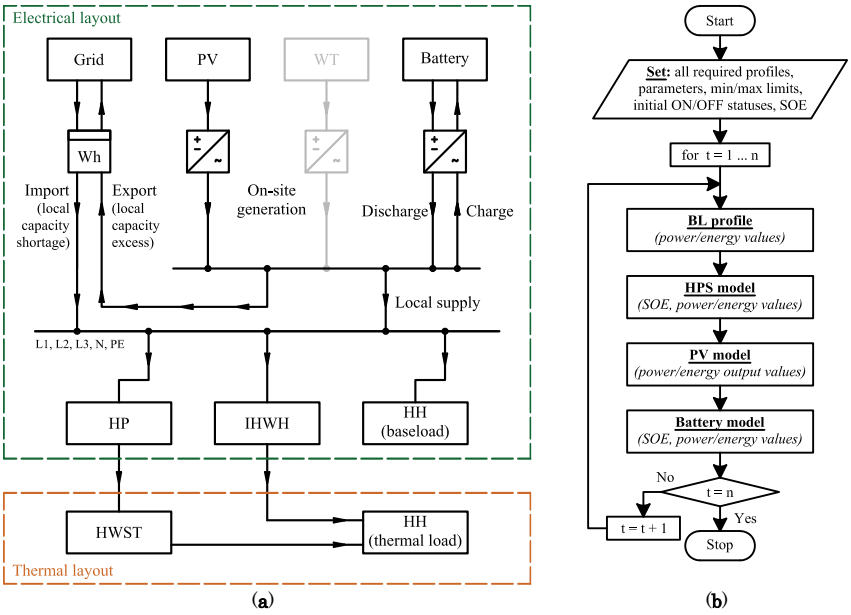

Figure 4.18. Building energy system setup according to scenario S6: (a) layout of electrical components; (b) layout of Matlab models.

The period of two days (22nd and 23rd of April, shown in Figure 4.19 below), demonstrates the simulation results of the behaviour of all the aforementioned components. As can be seen at about four o'clock in the morning, the energy level in the storage tank (red line) reached its minimum controllable level. At this moment, one can see that the heat pump was turned on and, accordingly, the HWST began to be charged with thermal energy. Since there was no generation of PV panels at this point (orange line) and the battery charge was at a minimum level (purple line), it can be seen that the entire load is fully covered by import of electricity from the grid. As soon as the level of own generation has exceeded demand (~ 09:30 am), it is observed that the battery charging process has begun (and lasts until ~ 15:30). Household heat demand all this time is covered by HWST until ~ 02:00 the next day. Once the SOE of the HWST has reached its minimum level again (at 02:00), the heat pump switching on can be seen again. This time, the battery was more than 70% charged. Since there was also no PV generation at this time, it can be seen that the entire peak demand of the household (i.e. the entire HWST charging cycle, which lasted about two hours) was fully covered by the battery. The latter moment, which wanted to be pointed out is the period between 12:00 to 16:00 on the second day. Very low demand and high generation can be observed during this time. In the first part of this period (12:00-14 00), it can be seen that all the energy generated by the PV panels was charged to

the battery. And once the battery charge has reached its maximum level, in the next two hours (14:00-16:00) all the excess generation is exported to the network.

Bar and pie charts shown in Figure 4.20 below depict the self-sufficiency and own consumption indices for this scenario and Table 4.8 provides a summary of these indices on an annual basis.

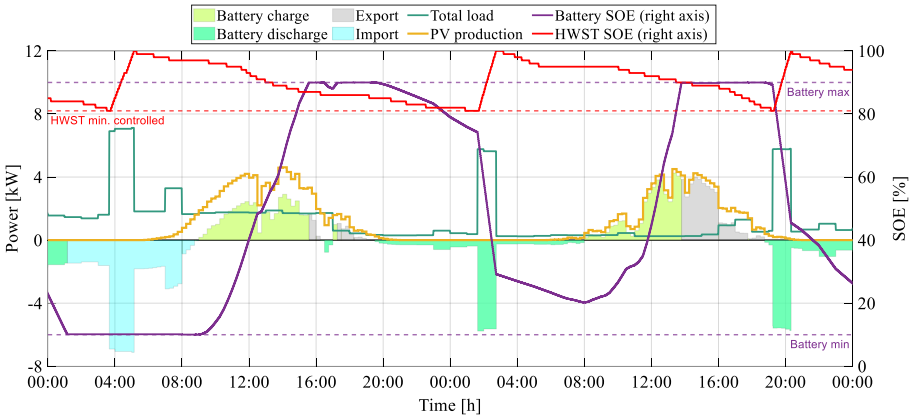

Figure 4.19. The performance of the energy system of building under scenario S6 (simulation results).

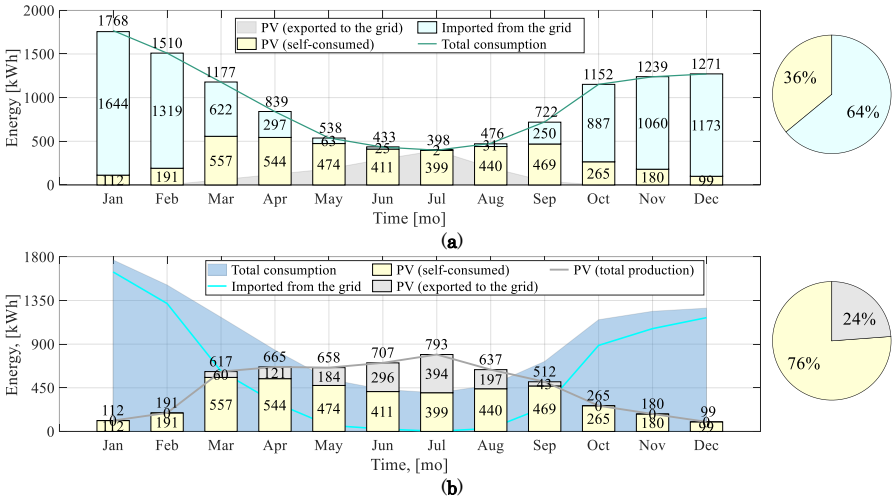

Figure 4.20. Monthly and annual self-sufficiency and own consumption indices under scenario S6: (**a**) self-sufficiency; (**b**) own consumption.

Table 4.8. Summary of the building's energy system performance under scenario S6.

Energy per year [kWh]			
Total load	*Imported from the grid*	*Own PV array production, which is*	
		Self-consumed	*Exported to the grid*
11,523	7,371	4,141	1,296

Comparing the performance of the system in this scenario with the previous one (without battery), it can be seen that all indices have improved almost twice. Self-sufficiency increased from 19% to 36%, respectively, imports decreased from 81% to 64%. Own consumption increased from 41% to 76% and, accordingly, exports fell from 59% to 24%. This indicates that the battery has a rather positive effect and, together with the increased load, enable increasing the use of own generated energy. Table 4.9 and Table 4.10 below summarizes energy values and percentages for all six scenarios.

Table 4.9. Summary of the building's energy system performance under all six scenarios (energy values).

Index	***Energy per year [kWh] under each scenario***							
	S1	***S2***	***S3***		***S4***		***S5***	***S6***
			Battery1	*Battery2*	*HWST1*	*HWST2*		
Imports	5,179	3,337	1,885	1,711	12,716	11,523	9,331	7,371
Self-consumption	–	1,842	3,282	3,445	–	–	2,207	4,141
Exports	–	3,616	2,176	2,013	–	–	3,230	1,296

Table 4.10. Summary of the building's energy system performance under all six scenarios (percentages).

Index	***PERCENTAGES [%]***													
	Baseload										***Baseload + HPS***			
	S1	***S2***			***S3***						***S4***		***S5***	***S6***
					Battery 1			*Battery 2*						
		PV	*WT*	*PV & WT*	*PV*	*WT*	*PV & WT*	*PV*	*WT*	*PV & WT*	*HWST1*	*HWST2*		
Self-sufficiency	–	36	38	57	64	57	84	67	63	87	–	–	19	36
Imports	100	64	62	43	36	43	16	33	37	13	100	100	81	64
Own consumption	–	34	44	30	60	66	44	63	72	45	–	–	41	76
Exports	–	66	56	70	40	34	56	37	28	55	–	–	59	24

4.2. ANALYTICS OF ENERGY CONSUMPTION OF A GROUP OF BUILDINGS

Another interesting aspect of the study is to analyse how the rearrangement of the integrated thermal and electrical energy systems of building impact the need for power supply from the grid and hence a feeder load in different months of the year. When it comes to aggregation, here, in contrast to self-sufficiency and own consumption indices (important for an individual household), the indicators of the total load of the feeder line and the transformer substation are much more important. Load profiles, together with monthly and annual energy consumption indicators, are essential both to ensure reliable power grid operation (for maintaining the power factor, voltage/current characteristics within the admissible level) and for proactive grid operation planning (to ensure a sufficient level of generating and reserve capacities). Since, having a load profile, using modern statistical estimation techniques, it is possible to predict potential consumption forward in time with great accuracy.

At this stage, a group of 25 buildings that belong to one 0.4 kV feeder line and where heat is supplied by the DH networks were selected for investigating and comparing all six aforementioned scenarios of building energy systems rearrangement (indicated at the beginning of this chapter). Based on the information described in Chapter 3 above, each of these buildings has an individual heat pump size, an HWST size, and a battery size. Considering also the above-described restrictions on RESs for individual use, the PV panels array size was chosen as the maximum allowable, namely 6 kW, for each house. Six different types of HPs, offered by the manufacturer [199], were selected for this study. The rated electric power values of each of these types are shown in Table 4.11. The suitable sizes of HWSTs are calculated based on the second method presented in Section 3.3.6, Eq. (3.32) (i.e. assuming that one hour of backup heat supply is a minimum requirement of inhabitants for not violating their thermal comfort preferences). While all the remaining parameters for all 25 houses are summarized in Table 4.12 below.

Table 4.11. Rated electric power for six different types of heat pumps.

HP type	*Rated Electric Power [kW]* (for maximum compressor speed at an outdoor air temperature [°C] in accordance with EN 14511)					
	–13°C	–7°C	+2°C	+7°C	+12°C	+20°C
Type 1	2.0	2.2	2.1	2.2	2.2	2.0
Type 2	2.8	3.1	3.1	3.1	2.7	2.0
Type 3	2.6	2.7	2.9	3.0	3.1	3.1
Type 4	3.7	3.6	3.5	3.6	3.3	3.1
Type 5	5.3	5.3	5.3	5.4	5.3	4.7
Type 6	5.3	6.1	6.1	5.9	5.3	4.7

Table 4.12. Input parameters used to simulate the behaviour of a group of 25 houses.

House №	Heat load		Electric baseload		*HPS*			*PV rated power [kW]*	*Battery*	
	Peak load [kW]	Annual consumpt. [kWh]	Peak load [kW]	Annual consumpt. [kWh]	HP type	IHWH [kW]	HWST volume [m³]		Power [kW]	Energy [kWh]
1	9.4	12,011	4.4	3,776	4	6	0.8	6	9.1	13.8
2	10.5	13,232	4.2	5,878	4	6	0.9	6	8.1	12.3
3	14.6	14,269	2.6	3,447	5	6	1.25	6	8.3	12.6
4	5.6	4,829	3.6	3,294	1	6	0.5	6	7.2	10.9
5	11.0	11,363	2.2	2,989	4	6	0.95	6	9.5	14.4
6	9.2	13,345	6.9	5,793	4	6	0.8	6	8.1	12.3
7	8.6	8,346	5.1	7,433	2	6	0.75	6	10.8	16.3
8	9.4	8,728	2.1	3,337	4	6	0.8	6	9.4	14.3
9	15.5	19,156	4.0	5,158	5	6	1.35	6	9.4	14.2
10	10.2	13,192	4.3	4,843	4	6	0.9	6	9.6	14.5
11	7.7	8,559	4.2	4,687	1	6	0.65	6	9.5	14.4
12	9.9	12,751	5.2	6,485	2	6	0.85	6	8.1	12.2
13	7.7	14,350	4.4	8,083	3	6	0.65	6	8.8	13.4
14	18.3	20,445	3.5	3,637	6	6	1.55	6	10.0	15.1
15	14.2	14,989	4.3	5,658	5	6	1.2	6	9.0	13.7
16	7.7	8,889	3.4	3,170	2	6	0.65	6	9.2	13.9
17	11.2	10,125	4.6	4,441	3	6	0.95	6	10.4	15.8
18	11.5	12,486	5.4	5,179	5	6	1	6	9.3	14.1
19	13.4	17,723	3.8	3,463	5	6	1.15	6	8.1	12.2
20	9.6	11,611	3.5	4,221	2	6	0.8	6	9.4	14.3
21	9.0	9,650	3.1	3,054	3	6	0.75	6	9.4	14.3
22	8.9	14,777	4.1	4,679	3	6	0.75	6	9.6	14.5
23	12.4	17,456	4.3	4,253	5	6	1.05	6	9.2	14.0
24	9.6	11,780	5.1	8,424	4	6	0.85	6	8.0	12.1
25	9.0	10,698	4.0	3,738	4	6	0.75	6	9.0	13.6

Power curve graphs, Figure 4.21, visually illustrate how the emergence of one or another resource (in accordance with scenarios S1...S6) changes the load of the feeder line throughout the year.

Graph **s1** is the baseload and the starting point against which everything is compared.

From the graph **s2**, as well as the Bar charts in Figure 4.22 (reflecting the total monthly indices for each of the six scenarios), it can be seen that in the second case (**s2**), the appearance of PV panels reduces the need for power supply from the grid (imports) almost two times from March to September. However, at the same time, it can be seen that by adding PV panels to each house, a very significant generation into the grid (exports) also appeared, which, depending on the permissible characteristics of the network infrastructure, can have negative consequences.

The appearance of the battery in each house (graph **s3**) significantly reduces the load of the feeder line. When moving a step further and looking at the bar chart **s3** Figure 4.21, it can also be seen that there is practically no consumption during the March-September period. Nevertheless, export indices fell by only a third. Graph **s3**, Figure 4.21, in turn, shows that the peak load remained at the same level, although the periodicity is rare.

The **s4** graph in Figure 4.21, as well as the **s4** bar chart in Figure 4.22, show how much the demand for electricity has increased with the advent of the heat pump. Comparing with the baseload (**s1**), it can be seen that in the month when the heat pumps operate at maximum load, that is, during the heating season, the load on the grid has increased almost threefold. Again, depending on the state of the grid infrastructure, such an increase in load can cause severe voltage drops at the end of the feeder line and cause unplanned overload shutdowns.

The appearance of solar panels practically does not change the situation during the heating season (graph and bar chart **s5**) and only partially during the non-heating, while increasing exports.

The last graph and bar chart **s6** show that the presence of own PV panels and batteries practically does not change the load curve and, during the heating season, have a very insignificant effect on imports. Compared to the scenario without a battery (**s5**), it can be seen that the presence of the latter significantly reduced some of the exports to the grid, but did not completely deprive it. From June to August, exports exceed demand three times, which may cause overvoltage and tripping of protective equipment at distribution switchboards and transformer substation.

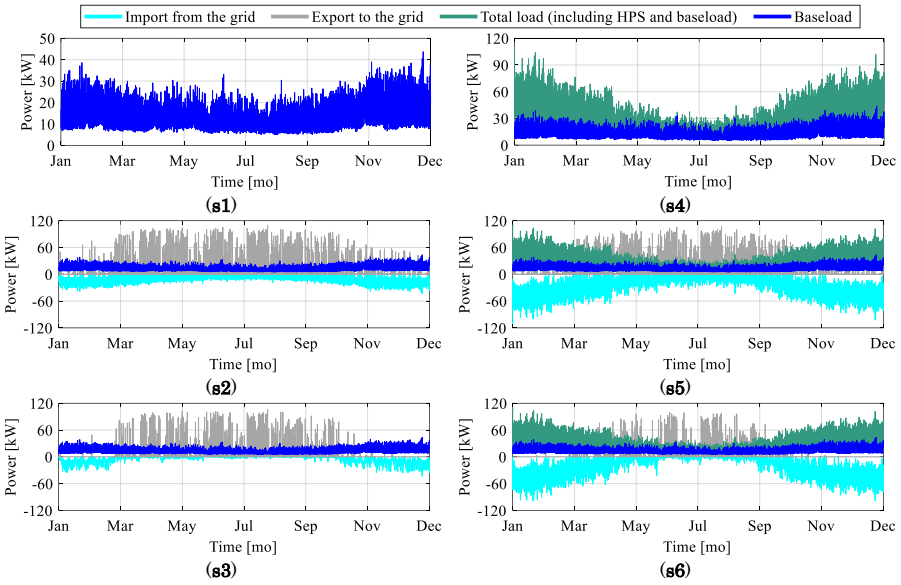

Figure 4.21. Electric load profiles of a group of 25 houses under each of six scenarios: (**s1**) Baseload; (**s2**) Baseload + PV; (**s3**) Baseload + PV + Battery; (**s4**) Baseload + HPS; (**s5**) Baseload + HPS + PV; (**s6**) Baseload + HPS + PV + Battery.

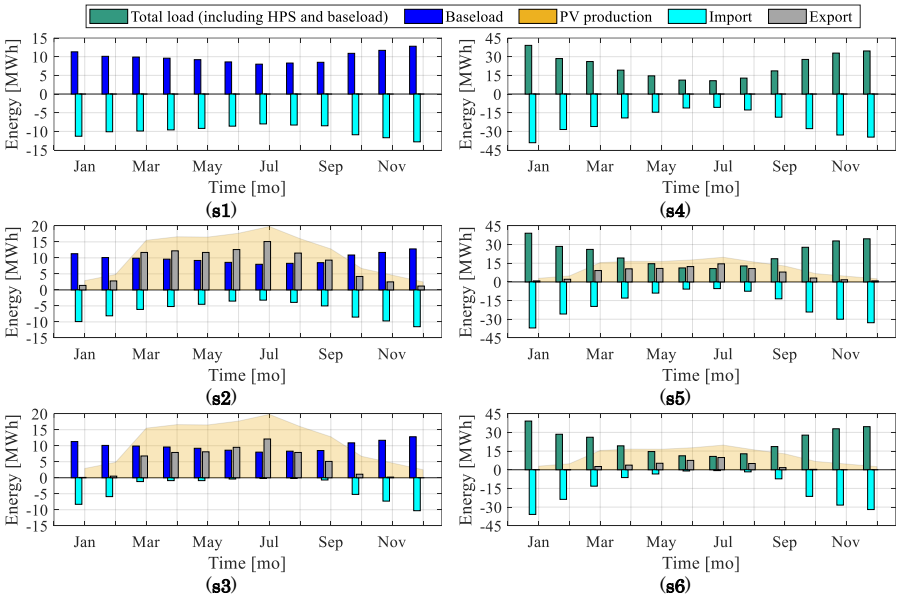

Figure 4.22. Monthly electric energy consumption indices for each of six scenarios: (**s1**) Baseload; (**s2**) Baseload + PV; (**s3**) Baseload + PV + Battery; (**s4**) Baseload + HPS; (**s5**) Baseload + HPS + PV; (**s6**) Baseload + HPS + PV + Battery.

Figure 4.23 depicts the total annual indices for each of the investigated scenarios. It is obvious that neither PV panels nor PV panels together with the battery do not change the situation regarding imports drastically, which cannot be said about the large-scale expansion of heat pumps. The latter has an extremely large impact on the power grid during the heating season, increasing the grid load more than twice. PV panels in combination with a battery, on the contrary, show the best joint performance precisely in the non-heating season. That is why more flexible load utilization, with the ability to deviate from the reference profile, as well as to be able to shave the load immediately on demand, is essential for a stable, secure grid operation. And such flexible use can be mutually beneficial for both the grid companies and prosumers. This will be explored in the next chapter.

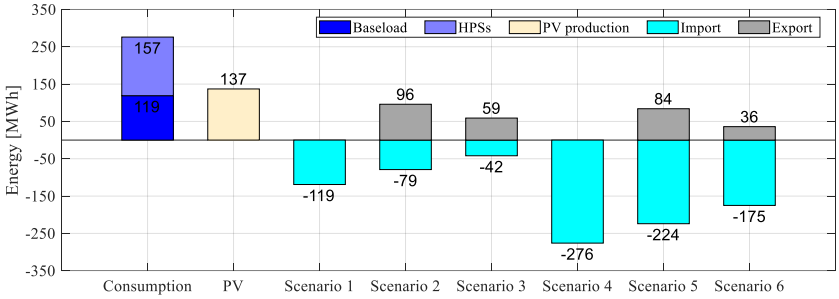

Figure 4.23. Annual electric energy consumption and imports/exports indices for each of six scenarios.

An increase or decrease in the share of import and export in all six scenarios of household energy systems modernization is shown in Table 4.13. An increase/decrease in imports is shown in relation to the reference scenario S1 (baseload), while an increase/decrease in exports is illustrated with respect to scenario S2 (Baseload + PV).

Table 4.13. Indices of an increase or decrease in the share of imports and exports.

	Percentage increase or decrease in different scenarios [%]					
	S1	***S2***	***S3***	***S4***	***S5***	***S6***
Export	-	100	-39	-	-13	-63
Import	100	-34	-65	+132	+88	+47

The table shows that the best result was achieved under scenario S3, reducing the share of imports by –65%, while the appearance of a heat pump (S4) increased this share by +132%. PV panels and batteries are able to only partially compensate for the increase in load while leaving a great share of imports. At the same time, as can be seen, even the significant demand and availability of a battery (S6) is not able to ensure full

consumption of own generated electricity, reducing the share of exports by a maximum of –63%.

4.3. CHAPTER SUMMARY

This chapter has demonstrated the changes that in-building energy system modernization (by using certain DER components) can make to the conventional power supply of the household and to the power grid. Six different scenarios for combining renewable sources and a heat pump with different storage tanks and batteries were analysed. Based on the above information, the following conclusion can be drawn.

It is obvious that the emergence of on-site renewable sources increases the energy efficiency of a single house by increasing its self-sufficiency indices. Replacement of the traditional heat source, where fossil fuel might have been employed, with HPS, in turn, rises this energy efficiency index on the other (district heating dependency reduction) side. Nevertheless, it can also be clearly stated that on-site RESs coupled with batteries are not able to fully compensate for this heat source shift by covering the increased power demand with local generation. The permissible size limit of 6kW for the domestic rooftop PV installation even with the fairly large battery is insufficient to cover neither peak power demand nor monthly/annual energy needs. On the other hand, even this size causes quite large exports in the non-heating season, which can lead to various consequences in grid operation (such as overvoltage, reverse power flow, unplanned outages and others). Therefore, ordinary use of on-site RESs with battery (while simply exporting the excess of local production to the grid without the use of specific model predictive control or optimal scheduling) should not be considered significant load reduction to the power system. Rather the improvement of energy efficiency and response in supporting the global emission reduction.

To improve this index, the solution may be found in the flexible use of HPS wherein, with the help of more intelligent control, the option to deviate from the reference profile (i.e. the ability of shaving, shifting or shaping the load) can be enabled.

5 ACTIVE INTERCONNECTION BETWEEN SMART BUILDINGS AND THE GRID

This chapter examines several aspects of energy flexibility service provisioning. The first section presents the general concept of providing demand-side energy flexibility services, which is applied in this study.
The second section explores the energy flexibility that can be provided by a single residential building equipped with a heat pump system and PV panels coupled with a battery. The flexibility potential (and hence the ability to reduce peak loads) is estimated as a percentage and quantified using an artificially simulated signal generated on the basis of the peak load of a 20/0.4kV transformer substation. To determine the peak hours, the historical baseload data of 129 houses of different types, which are powered by this transformer substation, were used.
The third section explores how the aggregated flexibility of 25 active houses connected to a single feeder can help to address the voltage drop issues occurring in that feeder. To do this, a load flow analysis is performed, and a feedback voltage-based signal (voltage drop-based, in this case) is sent to all involved households. For providing a response to these signals, as well as calculating the amount of peak energy shaved, a rule-based management strategy (low-level control) has been developed. Another centralized coordinating control strategy was designed for the smooth restart of all respondents, thereby preventing simultaneous turning ON of all heat pumps that cause much more serious voltage fluctuation. The main advantage of these strategies is that having a generally non-obligatory basis for giving responses, such a DR application helps to eliminate most of the voltage drop events occurring in that feeder during an ordinary operation. Non-obligatory, in this context, implies responding in such a way so as not to violate the thermal comfort of inhabitants (while considering all the features of the HPS operation, i.e., delays, defrost cycle, pre-set power-on time). Whereas the main benefit of this analysis is the ability to track the behaviour/reaction of each house individually.

5.1. THE CONCEPT OF DEMAND-SIDE FLEXIBILITY SERVICE PROVISIONING

The provision of energy flexibility services on the demand side has been a popular and interesting topic in recent years. There are various research

pilot projects, with real installations, such as [262]–[264], and many others that investigate DSF. Nevertheless, flexibility has not yet been widely adopted as of today. One of the most popular control schemes, where heat pumps are involved, is direct load control (DLC, see Section 2.2.8) allowing energy flexibility program providers (aggregators) to either fully remotely control heat pumps or send request (on/off) signals with the mandatory reaction. Failure to respond to such signals usually entails penalties, which are quite severe. This is one of the reasons why not every flexible resource owner is interested in participating in such programs.

In contrast to the above-mentioned DLC scheme, the concept applied in this study involves the creation of conditions where responding to input signals is possible on a non-obligatory basis (without imposing any penalties for failure to respond). Referring to Section 2.2.4 above, the concept proposed here is directly related to the Peak clipping objective of DSM (shown Figure 2.5) and is designed to reduce the peak load in the local low voltage 0.4 kV grid. The proposed concept is associated with the provision of explicit energy flexibility services (incentive-based DR) and is most similar to existing Curtailable/Interruptible load or Emergency Demand Response programs described in Section 2.2.5 above. However, unlike the above-described programs, which allow only large consumers to participate (over 100kW, with a significant impact on the grid), this concept involves participation of small aggregated loads, such as an ordinary household. Peak load reduction is realized by sending technical signals to all participants with energy-flexible loads. Technical signals, in turn, also have a different background.

From the fundamentals of the electric power industry, it is known that the stable and reliable operation of the power grid is influenced by many different factors. Each important grid node, such as a transformer substation, switchgear, bus, as well as feeder line, is usually designed with its own tolerance limit, the so-called hosting capacity threshold. Depending on many different factors, such as, for example, load of transformers, buses, nominals and setpoints of protective equipment, permissible long-term current that can flow across cable lines, the voltage drop at the end of the lines, harmonic distortion level, reactiveness of load etc., these thresholds are very individual for each node. In the nowadays contemporary power system, where the amount of RESs and flexible loads is growing exponentially every day, the selection of proper acceptability limit becomes a very tough (yet not least important) task. Grid codes of all countries in the world, determine that maintaining such basic parameters as voltage and frequency deviations within the permitted limits is the key to the stable operation of the power grid. Frequency today is regulated at a high voltage level by transmission operators using various reserves (as

described in Section 2.1.2 above) and this regulation is so far adequate up to the end-use customer level. It is up to DSOs to maintain voltage stability at low voltage level, and it is the voltage at the DSOs responsibility level that potential household demand response can contribute to.

Hence, when coming back to signals topology, in the case of investigating the flexibility potential, this dissertation implies the use of signals based on the loading of the transformer substation. Whereas, when studying the impact on the grid, these signals are based on the voltage of the feeder line, namely, the voltage drop at the weakest bus, and are generated as feedback signals as a consequence of a load flows analysis. The concept also takes into account the fact that all relationships between suppliers and consumers of electricity are market-based today, and therefore all communications take place through the DataHub and aggregators. It is also assumed that each HP is connected to the grid through an individual electricity meter, so the activation time of the service and the amount of energy reduced, can also be estimated based on historically recorded time-series data. An overview of this concept is shown in Figure 5.1.

The scheme underlying this concept is similar to the already implemented principles of activation of frequency reserves at the transmission level (described in the section Ancillary services, Section 2.1.2). In this concept, it is assumed that in the near future the most important strategic nodes of low-voltage distribution networks will be modernized (equipped with RTU or PMU units) and the DSO will be able to remotely monitor all the necessary indices. DSO, having an understanding of how much flexibility may be required to keep the grid stable at each particular time of the day, makes requests for this flexibility in the electricity markets. This could be, for example, a day-ahead, an intraday platform, as well as a perspective new flexibility market. In this connection, geotags that is, the specific location of potentially congested nodes play a very important role. Aggregators related to that geolocation (there may be several aggregators, similar to electricity supply companies), knowing the flexibility potential of their customers, make preliminary offers on the other side of the auction. Bids and offers are matched and the price of each kWh of energy flexibility is determined following the marginal price principle and is formatted on a minutely (5-minute or at least 15-minute) basis. At the moment when one of the aforementioned limits goes beyond the acceptable thresholds, during the operation of the system, DSO sends signals to activate flexibility to those aggregators whose rates are approved. Aggregators, in turn, redirect signals to all houses participating in the program. Since metered time series values cannot be used for the settlement purpose (due to obvious reasons – the load is turned off), settlement for those players whose bids have been activated is done based

on the calculated/estimated energy values. These energy values, in turn, are obtained based on the rated electric power of each individual heat pump and the response signals reflecting the duration of the activation period of each individual unit (i.e. the number of minutes where the heat pump reacts to the request signals). This will be explained in more detail when reviewing the DR strategy presented in Section 5.2.3. The settlement, in turn, should be done at the end of each day of operation and all discrepancies between pre-agreed and actual flexibility are expected to be settled similarly to the principles of the real-time market described in Section 2.2.1 above.

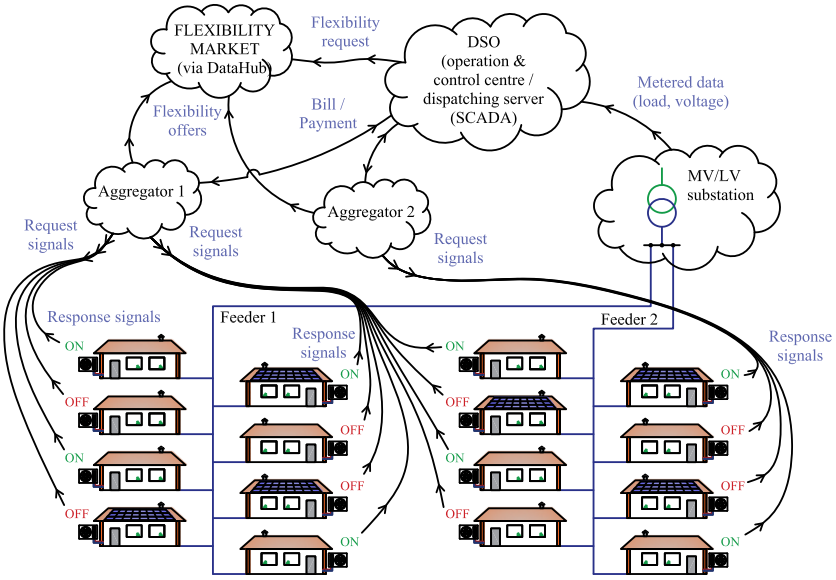

Figure 5.1. Overview of the concept of demand-side flexibility service provisioning.

In the context of the flexibility potential and the aforementioned non-obligatory response framework (without levying penalties), the simultaneity factor is an important point. Having, for example, 25 houses in the portfolio, the aggregator bets on only 6-7 houses, knowing that only 6-7 simultaneous responses can be guaranteed in any case. At the same time, only those 6-7 houses that have been activated receive monetary rewards. The simultaneity factor, in turn, should also be publicly available to all owners of flexible sources, for the possibility of tracking and additional control of earnings. Referring to Section 2.2.8 above, it can also be said that this concept covers local and partially centralized coordination controls. Since the original decision was made to investigate the topology

of energy systems integrated into a building, shown in Figure 3.8 **a**, (see Section 3.6.2 above), local control is mainly applied to the heat pump system. However, it also takes into account the presence of an on-site PV array and a battery by checking whether the household (at the moment of receiving the flexibility request) is powered from the grid or fully covered by on-site resources. Coordination control is limited to sending technical (request and restart) signals.

5.2. FLEXIBILITY POTENTIAL AND DEMAND RESPONSE BASED ON A SIMULATED SIGNAL

The section aims to answer research questions: «What energy flexibility can a single average household, equipped with DERs, provide and how does energy storage capacity (both electrical and thermal) affect the degree of flexibility and the duration of the activation period». Flexibility, in this section, is investigated by applying peak load-based technical signals. For generating an artificial signal, peak load hours should be determined first.

5.2.1. Peak hours in LV and HV

Having no low-voltage grid data available at the very initial stage of this project, for the creation of peak load based DR signal, overall Denmark's electricity demand data, available in public in [10], were used first. However, as further research and simple data analytics have shown, peak load periods at the national transmission level and at the local distribution 0.4 kV level of the power grid are very different. The results of this analysis are presented for a visual comparison in Figure 5.2. From the **a2** graph, it can be seen that, at the transmission level, the grid load exceeds the annual arithmetic mean value already at about 06:00 in the morning and all day long, until 20:00, remain above this level. Load at the local distribution level on the contrary. Graph **b2** shows that for most of the day it remains below the arithmetic mean, and grows only in the evening time. The maximum peak load can be clearly seen from 16:00 to 20:00. For the flexibility study, this basically means that the use of national-level data is not suitable for solving local grid peak load shaving issues.

5.2.2. DR request signal simulation

Artificial demand response (request) signal has been generated following the logic below. For ease of understanding, the below-described process is also reflected in Figure 5.3. In this study, it is assumed that exceeding the value of an average annual load of the transformer substation by 25% is the peak threshold of one of the aforementioned hosting capacity indices.

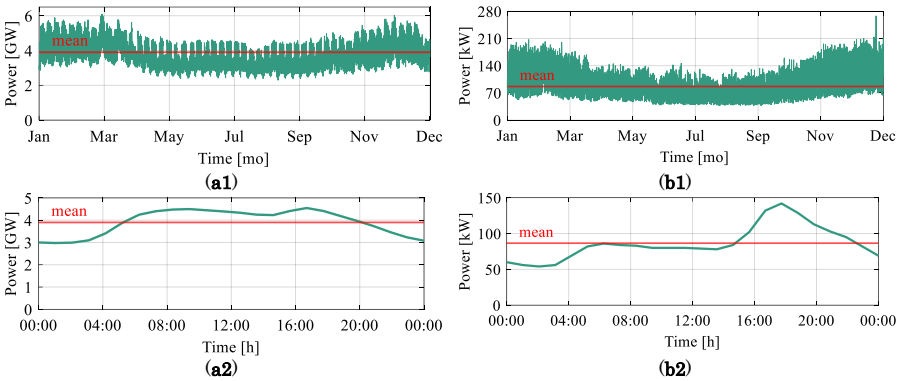

Figure 5.2. Electric load profiles: (**a**) national transmission level; (**b**) local distribution 0.4 kV level; (**1**) overall electricity demand; (**2**) average hourly demand throughout the year.

Having data with an hourly time resolution and a time span of one year, the events when the load exceeds the aforementioned limit were determined and counted for each particular hour of the day for all 365 days of the year, as shown in Figure 5.3**c**. In the next step, a 24-hour probability distribution profile was created, in which the sum of exceeding events at any particular hour of a day, equal to 365, is considered 100% (i.e. when the load exceeds the limit every single day during a year) and 0 exceeding events – 0% respectively (see Figure 5.3 **d**). This is made to convert these hourly measured peak events, to 15-minute values, following the same probability for a peak load occurrence at a certain hour during the day, as for the hourly events throughout the year. Also, for the reason to making these signals more realistic and versatile in terms of load variation within one hour. Finally, each 15-minute peak event was simply split into a series of one-minute intervals keeping the same value for all 15 one-minute steps. This is done simply considering that the flexibility service duration of 15-minute is more realistic than multiple one-minute periods. Also in order to be able to run simulation at a lower time resolution. Thus, based on the above, with a total number of peak hour events (signals) of 1,852 for hourly resolution, 7,408 signals were generated with 15-minute time intervals following the same probability as for the hourly events. The latter ones have subsequently been granulated into a series of 111,120 signals with a 1-minute time resolution. As opposed to a simple multiplication of the initial value by 4 and thereafter by 15 (and then always keep using the same series of signals), this methodology allows generating an absolutely new time series. New series of signals distributed throughout the year (while following the initial probability for a peak load occurrence at a certain hour during the day) could be applied to validate the model behaviour or to verify the accuracy of the results.

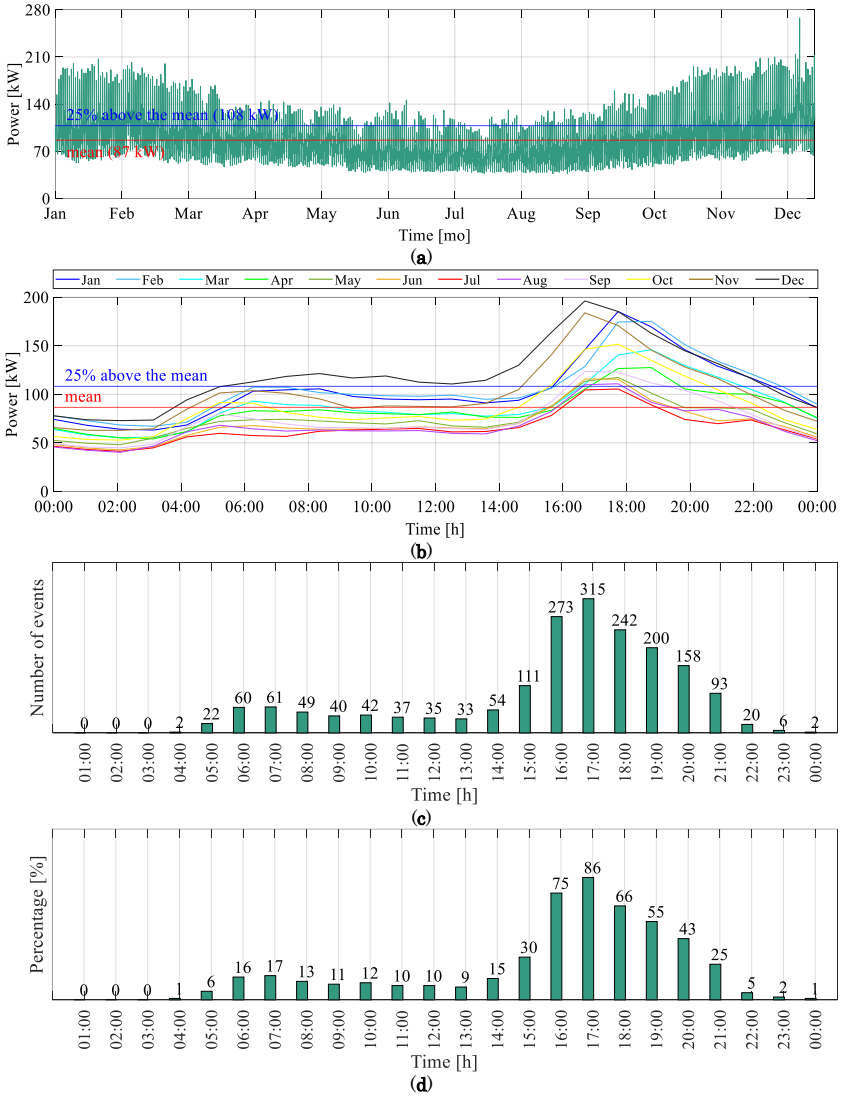

Figure 5.3. Peak hour distribution in the local power low-voltage grid 0.4 kV: (**a**) overall electricity demand; (**b**) average hourly demand at a specific month; (**c**) number of events occurring above the prespecified threshold; (**d**) percent of events occurring above the pre-specified threshold.

5.2.3. Strategy for responding to DR signal (local low-level control)

The methodology for providing a response to a DR signal follows a rule-based management strategy (i.e. decision tree). In this regard, local low-

level control implies that the decision to either provide a response to the requested DR signal or not is made exclusively locally by following a predetermined set of rules. The set of rules, in turn, has been developed and structured in such a way that the thermal comfort of residents is always a top priority. As is already noted in the concept section above, despite having created PV and battery models, the strategy proposed here is primarily concerned with the HPS model. In this regard, it is also worth mentioning that the primary focus of this strategy is being made on solving overloading and undervoltage issues. This is done by reducing the HP load. The role of PV and battery is very limited. In relation to these two components, it is only checked whether power is imported from the grid or not. Since the optimal scheduling or model predictive control, are not included in the scope of this research work, the option of solving overvoltage issues is not considered. To enable this option, at the same time to maximize the utilization of local PV production and avoid unwanted curtailment, the advanced control methods and accurate forecasting techniques are absolutely vital. The block diagram in Figure 5.4 illustrates the layout of all the model elements involved in this study.

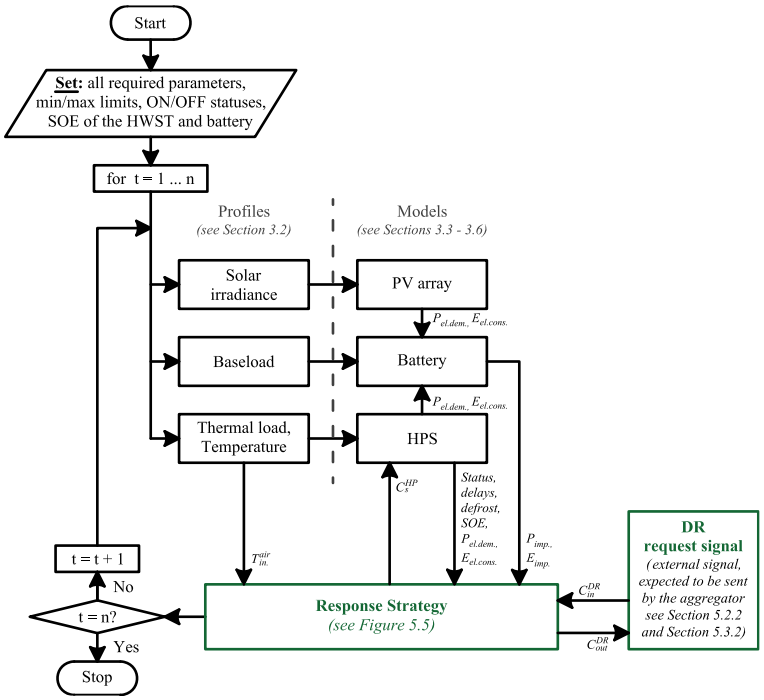

Figure 5.4. Block diagram demonstrating the layout of all the building model components involved in the provision of a demand response service.

Figure 5.5 denotes a set of decision-making conditions necessary to provide a response. All the conditions are described right below the flowchart

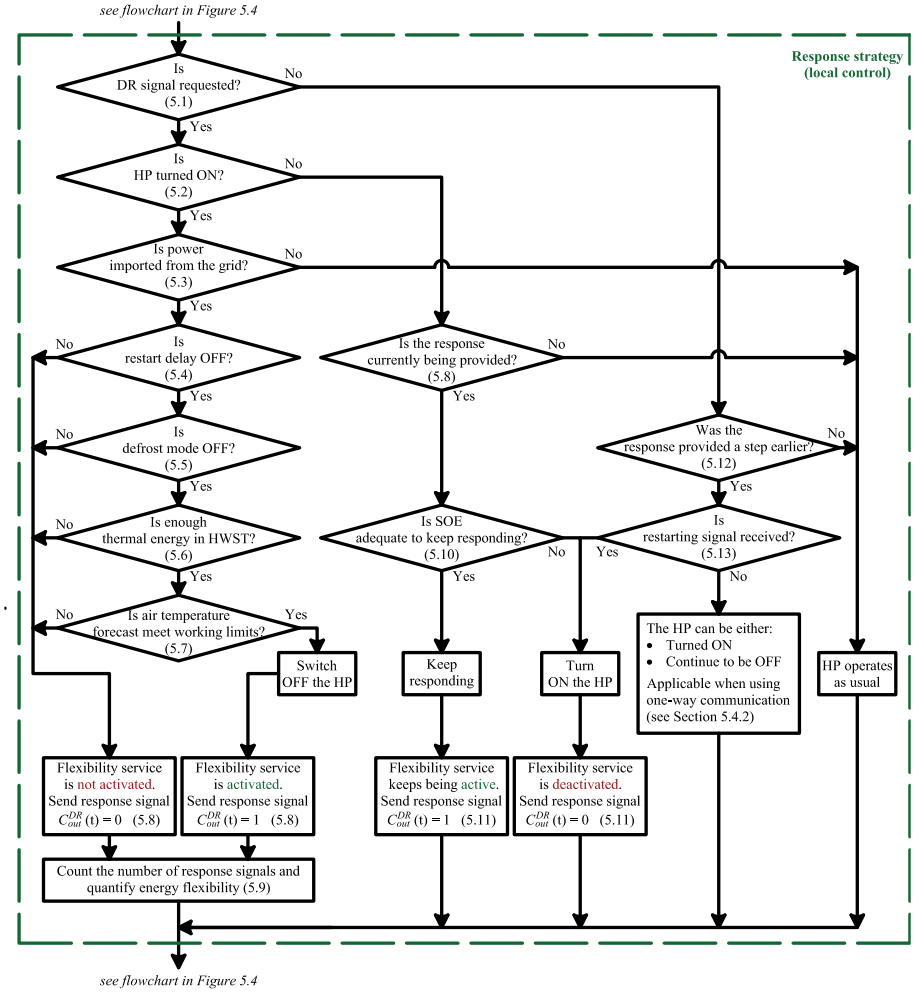

Figure 5.5. Flowchart demonstrating the strategy for responding to DR signal (local low-level controller).

First, all the necessary parameters and statuses are initialized and the necessary data for each component of the building model is loaded. The heat output and electric input power of the HPS, SOE of the HSWT, output power of the PV panels and SOE of the battery are calculated as described in detail in Chapter 3. When these outputs values have already been obtained, the first step in the proposed DR strategy is to verify whether

the technical signal (C_{in}^{DR}), at the moment, is requested by the aggregator. This condition is simply denoted as:

$$C_{in}^{DR}(t) = \begin{cases} 1, & if \ \ requested \\ 0, & if \ \ not\ requested \end{cases} \tag{5.1}$$

where,

C_{in}^{DR} – technical DR signals (1 – flexibility is requested, 0 – not requested)

The next step checks to see whether the HP is in operating mode, wherein all the initial conditions for turning the HP unit ON or OFF are listed in Eq. (3.25), Section 3.3.3. Starting from the next loop, the HPs ON/OFF status depends primarily on the fulfilment of the conditions listed below in this section.

$$HP_{status}(t) = \begin{cases} ON, & if \ \ C_s^{HP}(t-1) = 1 \\ OFF, & if \ \ C_s^{HP}(t-1) = 0 \end{cases} \tag{5.2}$$

Then, it is checked whether electricity is imported from the grid, or the house is powered by on-site resources (a detailed description of all import conditions is given in Section 3.6.3).

$$if \ \ P_{imp.}^{GRID}(t) > 0 \tag{5.3}$$

Two conditions specified in (5.4), in this context, have the same purpose and are intended to check if the heat pump has been operating for more than 30 minutes. The minimum duration of continuous operation of 30 minutes was chosen as a reasonable time to prevent short cycles, which have a detrimental effect on the lifetime of HP's components. Short cycles can be caused, including through a series of input DR signals, accordingly, no response can be provided during this time.

$$if \ \ \tau_{rest.}(t-25, \dots, t) = 0 \ \ \& \ \ \tau_{oper.}(t-30, \dots, t) = 0 \tag{5.4}$$

Following the sequence, the next step verifies that HP is not performing a defrost cycle, which is also an important component of the smooth operation of the system (see Section 3.3.1).

$$if \ \ \tau_{defr.}(t) = 0 \tag{5.5}$$

The condition indicated in (5.6) reflects the minimum energy threshold in the HWST (with the HP operating) at which a response to the requested DR signal can be provided. Since the basic HPS control is realised in the HWST water temperature range from +55°C to +65°C (or between

$SOE^{HWST}_{min.ctrl.}$ and SOE^{HWST}_{max}, see Section 3.3.3), this threshold is selected to be greater or equal to +60°C, reflecting at least 50% of the controlled energy range. The equivalent SOE setpoint for this temperature level is expressed below. Estimation of the SOE for 11 steps ahead (i.e., the second sub-condition) is designed to prevent the HWST's energy level from falling below the minimum controllable band, thereby ensuring a stable heat supply during restart and conversion delay periods. This estimation is especially relevant for small size HWSTs that can be rapidly discharged due to peak heat demand.

$$\begin{gathered} if\ \ SOE^{HWST}(t) \geq SOE^{HWST}_{min.ctrl.} + (SOE^{HWST}_{max} - SOE^{HWST}_{min.ctrl.}) \times 0.5 \\ \& \\ SOE^{HWST}(t) - \sum_{t}^{t+11} \left(\frac{Q^{HH}_{th.cons.}(t) + Q^{HWST}_{th.loss}(t)}{Q^{HWST}_{total}} \times 100 \right) > SOE^{HWST}_{min.ctrl.} \end{gathered} \tag{5.6}$$

where,

$SOE^{HWST}_{min.ctrl.}, SOE^{HWST}_{max}$ – minimum and maximum controlled energy levels of the HWST [%]

The latter condition in (5.7) estimates the outdoor air temperature for the same 11 steps ahead to ensure that the HP is turned ON when needed, and thus, undesirable activation of the IHWH is avoided.

$$if\ \ T^{air}_{in.min} < T^{air}_{in}(t, \dots, t+11) < T^{air}_{in.max} \tag{5.7}$$

Finally, when all the prerequisites are met, the HP is turned OFF ($C^{HP}_{s}(t) = 0$) and a response signal is sent back to the aggregator informing that the service has been activated. Accordingly, if any of the above conditions are not met, the service cannot be provided.

$$C^{DR}_{out}(t) = \begin{cases} 1, & if\ \ activated \\ 0, & if\ \ not\ activated \end{cases} \tag{5.8}$$

The amount of energy flexibility* is determined as shown in (5.9)

* The energy flexibility, in this context, is considered an estimated energy value that could have been used by the HP unit, but not used due to cutting its power OFF. It is also worth noting that, in the context of this study, the conditions outlined in (5.6, 5.10, 5.7) imply the use of only historically measured time-series data several steps ahead. However, for the full-fledged application of these estimates, a specific short-term load forecasting technique should be applied. An appropriate model for implementation (such as artificial neural networks, regression, time series, support vector machine, bottom-up, etc.) can be selected based on the reviews made in [270], [271].

$$E_{flex.}^{HH^*} = \begin{cases} \frac{1}{60} \int P_{el.rt.}^{HP} \times C_{out}^{DR} \times dt, & if \quad P_{imp.}^{GRID}(t) > P_{el.rt.}^{HP}(t) \\ \frac{1}{60} \int P_{imp.}^{GRID} \times C_{out}^{DR} \times dt, & if \quad P_{imp.}^{GRID}(t) < P_{el.rt.}^{HP}(t) \end{cases} \tag{5.9}$$

where,

$E_{flex.}^{HH}$ – energy flexibility provided by the household (estimated per minute value) [kWh],

C_{out}^{DR} – binary control signal, which defines the DR activation (and thus the duration of an actual response), where activated = 1, not activated = 0.

If a request signal has been received (5.1), but the heat pump has already been switched off (5.2), in this case, it is checked whether the cause of the switch-off is a previously activated service (i.e. $C_{out}^{DR}(t-1) = 1$ according to (5.8)), or an ordinary HWST discharge cycle (i.e. $C_s^{HP}(t) = 0$ according to (3.25), while running the first loop), or the fact that any of the conditions listed above are not met. If the reason is the active provision of the flexibility service, it is then checked whether the energy level of the tank is sufficient to continue providing this service. For this purpose, condition (5.10), estimates the SOE for 6 steps forward in time and, unlike (5.6), reflects the energy threshold of the tank, upon reaching which (if the condition is not met), the HP must be turned ON. Accordingly, DR activation must be interrupted. Conversely, if the condition is successfully met, the service continues to be provided (5.11). The six-step estimate is created for a similar purpose as (5.6) – that is to prevent the energy of the HWST from falling below the minimum controllable level, and also to cover the period of conversion delay, thereby not violating the thermal comfort of inhabitants. Nonetheless, in contrast to (5.6), in this case, the 5-minute restart delay time is not counted due to the fact that the HP, by default, must already be switched off for at least 5 minutes.

$$SOE^{HWST}(t) - \sum_{t}^{t+6} \left(\frac{Q_{th.cons.}^{HH}(t) + Q_{th.loss}^{HWST}(t)}{Q_{total}^{HWST}} \times 100 \right) > SOE_{min.ctrl.}^{HWST} \tag{5.10}$$

subject to

$$C_s^{HP}(t) = \begin{cases} 1, & if \quad (5.10)\ is\ false \quad \rightarrow \quad C_{out}^{DR}(t) = 0 \\ 0, & if \quad (5.10)\ is\ true \quad \rightarrow \quad C_{out}^{DR}(t) = 1 \end{cases} \tag{5.11}$$

If the DR signal is not requested (5.1) and the response has not been given before (i.e. $C_{out}^{DR}(t-1) = 0$ according to (5.12)), the heat pump operates

following the standard regulations described in Eq. (3.25), Section 3.3.3. If the signal was requested before and the response has been provided to it, but at the moment is no longer requested, in this case, everything depends on how the information is exchanged between the aggregator and the building energy management system (i.e. one-way or two-way communication).

$$C_s^{HP}(t) = \begin{cases} see\ (3.25), & if\ \ C_{in}^{DR}(t) = 0\ \ \&\ \ C_{out}^{DR}(t-1) = 0 \\ see\ (5.13), & if\ \ C_{in}^{DR}(t) = 0\ \ \&\ \ C_{out}^{DR}(t-1) = 1 \end{cases} \tag{5.12}$$

This section deals with one-way communication only. Since the request signals have been artificially created to just mimic some grid issues and to investigate the HPS behaviour, there is no centralised control implied in this part of the study even though the feedback signal option is shown in the block diagram. In the context of the study of the energy flexibility potential, the control is implemented in such a way that after the signal has elapsed, the heat pump is automatically switched on and continues the HWST charging cycle not completed earlier (interrupted by DR). These conditions are shown below.

$$C_s^{HP}(t) = \begin{cases} 1, & if\ \ C_{restart}^{DR}(t) = 1 \\ 1\ (for\ this\ study)^{*}, & if\ \ C_{restart}^{DR}(t) = 0 \end{cases} \tag{5.13}$$

As further research has shown, turning on the heat pump immediately after the termination of the request signal has a negative impact on the stable operation of the network, namely the voltage stability. That is why the strategy has been adapted and in fact can be used for both one-way and two-way information exchange (demonstrated in Section 5.3.2), without losing the main idea – respecting the priority of consumer comfort. The impact and negative consequences of automatic turning on heat pumps will be described in more detail in Section 5.3.2. For a clear demonstration of the above strategy, the scenario designated as S6 in the previous chapter was chosen, namely Baseload + HPS + PV + battery, with an HWST volume of 1m^3.

Figure 5.6 shows the behaviour of the integrated energy systems of a household and the response of these systems to a series of requested DR signals following the above strategy. Both graphs below should be considered as one in common and separated only for ease of perception.

* Can be either 0 or 1 in the case of using one-way communication. However, this should not be the case in general when using two-way communication and is considered a communication error. For more details, see Section 5.3.2.

The period from 00:00 to 05:00 reflects the situation when the heat pump is switched off and the HWST energy level is sufficient to cover all heat demand. At 02:30 it can be seen, that the air temperature has dropped, heat demand has increased and the intense discharge of the HWST can be observed. At 05:00 the SOE level of the tank reached a minimum, which caused the heat pump to turn on. Since there is no PV generation at this time, as well as the battery SOE is at a minimum level, all electricity is imported from the grid. At 05:30 it can be seen that the first series of DR signals are sent by the aggregator, requesting to reduce the load. Since the heat pump has not run for enough time since it was switched on (i.e. at least 30 minutes, as indicated (5.4), the first series of signals can be seen to be ignored. From the SOE of the HWST curve, it can be seen that several minutes before 06:00 (namely at 05:52) the tank charging has stopped. Since the outdoor temperature was below the freezing point at this time and the heat pump was running for more than 55 minutes, the heat pump went into defrosting mode. At 06:00 the next series of signals arrived. Since the defrost cycle (programmed for 5 minutes) has ended (5.5), the energy level in the tank has reached a sufficient level to meet condition (5.6) and the temperature requirements have been met – a response has been provided. The heat pump was switched OFF, which is also reflected in the power import from the grid. As the signal lasted 15 minutes, at 06:15 the heat pump turned on again. From the SOE of the HWST curve, it can be seen again that the tank charging started only after a few minutes, which is due to a five-minute conversion delay. After working for exactly 30 minutes, the next 15-minute series of request signals was received (06:45 - 06:59), which has also been successfully answered, as well as the signals between 07:30 - 07:44. Since the last morning series of signals was received only 16 minutes after the heat pump was turned on (meaning less than 30 minutes as indicated in condition (5.4)), the response was ignored. Then the tank was charged to 100% and the discharge cycle began. From 08:00 to 19:00, the active PV generation can be observed, which is also reflected in the battery SOE level. Having low energy consumption, almost all of the energy is charged to the battery. At 13:13 the HWST energy level reached the minimum controllable level and the heat pump turned ON. Since there was a high PV generation during this period and the battery was fully charged, all the peak load is covered only by local resources. For the same reason there is no power import, and all afternoon and evening signals are ignored.

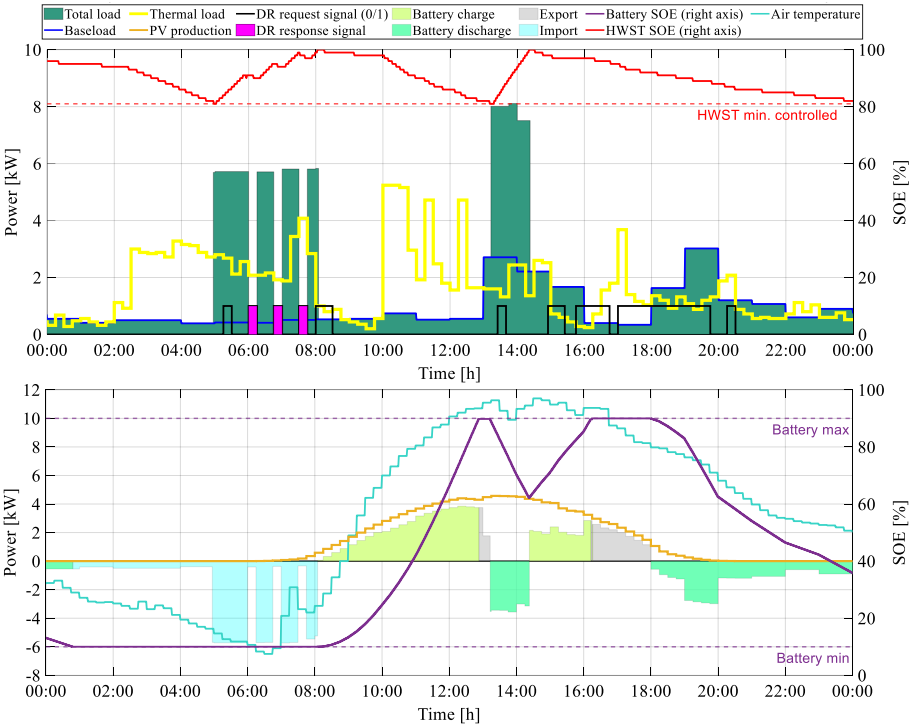

Figure 5.6. Behaviour of the integrated energy systems of a household as a demonstration of the DR signal response strategy (Aptil 4).

The results of numerous simulations have shown that the application of this strategy for responding to DR signals has practically no effect on the final annual electricity consumption. This is shown in the example of a scenario with a 1m³ tank (without a battery), where the difference in results is very insignificant, namely 0.85%. The result can be seen in Table 4.6.

Table 5.1. Summary of the building's energy system performance under scenario S4.

HWST volume [m³]	*Electrical energy consumption per year [kWh]*		*Percentage difference [%]*
	Without DR application	With DR application	
1.0	11,523	11,621	0.85

More scenarios can be seen in [190], [265]. This generally means that having a fixed electricity tariff, the application of such a DR scheme will not increase the final annual electricity bill.

5.2.4. Flexibility rate and amount of peak-hour energy shaved

Flexibility potential in percentage, in the context of this study, is considered as the ratio of the sum of all response signals to the sum of all requested signals. It can be either a daily, a seasonal or an annual index. Let us consider the impact of on-site PV panels, battery and two different HWST sizes on the number of responses provided. For example, scenarios with two different tanks 0.2m^3 and 1m^3 and "with" and "without" PV&Battery were used (four scenarios in total). The results shown in Table 5.2 demonstrates the highest flexibility percentage in the scenario **s4** (with a 1m^3 tank and without PV&Battery) and the smallest in the scenario **s1** (with a 0.2m^3 tank and with PV&Battery). Based on this a simple conclusion can be made that the larger the tank, the greater the number of responses. This can be attributed to longer charging cycles, which in turn cover a larger number of requested signals. The fact that flexibility in scenarios with a tank of 0.2 m^3 is scantily small can be explained by the fact that HWSTs of this size are primarily intended to optimize the operating cycles of the heat pump and are not intended to bridge power OFF periods, as well as provide backup heat supply for a long time. The volume, as well as the controllable thermal energy range, are too small for these purposes (see Table 4.5 in Section 4.1.4). The lower percentage in scenarios with PV and battery can be explained by the fact that having on-site RES and battery, less energy is imported from the grid and there is no need to respond to all requested signals.

The proposed approach is an example of estimating the flexibility of a single house, which can be successfully applied to calculate the potential of aggregated flexibility of a group of houses. The correctness of this method can be verified by raising the peak load limit described in Section 5.2.2. By changing the threshold from 25% to 35% above the yearly mean, the number of peak events and thus the requested signals decrease. Accordingly, the number of responses provided is also smaller. However, even though the number of responses is smaller, the ratio of responses to the sum of requests remains almost unchanged. Analysis of the results in Table 5.2 showed that by changing the threshold from 25% to 35%, the difference does not exceed 1.0%, which does not significantly affect the overall assessment of the flexibility potential.

Table 5.2. Summary of percentages of responses to the DR signal.

Scenario	*HWST volume [m³]*	*PV & Battery*	*Percentage of responds per year [%]*		*Percentage difference [%]*
			The threshold is set to +25 above the yearly mean, and the number of signals requested per year is 111,120	The threshold is set to +35 above the yearly mean, and the number of signals requested per year is 82,260	
S1	0.2	with	0.54	0.49	0.05
S2		without	0.57	0,51	0,06
S3	1.0	with	13.21	12,95	0,26
S4		without	17.62	16.95	0.67

If the percentage flexibility is needed to just estimate the potential, the value in kWh is required for specific financial settlements (for billing and payment). The results of the above four scenarios in kWh equivalent are summarized in Table 5.3.

Table 5.3. Summary of the energy flexibility provision in four different scenarios.

Scenario	*HWST volume [m³]*	*PV & Battery*	*Number of signals per year [ones]*		*Amount of peak-hour energy per year [kWh]*		*Percentage [%]*
			Requested	Responded	Requested to be shaved	Shaved	
S1	0.2	with	111,120	599	9,816	53	0.54
S2		without		629		56	0.57
S3	1.0	with		14,674		1,296	13.21
S4		without		19,578		1,729	17.62

From both tables above it can also be seen that the total number of responses provided, or kWh of energy shaved, is very small compared to the number of requests (the highest rate is 17.62%). Such a small number of responses can be explained by several factors.

- First, this can be explained by the need to fulfil all the prerequisites specified in the strategy above, so as not to violate the comfort of residents.
- Second (as noted above), is the amount of energy controlled in the tank. This amount, which plays an extremely important role, in turn, directly depends on the volume of the tank and the temperature difference (see (3.21)). The water temperature difference, in turn, depends on the ability of the heat pump to deliver hot water in the mono-mode application (i.e. without the use of a supplemental heater). The higher the water temperature can the HP produce, the greater the controllable temperature range inside the HWST (hysteresis) and hence the greater amount of controllable heat energy. The greater amount of heat energy

controlled simply means longer backup heat supply time without turning ON the HP, therefore longer lasting DR activation period, and hence, the larger amount of energy (not power) can be shifted in time. Not so long time ago, most residential A2W type heat pumps were able to deliver maximum +55°C water (over a wide outdoor temperature range). Nowadays, this limit increased up to +65-70°C and keeps growing with new developments in this field.

- Third, even though HWST volume plays an incredibly important role, the increase in tank size is not the unique solution for increasing this flexibility rate. One of the possible options for increasing this rate may be to improve the algorithm and strengthen it with better prediction of outdoor temperature, heat demand, heat production as well as SOE of the HWST. Optimal scheduling of the HWST charging cycles (taking into account the PV production), or the model predictive control (which, by offering the best system behaviour a few steps forward in time, allows shifting the load over time), could be considered perspective solutions for improvement.

5.3. GRID IMPACT AND VOLTAGE SUPPORT VIA DEMAND RESPONSE

The section aims to answer research questions: «How exactly can the activation of energy assets of buildings with new control and management schemes and further utilisation of energy flexibility from these DERs *support the grid* operation? In this connection, can the voltage-based DR control strategy for such kinds of active buildings help to solve grid peak hours issues (i.e. overloading, undervoltage) thereby reducing or postponing the need for grid reinforcement? What energy flexibility can an aggregate group of such kinds of houses provide»?

At the first stage, it is interesting to investigate what impact, in general, the modernization of the energy systems of the households have on the voltage stability in the power distribution grids. As the studies reviewed in Section 2.1.2 show, for example [101], it is with a voltage drop (not with overvoltage due to RESs) at a low voltage level of 0.4 kV that potential problems can arise. Since a significant increase in load, which is the main cause of voltage drop, occurs during the heating season and is directly related to heat pumps (as shown in Figure 4.21 **s4** in Section 4.2), the impact of heat pumps on voltage fluctuations in the local distribution grid is the most logical to investigate. Given the fact that the presence of PV&Battery (for the actual case) does not dramatically change neither the peak load (Figure 4.21 **s4** – **s6**) nor the amount of flexibility (Table 5.3

shows the difference between "with" and "without" <4.5%) further research and DR strategy for voltage support proposed later in this section only apply to heat pumps.

5.3.1. Grid impact

To investigate the impact of the expansion of such buildings on the local low voltage distribution grid, a part of the network, that is, one low-voltage 0.4 kV feeder that feeds 25 residential buildings, was selected. This feeder has 13 buses, each of which feeds several houses. A single-line diagram of this part of the network is shown in Figure 5.7, while a more detailed description of all parameters of cables, impedance, etc., necessary for further analysis of voltage deviation, and DR application, can be found in the Appendix C.

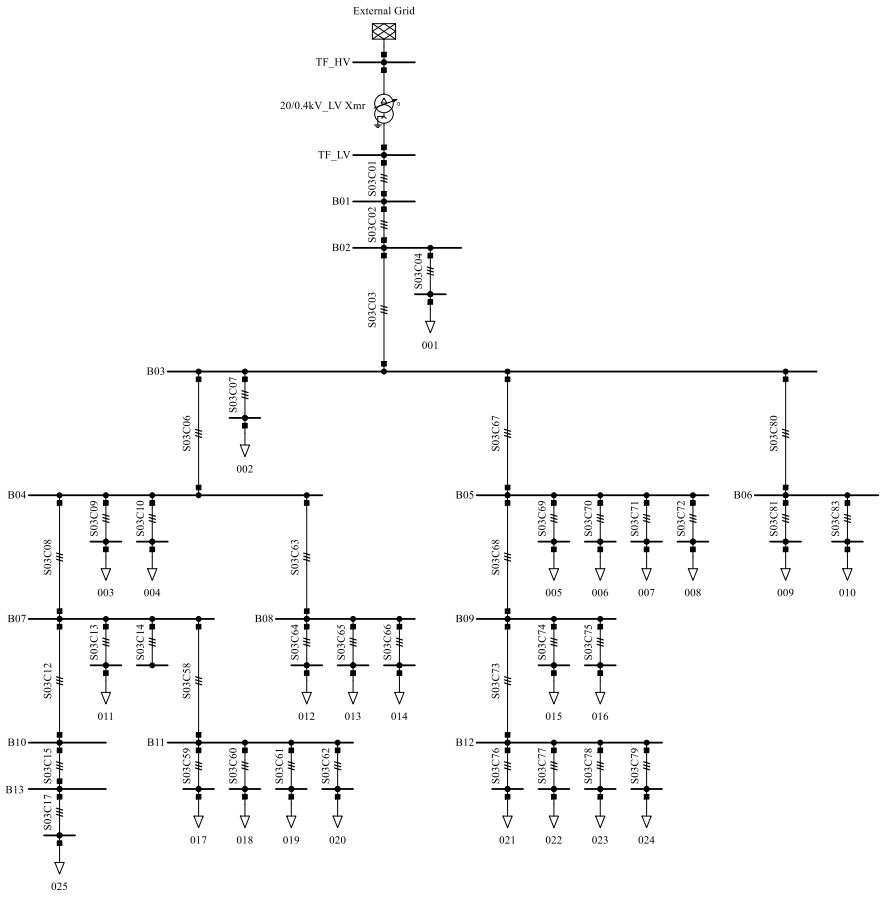

Figure 5.7. Single-line diagram of a part of the distribution grid 0.4 kV.

It was decided to investigate the voltage deviation on this feeder by carrying out Load flow analysis using the Newton-Raphson method, described in detail in [266]. The load profiles required for the analysis were generated following the approach shown in the figure below. The flowchart in Figure 5.8 shows the sequence of analysis. First, the initial data matrices of the network (transformer, bus, cables), as well as the baseload profiles of the households are loaded. Having different heat load profiles and, accordingly, individual sizes of heat pumps in each household, the system behaviour and heat pump electric load profiles are simulated/generated for each household individually using the model created in Section 3.3. The active and reactive power required for this analysis are obtained from equations (3.29), (3.30) in Section 3.3.5. In the next stage, these profiles (BL + HPS) are summed, forming the total load of the house. With active and reactive loads, a matrix of 25 house profiles is created, which serves as input for Load Flow analysis. Actually, the analysis is carried out and the cycle is repeated every new step from 1 to n (that is, 525600 steps for a corridor of one year).

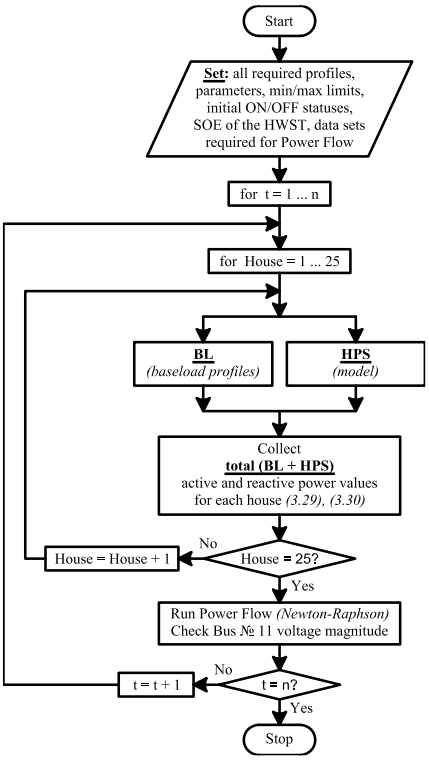

Figure 5.8. Flowchart showing the sequence of performing the power flow analysis.

The result of the analysis showed that the investigated feeder is strong enough and can normally accommodate all heat pumps without the need to strengthen the lines. Figure 5.9 illustrates voltage fluctuation curves at baseload only (graph **a**) and with heat pumps (graph **b**). Both figures show that the voltage is very stable and even with the emergence of heat pumps in 100% of households in Figure 5.9 **b**, it can be seen that the voltage during the year is within acceptable limits and does not violate the requirements of standards. DS EN50160 [267], in this context, stipulates that the steady-state supply voltage must be maintained within ±10% of the nominal value under normal operating conditions. DS EN 60204-1 [268], in turn, reinforces the above statement indicating that the conductors and cables voltage drop should not exceed 5% at any point of the circuit starting from the supply point to the load. The latter value has been selected as a basis in this study.

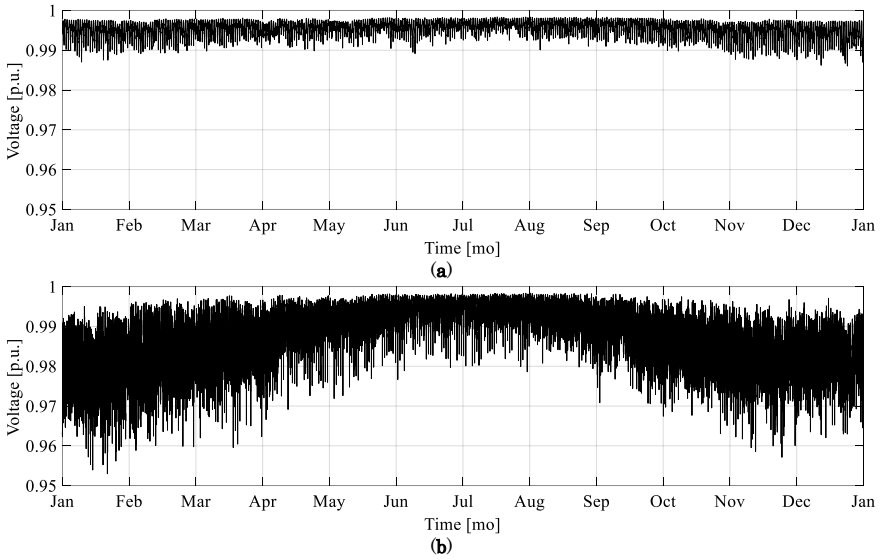

Figure 5.9. The voltage magnitude on the weakest bus № 11: (**a**) Baseload; (**b**) Baseload + HPS.

Since far not all electrical networks have such a strong infrastructure, for further research on the DR application, it was decided to artificially simulate the voltage problem in the network. This has been done by extending the length of the central cable line from bus B01 to B013 by 2.5 times. The result of such simulation is presented in Figure 5.10. From Figure 5.10 **b** one can see a lot of periods during the entire heating season (from October to April) when the voltage drops below the permitted 0.95 p.u. While January is the most saturated month in terms of voltage drop. Table 5.4summarizes the total number of voltage drop events during the

year and separately in January. This month will be used to compare the performance of the strategy proposed below and the ability of the latter to resolve the voltage drop issue in the network.

Table 5.4. Summary of voltage drop events under the base case scenario.

Minutes of voltage drop [m]		
Per one week in January	*Per full month, January*	*Per year*
722	4,126	20,280

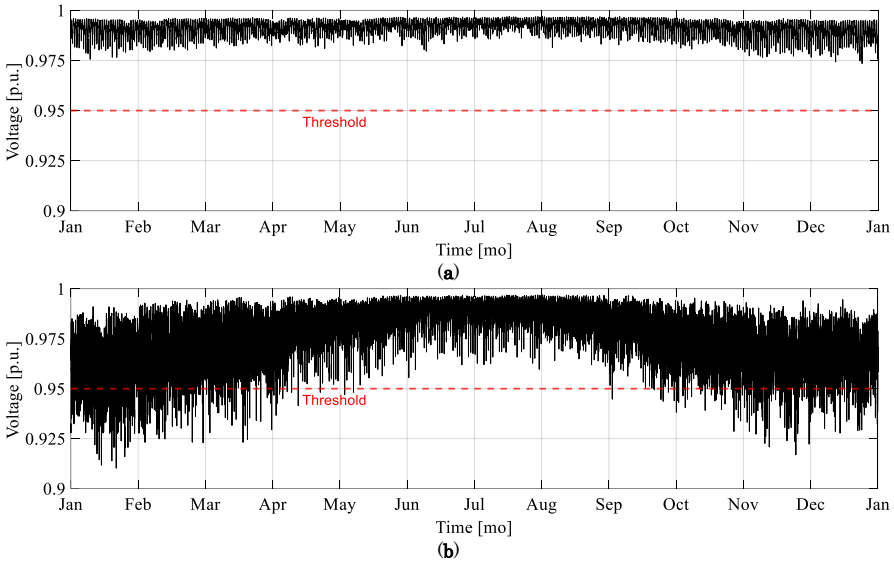

Figure 5.10. The voltage magnitude on the weakest bus № 11 with extended cable length: (**a**) Baseload; (**b**) Baseload + HPS.

5.3.2. Demand Response application from the perspective of aggregators. Flexibility request strategy for voltage support (centralized coordination control).

This section demonstrates the effect of automatic turning on of heat pumps immediately after the DR request signal has elapsed, as one of the likely consequences of using control with one-way communication. A strategy for avoiding such consequences and overcoming voltage drop issues in a low-voltage network of 0.4 kV is also proposed. Going back to Figure 5.4, it can be said that the developed strategy is what happens inside the "DR request signal" block and is considered a centralized control for aggregators. The first part of this strategy is structured as follows. Performing power flow analysis, the weakest bus was determined first. In this case, this is bus №11. It is assumed that this bus is equipped with a PMU unit and DSO,

has complete information about the status of all important indices of this network node. When the voltage on this bus falls below the pre-set level (in this case 0.95 p.u.) the PMU is signalling this DSO. Then, the DSO makes a request for flexibility to the aggregator, and the latter, in turn, sends a series of signals to all involved houses with heat pumps. Heat pumps respond to these signals whenever possible by following the "response strategy" described in Section 5.2.3. As the result of the simulations showed, the voltage stabilizes almost immediately after the response has been provided by several heat pumps, regardless of the duration of the request signal. However, the most important aspect for further compliance with this voltage within the permitted limits is precisely the behaviour of heat pumps after voltage stabilization and after the signal has ceased. Starting from this moment, many different scenarios for the development of events have been investigated, among which the following three can be highlighted:

- S1. Turning ON and continuing the HWST charge cycle;
- S2. HPs continue to be switched OFF initiating HWSTs' discharge cycles;
- S3 Smooth uniform (cascade) restart of each heat pump individually at specified intervals.

In the first two points (S1, S2), centralized control comes down to sending voltage-based flexibility request signals with a specified duration. Such a scheme provides only one-way communication and all subsequent decisions after receiving the signal are made exclusively at the local level, as described in Section 5.2.3. In the context of one-way communication, the scenarios of sending signals lasting 5-10-15-20-25-30 minutes were analyzed. Considering the specifics of the heat pump operation (delays, defrost), signals with a longer duration showed better results, allowing a more even distribution of heat pump operation over time. The longer signal duration also allows reducing the share of wasteful energy due to the conversion delay before each start of the heat pump. However, the signal duration has yet a secondary importance, while the most important is the fact of whether the heat pump is turned on after the termination of the request signal or not, and how.

S1. Turning ON and continuing the HWST charge cycle

Figure 5.11 shows the severe voltage destabilization resulting from at simultaneous activation of all involved heat pumps immediately after the end of each new series of request signals from aggregators. The period of one day on the first of January in the graphs below demonstrates the voltage magnitude on bus 11 and the behaviour of one house powered by this bus. Each subsequent response to a series of signals is clearly reflected

in both the load change (due to HP switching OFF) and the voltage change. Since the installed capacity of the heat pumps is quite large, one can see a significant increase in voltage immediately after responding to the request signal, as well as a significant voltage drop after each simultaneous switching on of all 25 heat pumps. In this context, the analysis of the signal duration is of the least importance, since, as can be seen from the graphs, such a DR scheme has a negative effect on the stability of the voltage in the network.

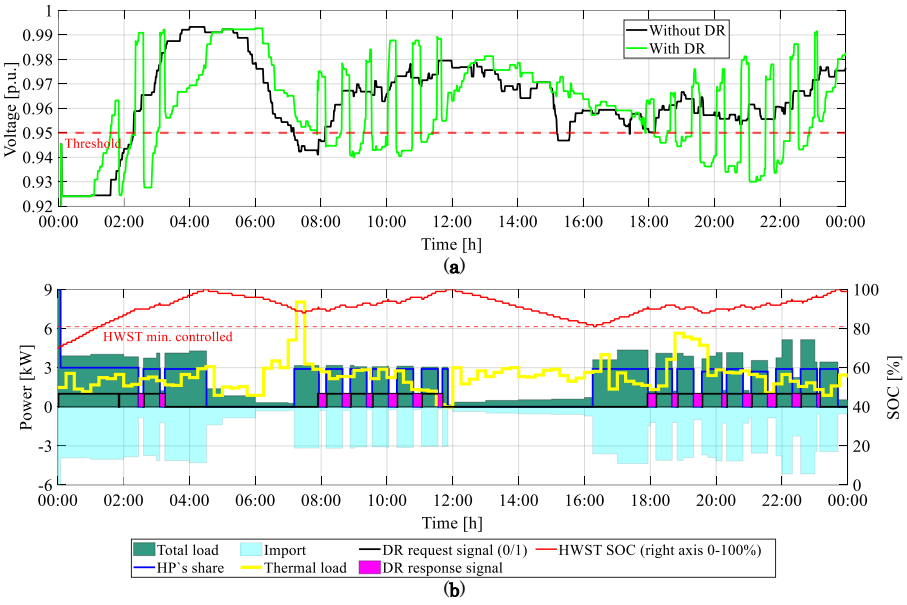

Figure 5.11. Demonstration of DR application under scenario S1 (**a**) voltage magnitude at the weakest bus №11; (**b**) behaviour of a single house №17 powered by this bus.

Table 5.5 shows the result of the weekly simulation, summing the number of voltage drops in two cases - with DR application and without. As can be seen from the table - the total number of minutes of voltage drop has more than doubled, which once again confirms the negative impact of such DR application.

Table 5.5. Summary of voltage drop events under scenario S1.

DR application	*Minutes of voltage drop per one week in January [m]*	*Percentage increase [%]*
Without	722	+116.9
With	1566	

S2. HPs continue to be switched OFF initiating HWSTs' discharge cycles

Since S1 showed an unsatisfactory result, it was decided to investigate the voltage in the network when the HPs continue to be in power-off mode after each elapsed signal, following the basic temperature control, until one of the conditions in (3.25) is met. This scenario is also relatively easy to implement, both in terms of communication and in terms of local controller settings, changing only one default value of the resulting HP control signal from $C_s^{HP} = 1$ to $C_s^{HP} = 0$ (as is shown in Eq. 5.13). The result of such readjustments obviously has a better effect on the grid voltage. Figure 5.12 illustrates the same period as in scenario S1, voltage magnitude at the bus №11 and the reaction of two houses, namely №19 and 25. As in S1, one of the worst-case scenarios was chosen for the demonstration, starting the simulation with the initial state of energy of the HWST of 70%. Not fully charged HWST implies the simultaneous starting up of all 25 HPs, which is clearly reflected in both the request signals and the significant undervoltage during the first hour. The graph shows that such a scheme allows stabilizing the voltage in the network and keeping it within the normal range during the day. There are only a few short-term voltage drops observed, which are instantly counterbalanced by sending new signals and responses to these signals. The table below, based on the result of a simulation of one week, in turn, also demonstrates a significant reduction of voltage drop minutes in the case of DR application showing a percentage of improvement of 70.8%.

Table 5.6. Summary of voltage drop events under scenario S2.

DR application	*Minutes of voltage drop per one week in January [m]*	*Percentage decrease [%]*
Without	722	-70.8
With	211	

Nevertheless, the main disadvantage and issue of such a DR application are how the settlement will be performed. How can the aggregator, as a potential flexibility program provider, know the specific activation period for a particular respondent, using one-way communication? How to find how many HSs are still responding, and which ones have already been transferred to discharge mode? From graphs **b** and **c**, it can be seen that with the same duration of the request signal, the activation periods can be very different (see the period between 01:00 – 02:00). Since these periods cannot be measured with a conventional electricity meter, the question remains open. The use of techniques such as, for example, nonintrusive load monitoring [13], in this context is also not rational, due to the actual transition to the discharge cycle of the HWST (HP keeps being OFF), as well as the specifics of the heat pump operation, as for example, the defrost

cycle, which can be mistakenly considered as flexibility activation. This only emphasizes the importance of two-way communication.

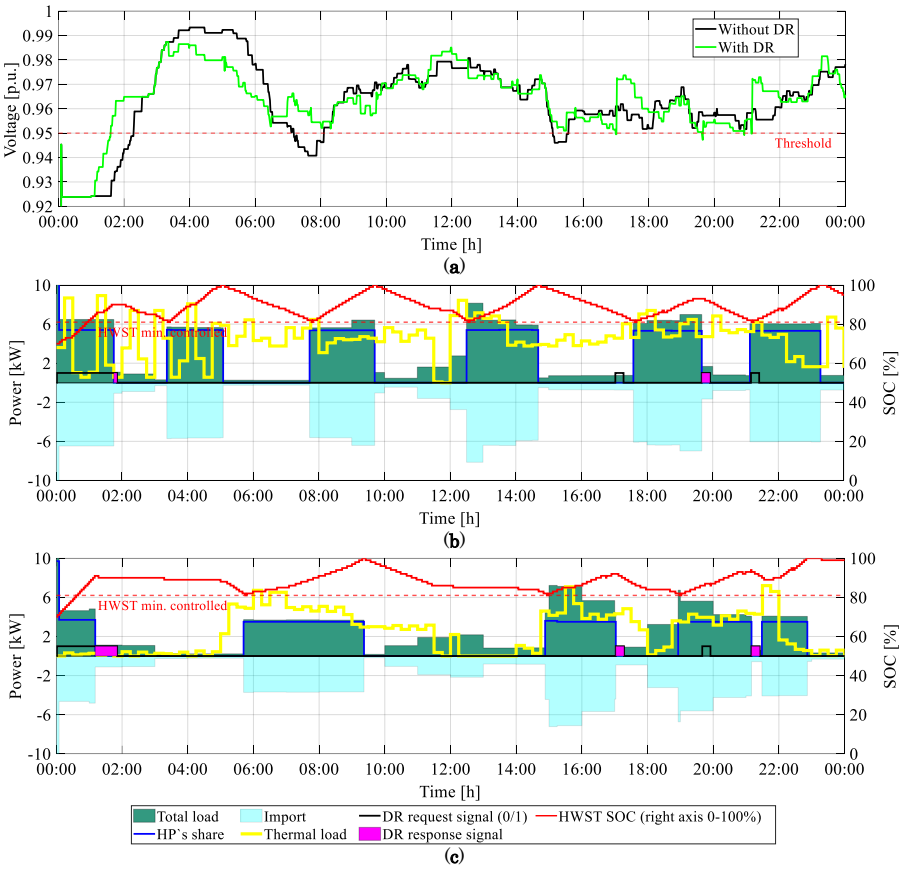

Figure 5.12. Demonstration of DR application under scenario S2 (**a**) voltage magnitude at the weakest bus №11; (**b, c**) behaviour of a house №19, 25.

S3. Smooth uniform (cascade) restart of each heat pump individually at specified intervals

Special attention of this section is paid to the strategy described below since it is this strategy is considered a centralized coordination control and it is this strategy involves the use of two-way communication. Demand Response application, in this context, consists of:

- sending voltage-based flexibility request signals,
- receiving activation signals back from each respondent, and
- sending heat pump restart signals to each respondent individually (to each activated unit) at certain intervals.

It is this exchange of information that makes it possible to accurately calculate the activation periods of each respondent and, accordingly, the exact amount of flexibility provided, which is important for all parties concerned in this process. It is the application of this strategy (as shown in Figure 5.13 and described below) that allows a more uniform distribution of the heat pumps' work in time, thereby preventing the simultaneous activation of all responders at once after the signal has ceased. And it was this scheme that showed the best voltage stabilization results, reducing voltage drop periods that occurred during an ordinary operation (without DR application) by 81%. For ease of understanding, the main idea of this strategy is also presented in Figure 5.14. The process is as below.

First, the total load (active and reactive) of each household is collected individually, a Power Flow analysis is performed and the voltage magnitude on the weakest bus №11 is determined. At the moment when the voltage on this bus drops below the set threshold (0.95 p.u. in this case), the flexibility **request** signal is sent to all 25 involved houses (heat pumps). The next time step is to determine the ability of each heat pump individually to provide a response, following the response strategy presented in Section 5.2.3, Figure 5.5. According to that strategy, all responding households send a "**response**" signal in the opposite direction informing about the "**activated**" status. The cycle repeats until the voltage exceeds 0.95 p.u. Hysteresis control (in the range of 5 volts) is set between 0.95 – 0.9625 p.u. (380 – 385 V). As soon as the voltage has exceeded the lower limit of 0.95 p.u., the system identifies all respondents, and until the upper limit is reached (0.9625 p.u.), the request signals are sent only to them. From the moment the upper limit is exceeded (0.9625 p.u.), a restart count/delay begins, during which signals still continue to be sent to all respondents. If the voltage was stable during the delay time (15 minutes in this case), the next step is to check how many respondents can be turned on. If the voltage during the whole time was above 0.9675 p.u. (387 V) the "**restart**" signal is sent to the 20% of respondents who responded the longest. Accordingly, the request signals continue to be sent to the remaining 80%. If for the next 15 minutes the voltage fluctuates between 0.9675 – 0.9625 p.u., only the next 10% of respondents receive a restart signal this time (and the request signals, respectively, continue to be sent to the remaining 70% of respondents). In order to realize the ability to turn on all respondents after voltage stabilization, the number of respondents that have to be restarted is determined as shown in (5.14). If the voltage drops below 0.95 p.u. the signals are sent to all houses again and the cycle repeats.

$$NrToBeON = \begin{cases} ceil\left(\frac{TotalNrResp \times 20 \times (k/15)}{100}\right), & if \quad U > 0{,}9675 \\ ceil\left(\frac{TotalNrResp \times 10 \times (k/15)}{100}\right), & if \quad 0{,}9625 < U < 0{,}9675 \end{cases} \tag{5.14}$$

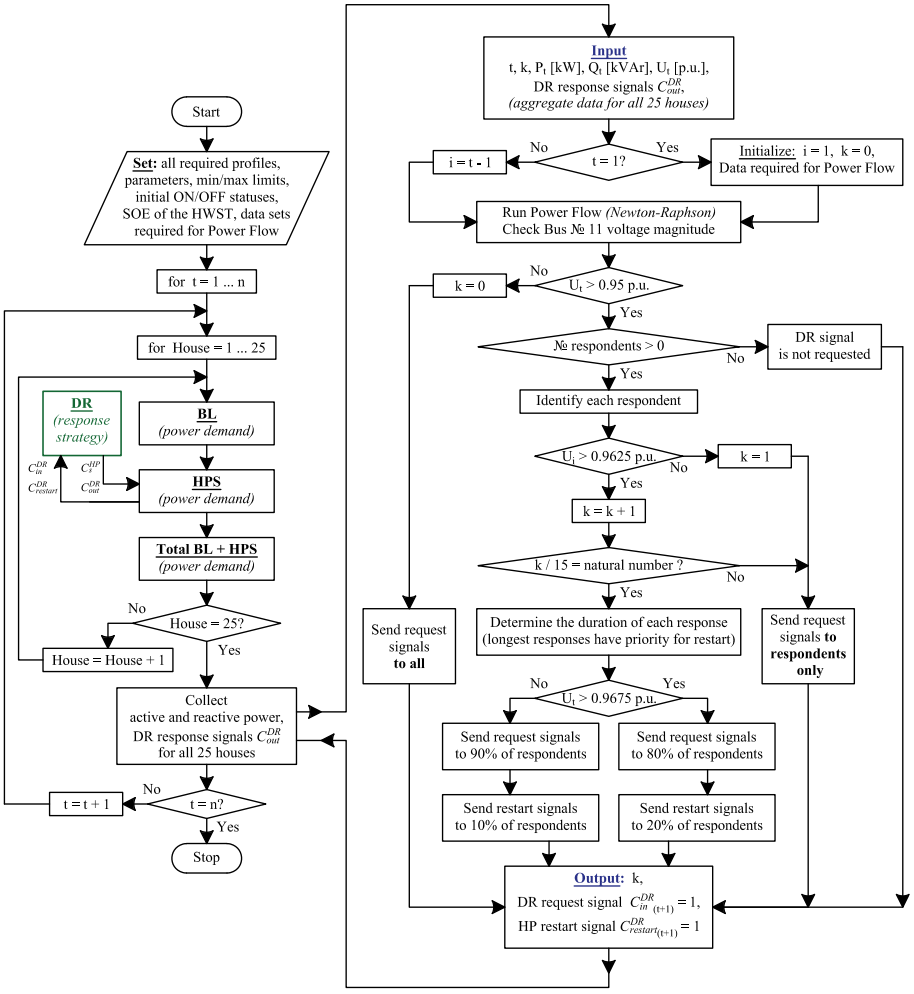

Figure 5.13. Flowchart demonstrating the flexibility request strategy for voltage support (centralized coordination control).

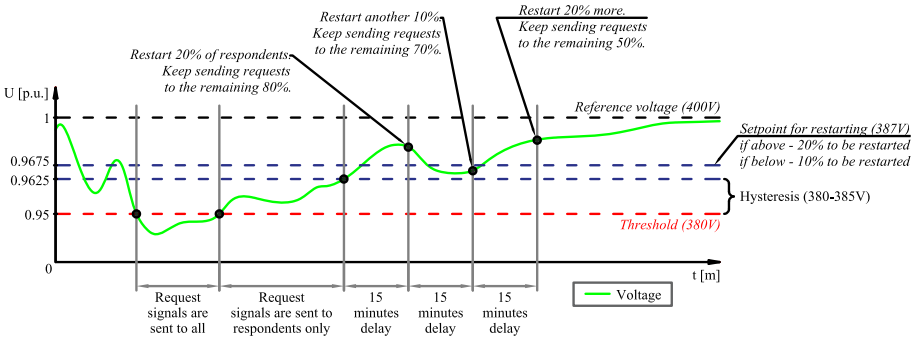

Figure 5.14. Simplified description of a voltage-based strategy.

For clarity, the above processes are demonstrated using the example of the behaviour of three houses in Figure 5.15, while the complete chronology of events (sending request/response/restart signals) can be tracked in Table 5.7.

At 17:02 the voltage reached the lower-controlled level and the flexibility request signal was sent to all 25 houses. The system identified that the response was provided by 10 houses. Over the next 15 minutes, request signals continue to be sent to all 10 respondents. Since the voltage during these 15 minutes was in the range of 0.95 p.u.<U<0.9675 p.u. it was decided to turn ON 10% of respondents (i.e. 1 house). Since house №20 had provided flexibility service earlier, it received a restart signal (at 17:17). Since subsequent periods the voltage was below 0.9625 p.u. restart signals were no longer sent. Requests, however, continued to be sent to all respondents. Providing a response (by being off) over a long period of time, the heat pumps began to gradually turn on following the local temperature control (clearly seen from Table 5.7). This gradually led again to a voltage drop below the allowable threshold and the flexibility request signal was again sent to everyone (at 21:50). From this moment it can be seen that the voltage was above the upper controlled limit by the end of the day, and therefore the operation of the heat pumps was gradually restored in increments of at least 15 minutes.

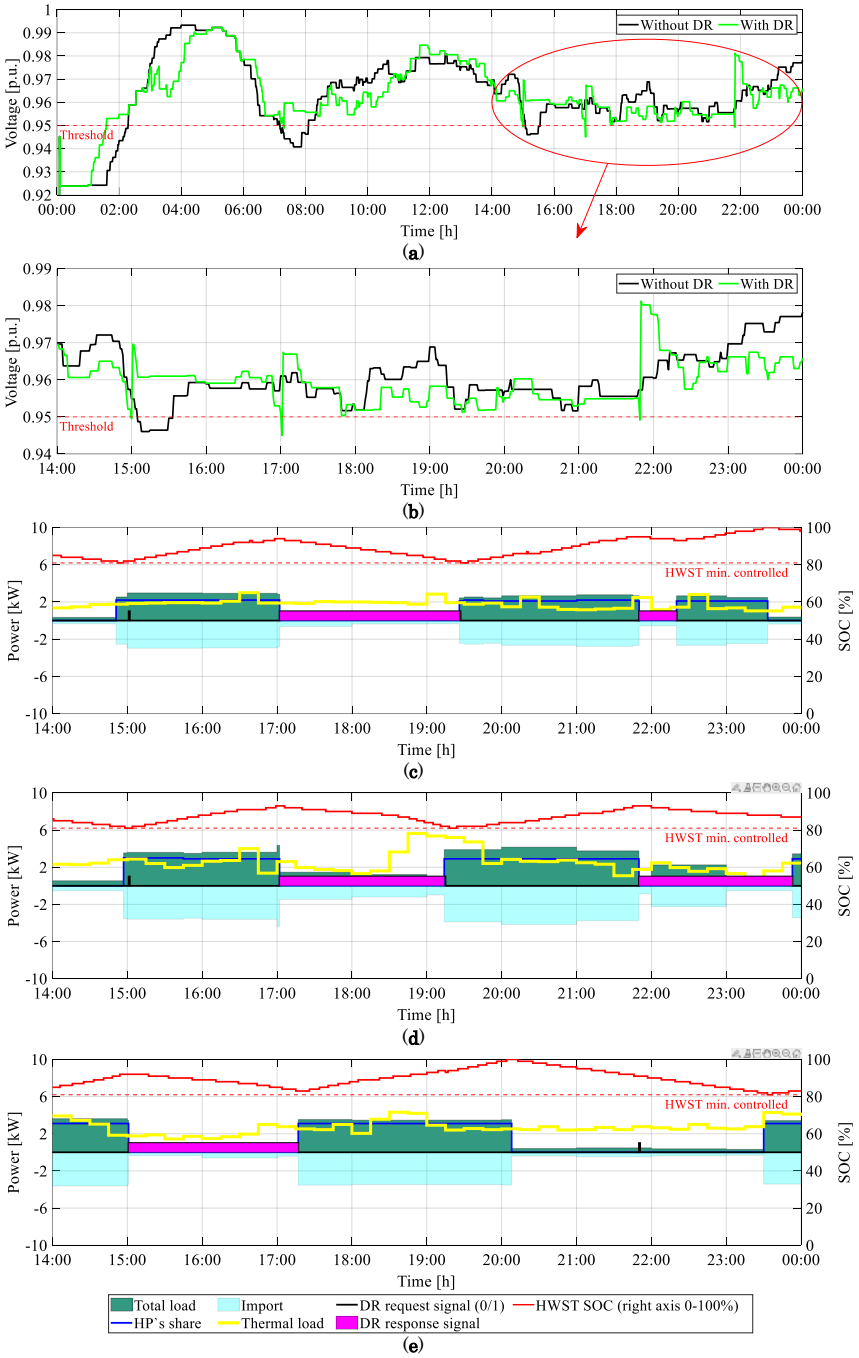

Figure 5.15. Demonstration of DR application under scenario S3 (**a, b**) voltage magnitude at the weakest bus №11; (**c, d, e**) behaviour of houses №11, 17, 20.

Table 5.7. Chronology of events applying voltage based DR strategy.

Time	*House №*			
	Request signals are sent to:	*Response signals are sent back by:*	*Restart signal is sent to:*	*Local decision to restart*
15:01	to all	1,6,18,19,20,22		
15:52	1,18,19,20,22	1,×,18,19,20,22		6
16:45	18,19,20,22	× 18,19,20,22		1
16:54	9,20,22	×,19,20,22		18
17:01	20,22	×,20,22		19
17:02	to all	3,5,9,11,12,15,17,20,22,25		
17:17	3,5,9,11,12,15,17,22,25	3,5,9,11,12,15,17, × ,22,25	**20**	
17:24	3,5,9,11,12,15,17,25	3,5,9,11,12,15,17 × ,25		22
18:30	3,5,9,11,12,17,25	3,5,9,11,12, × ,17 25		15
18:44	3,5,9,11,12,17	3,5,9,11,12 17 ×		25
19:14	3,5,9,11,12	3,5,9,11,12 ×		**17**
19:26	3,5,9,12	3,5,9, × ,12		**11**
19:38	3,9,12	3,×,9 12		5
19:56	3,9	3 9 ×		12
20:23	9	× 9		3
21:50	to all	3,4,5,7,9,11,12,14,15,16,17,22,24,25		
21:58	3,4,5,7,11,12,14,15,16,17,22,24,25	3,4,5,7,×,11,12,14,15,16,17,22,24,25		9
22:05	7,11,12,14,15,16,17,22,24,25	×,×,×,7, ,11,12,14,15,16,17,22,24,25	3,4,5	
22:20	12,14,15,16,17,22,24,25	× × ,12,14,15,16,17,22,24,25	7,**11**	
22:52	14,15,16,17,22,24,25	× 14,15,16,17,22,24,25	12	
23:15	15,16,17,22,24,25	×,15,16,17,22,24,25	14	
23:25	15,17,22,24,25	15, × ,17,22,24,25		16
23:32	17,22,24,25	× ,17,22,24,25	15	
23:53	22,24,25	× ,22,24,25	**17**	
00:08	25	× , × ,25	22,24	
00:23		×	25	

Table 5.8 below shows the result of the one-week simulation, summing the number of voltage drops in two cases - "with" and "without" DR application. From the table one can see that the application of this strategy demonstrates a significant reduction of voltage drop minutes, showing an improvement percentage of 81.2%.

Table 5.8. Summary of voltage drop events under scenario S3.

DR application	*Minutes of voltage drop per one week in January [m]*	*Percentage decrease [%]*
Without	722	-81.2
With	136	

The presence of voltage drop minutes (which in this case 136) can be explained primarily by the fact that all simulations results presented in this chapter are related to the worst-case scenario. The worst-case scenario, in this context, implies starting the simulation with not fully charged HWSTs, and consequently simultaneous operation of all 25 heat pumps within the first hour and a half (97 minutes, to be more precise). This is, of course, reflected in voltage deviation, which is below 0.95 p.u.

during this time (see Figure 5.15 **a**). The next 39 minutes of voltage drop (136 - 97 = 39) can be explained by the fact that the Matlab model is built in such a way that heat pumps react to request signals only from the next time step. Since the simulation is performed in 1-minute increments, the moment of reaching the threshold of 0.95 p.u. is always counted as one minute of voltage drop.

The amount of energy flexibility requested by DSO and expected to be provided by each individual house, as well as the aggregated flexibility from the group of 25 houses at each time step (t), and the total flexibility during the entire investigated period is determined following the algorithm shown in Figure 5.16. Since the main flexibility resource is the heat pump, the amount of flexibility expected from each individual household is directly associated with the rated power of each heat pump and the time during which each particular HP is expected to be switched OFF. The time in this case is the duration of a series of one-minute **request** signals that (following the strategy presented above) are sent to each household individually (unlike actually provided flexibility, where the response signals are used, see (5.9)). The presented algorithm is described for the Matlab environment.

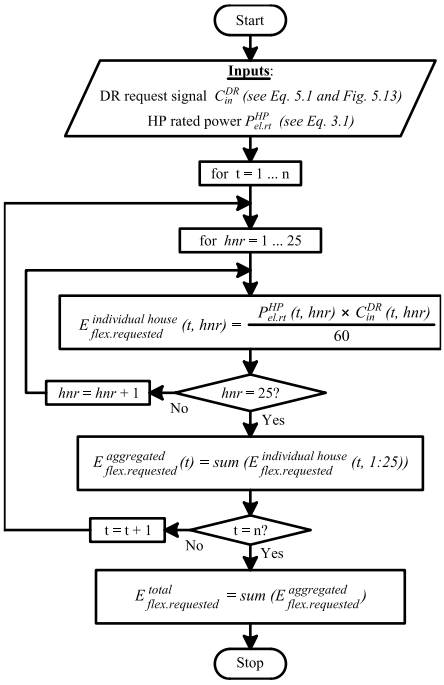

Figure 5.16. Flowchart demonstrating the process for calculating the amount of energy flexibility requested.

Following this algorithm, the total amount of energy flexibility requested from 25 houses during the first week in January, and the actual flexibility provided by these houses (following (5.9)) are shown in Table 5.9.

Table 5.9. Summary of demand-side energy flexibility provision following the voltage-based strategy

Total aggregated energy consumption per one week in January [kWh]	*Amount of energy flexibility per one week in January [kWh]*		*Percentage of energy flexibility out of total consumption [%]*		*Percentage of service provision (provided from requested) [%]*
	Requested	*Provided*	*Requested*	*Provided*	
8,727	1,623	1,451	18.6	16.6	89.4

In addition to the strategy described above, it is also worth noting that voltage setpoints presented here are not rigidly fixed (given only to demonstrate the use of DSF) and should be selected for each network individually depending on the grid infrastructure and hosting capacity indices. An important factor in choosing the right setpoints will also be cost optimization analysis, including how much DSO will be willing to pay for such flexibility, how long and what is more profitable compared to reinforcement (this, again, is very individual for each section of the network). On the other hand, these thresholds can serve as a kind of marker for the need to strengthen the grid. Raising the lower threshold results in an increase in the number of request signals. A large number of request signals to reduce the load means that it becomes difficult to keep the voltage within these limits, and therefore the network should be reinforced or at least reconfigured. In addition, although this study demonstrated a restart at 15-minute intervals, the use of 10-minute and 5-minute intervals also showed a high rate of improvement (decreasing the total number of voltage drop events by 78.9% and 77.9% under the worst case scenario) and even slightly lower need for flexibility. However, a longer interval allows the heat pump operation to be better distributed over time and thus avoid simultaneity, which is the main cause of voltage drops.

5.4. CHAPTER SUMMARY

This section presented the concept of providing flexibility services through market mechanisms, the method of estimating the flexibility potential, the impact of heat pumps on the voltage in the distribution network, as well as the methodology of maintaining this voltage within acceptable limits. The results showed that the above strategies can be successfully applied

both to assess the flexibility potential of an individual house and a group of houses and to stabilize the voltage in the local power distribution grid.

In the second section of this chapter, it was shown that the amount of energy flexibility that can be obtained from a heat pump with HWST is very limited due to the small controlled amount of energy in the tank and the specificity of the heat pump operation. However, as shown in the third section, even though the controllable range of the HWST is very limited, the DR application (based on the presented voltage-based strategy) can be very helpful in solving low voltage network voltage drop problems.

The voltage-based strategy described above showed that the use of such flexibility helps to reduce the number of minutes of voltage drop in the network by 81.2% in the worst-case scenario. The overall percentage of flexibility is demonstrated to be 89.4%, with all responses provided on a non-obligatory basis, prioritizing consumer comfort and not levying penalties for not responding.

6 CONCLUSIONS AND PLANS FOR FUTURE WORK

This section briefly summarizes what has been done in this dissertation and gives conclusions on all the main outcomes of this research work.

6.1. THESIS SUMMARY

At the very beginning of this dissertation, environmental issues and the importance of switching to renewable energy sources were highlighted. This was followed by the discussion of issues that system operators in many countries faced due to the growing penetration of RESs into the power grid and electrification (as a consequence of decarbonisation) of the heat and transport sectors. The importance of energy flexibility of buildings on the path of transformation of the energy sector was emphasized, and the resources of flexibility to which the largest emphasis is being made today are analysed. To investigate the impact of the emergence of such resources on the building's need for electricity from the grid and, in fact, the network itself, energy models of various DERs were created, in particular, PV panels, wind turbine, battery, and heat pump system coupled with hot water storage tank. Then, the self-sufficiency and own consumption shares were analysed when combining these DERs under a single coordinating algorithm. In the next stage, the flexibility potential that can be provided by a household equipped with such DERs was assessed using artificially generated DR signals and a rule-based management strategy for providing a response to these signals. This was followed by investigating the impact of a group of 25 such houses on the electricity grid. The impact was studied by performing a load flow analysis using the Newton-Raphson method. The DR application was investigated on the example of a heat pump, and all the positive and negative consequences of such flexibility service provisioning were highlighted in detail. Finally, the flexibility request strategy was proposed to support the voltage regulation in a low voltage 0.4 kV network (namely, to support

solving voltage drop problems). The strategy also involves the coordinated restart of active respondents, made to avoid simultaneous turning on after the signal is elapsed.

6.2. CONCLUSIONS ON THE PROPOSED HYPOTHESES

The conclusion on the proposed hypothesis is presented in brief, since all research questions associated with this hypothesis have been addressed in detail in each chapter summary. Based on the simulation results obtained during this study, the following conclusions can be drawn.

- It is unambiguous that the integration of on-site renewable sources increases the energy efficiency of an individual household by rising its self-sufficiency share, as well as clear that the utilisation of heat pump system increases this efficiency on the other (fossil fuel dependency reduction) side.
- The permissible size limit of 6kW for the domestic rooftop PV installation in Denmark, does not allow to fully cover the increase in load caused due to the heat pump. The presence of a battery, in this respect, even a fairly large size, is not able to completely reduce dependence on the grid, including the need to export excess RESs generation, which can also be explained by the aforementioned limits.
- Furthermore, a usual net metering scheme, while simply exporting the surplus of on-site RES production to the grid (implying no special control), is not the best solution that can be described as a load reduction to the power system. In non-heating season, when heat pumps are much rarely used, and there are many sunny days, even such allowable limits for PV installations induce a large energy export to the grid. The latter could have a negative impact on grid operation such as overvoltage, reverse power flow, unplanned outages, and others. Consequently, more advanced control methods for these RESs, battery, and HPS, which involve prediction and optimal scheduling, model predictive control (thereby improving the self-sufficiency and own-consumption indices) are absolutely vital.
- Since the main focus of this work was on the use of energy flexibility that can be provided by the heat pump, it can be said that the amount of such flexibility depends on the amount of energy controlled in the storage tanks and the specifics of the heat pump operation. The application of the developed rule-based strategy, which takes into account this specificity and is aimed at the thermal comfort of consumers, allowed to obtain the maximum

percentage of the flexibility of a single house of 17.6%. While the application of centralized coordination control strategy showed a percentage of aggregated flexibility of 89.4%. Analysis of scenarios with PV and battery showed that the presence of the latter has the opposite effect on the percentage of flexibility. Since part of the peak load is covered by on-site resources (implying less energy is imported from the grid) the number of DR signals to be responded is also less.

The main objective of this research work was to develop a solution for energy management of residential buildings, aimed at providing system services to support technical issues that occurred during the operation of the distribution grid. To achieve this objective detailed models of the key active flexible components of the building (such as heat pump and HWST), as well as the performance models of local renewable generation and storage units (such as PV panels, wind turbine, and battery), were created.

The created models can be considered one of the major outcomes that allowed to execute all subsequent simulations and analyses. Special attention, among these models, was paid to the heat pump system. This model was created to mimic the heat supply system behaviour as close as possible to the real system (including delays, defrost mode, and guaranteed power-on time) and is considered the main flexibility source in this thesis.

Nevertheless, the most meaningful outcomes of this dissertation are the rule-based management strategy developed for responding to a technical demand response signal and a centralized coordinating control strategy for addressing the voltage drop issues in the 0.4 kV feeder. These two strategies are considered a targeted solution outlined as the main objective of this work.

The performance of the developed DR strategies has been demonstrated in the example of a single 0.4 kV radial feeder. The utilization of energy flexibility of 25 households connected to that feeder showed the ability to solve 81% of voltage drop periods occurring in that feeder during ordinary operation, applying the worst-case scenario. The obtained percentage confirms the fact that applying such a strategy can provide enhanced voltage regulation support to distribution system operators. On the other hand, a concept implying incentive payments for each kWh of energy flexibility provided, without incurring penalties for nonresponse, while at the same time placing the thermal comfort of inhabitants as the top priority, can be an excellent motivation for household owners to participate. Despite the fact that the performance of proposed strategies

were evaluated on the example of a particular LV feeder, the proposed strategies are generic and can be applied to any LV distribution grid which is fully consistent with the goal.

6.3. FUTURE PERSPECTIVES

In this work, various aspects were explored and addressed. However, during the research process, some other points were identified that may extend or enhance the outcomes presented in this thesis. Among them:

- Strengthening the proposed DR strategies with forecasting. The ability to accurately predict the behaviour of various active components of the house can bring the provision of flexibility services to a whole new level. The power output of RESs and consequently the battery SOE is directly dependent on weather forecast and consumption. Predicting the heat pump consumption and, accordingly, the SOE of the HWST depends on the outside air temperature, as well as heat demand, which in turn depends on the behaviour of the residents. Having predictions of the behaviour of all these components, the strategies can be enhanced by solutions such as optimal scheduling or model predictive control (MPC).
- Optimal scheduling and MPC is another area that can significantly maximize the provision of flexibility services. Having predictions and detailed models of various building components, MPC can plan the best optimal solution for the system behaviour for a short horizon forward in time. This could allow, for example, to schedule the HWST charging to the hours when there is a lot of PV production, thereby shifting the great amount of HPs load to off-peak hours.
- Make the proposed DR strategies more versatile in relation to:
  - a wider range of issues that can be solved such as, for example, overvoltage issues, where the aforementioned optimal scheduling of RESs, battery and load are crucial, or a frequency support;
  - a wider range of active components, for example, the use of electric vehicles or electrolysers, again, along with optimal scheduling or MPC.
- Conduct an economic analysis that can assess the impact of such flexibility on the need for grid reinforcement or a cost-benefit analysis for flexible load owners.

BIBLIOGRAPHY

[1] IEA (2020), "Key World Energy Statistics 2020," *IEA, Paris*. https://www.iea.org/reports/key-world-energy-statistics-2020.

[2] Energinet, "REPORT 2017 Energinet's analysis assumptions," 2017. [Online]. Available: https://bit.ly/2J2QOeW.

[3] IEC, "Coping with the Energy Challenge. The IEC's Role from 2010 to 2030. Smart electrification - The Key to Energy Efficiency," 2010. [Online]. Available: https://www.iec.ch/smartenergy/downloads/.

[4] IEA (2020), "CO2 Emissions from Fuel Combustion: Overview," *IEA, Paris*. https://www.iea.org/reports/co2-emissions-from-fuel-combustion-overview.

[5] United Nations, "Paris Agreement," 2015. https://treaties.un.org/pages/ViewDetails.aspx?src=TREATY&mtdsg_no=XXVII-7-d&chapter=27&clang=_en.

[6] European Commission, "Climate strategies & targets." https://ec.europa.eu/clima/policies/strategies_en.

[7] IRENA, "Renewable capacity highlights," 2020. [Online]. Available: https://www.irena.org/Statistics/View-Data-by-Topic/Capacity-and-Generation/Statistics-Time-Series https://tabsoft.co/38uvMjl.

[8] The Danish Ministry of Climate Energy and Utilities, "National Energy and Climate Plan," 2019.

[9] State of Green, "Denmark: The Most Wind Energy Producing Country Per Capita," *August 09*, 2017. https://bit.ly/3nWU5e5.

[10] Nord Pool AS, "Historical Market Data." https://bit.ly/2N6iYqR and https://bit.ly/2XJnA8F.

[11] The Danish Energy Agency, "Electricity Supply.," *Annual and monthly statistics*. https://bit.ly/2XOUjct.

[12] The Danish Energy Agency, "Overview map of the Danish power infrastructure in 1985 and 2015.," *Energy infomaps*. https://bit.ly/3r88ebe.

[13] K. Kouzelis, "Load and Flexibility Models for Distribution Grid

Management," Aalborg University (AAU), 2015.

[14] Energinet, "ROLES & RESPONSIBILITIES. Who does what in the Danish electricity market?," 2021. https://bit.ly/37ox1Q2.

[15] K. Nainar, "Hierarchical Distributed Control of Active Electric Power Distribution Grids," Aalborg University (AAU), 2019.

[16] Energinet, "Regulation C1 – Terms of balance responsibility," no. 16/04092–15. pp. 1–30, 2016, [Online]. Available: https://bit.ly/2Pc8OpF.

[17] Energinet, "Regulation C3 Handling of notifications and schedules - daily procedures," no. 158912–07 Rev. 3 November. p. 31, 2011, [Online]. Available: https://bit.ly/2Pc8OpF.

[18] Klima- Energi- og Bygningsmin. Energistyrelsen, *Bekendtgørelse BEK nr 1358 af 03/12/2013*. Danmark, 2013.

[19] Energistyrelsen, "Data for eksisterende og afmeldte anlæg (ultimo 11 2020) – uploadet 21. december 2020," *Data: Oversigt over energisektoren*. https://bit.ly/3nRSGoU.

[20] Danish Ministry of Climate Energy and Building, "Smart Grid Strategy. The intelligent energy system of the future," 2013. [Online]. Available: https://bit.ly/3rE8NsC.

[21] Energinet, "MARKET MODEL 2.0," 2015. [Online]. Available: https://bit.ly/3adfvA3.

[22] J. R. Kristoffersen, "The Horns Rev Wind Farm and the Operational Experience with the Wind Farm Main Controller," *Proc. Copenhagen Offshore Wind*, no. October, pp. 1–9, 2005.

[23] H. Lund and W. Kempton, "Chapter 5. Analysis: Large-Scale Integration of Renewable Energy," in *Renewable Energy Systems: A Smart Energy Systems Approach to the Choice and Modeling of 100% Renewable Solutions.*, Second Edi., Elsevier Inc., 2014, pp. 79–129.

[24] Skatteministeriet, *Bekendtgørelse af lov om afgift af elektricitet*, no. LBK 1321 af 26/08/2020 § 2d. Stk3. Stk.1, litra c. Danmark: Lovtidende A, https://www.retsinformation.dk/eli/lta/2020/1321.

[25] H. Wirth, "Recent facts about photovoltaics in Germany, Fraunhofer ISE," Freiburg, 2021. [Online]. Available: https://bit.ly/3srSfG6.

[26] D. Q. Hung, N. Mithulananthan, and K. Y. Lee, "Determining PV penetration for distribution systems with time-varying load models," *IEEE Trans. Power Syst.*, vol. 29, no. 6, pp. 3048–3057, 2014.

[27] D. Fischer and H. Madani, "On heat pumps in smart grids: A review," *Renew. Sustain. Energy Rev.*, vol. 70, no. May 2016, pp. 342–357, 2017, doi: 10.1016/j.rser.2016.11.182.

[28] X. Xiu and B. Li, "Study on energy storage system investment decision based on real option theory," in *Proc. IET Sustainable Power Generation and Supply (SUPERGEN 2012)*, 2012, pp. 1–4.

[29] R. Høm Jensen, "Disconnected power cable to Bornholm offers unique test option," *DTU*, 2019. https://bit.ly/2ZjePmn.

[30] R. Halvgaard *et al.*, "Model predictive control for a smart solar tank based on weather and consumption forecasts," *Energy Procedia*, vol. 30, pp. 270–278, 2012.

[31] P. D. Lund, J. Lindgren, J. Mikkola, and J. Salpakari, "Review of energy system flexibility measures to enable high levels of variable renewable electricity," *Renew. Sustain. Energy Rev.*, vol. 45, pp. 785–807, 2015, [Online]. Available: http://dx.doi.org/10.1016/j.rser.2015.01.057.

[32] The European Parliament and the Council of the European Union, "DIRECTIVE (EU) 2018/844 of the European Parliament and of the Council of 30 May 2018 amending Directive 2010/31/EU on the energy performance of buildings and Directive 2012/27/EU on energy efficiency (factsheet attachment)," *Off. J. Eur. Union*, vol. L 156, p. 1, 2018.

[33] L. Gynther, B. Lapillonne, K. Pollier, and D. Bosseboeuf, "Energy Efficiency Trends and Policies in the Household and Tertiary Sectors (ODYSSEE-MURE project)," 2015. doi: DOI 10.1089/pho.2012.3369.

[34] Eurostat, "Archive:Consumption of energy." https://bit.ly/34lU646.

[35] Eurostat, "Energy consumption in households," *Data extracted in June 2020*. https://bit.ly/3ht1bW1.

[36] The European Parliament and the Council of the European Union, "DIRECTIVE 2012/27/EU of the European Parliament and of the Council of 25 October 2012 on energy efficiency, amending Directives 2009/125/EC and 2010/30/EU and repealing Directives 2004/8/EC and 2006/32/EC," *Off. J. Eur. Union*, vol. L 315, no. 14.11.2012, pp. 1–56, [Online]. Available: http://data.europa.eu/eli/dir/2012/27/2021-01-01.

[37] The European Parliament and the Council of the European Union, "DIRECTIVE 2009/125/EC of the European Parliament and of the Council of 21 October 2009 establishing a framework for the setting of ecodesign requirements for energy-related products (recast) (OJ L 285 31.10.2009, p. 10)," *Off. J. Eur. Union*, no. 2009L0125 — EN — 04.12.2012 — 001.001, pp. 1–40, 2009, [Online]. Available: http://data.europa.eu/eli/dir/2009/125/2012-12-04.

[38] The European Parliament and the Council of the European Union, "DIRECTIVE 2010/31/EU of the European Parliament and of the Council of 19 May 2010 on the energy performance of buildings (recast) (OJ L 153 18.6.2010, p. 13)," *Off. J. Eur. Union*, no. 02010L0031 — EN — 01.01.2021 — 003, pp. 1–35, 2021, [Online]. Available: http://data.europa.eu/eli/dir/2010/31/2021-01-01.

[39] Energinet and Danish Energy Association, "Smart grid in Denmark 2.0." [Online]. Available: https://bit.ly/2NjjUIS.

[40] J. R. Pillai, P. Thogersen, J. Moller, and B. Bak-Jensen, "Integration of Electric Vehicles in low voltage Danish distribution grids," in *IEEE Power and Energy Society General Meeting*, 2012, pp. 1–8, doi: 10.1109/PESGM.2012.6343948.

[41] J. M. Morales, A. J. Conejo, H. Madsen, P. Pinson, and M. Zugno, *Integrating Renewables in Electricity Markets. Operational Problems.*, vol. 205. Springer NewYork Heidelberg Dordrecht London, 2014.

[42] R. Weron, *Modeling and Forecasting Electricity Loads and Prices. A Statistical Approach.* Chichester: John Wiley & Sons Ltd, 2006.

[43] T. Soares, "Renewable energy sources offering flexibility through electricity markets," Technical University of Denmark (DTU),

2017.

[44] F. P. Sioshansi, *Evolution of Global Electricity Markets. New Paradigms, New Challenges, New Approaches.* Elsevier Inc., 2013.

[45] J. Lin and F. H. Magnago, *Electricity Markets. Theories And Applications*. John Wiley & Sons, Inc.Hoboken, New Jersey, IEEE Press, 2017.

[46] European Commission, "Commission Regulation (EU) 2015/1222 of 24 July 2015 establishing a guideline on Capacity Allocation and Congestion Management (CACM)," *Off. J. Eur. Union*, vol. L 197, no. 25.7.2015, pp. 24–72, [Online]. Available: https://eur-lex.europa.eu/legal-content/EN/TXT/?uri=CELEX%3A32015R1222.

[47] Nord Pool A/S, "Trade at the Nordic spot market (NordPool Spot AS) - The world's first international spot power exchange." Technical Report, 2004.

[48] "Nord Pool AS." https://www.nordpoolgroup.com/About-us/.

[49] Nord Pool AS, "Annual report 2019. Embracing New Challenges." pp. 1–36, 2020, [Online]. Available: https://www.nordpoolgroup.com/message-center-container/Annual-report/.

[50] Nord Pool AS, "Day-ahead Market Regulations. Nordic/Baltic Market and CE Market." pp. 1–9, 2021, [Online]. Available: https://www.nordpoolgroup.com/trading/Rules-and-regulations/.

[51] Nord Pool AS, "Product specifications. Nordic & Baltic Market Areas," no. June 12. pp. 1–6, 2018, [Online]. Available: https://www.nordpoolgroup.com/trading/Rules-and-regulations/.

[52] K. Skytte, "The regulating power market on the Nordic power exchange Nord Pool: An econometric analysis," *Energy Econ.*, vol. 21, no. 4, pp. 295–308, 1999, doi: 10.1016/S0140-9883(99)00016-X.

[53] Nord Pool AS, "Annual report 2012. The power of transparency." pp. 1–52, 2012, [Online]. Available: https://bit.ly/39R6uvS.

[54] Nord Pool AS, "Intraday Market Regulations." pp. 1–9, 2020, [Online]. Available: https://www.nordpoolgroup.com/trading/Rules-

and-regulations/.

[55] Energinet, "Introduktion til elmarkedet," no. 18/08514–1. pp. 1–16, 2019, [Online]. Available: https://energinet.dk/-/media/41F2C6A30A834208B0225DB3132560C7.PDF.

[56] Energinet, "Regulation A : Principles for the electricity market." Doc. 165915-07. Rev. 1., pp. 1–13, 2007, [Online]. Available: https://bit.ly/2Pc8OpF.

[57] Ramboll, "Ancillary Services From New Technologies. Technical Potentials and Market Integration." Report. Doc ID 1191289-2 / Version 3, 2019, [Online]. Available: https://energinet.dk/-/media/229625DCEA984813BF322090E7926844.pdf.

[58] Nord Pool Spot AS, "The Nordic Electricity Exchange and The Nordic Model for a Liberalized Electricity Market." pp. 1–18, 2011, [Online]. Available: https://bit.ly/3mM3Bli.

[59] Energinet, "Ancillary services to be delivered in Denmark - Tender conditions," Doc. 13/80940-127, 2021. [Online]. Available: https://en.energinet.dk/Electricity/Rules-and-Regulations#Market regulations.

[60] Energinet, "Regulation C2 : The balancing market and balance settlement," no. 13/91893-80. pp. 1–17, 2017, [Online]. Available: https://bit.ly/2Pc8OpF.

[61] T. Chen, Q. Alsafasfeh, H. Pourbabak, and W. Su, "The next-generation U.S. retail electricity market with customers and prosumers-A bibliographical survey," *Energies*, vol. 11, no. 1, 2018, doi: 10.3390/en11010008.

[62] The European Parliament and the Council of the European Union, "DIRECTIVE (EU) 2019/944 of the European Parliament and of the Council of 5 June 2019 on common rules for the internal market for electricity and amending Directive 2012/27/EU (recast)," *Off. J. Eur. Union*, vol. L 158, no. 14.6.2019, pp. 125–158, [Online]. Available: http://data.europa.eu/eli/dir/2019/944/oj.

[63] The European Parliament and the Council of the European Union, "REGULATION (EU) 2019/943 of the European Parliament and of the Council of 5 June 2019 on the internal market for electricity," *Off. J. Eur. Union*, vol. L158, no. 14.6.2019, pp. 54–124, [Online].

Available: http://data.europa.eu/eli/reg/2019/943/oj.

[64] Energinet, "The Danish Electricity Retail Market. Introduction to DataHub and the Danish supplier-centric model." Doc. 16/07474-4, 2018, [Online]. Available: https://bit.ly/3vP3YyD.

[65] Elpris.dk, "Fast pris og variabel pris." [Online]. Available: https://bit.ly/33mvBD8.

[66] Forsyningstilsynet, "Elprisstatistik 1. kvartal 2021." DEN 15. APRIL 2021, pp. 1–11, [Online]. Available: https://bit.ly/2SxKpwH.

[67] Energistyrelsen, "Fakta om flexafregning." April 2019, pp. 1–8, [Online]. Available: https://bit.ly/3ts2x7V.

[68] Energinet, "Flexafregning af produktionsanlæg på den årsbaserede ordning." [Online]. Available: https://bit.ly/2QVSR8C.

[69] Eurostat, "Electricity prices for household consumers, second half 2020 (EUR per kWh) v1." [Online]. Available: https://bit.ly/3eWZAH7.

[70] S. Sekizaki, I. Nishizaki, and T. Hayashida, "Electricity retail market model with flexible price settings and elastic price-based demand responses by consumers in distribution network," *Int. J. Electr. Power Energy Syst.*, vol. 81, pp. 371–386, 2016, doi: 10.1016/j.ijepes.2016.02.029.

[71] C. Gu, J. Wu, and F. Li, "Reliability-Based Distribution Network Pricing," *IEEE Trans. Power Syst.*, vol. 27, no. 3, pp. 1646–1655, 2012, doi: 10.1109/TPWRS.2012.2187686.

[72] M. Hong, "An Approximate Method for Loss Sensitivity Calculation in Unbalanced Distribution Systems," *IEEE Trans. Power Syst.*, vol. 29, no. 3, pp. 1435–1436, 2014, doi: 10.1109/TPWRS.2013.2288022.

[73] J. W. M. Lima, J. C. C. Noronha, H. Arango, and P. E. S. dos Santos, "Distribution pricing based on yardstick regulation," *IEEE Trans. Power Syst.*, vol. 17, no. 1, pp. 198–204, 2002, doi: 10.1109/59.982214.

[74] E. Litvinov, T. Zheng, G. Rosenwald, and P. Shamsollahi, "Marginal loss modeling in LMP calculation," *IEEE Trans. Power*

Syst., vol. 19, no. 2, pp. 880–888, 2004, doi: 10.1109/TPWRS.2004.825894.

[75] P. M. Sotkiewicz and J. M. Vignolo, "Towards a Cost Causation-Based Tariff for Distribution Networks With DG," *IEEE Trans. Power Syst.*, vol. 22, no. 3, pp. 1051–1060, 2007, doi: 10.1109/TPWRS.2007.901284.

[76] P. M. Sotkiewicz and J. M. Vignolo, "Nodal pricing for distribution networks: Efficient pricing for efficiency enhancing DG," *IEEE Trans. Power Syst.*, vol. 21, no. 2, pp. 1013–1014, 2006, doi: 10.1109/TPWRS.2006.873006.

[77] NordREG, "Electricity distribution tariffs. Report by the NordREG Network Regulation WG." Report 2/2021, Oslo, pp. 1–35, 2021, [Online]. Available: http://www.nordicenergyregulators.org/publications/.

[78] R. Poudineh, "Liberalized retail electricity markets:What we have learned after two decades of experience?" OIES Paper: EL 38. December 2019, pp. 1–36, doi: https://doi.org/10.26889/9781784671518.

[79] U.S. Department of Energy, "Benefits of Demand Response in Electricity Markets and Recommendations for Achieving Them," Feb. 2006. [Online]. Available: https://eta.lbl.gov/publications/benefits-demand-response-electricity.

[80] F. Lopes and H. Coelho, "Electricity Markets with Increasing Levels of Renewable Generation: Structure, Operation, Agent-based Simulation, and Emerging Designs," in *Studies in Systems, Decision and Control*, vol. 144, Springer, 2018, pp. 1–342.

[81] ACER, "Methodology for the European resource adequacy assessment in accordance with Article 23 of Regulation (EU) 2019/943 of the European Parliament and of the Council of 5 June 2019 on the internal market for electricity," no. October, 2020, [Online]. Available: https://bit.ly/3ofAesq.

[82] Energistyrelsen, "MARKEDSMODEL 3.0," 2021. [Online]. Available: https://bit.ly/3AJ4Ec2.

[83] Nordic Balancing Model, "Webinar - Nordic aFRR capacity

market." Webinar presentation, pp. 1–26, 2021, [Online]. Available: https://bit.ly/39Xk4Ov.

[84] Nordic Balancing Model, "Implementation Guide for market participants - for the common Nordic mFRR energy activation market." Webinar presentation, pp. 1–32, 2021, [Online]. Available: https://bit.ly/3s2VOQX.

[85] "All NEMOs Committee/Single Intraday Coupling (SIDC)." http://www.nemo-committee.eu/sidc.

[86] Universal Smart Energy Framework (USEF) Foundation, "Flexibility Value Chain," *White Paper*. Version 1.0. October 16, 2018, pp. 1–17, [Online]. Available: https://bit.ly/3hBT7nQ.

[87] H. Holttinen, N. A. Cutululis, A. Gubina, A. Keane, and F. Van Hulle, "Ancillary services : technical specifications, system needs and costs. Deliverable D 2.2.," *REserviceS*, no. November, 2012.

[88] ENTSO-E WGAS, "Survey on Ancillary Services Procurement, Balancing Market Design 2019," 2020. [Online]. Available: https://bit.ly/319SDMF.

[89] E. Ela, M. Milligan, and B. Kirby, "Operating Reserves and Variable Generation. A comprehensive review of current strategies, studies, and fundamental research on the impact that increased penetration of variable renewable generation has on power system operating reserves.," *Technical Report. NREL/TP-5500-51978*. NREL, Golden, Colorado, pp. 1–103, 2011, [Online]. Available: http://www.nrel.gov/docs/fy11osti/51978.pdf.

[90] ENTSO-E, "Market Report," 2020. [Online]. Available: https://www.entsoe.eu/news/2020/06/30/2020-entso-e-market-reports/.

[91] Energinet, "Introduktion til systemydelser," no. 14/02811-173. pp. 1–13, 2020, [Online]. Available: https://energinet.dk/El/Elmarkedet/Regler-for-elmarkedet/Markedsforskrifter#C1.

[92] NordREG, "Status report on regulatory aspects of demand side flexibility." pp. 1–41, 2016, [Online]. Available: http://www.nordicenergyregulators.org/2016/12/status-report-on-regulatory-aspects-of-demand-side-flexibility/.

[93] Energinet, "Behovsvurdering For Systemydelser 2021." Report. Dok. 20/06034-2, pp. 1–54, 2021, [Online]. Available: https://bit.ly/2QgwXwn.

[94] N. Qin, "Aalborg Universitet Voltage control in the future power transmission systems." Aalborg Universitetsforlag. Ph.d.- serien for Det Teknisk-Naturvidenskabelige Fakultet, Aalborg Universitet, 2016, [Online]. Available: https://doi.org/10.5278/vbn.phd.engsci.00178.

[95] G. Schett, "What is the problem with long distance underground and sub-sea HVAC cable transmission?," *17.04.2021*. LinkedIn/IEEE Smart Grid group, [Online]. Available: https://www.linkedin.com/feed/update/urn:li:activity:6789168955459166208.

[96] C. BENGTSSON, T. OLSSON, K. OLSSON, R. S. AL-NASSAR, and L. CHAVEZ, "Design and testing of 300 Mvar Shunt Reactors," *Power*. 42nd CIGRÉ session, Paris, pp. 1–9, 2008, [Online]. Available: https://bit.ly/3tz3ufr.

[97] Energinet, "Teknisk Forskrift 2.1.3. Krav for udveksling af reaktiv effekt (Mvar) i skillefladen mellem transmissions- og distributionssystemerne." Report. Dok. 18/05964-20, pp. 1–16, 2019, [Online]. Available: https://bit.ly/3x6fLKC.

[98] R. Sinha, B. B. Jensen, and J. Radhakrishnan Pillai, "Impact Assessment of Electric Boilers in Low Voltage Distribution Network," *IEEE Power Energy Soc. Gen. Meet.*, vol. 2018-Augus, 2018, doi: 10.1109/PESGM.2018.8586236.

[99] M. Akmal, B. Fox, J. D. Morrow, and T. Littler, "Impact of heat pump load on distribution networks," *IET Gener. Transm. Distrib.*, vol. 8, no. 12, pp. 2065–2073, 2014, doi: 10.1049/iet-gtd.2014.0056.

[100] M. H. J. Bollen and S. K. Rönnberg, "Hosting capacity of the power grid for renewable electricity production and new large consumption equipment," *Energies*, vol. 10, no. 9, 2017, doi: 10.3390/en10091325.

[101] M. Z. Degefa, H. Saele, and C. Andresen, "Analysis of Future Loading Scenarios in a Norwegian LV Network," 2019, doi: 10.1109/SEST.2019.8849081.

[102] M. Marinelli, S. Massucco, A. Mansoldo, and M. Norton, "Analysis of inertial response and primary power-frequency control provision by doubly fed induction generator wind turbines in a small power system," *17th Power Syst. Comput. Conf. PSCC 2011*, 2011, [Online]. Available: https://bit.ly/3ekS2gX.

[103] N. W. Miller and K. Clark, "Advanced controls enable wind plants to provide ancillary services," *IEEE PES Gen. Meet. PES 2010*, pp. 1–6, 2010, doi: 10.1109/PES.2010.5589787.

[104] L. Ruttledge and D. Flynn, "System-wide inertial response from fixed speed and variable speed wind turbines," *IEEE Power Energy Soc. Gen. Meet.*, pp. 1–7, 2011, doi: 10.1109/PES.2011.6038883.

[105] M. N. I. Sarkar, L. G. Meegahapola, and M. Datta, "Reactive power management in renewable rich power grids: A review of grid-codes, renewable generators, support devices, control strategies and optimization Algorithms," *IEEE Access*, vol. 6, pp. 41458–41489, 2018, doi: 10.1109/ACCESS.2018.2838563.

[106] S. Ahsan, Anwar Shahzad Siddiqui, and S. Khan, "Reactive power compensation for integration of wind power in a distribution network," in *IEEE 5th India International Conference on Power Electronics, IICPE*, 2012, no. December 2012, doi: 10.1109/IICPE.2012.6450465.

[107] F. D. González, M. Martínez-Rojas, A. Sumper, O. Gomis-Bellmunt, and L. Trilla, "Strategies for reactive power control in wind farms with STATCOM," *EPE Wind Energy Chapter Symp. 2010*, 2010, [Online]. Available: https://bit.ly/3eg39YJ.

[108] H. Sun *et al.*, "Review of Challenges and Research Opportunities for Voltage Control in Smart Grids," *IEEE Trans. Power Syst.*, vol. 34, no. 4, pp. 2790–2801, 2019, doi: 10.1109/TPWRS.2019.2897948.

[109] S. A. Rahman, "Novel Controls of Photovoltaic (PV) Solar Farms." Electronic Thesis and Dissertation Repository. 922., 2012, [Online]. Available: https://ir.lib.uwo.ca/etd/922/.

[110] N. Solanki and J. Patel, "Utilization of PV solar farm for Grid Voltage regulation during night; Analysis & control," *1st IEEE Int. Conf. Power Electron. Intell. Control Energy Syst. ICPEICES 2016*, no. July 2016, doi: 10.1109/ICPEICES.2016.7853390.

[111] Nordic Council of Ministers, "Demand side flexibility in the Nordic electricity market. From a Distribution System Operator Perspective." pp. 1–72, 2017, [Online]. Available: https://doi.org/10.6027/TN2017-564.

[112] E. Hillberg *et al.*, "Power Transmission & Distribution Systems Flexibility needs in the future power system." Discussion paper ISGAN Annex 6 Power T&D Systems, pp. 1–46, 2019, [Online]. Available: https://bit.ly/3eY7Hoz.

[113] E. Lannoye, D. Flynn, and M. O'Malley, "Evaluation of power system flexibility," *IEEE Trans. Power Syst.*, vol. 27, no. 2, pp. 922–931, 2012, doi: 10.1109/TPWRS.2011.2177280.

[114] S. Yilmaz, "Stochastic bottom-up modelling of household appliance usage to quantify the demand response potential in UK residential sector," Loughborough University, 2017.

[115] L. De Coninck, Roel; Helsen, "Bottom-Up Quantification of the Flexibility Potential of Buildings," *13th Conf. Int. Build. Perform. Simul. Assoc.*, 2013.

[116] R. De Coninck and L. Helsen, "Quantification of flexibility in buildings by cost curves - Methodology and application," *Appl. Energy*, vol. 162, pp. 653–665, 2016, [Online]. Available: http://dx.doi.org/10.1016/j.apenergy.2015.10.114.

[117] R. G. Junker *et al.*, "Characterizing the energy flexibility of buildings and districts," *Appl. Energy*, vol. 225, no. April, pp. 175–182, 2018, doi: 10.1016/j.apenergy.2018.05.037.

[118] M. Z. Degefa, I. B. Sperstad, and H. Sæle, "Comprehensive classifications and characterizations of power system flexibility resources," *Electr. Power Syst. Res.*, vol. 194, no. 107022, 2021, doi: 10.1016/j.epsr.2021.107022.

[119] IRENA (2018), "Power system flexibility for the energy transition, Part 1: Overview for policy makers," International Renewable Energy Agency, Abu Dhabi. [Online]. Available: www.irena.org/publications.

[120] S. Ø. Jensen *et al.*, "IEA EBC Annex 67 Energy Flexible Buildings," *Energy Build.*, vol. 155, pp. 25–34, 2017, [Online]. Available: https://doi.org/10.1016/j.enbuild.2017.08.044.

[121] M. Z. Degefa, H. Sale, I. Petersen, and P. Ahcin, "Data-driven Household Load Flexibility Modelling: Shiftable Atomic Load," 2018, doi: 10.1109/ISGTEurope.2018.8571836.

[122] A. Ionesi, M. Jradi, M. B. Kjærgaard, and C. T. Veje, "Towards seamless integration of model-based energy performance simulation and multi-objective optimization tools," in *14th International Conference of IBPSA - Building Simulation*, 2015, pp. 1173–1179.

[123] A. Arteconi, N. J. Hewitt, and F. Polonara, "State of the art of thermal storage for demand-side management," *Appl. Energy*, vol. 93, pp. 371–389, 2012, doi: 10.1016/j.apenergy.2011.12.045.

[124] R. De Coninck, R. Baetens, B. Verbruggen, J. Driesen, D. Saelens, and L. Helsen, "Modelling and simulation of a grid connected photovoltaic heat pump system with thermal energy storage using Modelica," *8th Int. Conf. Syst. Simul. Build.*, no. June, p. P177, 2010.

[125] K. Hedegaard, B. V. Mathiesen, H. Lund, and P. Heiselberg, "Wind power integration using individual heat pumps - Analysis of different heat storage options," *Energy*, vol. 47, no. 1, pp. 284–293, 2012, doi: 10.1016/j.energy.2012.09.030.

[126] N. J. Hewitt, "Heat pumps and energy storage - The challenges of implementation," *Appl. Energy*, vol. 89, no. 1, pp. 37–44, 2012, doi: 10.1016/j.apenergy.2010.12.028.

[127] K. Karlsson, O. Balyk, E. Zvingilaite, and K. Hedegaard, "SDWS2011 . 0809 District Heating Versus Individual Heating in a 100 % Renewable Energy System by 2050," p. 2050, 2011.

[128] A. L. M. Mufaris and J. Baba, "Local control of heat pump water heaters for voltage control with high penetration of residential PV systems," *2013 IEEE 8th Int. Conf. Ind. Inf. Syst. ICIIS 2013 - Conf. Proc.*, pp. 18–23, 2013, doi: 10.1109/ICIInfS.2013.6731948.

[129] D. Six, J. Desmedt, J. V. A. N. Bael, and D. Vanhoudt, "Exploring the Flexibility Potential of Residential Heat Pumps," *21st Int. Conf. Electr. Distrib.*, no. 0442, pp. 6–9, 2011.

[130] F. Tahersima, J. Stoustrup, S. A. Meybodi, and H. Rasmussen, "Contribution of domestic heating systems to smart grid control,"

Proc. IEEE Conf. Decis. Control, pp. 3677–3681, 2011, doi: 10.1109/CDC.2011.6160913.

[131] R. Parameshwaran, S. Kalaiselvam, S. Harikrishnan, and A. Elayaperumal, "Sustainable thermal energy storage technologies for buildings: A review," *Renew. Sustain. Energy Rev.*, vol. 16, no. 5, pp. 2394–2433, 2012, doi: 10.1016/j.rser.2012.01.058.

[132] J. Le Dréau and P. Heiselberg, "Energy flexibility of residential buildings using short term heat storage in the thermal mass," *Energy*, vol. 111, pp. 991–1002, 2016, doi: https://doi.org/10.1016/j.energy.2016.05.076.

[133] H. Johra, "Aalborg Universitet Integration of a magnetocaloric heat pump in energy flexible buildings," Aalborg University (AAU), 2018.

[134] R. Sinha, B. Bak Jensen, J. R. Pillai, and B. Møller-Jensen, "Unleashing Flexibility from Electric Boilers and Heat Pumps in Danish Residential Distribution Network," *CIGRE 2018 C6-206*, pp. 1–11, 2008.

[135] L. Carradore and R. Turri, "Electric Vehicles participation in distribution network voltage regulation," in *45th International Universities Power Engineering Conference UPEC2010*, 2010, pp. 1–6.

[136] K. Knezović, M. Marinelli, R. J. Møller, P. B. Andersen, C. Træholt, and F. Sossan, "Analysis of voltage support by electric vehicles and photovoltaic in a real Danish low voltage network," in *2014 49th International Universities Power Engineering Conference (UPEC)*, 2014, pp. 1–6, doi: 10.1109/UPEC.2014.6934759.

[137] K. Knezović, M. Marinelli, P. Codani, and Y. Perez, "Distribution grid services and flexibility provision by electric vehicles: A review of options," *Proceedings of the Universities Power Engineering Conference (UPEC)*. 2015, doi: 10.1109/UPEC.2015.7339931.

[138] J. Salpakari, T. Rasku, J. Lindgren, and P. D. Lund, "Flexibility of electric vehicles and space heating in net zero energy houses: an optimal control model with thermal dynamics and battery degradation," *Appl. Energy*, vol. 190, pp. 800–812, 2017, doi: 10.1016/j.apenergy.2017.01.005.

[139] J. Hu, A. Saleem, S. You, L. Nordström, M. Lind, and J. Østergaard, "A multi-agent system for distribution grid congestion management with electric vehicles," *Eng. Appl. Artif. Intell.*, vol. 38, pp. 45–58, 2015, doi: https://doi.org/10.1016/j.engappai.2014.10.017.

[140] H. M. Marczinkowski and P. A. Østergaard, "Residential versus communal combination of photovoltaic and battery in smart energy systems," *Energy*, vol. 152, pp. 466–475, 2018, doi: 10.1016/j.energy.2018.03.153.

[141] D. P. Jenkins, J. Fletcher, and D. Kane, "Model for evaluating impact of battery storage on microgeneration systems in dwellings," *Energy Convers. Manag.*, vol. 49, no. 8, pp. 2413–2424, 2008, doi: 10.1016/j.enconman.2008.01.011.

[142] R. R. Mosbæk and I. Katic, "PV Battery System Tested with Real-Life Consumption Data," 2015, [Online]. Available: https://bit.ly/3DpHEjQ.

[143] M. Murnane and A. Ghazel, "A Closer Look at State of Charge (SOC) and State of Health (SOH) Estimation Techniques for Batteries," *Analog devices*, 2017, [Online]. Available: http://www.analog.com/media/en/technical-documentation/technical-articles/A-Closer-Look-at-State-Of-Charge-and-State-Health-Estimation-Techniques-....pdf.

[144] X. Hu, C. Zou, C. Zhang, and Y. Li, "Technological Developments in Batteries: A Survey of Principal Roles, Types, and Management Needs," *IEEE Power Energy Mag.*, vol. 15, no. 5, pp. 20–31, 2017, doi: 10.1109/MPE.2017.2708812.

[145] C. W. Gellings, "Evolving practice of demand-side management," *J. Mod. Power Syst. Clean Energy*, vol. 5, no. 1, pp. 1–9, 2017.

[146] C. W. Gellings and J. H. Chamberlin, *Demand-Side Management: Concepts and Methods*, 2nd ed. Lilburn, GA : Fairmont Press, 1993.

[147] P. Warren, "Demand-Side Management Policy : Mechanisms for Success and Failure by," University College London (UCL), 2015.

[148] A. S. CHUANG and C. W. Gellings, "Demand-side Integration in a Restructured Electric Power Industry," C6-105, CIGRE 2008, 2008.

[149] CIGRE Working Group C6.09, *Demand Side Integration*, no.

August. 2011.

[150] G. Strbac, "Demand side management: Benefits and challenges," *Energy Policy*, vol. 36, no. 12, pp. 4419–4426, 2008.

[151] D. S. Kirschen, "Demand-side view of electricity markets," *IEEE Trans. Power Syst.*, vol. 18, no. 2, pp. 520–527, 2003, doi: 10.1109/TPWRS.2003.810692.

[152] Rocky Mountain Institute, "Demand Response: An Introduction. Overview of programs, technologies, & lessons learned," for Southwest Energy Efficiency Project, 2006.

[153] K. Herter, "Residential implementation of critical-peak pricing of electricity," *Energy Policy*, vol. 35, no. 4, pp. 2121–2130, 2007, doi: 10.1016/j.enpol.2006.06.019.

[154] C. Triki and A. Violi, "Dynamic pricing of electricity in retail markets," *4or*, vol. 7, no. 1, pp. 21–36, 2009.

[155] H. Allcott, "Real Time Pricing and Electricity Markets," *Group*, pp. 1–77, 2009, [Online]. Available: http://www.erb.umich.edu/HTML-Email/speakers/Post-docCandidates/documents/jmp-allcott.pdf.

[156] M. G. Arentsen, H. Juhler-Verdoner, J. Møller Jørgensen, U. Stougaard Kiil, and M. Holst, "MARKET MODELS FOR AGGREGATORS – Activation of flexibility," *Working group of Danish Energy Association, Danish Intelligent Energy Alliance, Energinet, Confederation of Danish Industry*. pp. 1–14, 2017, [Online]. Available: https://bit.ly/3bklIdL.

[157] Smart Energy Demand Coalition (SEDC), "Explicit and Implicit Demand-Side Flexibility. Complementary Approaches for an Efficient Energy System.," *Position Paper*, no. September. 2016, [Online]. Available: https://bit.ly/2SV52mH.

[158] Smart Energy Demand Coalition (SEDC), "Explicit Demand Response in Europe. Mapping the Markets 2017." pp. 1–223, 2017, [Online]. Available: https://bit.ly/3fkpOn7.

[159] Universal Smart Energy Framework (USEF) Foundation, "The Framework explained." November 2, 2015, pp. 1–55, [Online]. Available: https://bit.ly/3bx0hpF.

[160] B. P. Bhattarai, "Intelligent Control and Operation of Distribution System," Aalborg University (AAU), 2015.

[161] M. Ifland, N. Exner, and D. Westermann, "Appliance of Direct and Indirect Demand Side Management," in *IEEE 2011 EnergyTech*, 2011, pp. 1–6, doi: 10.1109/EnergyTech.2011.5948534.

[162] K. Heussen, S. You, B. Biegel, L. H. Hansen, and K. B. Andersen, "Indirect control for demand side management - A conceptual introduction," in *2012 3rd IEEE PES Innovative Smart Grid Technologies Europe (ISGT Europe)*, 2012, pp. 1–8, doi: 10.1109/ISGTEurope.2012.6465858.

[163] A. M. Kosek, G. T. Costanzo, H. W. Bindner, and O. Gehrke, "An overview of demand side management control schemes for buildings in smart grids," *IEEE Int. Conf. Smart Energy Grid Eng. SEGE*, 2013, doi: 10.1109/SEGE.2013.6707934.

[164] T. Hesser and S. Succar, "Renewables Integration Through Direct Load Control and Demand Response," *Smart Grid*, pp. 209–233, Jan. 2012, doi: 10.1016/B978-0-12-386452-9.00009-7.

[165] R. Dong and L. J. Ratliff, "Energy Disaggregation and the Utility-Privacy Tradeoff," *Big Data Appl. Power Syst.*, pp. 409–444, Jan. 2018, doi: 10.1016/B978-0-12-811968-6.00018-8.

[166] V. Lakshmanan, "Demand Response on domestic thermostatically controlled loads," Technical University of Denmark (DTU), 2016.

[167] D. S. Callaway, "Tapping the energy storage potential in electric loads to deliver load following and regulation, with application to wind energy," *Energy Convers. Manag.*, vol. 50, no. 5, pp. 1389–1400, May 2009, doi: 10.1016/J.ENCONMAN.2008.12.012.

[168] D. Feng, "New real-time market facilitating demand-side resources for system balancing," in *2011 IEEE Power and Energy Society General Meeting*, 2011, pp. 1–6, doi: 10.1109/PES.2011.6039103.

[169] R. Sinha, B. Bak-Jensen, and J. R. Pillai, "Autonomous controller for flexible operation of heat pumps in low-voltage distribution network," *Energies*, vol. 12, no. 8, Apr. 2019, doi: 10.3390/EN12081482.

[170] B. P. Bhattarai, I. D. de C. Mendaza, B. Bak-Jensen, and J. R.

Pillai, "Local Adaptive Control of Solar Photovoltaics and Electric Water Heaters for Real-time Grid Support," *Cigré Session*. CIGRE (International Council on Large Electric Systems), Aug. 2016, [Online]. Available: https://bit.ly/3d1Fnjx.

[171] J. Kondoh, H. Aki, H. Yamaguchi, A. Murata, and I. Ishii, "Consumed power control of time deferrable loads for frequency regulation," in *IEEE PES Power Systems Conference and Exposition, 2004.*, 2004, pp. 1013–1018 vol.2, doi: 10.1109/PSCE.2004.1397726.

[172] D. Kullmann, O. Gehrke, and H. Bindner, "Asynchronous control of Distributed Energy Resources using behaviour descriptions," in *2012 International Conference on Computing, Networking and Communications (ICNC)*, 2012, pp. 216–220, doi: 10.1109/ICCNC.2012.6167414.

[173] P. Piagi and R. H. Lasseter, "Autonomous control of microgrids," in *2006 IEEE Power Engineering Society General Meeting*, 2006, p. 8 pp., doi: 10.1109/PES.2006.1708993.

[174] S. Behboodi, D. P. Chassin, N. Djilali, and C. Crawford, "Transactive control of fast-acting demand response based on thermostatic loads in real-time retail electricity markets," *Appl. Energy*, vol. 210, pp. 1310–1320, Jan. 2018, doi: 10.1016/J.APENERGY.2017.07.058.

[175] S. H. Clearwater, *Market-Based Control. A Paradigm for Distributed Resource Allocation*. Singapore: World Scientific Publishing Co. Pte. Ltd., 1996.

[176] European Smart Grids Task Force Expert Group 3, "Demand Side Flexibility - Perceived barriers and proposed recommendations," no. April, pp. 1–50, 2019, [Online]. Available: https://bit.ly/3eT8JC0.

[177] Energinet, "Regulation I : Master data." Doc. 16/04092-13. Version 2.11., pp. 1–42, 2016, [Online]. Available: https://bit.ly/2Pc8OpF.

[178] Energinet, "Regulation D1 : Settlement metering." Doc. 16/04092-18. Version 4.11., pp. 1–78, 2016, [Online]. Available: https://bit.ly/2Pc8OpF.

[179] E. Lannoye, D. Flynn, and M. O'Malley, "Power system flexibility

assessment State of the art," *IEEE Power Energy Soc. Gen. Meet.*, pp. 1–6, 2012, doi: 10.1109/PESGM.2012.6345375.

[180] CIMNE-BEE Group, "Data driven models and time series analysis," *CORDIS. EU research results*. Record number: 122862, pp. 1–3, 2018, [Online]. Available: https://bit.ly/3yJOYVl.

[181] R. De Coninck, F. Magnusson, J. Åkesson, and L. Helsen, "Toolbox for development and validation of grey-box building models for forecasting and control," *J. Build. Perform. Simul.*, vol. 9, no. 3, pp. 288–303, 2016, doi: 10.1080/19401493.2015.1046933.

[182] M. J. Jiménez, H. Madsen, J. J. Bloem, and B. Dammann, "Estimation of non-linear continuous time models for the heat exchange dynamics of building integrated photovoltaic modules," *Energy Build.*, vol. 40, no. 2, pp. 157–167, 2008, doi: 10.1016/j.enbuild.2007.02.026.

[183] J. Holst, U. Holst, H. Madsen, and H. Melgaard, "Validation of Grey Box Models," *IFAC Proc. Vol.*, vol. 25, no. 14, pp. 53–60, 1992, doi: 10.1016/S1474-6670(17)50712-0.

[184] Z. Yang *et al.*, "Investigating Grey-Box Modeling for Predictive Analytics in Smart Manufacturing," in *Proceedings of the ASME 2017 International Design Engineering Technical Conferences and Computers and Information in Engineering Conference. IDETC/CIE 2017*, Aug. 2017, pp. 1–10, doi: 10.1115/DETC2017-67794.

[185] Q. Navid and A. Hassan, "An Accurate and Precise Grey Box Model of a Low-Power Lithium-Ion Battery and Capacitor/Supercapacitor for Accurate Estimation of State-of-Charge," *Batteries*, vol. 5, no. 3. 2019, doi: 10.3390/batteries5030050.

[186] P. Bacher and H. Madsen, "Identifying suitable models for the heat dynamics of buildings," *Energy Build.*, vol. 43, no. 7, pp. 1511–1522, Jul. 2011, doi: 10.1016/J.ENBUILD.2011.02.005.

[187] Nordic Council of Ministers, "Flexible demand for electricity and power. Barriers and opportunities." pp. 1–83, 2017, [Online]. Available: https://bit.ly/3fm5P7x.

[188] N. Good, K. A. Ellis, and P. Mancarella, "Review and classification of barriers and enablers of demand response in the smart grid,"

Renew. Sustain. Energy Rev., vol. 72, no. January, pp. 57–72, 2017, doi: 10.1016/j.rser.2017.01.043.

[189] L. Feifer, M. Imperadori, G. Salvalai, A. Brambilla, and F. Brunone, *Active House: Smart Nearly Zero Energy Buildings*. SpringerBriefs in Applied Sciences and Technology. PoliMI SpringerBriefs, 2018.

[190] V. Stepaniuk, J. R. Pillai, and B. Bak-Jensen, "Estimation of Energy Activity and Flexibility Range in Smart Active Residential Building," *Smart Cities*, vol. 2, no. 4, pp. 471–495, 2019, [Online]. Available: https://doi.org/10.3390/smartcities2040029.

[191] R. Sinha, "Flexible Control for Local Heating and Transportation Units in Low Voltage Distribution System," Aalborg University (AAU), 2019.

[192] "Weather Data." https://sam.nrel.gov/weather-data.

[193] I. D. de C. Mendaza, "An Interactive Energy System with Grid , Heating and Transportation Systems," Aalborg University (AAU), 2014.

[194] Viessmann Werke GmbH & Co. KG, "Technical guide. VITOCAL Air/water heat pumps." pp. 1–228, 2017, [Online]. Available: www.viessmann.com.

[195] K. Hedegaard, "Wind power integration with heat pumps, heat storages, and electric vehicles – Energy systems analysis and modelling," Technical University of Denmark, 2013.

[196] M. P. Nielsen and K. Sørensen, "Heat Pump System Modelling ," *"LOCAL HEATING CONCEPTS", EUDP 64017-0030* . Sep. 2020.

[197] M. P. Nielsen and K. Sørensen, "Dynamic modeling of heat pumps for ancillary services in local district heating concepts ," vol. No. 176. Linköping University Electronic Press , pp. 39-46 BT-Proceedings of The 61st SIMS Conferen, Mar. 03, 2021, doi: https://doi.org/10.3384/ecp2017639.

[198] W. J. B. Heffernan, N. R. Watson, and J. D. Watson, "Heat-pump performance: voltage dip/sag, under-voltage and over-voltage," *J. Eng.*, vol. 2014, no. 12, pp. 640–657, Dec. 2014, doi: https://doi.org/10.1049/joe.2014.0180.

[199] Vaillant A/S, "Air to water heat pump aroTHERM plus." 2021, [Online]. Available: https://bit.ly/3DuajnS.

[200] Daikin Europe N.V., "Daikin Altherma. Product catalogue 2021. Heating. All-in-one comfort for residential applications." 2021, [Online]. Available: https://bit.ly/3yjQGeo.

[201] Panasonic Marketing Europe GmbH, "Panasonic Aquarea air-to-water heat pumps. Planning and Installation Manual for split systems and compact systems." 2018, [Online]. Available: https://bit.ly/3dhudaj.

[202] C. M. Hvenegaard, S. V. Pedersen, D. Mikkelsen, and J. B. Jensen, "Den lille blå om Varmepumper." Dansk Energi, 2019, [Online]. Available: https://bit.ly/3CXjYmN.

[203] *Norm for vandinstallationer (Code of Practice for domestic water supply installations): DS 439.*, 4. udg. Charlottenlund: Dansk Standard, 2009.

[204] Toshiba Carrier Corporation, "Circular-heating Heat Pump for High Temperature Water," [Online]. Available: https://bit.ly/3hkWOwz.

[205] J. K. Jensen, "Industrial heat pumps for high temperature process applications.," *A numerical study of the ammonia-water hybrid absorption-compression heat pump*. Technical University of Denmark, Kgs. Lyngby, 2016, [Online]. Available: https://bit.ly/3AbAazj.

[206] Danish Energy Agency and Energinet, "Technology Data for Heating Installations," no. 0003, pp. 1–109, 2021, [Online]. Available: http://www.ens.dk/teknologikatalog.

[207] Viessmann Werke GmbH & Co. KG, "New developments 2021. Co-create climate for life. VITOCAL 150-A, 250-A," [Online]. Available: https://bit.ly/3DCHeXE.

[208] Vaillant A/S, "Personal communication with a representative of Vaillant Denmark." 2021.

[209] EnerGuide Natural Resources Canada's Office of Energy Efficiency, "Heating and Cooling With a Heat Pump," 2004.

[210] M. Brunner, S. Tenbohlen, and M. Braun, "Heat pumps as important contributors to local demand-side management," *2013 IEEE Grenoble Conf. PowerTech, POWERTECH 2013*, no. year, 2013, doi: 10.1109/PTC.2013.6652381.

[211] M. Wahl, T. Droscher, J. Sprey, and A. Moser, "Modelling of Heat Pump Load Profiles for Grid Expansion Planning," *Proc. - 2018 53rd Int. Univ. Power Eng. Conf. UPEC 2018*, 2018, doi: 10.1109/UPEC.2018.8541958.

[212] C. M. R. Do Carmo, "Modelling and Development of an Innovative Dual-Mode Heat Pump with HP2Grid functionality," Aalborg University (AAU), 2016.

[213] Danish Energy Agency and Energinet, "Technology Data Catalogue for Electricity and district heating production." Version number: 0009 - Updated April 2020, pp. 1–414, 2020, [Online]. Available: https://bit.ly/2RZgSfu.

[214] J. Perko, V. Dugeč, D. Topić, D. Šljivac, and Z. Kovač, *Calculation and Design of the Heat Pumps*. 2011.

[215] Wärmepumpen-Testzentrum Buchs (WPZ) and NTB Interstaatliche Hochschule für Technik Buchs, "Test results of air to water heat pumps based on EN 14511 : 2018 / EN 14511 : 2013 / EN 14511:2011 / EN 14511:2007 / EN 14511:2004 / EN 14825 : 2016 and EN 14825 : 2013." https://www.ntb.ch/fue/institute/ies/wpz/pruefresultate-waermepumpen/.

[216] T. Kreuzinger, M. Bitzer, and W. Marquardt, "Mathematical modelling of a domestic heating system with stratified storage tank," *Math. Comput. Model. Dyn. Syst.*, vol. 14, no. 3, pp. 231–248, 2008, doi: 10.1080/13873950701844907.

[217] J. D. Chung and Y. Shin, "Integral approximate solution for the charging process in stratified thermal storage tanks," *Sol. Energy*, vol. 85, no. 11, pp. 3010–3016, 2011, doi: https://doi.org/10.1016/j.solener.2011.08.042.

[218] A. Campos Celador, M. Odriozola, and J. M. Sala, "Implications of the modelling of stratified hot water storage tanks in the simulation of CHP plants," *Energy Convers. Manag.*, vol. 52, no. 8, pp. 3018–3026, 2011, doi: https://doi.org/10.1016/j.enconman.2011.04.015.

[219] R. Sinha, B. B. Jensen, J. R. Pillai, C. Bojesen, and B. Moller-Jensen, "Modelling of hot water storage tank for electric grid integration and demand response control," *2017 52nd Int. Univ. Power Eng. Conf. UPEC 2017*, vol. 2017-Janua, no. 1, pp. 1–6, 2017, doi: 10.1109/UPEC.2017.8231964.

[220] O. Dumont, C. Carmo, R. Dickes, E. Georges, S. Quoilin, and V. Lemort, "Hot water tanks," *CLIMA 2016 - 12th REHVA World Congress, 22-25 May 2016, Aalborg, Denmark*. Department of Civil Engineering, Aalborg University, Aalborg, May 2016, [Online]. Available: https://bit.ly/3wkB8pM.

[221] R. K. Rajput, "Engineering Thermodynamics." Third Edition. Laxmi Publications Pvt Limited, 2010, [Online]. Available: https://bit.ly/3dJHSas.

[222] W. De Soto, S. A. Klein, and W. A. Beckman, "Improvement and validation of a model for photovoltaic array performance," *Sol. Energy*, vol. 80, no. 1, pp. 78–88, 2006, doi: https://doi.org/10.1016/j.solener.2005.06.010.

[223] M. K. Fuentes, "A simplified thermal model for Flat-Plate photovoltaic arrays," *Mater. Sci.*, 1987, [Online]. Available: https://bit.ly/35DbB0c.

[224] M. G. Villalva, J. R. Gazoli, and E. R. Filho, "Comprehensive Approach to Modeling and Simulation of Photovoltaic Arrays," *IEEE Trans. Power Electron.*, vol. 24, no. 5, pp. 1198–1208, 2009, doi: 10.1109/TPEL.2009.2013862.

[225] A. D. Hansen, P. E. Sørensen, L. H. Hansen, and H. W. Bindner, "Models for a stand-alone PV system." 2001, [Online]. Available: https://bit.ly/3wtM6KH.

[226] N. Mohammad, M. Quamruzzaman, M. Hossain, and M. Alam, "Parasitic Effects on the Performance of DC-DC SEPIC in Photovoltaic Maximum Power Point Tracking Applications," *Smart Grid Renew. Energy*, vol. 04, pp. 113–121, Jan. 2013, doi: 10.4236/sgre.2013.41014.

[227] M. J. E. Alam, K. M. Muttaqi, and D. Sutanto, "Distributed energy storage for mitigation of voltage-rise impact caused by rooftop solar PV," in *2012 IEEE Power and Energy Society General Meeting*, 2012, pp. 1–8, doi: 10.1109/PESGM.2012.6345726.

[228] A. Samadi, R. Eriksson, L. Söder, B. G. Rawn, and J. C. Boemer, "Coordinated Active Power-Dependent Voltage Regulation in Distribution Grids With PV Systems," *IEEE Trans. Power Deliv.*, vol. 29, no. 3, pp. 1454–1464, 2014, doi: 10.1109/TPWRD.2014.2298614.

[229] M. J. E. Alam, K. M. Muttaqi, and D. Sutanto, "Mitigation of Rooftop Solar PV Impacts and Evening Peak Support by Managing Available Capacity of Distributed Energy Storage Systems," *IEEE Trans. Power Syst.*, vol. 28, no. 4, pp. 3874–3884, 2013, doi: 10.1109/TPWRS.2013.2259269.

[230] V. P. Singh, V. Vijay, M. S. Bhatt, and D. K. Chaturvedi, "Generalized neural network methodology for short term solar power forecasting," in *2013 13th International Conference on Environment and Electrical Engineering (EEEIC)*, 2013, pp. 58–62, doi: 10.1109/EEEIC-2.2013.6737883.

[231] A. Alqahtani, M. Alsaffar, M. El-Sayed, and B. Alajmi, "Data-Driven Photovoltaic System Modeling Based on Nonlinear System Identification," *Int. J. Photoenergy*, vol. 2016, p. 2923731, 2016, doi: 10.1155/2016/2923731.

[232] J. Leloux, L. Narvarte, and D. Trebosc, "Review of the performance of residential PV systems in France," *Renew. Sustain. Energy Rev.*, Feb. 2012, doi: 10.1016/j.rser.2011.10.018.

[233] Danish Energy Agency and Energinet, "Technology Data - Energy Plants for Electricity and District heating generation," pp. 1–414, 2016, [Online]. Available: http://www.ens.dk/teknologikatalog.

[234] "SunPower. Support and Resources." https://us.sunpower.com/solar-resources.

[235] T. Ouyang, A. Kusiak, and Y. He, "Modeling wind-turbine power curve: A data partitioning and mining approach," *Renew. Energy*, vol. 102, no. October, pp. 1–8, 2017, doi: 10.1016/j.renene.2016.10.032.

[236] M. Lydia, S. S. Kumar, A. I. Selvakumar, and G. E. Prem Kumar, "A comprehensive review on wind turbine power curve modeling techniques," *Renew. Sustain. Energy Rev.*, vol. 30, pp. 452–460, 2014, doi: 10.1016/j.rser.2013.10.030.

[237] A. Kusiak, H. Zheng, and Z. Song, "On-line monitoring of power curves," *Renew. Energy*, vol. 34, no. 6, pp. 1487–1493, 2009, doi: https://doi.org/10.1016/j.renene.2008.10.022.

[238] V. Thapar, G. Agnihotri, and V. K. Sethi, "Critical analysis of methods for mathematical modelling of wind turbines," *Renew. Energy*, vol. 36, no. 11, pp. 3166–3177, 2011, doi: https://doi.org/10.1016/j.renene.2011.03.016.

[239] M. Sathyajith, *Wind Energy: Fundamentals, Resource Analysis and Economics*. Berlin, Heidelberg: Springer Berlin / Heidelberg, 2006.

[240] Г. Півняк, Ф. Шкрабець, Н. Нойбергер, and Д. Ципленков, "Основи вітроенергетики." НГУ, Дніпропетровськ, pp. 1–335, 2015, [Online]. Available: https://bit.ly/3kZEInx.

[241] Danish Wind Industry Association, "Describing Wind Variations: Weibull Distribution. The General Pattern of Wind Speed Variations," 2003. https://bit.ly/3rrsYLH.

[242] V. Sohoni, S. C. Gupta, and R. K. Nema, "A Critical Review on Wind Turbine Power Curve Modelling Techniques and Their Applications in Wind Based Energy Systems," *J. Energy*, vol. 2016, no. region 4, pp. 1–18, 2016, doi: 10.1155/2016/8519785.

[243] J. F. Manwell, J. G. McGowan, and A. L. Rogers, *Wind Energy Explained: Theory, Design and Application,* 2nd ed. John Wiley & Sons, Ltd., 2009.

[244] M. R. Patel, *Wind and Solar Power Systems: Design, Analysis, and Operation, Second Edition*. Baton Rouge: CRC Press, 2006.

[245] G. M. Shafiullah, A. M.t. Oo, A. B. M. Shawkat Ali, and P. Wolfs, "Potential challenges of integrating large-scale wind energy into the power grid-A review," *Renew. Sustain. Energy Rev.*, vol. 20, pp. 306–321, 2013, doi: 10.1016/j.rser.2012.11.057.

[246] Klima- Energi- og Forsyningsministeriet, "Bekendtgørelse om teknisk certificering og servicering af vindmøller." BEK nr 1773 af 30/11/2020, Danmark, 2020, [Online]. Available: https://www.retsinformation.dk/eli/lta/2020/1773.

[247] The Danish Energy Agency and Energinet, "Technology data

catalogue for energy storage." pp. 1–234, 2020, [Online]. Available: https://bit.ly/3hTi9NO.

[248] L. Guzzella and A. Sciarretta, "Vehicle propulsion systems: Introduction to modeling and optimization." pp. 1–419, 2013, doi: 10.1007/978-3-642-35913-2.

[249] M. Chen and G. A. Rincon-Mora, "Accurate electrical battery model capable of predicting runtime and I-V performance," *IEEE Trans. Energy Convers.*, vol. 21, no. 2, pp. 504–511, 2006, doi: 10.1109/TEC.2006.874229.

[250] S. Panchal, M. Mathew, R. Fraser, and M. Fowler, "Electrochemical thermal modeling and experimental measurements of 18650 cylindrical lithium-ion battery during discharge cycle for an EV," *Appl. Therm. Eng.*, vol. 135, pp. 123–132, 2018, doi: https://doi.org/10.1016/j.applthermaleng.2018.02.046.

[251] L. Song and J. Evans, "Electrochemical-Thermal Model of Lithium Polymer Batteries," *J. Electrochem. Soc.*, vol. 147, pp. 2086–2095, Jun. 2000, doi: 10.1149/1.1393490.

[252] J. Loukil, F. Masmoudi, and N. Derbel, "Modeling of internal parameters of a lead acid battery with experimental validation," in *2016 13th International Multi-Conference on Systems, Signals & Devices (SSD)*, 2016, pp. 478–483, doi: 10.1109/SSD.2016.7473738.

[253] H. Bindner, T. Cronin, P. Lundsager, J. F. Manwell, U. Abdulwahid, and I. Baring-Gould, "Lifetime modelling of lead acid batteries." 2005, [Online]. Available: https://bit.ly/3xxUhpT.

[254] J. Hu, "Control strategies for power distribution networks with electric vehicle integration," Technical University of Denmark, 2014.

[255] P. T. Moseley and J. Garche, *Electrochemical Energy Storage for Renewable Sources and Grid Balancing*. 2014.

[256] O. Sundström and C. Binding, "Flexible Charging Optimization for Electric Vehicles Considering Distribution Grid Constraints," *IEEE Trans. Smart Grid*, vol. 3, pp. 26–37, Mar. 2012, doi: 10.1109/TSG.2011.2168431.

[257] O. Sundstrom and C. Binding, "Flexible Charging Optimization for

Electric Vehicles Considering Distribution Grid Constraints," *IEEE Trans. Smart Grid*, vol. 3, no. 1, pp. 26–37, 2012, doi: 10.1109/TSG.2011.2168431.

[258] Fronius International GmbH, "Creating a Green Future We Can Look Forward To. We Are Revolutionising the Energy Supply of the Future. Services and product programme 2017/18.," 2017. [Online]. Available: https://bit.ly/2Ydzvir.

[259] Nord Pool AS, "Market data. Day-ahead prices." 2021, [Online]. Available: https://bit.ly/3ypH1TD.

[260] TESLA.COM/ENERGY, "Tesla Powerwall." 2021, [Online]. Available: https://bit.ly/3BsjUtQ.

[261] Danish Ministry of Environment and Environmental Protection Agency, "Statutory Order on Noise from Wind Turbines," vol. 7, no. 1284, pp. 1–14, 2011, [Online]. Available: https://bit.ly/2XCUtr5.

[262] Dansk Energi, "EcoGrid 2.0 Main Results and Findings." pp. 1–58, 2019, doi: 10.1007/978-3-658-27469-6_5.

[263] Aalborg University, "Smart Island Energy Systems," no. 731249, pp. 1–50, 2018.

[264] "ModFlex - Modelling Flexible Resources in Smart Distribution Grid." https://www.sintef.no/en/projects/2016/modelling-flexible-resources-in-smart-distribution/.

[265] V. Stepaniuk, J. R. Pillai, and B. Bak-Jensen, "Quantification of demand-side flexibility of a smart active residential building," *The 9th International Conference on Renewable Power Generation*. IET Conference Proceeding, 2021, [Online]. Available: https://doi.org/10.1049/icp.2021.1376.

[266] H. Saadat, *Power System Analysis*, 3rd ed. PSA Publishings https://www.psapublishing.com, 2010.

[267] *DS/EN 50160. Karakteristika for spændingen i offentlige elektricitetsforsyningsnet. Voltage characteristics of electricity supplied by public electricity networks.*, 4. udg. København: Dansk Standard, 2010.

[268] *DS/EN 60204-1:2018. Maskinsikkerhed – Elektrisk udstyr på*

maskiner – Del 1 : Generelle krav. Safety of machinery – Electrical equipment of machines – Part 1: General requirements. København: Dansk Standard, 2018.

[269] Klima- Energi- og Forsyningsministeriet, "Bekendtgørelse af lov om elforsyning." LBK nr 119 af 06/02/2020, Danmark, 2020, [Online]. Available: https://bit.ly/2RzNhII.

[270] C. Deb, F. Zhang, J. Yang, S. E. Lee, and K. W. Shah, "A review on time series forecasting techniques for building energy consumption," *Renew. Sustain. Energy Rev.*, vol. 74, no. July 2016, pp. 902–924, 2017, doi: 10.1016/j.rser.2017.02.085.

[271] C. Kuster, Y. Rezgui, and M. Mourshed, "Electrical load forecasting models: A critical systematic review," *Sustain. Cities Soc.*, vol. 35, no. July, pp. 257–270, 2017, doi: 10.1016/j.scs.2017.08.009.

APPENDICES

A. THE IMPORTANCE OF LOW-RESOLUTION MODELLING AND ISSUES WHEN PERFORMING 15-MINUTE TIME STEP SIMULATION

The text below emphasizes the importance of moving to a one-minute simulation step and illustrates the problematic aspects of performing simulations with a 15-minute and larger step. The section describes the situations that had to be faced by combining all the components of the energy model of a building under a single coordination algorithm and running a simulation of the behaviour of these components with a 15-minute time step (i.e. what had been done initially, before moving to a 1-minute step). To be noted, if simulating only individual components separately, the situations described below will not have such a significant impact and will be rather informational in nature, that is something that is worth paying attention to. However, combining several components into a single model, such situations lead to numerous errors, the solution of which will complicate the model a lot.

First of all, it should be noted that in energy studies, when simulating the behaviour of a system with 15-minute (and larger) steps, all calculations are carried out with energy (not with power). Unlike low-resolution modelling, where calculations are usually performed with power and to determining energy, the power value is multiplied by a specific activation time (e.g., the duration of the HP power ON period), in energy models with a 15-minute step or more, usually, the opposite is true. To determine the value of instantaneous power, the resulting energy value is commonly divided by the simulation step, and that is the place where the stumbling block is hidden. The main difference and the main cause of errors is that the simulation step and the specific activation time are two different values. Unlike low-resolution modelling, where the activation time is known (can easily be tracked) and there is not even a single difficulty with determining the energy, in the case of 15-minute models, the exact activation time is unknown – the only energy value and the simulation step (e.g., 15 minutes) are obvious. Since the activation may take less than 15 minutes, dividing the energy value by the entire time step to determine the power will give the wrong result.

With such interconnected building components as own RESs with battery and heat pump with HWST, the total amount of energy, during this single time step, is directly dependant on the behaviour of all these components and to the greatest extent on SOE of the battery and HWST. The larger the simulation step, respectively, the more energy is involved during that step and the more energy is added or subtracted to/from the previous SOE

during that step (see Eq. 3.23, Section 3.3.2 for an HWST or Eq. 3.49, Section 3.6.3 for battery). Accordingly, the faster the maximum/minimum levels are reached. Simulating a model with a 15-minute step, and at the same time, having a relatively small controlled SOE range in the HWST (between 81% and 100%), it often happens that the energy level reaches its maximum/minimum value somewhere in the middle or already in the first minutes of 15-minute step. Accordingly, somewhere in the middle of one step, the heat pump should be switched off (by reaching SOE_{max}^{HWST}) or turned on (by reaching $SOE_{min.ctrl.}^{HWST}$). Changes in heat pump consumption lead to the fact that the share of energy covered by own RESs, and, consequently, those parts of energy charged/discharged to the battery or imported/exported from/to the grid, will also be changed in the middle of a single time step. Determining, for example, the share of power delivered from the grid (required to perform a load flow analysis), while taking into account the exact HP's activation time (which is unknown in the case of a 15-minute step simulation), complicates the process a lot.

An example could be the HPS with an HWST volume of 0.2 m^3. The controlled range for this tank (i.e. 81-100%) is equivalent to just 2.3 kWh of thermal energy. Having maximum thermal demand of the household of 11.5 kW this will be enough for 12 minutes only (i.e. 12 minutes of heat supply without turning on the HP). Considering that the SOE of HWST is far not always at its maximum level (not always 100% charged), the HP turning on and off in the middle of a single 15-minute time step is a quite often phenomenon. Thus, the HPs energy consumption will also be reduced compared to how it would normally have been consumed during a full 15-minute time step, say only 1.2 kWh out of 2kWh (figures are given as an example only and have no ties to the actual energy consumption). Dividing this 1.2 kWh by 15 minutes, the power value will be greatly underestimated compared to the truth value (i.e. 1.2 / 0.25 = 4.8 kW where it should be 8 kW). And such situations are quite common. Let's consider a few of these situations.

All the graphs in Figure 6.1 below represent a time span of 15 minutes (i.e. a single time step) and can be divided into those where RES production covers the major part of the demand (i.e. graphs **a**, **b**) and the minor part (graphs **c**, **d**). 15-minute step is divided into three equal 5-minute segments ($\Delta t_1, \Delta t_2, \Delta t_3$) just for ease of perception, however, the duration of each of them can be completely different. Graphs (**a**, **b**) describe a situation when RES production is in excess ($\Delta P > 0$) for the first period of time, and then a shortage (i.e. when $\Delta P < 0$) for the remaining time. Graphs (**c**, **d**) depict a situation when own RES generation is not sufficient to cover demand, therefore a shortage is observed throughout the entire time step.

Graph (**a**) shows the case when the battery is completely discharged. For the first 5 minutes, battery charge and HWST discharge can be observed. The decrease in heat energy level in the HWST down to the minimum level led to the activation of the heat pump and an increase in the total electricity demand (starting from the 5th minute). The growth of consumption, in turn, led to a lack of RES generation and battery discharge, but since the energy stored in the battery is not enough to cover the demand, part of the energy is imported from the grid. When the battery level reached its minimum (10th minute), a share of imports increased.

Graph (**b**) shows the battery charge (first 5 minutes) and then the grid export (next 5 minutes after reaching the maximum battery level). However, when the thermal energy in the HWST reached the minimum level (10th minute), the heat pump turned on and, accordingly, the increase in demand caused the battery to discharge.

Graph (**c**) illustrates battery discharge and grid import. As demand increased, the share of energy discharged from the battery also increased, but since demand has exceeded the rated power of the battery inverter, both battery discharge and import from the grid occurred simultaneously. Once the battery is completely discharged (at the 10th minute) – only import can be observed.

Graph (**d**) represents both battery discharge and import from the grid. The graph is provided only to visualise how the energy shares may change depending on when the battery and HWST reach their minimums.

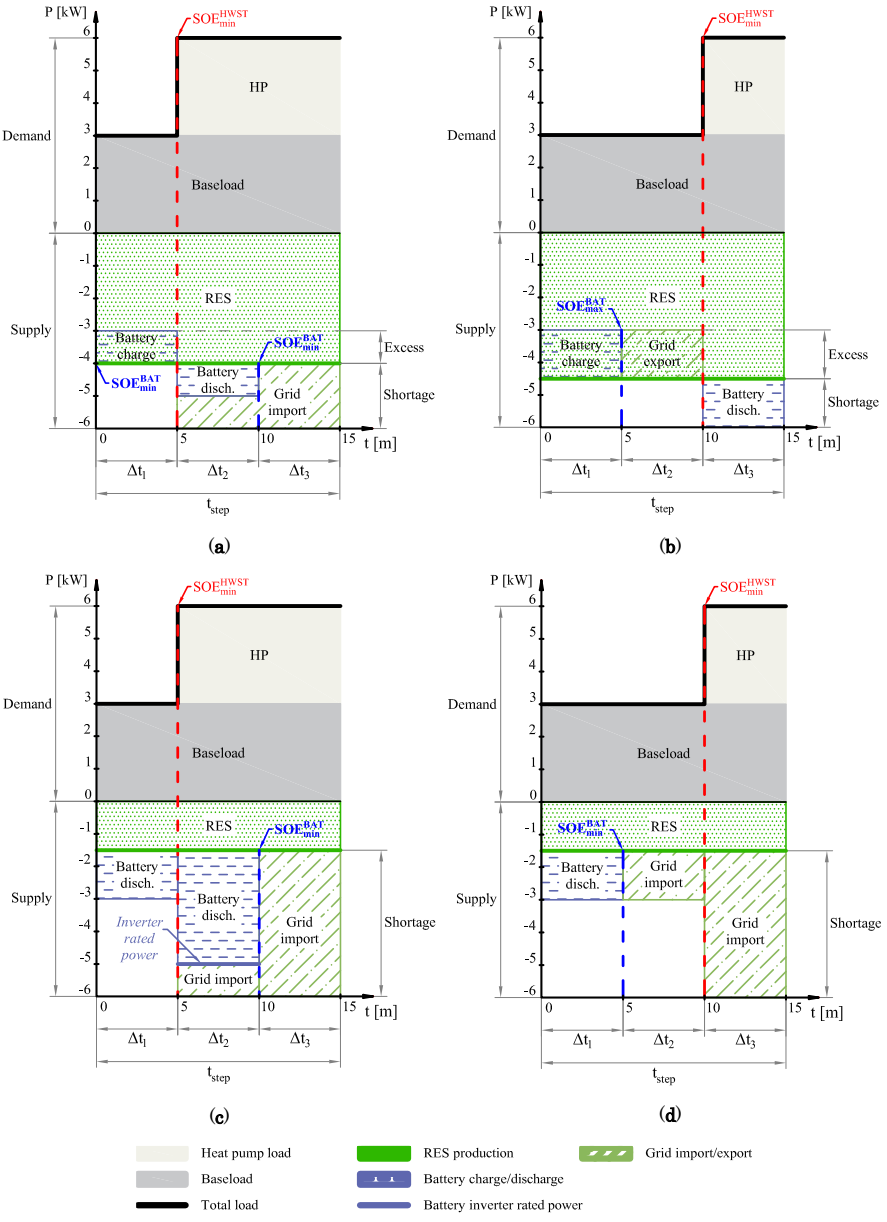

Figure 6.1. Examples of problematic cases that complicate quantification and arise when running simulations in 15-minute increments.

All the graphs in Figure 6.2 show similar situations in relation to battery discharge/charging, as well as import from the grid, however, the main

focus, in this case, should be on energy flexibility, which is one of the main aspects of this study. All four graphs show situations where the HWST is "charged" with thermal energy, in particular situations where the heat pump has already been turned on long enough to be able to switch off to provide an energy flexibility service (in response to DR signal). However, the biggest difficulty in these cases is to separate and quantify exactly that part of HP's power demand and energy consumption that is imported from the grid. Since the battery is not charged from the grid, only from RESs (implying no flexibility from the battery side), it is this part of the total HP consumption (which is imported from the grid) that will be considered as potential energy flexibility, and it is this part of the flexible consumption that must subsequently be paid by the Aggregator.

The graphs illustrate that, due to the fact that the heat pump can be switched off or the battery minimum/maximum level can be reached in the middle of a given time interval, the energy flexibility can, in principle, take different forms, and the duration of the flexibility provision period can also be less than 15 minutes. Having a large simulation step, like 15 minutes, and a small controllable SOE range of the HWST, this flexibility (especially when there is a high heat demand) simply will not be observed. All this complicates the process of subtracting this energy flexibility share exponentially. A good example is graph (**a**). On the other hand, graph (**d**) depicts an ideal situation where the energy is continuous during an entire time step, and at the same time shows that the battery power limit (i.e. the inverter rated power) is not an obstacle for executing calculations.

Summing up the aforementioned, it can be said that difficulties arise:

- due to the small controllable SOE range of the HWST;
- due to the large time interval of the simulation;
- predominantly when the SOE of the HWST or battery is close to the maximum/minimum levels.

The simple solution is to modify the charging/discharging algorithm in such a way so that the excess/shortage of local production remain inseparable into parts within a single time step. By reaching the maximum SOE level, the excessed energy can be either charged to the battery or exported to the grid and vice versa (discharged/imported by reaching the minimum level). It would be logical and reasonable to note that, in these cases, the battery will be undercharged to the maximum (under-discharged to the minimum) level to some extent (especially while having a 15-minute and larger time step). Assuming that this may also lead to a decrease in the accuracy of computation, it is decided to minimise this error by swapping to a lower time interval. With a simulation step of one minute, the error is absolutely neglectable. The result showed that

undercharging to the maximum level, in such cases, is less than 1% and is varied between 0.003-0.74% (based on the simulation period of one year).

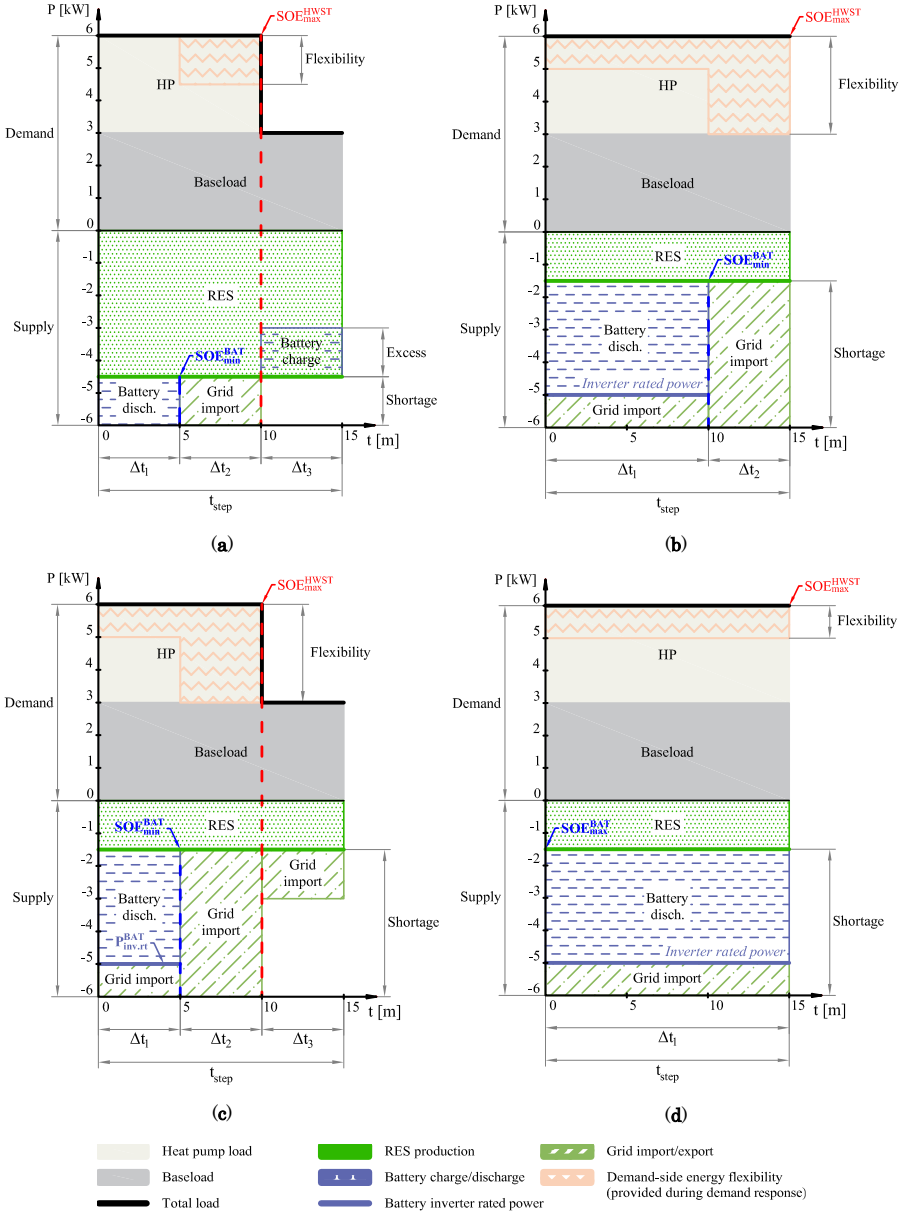

Figure 6.2. Examples of problematic cases that arise when running simulations in 15-minute increments, associated with energy flexibility quantification.

In this section, only a few situations have been visualized, while in reality there can be much more, depending on the demand and the level of RES generation, as well as SOE of the Battery and HWST. It is also worth noting that among the variety of advantages of a one-minute step, the main disadvantage, however, is the computation time, which, in some cases can be as long as 30-35 hours.

B. MICRO WIND TURBINE DATASHEET

Proven Energy Products Ltd

HAWT – From 0,6 kW to 15 kW

Contact name: David Watson
Address: Wardhead Park, Stewarton, Ayrshire, KA3 5 LH, Scotland
Telephone: +44 (0) 1560 485 570
Country : **United Kingdom**

Proven WT 6 000 references

Site	Use	Country

Proven WT 6 000/ 6 kW

Technical information

POWER		Unit
1) Rated power	6	KW
2) Rated wind speed	12	m/s
3) Cut-in wind speed	2,5	m/s
4) Cut-out wind speed	None	m/s
5) Maximum wind speed the turbine can withstand	234	Km/h
DIMENSIONS		
6) Rotor weight	539	Kg
7) Rotor diameter	5,5	m
8) Rotor height (for VAWT only)		m
9) Swept area	23,76	m^2
10) Height of the mast	9 / 15	m
OTHER INFORMATION		
11) Maximum rpm		At rated wind speed
12) Gear box type		
13) Brake system		
14) Number of blades		3
15) Blades material		Wood/ Epoxy / P.U.
16) Output voltage	48 to 300	V
17) Minimum operation temperature	Artic circle	°C
18) Maximum operation temperature	South America	°C
19) Acoustic levels at a distance of 20 m ? at nacelle ? (wind = 5 m/s)	45 dB at mast 36 dB at 20 m	DB
20) Lifetime	20-25	Years
21) Is the machine self-starting		Yes
22) Use of an asynchronous generator		No
23) Yaw control system		
24) Upwind or downwind		Downwind

Calculated power curve

Wind speed (m/s)	Power (W)
1	0
2	0
3	100
4	450
5	1 000
6	1 500
7	2 050
8	3 000
9	4 000
10	5 000
11	6 000
12	6 200
13	6 250
14	6 150

Power curve:

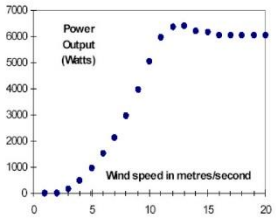

C. LOCAL LV DISTRIBUTION GRID DATA REQUIRED FOR POWER FLOW ANALYSIS

Bus data											
	1	2	3	4	5	6	7	8	9	10	11
Name	Bus / Terminal / Node №	Bus code	Voltage	Angle	Load		Generator				Inject
			Magn.	Degree	P (MW)	Q (MVar)	P (MW)	Q (MVar)	Q (min)	Q (max)	Q (MVar)
TF_LV	1	1	1	0	0	0	0	0	0	0	0
B01	2	0	1	0	0	0	0	0	0	0	0
B02	3	0	1	0	0	0	0	0	0	0	0
B03	4	0	1	0	0	0	0	0	0	0	0
B04	5	0	1	0	0	0	0	0	0	0	0
B05	6	0	1	0	0	0	0	0	0	0	0
B06	7	0	1	0	0	0	0	0	0	0	0
B07	8	0	1	0	0	0	0	0	0	0	0
B08	9	0	1	0	0	0	0	0	0	0	0
B09	10	0	1	0	0	0	0	0	0	0	0
B10	11	0	1	0	0	0	0	0	0	0	0
B11	12	0	1	0	0	0	0	0	0	0	0
B12	13	0	1	0	0	0	0	0	0	0	0
B13	14	0	1	0	0	0	0	0	0	0	0
Load 01	15	0	1	0	0.0009	0.0003	0	0	0	0	0
Load 02	16	0	1	0	0.0009	0.0003	0	0	0	0	0
Load 03	17	0	1	0	0.0009	0.0003	0	0	0	0	0
Load 04	18	0	1	0	0.0007	0.0002	0	0	0	0	0
Load 05	19	0	1	0	0.001	0.0003	0	0	0	0	0
Load 06	20	0	1	0	0.0008	0.0003	0	0	0	0	0
Load 07	21	0	1	0	0.001	0.0003	0	0	0	0	0
Load 08	22	0	1	0	0.0008	0.0003	0	0	0	0	0
Load 09	23	0	1	0	0.0007	0.0002	0	0	0	0	0
Load 10	24	0	1	0	0.0008	0.0003	0	0	0	0	0
Load 11	25	0	1	0	0.0009	0.0003	0	0	0	0	0
Load 12	26	0	1	0	0.0005	0.0002	0	0	0	0	0
Load 13	27	0	1	0	0.001	0.0003	0	0	0	0	0
Load 14	28	0	1	0	0.001	0.0003	0	0	0	0	0
Load 15	29	0	1	0	0.0008	0.0003	0	0	0	0	0
Load 16	30	0	1	0	0.0008	0.0002	0	0	0	0	0
Load 17	31	0	1	0	0.001	0.0003	0	0	0	0	0
Load 18	32	0	1	0	0.001	0.0003	0	0	0	0	0
Load 19	33	0	1	0	0.001	0.0003	0	0	0	0	0
Load 20	34	0	1	0	0.0009	0.0003	0	0	0	0	0
Load 21	35	0	1	0	0.0008	0.0002	0	0	0	0	0
Load 22	36	0	1	0	0.001	0.0003	0	0	0	0	0
Load 23	37	0	1	0	0.001	0.0003	0	0	0	0	0
Load 24	38	0	1	0	0.0009	0.0003	0	0	0	0	0
Load 25	39	0	1	0	0.0009	0.0003	0	0	0	0	0
CBN	40	0	1	0	0	0	0	0	0	0	0

Line data								
			1	2	3	4	5	6
Length km	From Node	To Node	From Node №	To Node №	R' p.u.	X' p.u.	1/2 B p.u.	TAP
0.085	TF_LV	B01	1	2	11.05	2.7625	0	1
0.056	B01	B02	2	3	7.28	1.82	0	1
0.037	B02	B03	3	4	4.81	1.2025	0	1
0.012	B02	Load01	3	15	13.725	0.7275	0	1
0.072	B03	B04	4	5	9.36	2.34	0	1
0.014	B03	Load02	4	16	16.0125	0.84875	0	1
0.05	B04	B07	5	8	6.5	1.625	0	1
0.011	B04	Load03	5	17	12.58125	0.666875	0	1
0.058	B04	Load04	5	18	66.3375	3.51625	0	1
0.06	B07	B10	8	11	7.8	1.95	0	1
0.022	B07	Load11	8	25	25.1625	1.33375	0	1
0.023	B07	CBN	8	40	26.30625	1.394375	0	1
0.025	B10	B13	11	14	3.25	0.8125	0	1
0.014	B13	Load25	14	39	16.0125	0.84875	0	1
0.037	B07	B11	8	12	14.82313	1.34125	0	1
0.019	B11	Load17	12	31	21.73125	1.151875	0	1
0.018	B11	Load18	12	32	20.5875	1.09125	0	1
0.013	B11	Load19	12	33	14.86875	0.788125	0	1
0.011	B11	Load20	12	34	12.58125	0.666875	0	1
0.043	B04	B08	5	9	17.22688	1.55875	0	1
0.019	B08	Load12	9	26	21.73125	1.151875	0	1
0.017	B08	Load13	9	27	19.44375	1.030625	0	1
0.013	B08	Load14	9	28	14.86875	0.788125	0	1
0.037	B03	B05	4	6	7.4	1.24875	0	1
0.051	B05	B09	6	10	10.2	1.72125	0	1
0.02	B05	Load05	6	19	22.875	1.2125	0	1
0.022	B05	Load06	6	20	25.1625	1.33375	0	1
0.011	B05	Load07	6	21	12.58125	0.666875	0	1
0.016	B05	Load08	6	22	18.3	0.97	0	1
0.037	B09	B12	10	13	7.4	1.24875	0	1
0.019	B09	Load15	10	29	21.73125	1.151875	0	1
0.017	B09	Load16	10	30	19.44375	1.030625	0	1
0.019	B12	Load21	13	35	21.73125	1.151875	0	1
0.018	B12	Load22	13	36	20.5875	1.09125	0	1
0.011	B12	Load23	13	37	12.58125	0.666875	0	1
0.01	B12	Load24	13	38	11.4375	0.60625	0	1
0.05	B03	B06	4	7	20.03125	1.8125	0	1
0.01	B06	Load09	7	23	11.4375	0.60625	0	1
0.024	B06	Load10	7	24	27.45	1.455	0	1

ISSN (online): 2446-1636
ISBN (online): 978-87-7573-977-6

AALBORG UNIVERSITY PRESS